WCAP-15129
Revision 3

◆ ◆ ◆ ◆ ◆ ◆ ◆ ◆ ◆ ◆

Depth-Based SG Tube Repair Criteria for Axial PWSCC at Dented TSP Intersections

Westinghouse Electric Company LLC

WCAP-15129
Revision 3

Depth-Based SG Tube Repair Criteria for Axial PWSCC At Dented TSP Intersections

T. A. Pitterle
R. F. Keating
D. D. Malinowski
W. K. Cullen
G. P. Lilly
A. Sagar

June 30, 2000

Depth Based SG Tube Repair Criteria for
Axial PWSCC at Dented TSP Intersections

Table of Contents

Table of Contents (Continued)

Table of Contents (Continued)

1.0   INTRODUCTION

This report provides the technical bases for a depth based ARC for axial PWSCC indications at dented TSP intersections. Repair limits are developed for indications within the TSP or with limited extension outside the TSP. The ARC repair limits of this report apply to axial PWSCC indications $\geq 40\%$ maximum depth since indications $< 40\%$ depth are left in service per the existing Technical Specification repair limit of 40% depth. The ARC and supporting requirements including inspection, burst analyses and leak rate analyses are described in this report. The ARC is conservatively based upon the assumption that the indications are freespan at SLB conditions and applies to axial indications that are located within or extending outside the TSP. Only indications within the TSP are left in service with maximum depths $\geq 40\%$. Requirements for including NDE uncertainties in the ARC analyses are also defined. The ARC satisfies steam generator tube integrity guidelines consistent with the requirements of NEI 97-06, draft Regulatory Guide 1.121 and draft Regulatory Guide DG-1074. The depth based repair limits are based upon establishing a high confidence that the indications will burst or result in unacceptable leak rates under SLB conditions at the end of the operating cycle.

The ARC is based on the use of crack depth profiles obtained from +Point analyses. Burst pressures are calculated from the depth profiles by searching the total crack length for the partial length that results in the lowest burst pressure. Because the burst pressure can be lower than that for the longest allowable crack length at its average depth, a fixed repair limit cannot be established. The repair basis is obtained by projecting the crack profile to the end of the next operating cycle and determining if the burst pressure and SLB leak rate for the projected profile satisfy the burst margin and acceptable leakage limit requirements. If the projected EOC burst margin and leakage requirements are satisfied, the indication can be left in service. Thus, the repair basis corresponds to demonstrating that the operational assessment requirements are satisfied. Crack length limits are defined so that crack extension and growth outside of the TSP provide adequate margin against burst for the freespan length in addition to the total crack length.

Section 2 provides the summary and conclusions of the report. The pulled tube and laboratory database supporting the NDE database for axial PWSCC at dented TSP intersections is described in Section 3. The qualification of NDE techniques for detection and sizing of PWSCC in dented TSPs is discussed in Section 4. This section describes the NDE analysis guidelines, results of blind analyses tests, the results of Appendix H qualification, the results of a NDE Performance test and PWSCC growth rates. The development and description of the methodology to predict the burst pressure of SG tubes with axial, stress corrosion cracks which extend partly through the tube wall is presented in Section 5. In Section 6, the available crack leak rate database is used to correlate CRACKFLO Code predicted leak rates at SLB conditions with test results. This approach permits the development of statistical analyses of the CRACKFLO Code predictions vs. measured crack leak rates at SLB conditions. The resulting correlation permits calculations of SLB leak rates with defined uncertainties based on the throughwall length of the crack. The ARC is based on the use of crack depth profiles which permit prediction of the EOC length when NDE uncertainties and growth, where required, are included in the analyses. A ligament tearing model is applied to calculate the throughwall crack length from the EOC crack profile. Applicable structural limits, NDE uncertainties and growth rates are described in Section 7. Repair bases to satisfy burst and leakage requirements are also developed in Section 7. In addition, the inspection requirements for application of the ARC are described in Section 7. Section 8 provides a list of references for the report.

2.0 SUMMARY AND CONCLUSIONS

2.1 ARC Summary

The ARC repair limits of this report apply to axial PWSCC indications ≥ 40% maximum depth. Indications < 40% maximum depth are left in service per the existing Technical Specification repair limit of 40% depth. Both repair limits are applied for axial PWSCC at dented TSP intersections since indications ≥ 40% depth require location and length limits that are not necessary below 40% maximum depth.

2.1.1 Repair Limits

The existing Technical Specification repair limits at ≥ 40% maximum depth are applied as follows:

- Indications with < 40% maximum depth are left in service per the existing Technical Specification limits without the additional location and analysis requirements for the ARC indications having ≥ 40% maximum depth
- The Technical Specification repair limit of 40% maximum depth applies to the freespan length (length outside the TSP) of indications entirely outside the TSP or with one or both crack tips extending outside the edge of the TSP
- Condition monitoring and operational assessment requirements for these indications are imposed by NEI 97-06 rather than the specific ARC requirements of this report

The ARC repair limits apply to indications within the TSP, within and extending outside the TSP or at the edge of the TSP with ≥40% maximum depth limited to within the TSP. The repair bases, which apply updated growth data, cycle lengths, T_{hot} and steam pressures for each cycle are:

- Length requiring repair
  - Indications having ≥ 40% depth at > 0.375 inch from the centerline of the TSP (i.e., outside the TSP)
- Operational assessments against burst margins and leakage limits are performed to identify indications requiring repair. The operational assessments include:
  - Single indication Monte Carlo analyses to compare the burst pressure for the projected EOC crack distribution against deterministic burst margin requirements
  - Measured crack depth profiles from +Point analyses are increased in length and depth based on growth and NDE uncertainties to obtain the projected EOC crack distributions.
  - Burst pressures are based on searching the EOC crack profile for the partial crack length resulting in the lowest burst pressure. Burst pressures are predicted based on a correlation of burst pressure measurements with an analytical model for part throughwall cracks.
  - SLB leak rates are based on searching the EOC crack profile for the crack lengths predicted to be throughwall at EOC including predictions of ligament tearing. SLB leak rates are predicted from the throughwall crack length applying a correlation of SLB leak rate measurements with an analytical leak rate model.
  - Burst margin requirements of $1.43\Delta P_{SLB}$ are applied to the total crack length and $3\Delta P_{NO}$ are applied to the length outside the TSP.
  - Allowable leakage limits are 1 gpm for freespan indications and the plant specific licensing basis limit for constrained crack indications. The 1 gpm freespan leakage limit applies to the sum of leak rates predicted for freespan axial PWSCC crack lengths left in service and for all other freespan degradation mechanisms predicted to have leakage in their respective operational

assessments. The constrained crack leakage limit applies to the sum of leak rates predicted for the total PWSCC crack lengths left in service, axial ODSCC at TSP intersections left in service under the GL 95-05 ARC and axial indications within the tubesheet left in service under the W* ARC.

- Burst margin and SLB leakage requirements are to be satisfied at 95% probability at 95% confidence on the projected EOC values.
- For the Diablo Canyon SGs, tube/TSP intersections excluded from application of the voltage based repair limits for ODSCC due to LOCA + SSE considerations are also excluded from application of the depth based repair limits for PWSCC of this report (PWSCC ≥40% maximum depth). In addition, some tubes at the top TSP of the Diablo Canyon SGs are excluded from the ARC due to bending stresses potentially exceeding the yield strength under FLB + SSE conditions. No tubes are excluded from application of the ARC for the Sequoyah SGs.
• Typical plant operating conditions, which would be updated prior to each inspection, are:
- Sequoyah SGs: $T_{hot} = 611°F$, 1.25 EFPY, $3\Delta P_{NO} = 4209$ psi
- Diablo Canyon SGs: $T_{hot} = 603°F$, 1.42 EFPY, $3\Delta P_{NO} = 4383$ psi

The NDE uncertainties and growth rates for calculating plant specific repair limits are given below. In these equations, ΔG = growth rate per EFPY; ΔNDE = NDE uncertainty; AD = average depth; MD = maximum depth, L = length; and subscript BE = best estimate or "truth" inferred from correlation with NDE data.

NDE Uncertainties

• Average Depth NDE Uncertainty
- Correlation: $[AD_{BE} = 0.914AD_{NDE} + 0.687]^g$
- Standard deviation = $[7.8\%]^g$
- NDE Uncertainty at +95% confidence ($\Delta NDE_{AD95\%}$) = [10.1% for indication at ≈40% average depth]^g
• Maximum Depth NDE Uncertainty
- Correlation: $[MD_{BE} = 0.939MD_{NDE} - 0.923]^g$
- Standard deviation = $[14.2\%]^g$
- NDE Uncertainty at +95% confidence ($\Delta NDE_{MD95\%}$) = [19.2% for indication at 55% maximum depth]^g
• Length NDE Uncertainty
- Correlation: $[L_{BE} = 1.008L_{NDE} + 0.010]^g$
- Standard deviation = $[0.14$ inch$]^g$
- NDE Uncertainty at +95% confidence ($\Delta NDE_{L95\%}$) =[approximately 0.25 inch for indications between 0.75 and 1.25 inch length]^g

PWSCC Growth Rates

• Growth rate distributions for length, average depth and maximum depth are applied with separate distributions for Sequoyah SGs and for Diablo Canyon SGs. Growth rates are to be updated following each inspection to incorporate the latest data in the growth distributions. Examples at 95% probability are given below.
• Average depth growth at 95% probability ($\Delta G_{AD95\%}$) = [17.9% per EFPY at 611°F for Sequoyah and 13.2% per EFPY at 603°F for Diablo Canyon]^g

- Maximum depth growth at 95% probability ($\Delta G_{MD95\%}$) = [20.4% per EFPY at 611°F for Sequoyah and 15.5% per EFPY at 603°F for Diablo Canyon] [g]
- Length growth at 95% probability ($\Delta G_{L95\%}$) = [0.21 inch per EFPY at 611°F for Sequoyah and 0.15 inch per EFPY at 603°F] [g]

2.1.2 Inspection Requirements

To support the ARC for axial PWSCC at dented TSP intersections, inspection requirements are identified for the extent of inspection and NDE data analysis.

Extent of Inspection

The bobbin coil probe is applied for sizing of dent voltages and for detection of axial PWSCC indications at TSP intersections with less than or equal to 2.0 volt dents for which the bobbin probe qualification is described in Section 4. The +Point probe is applied for sizing of bobbin detected indications and for detection and sizing at intersections with greater than 2.0 volt dents. The extent of inspection required for the ARC is then:

- 100% bobbin coil inspection of all TSP intersections
- +Point coil inspection of all bobbin coil indications at dented TSP intersections
- +Point coil inspection of all prior PWSCC indications left in service.
- On a SG basis, +Point coil inspection of all TSP intersections having > 2.0 volt dents up to the highest TSP for which PWSCC has been detected in the prior and current inspection and 20% of dents > 2.0 volts at the next highest TSP

NDE Analysis Requirements

In addition to general reporting requirements such as tube location, TSP number and crack location relative to the center of the TSP, the following data are required from the inspection. For the bobbin coil, dent voltage and the detection call as NDD or PI (or equivalent) with the associated bobbin flaw voltage. Dent voltages must be determined to at least a minimum of 2 volt dents in order to define the +Point inspection requirements. When it is established that denting has been arrested and dents are not growing, dent voltages for TSP intersections can be established one time and applied for subsequent inspections. For the + Point Probe, the flaw call shall be reported as ID or OD, NDD, SAI or MAI for each dented intersection inspected. In addition, the crack length versus depth and voltage profile with axial positions defined relative to the center of the TSP shall be reported. The NDE profiles are adjusted for length and depth (if maximum voltage ≤ 1.0 or ≥ 4.5 volts) per the adjustment procedure given in Section 4.

When PWSCC indications at dented TSP intersections are to be left in service, the +Point data shall be applied to evaluate the TSP for cracked ligaments. If cracked ligaments are detected, the PWSCC indication shall be repaired.

2.1.3 Condition Monitoring and Operational Assessments

The ARC condition monitoring assessment is a probabilistic SLB calculation. Crack lengths dominantly inside the TSP must satisfy $1.43\Delta P_{SLB}$ burst margins. Indication lengths outside the TSP must satisfy $3\Delta P_{NO}$ burst margins and probabilistic SLB calculations are not an acceptable option. All indications are conservatively assumed to be free span indications (postulated SLB TSP displacements) for the

condition monitoring analyses even if the indication is inside the TSP. If the indication is outside the TSP, in situ pressure and leak testing can be performed for the condition monitoring assessment. The total leakage from axial PWSCC, ODSCC at TSP intersections and tubesheet W* indications must be less than the allowable dose based leakage limit for constrained indications in the licensing basis. Leakage from freespan indications must be less than 1 gpm for the sum of leak rates from PWSCC indications and any other freespan indications found to leak in their respective condition monitoring assessments. The condition monitoring requirements are to be satisfied at 95% probability and 50% confidence. If the condition monitoring requirements are not satisfied for burst and/or leakage, the causative factors for EOC indications exceeding the expected values should be evaluated.

As a minimum, growth rates for large indications that could impact the upper tail of the growth distribution shall be evaluated. If the growth data for new indications causes the growth distribution above 90% probability to be more conservative, the new growth data shall be added to the growth distribution for the operational assessment.

The ARC operational assessment is satisfied by the methods used to identify indications requiring repair and no further operational assessment is required. If the condition monitoring assessments satisfy burst and leakage requirements, no adjustments of the repair bases are required other than updates to the growth rates, cycle length, T_{hot} and/or steam pressure.

2.1.4 Tube Removal Requirements for ARC Applications

The following define the requirements for pulling tubes in association with implementation of the alternate repair criteria of this report for axial PWSCC at dented TSP intersections.

- Plants shall pull a tube prior to or subsequent to implementing the PWSCC ARC to support +Point sizing of the indication and crack morphology consistent with the PWSCC database.
- When a tube pull is required to support +Point sizing, the tube selected for removal shall have a high probability of leaking in order to contribute to the leak rate database. The requirements for a tube removal to enhance the likelihood of finding a leaker are given below. The tube pull may be performed in the cycle following ARC implementation or later as necessary to obtain an indication satisfying the requirements for removal. No TSP intersection above the potentially leaking intersection should be removed due to the increased likelihood of damage to the desired intersection.
- The destructive exam for the removed tube shall include, as a minimum, a leak test at operating temperature, a burst test, fractography to obtain the depth profile of the burst crack and a second major crack if present and one or more transverse metallographic sections (cross sections of the tube) to characterize secondary cracking if present. If the tube section removed to obtain the potential leaking section includes a lower TSP with a PWSCC indication, this second intersection shall also be destructively examined.

The leakage based requirements that must be satisfied to pull a tube are:

1. The indication is found to leak in an in situ test, or
2. The indication has a predicted leak rate ≥ 0.01 gpm at 50% probability from the Monte Carlo leak rate distribution performed as part of the condition monitoring assessment

2.1.5 Risk Assessment

The depth based repair limits are conservatively established to provide deterministic margins against burst under normal operation and accident conditions. Burst margins of $3\Delta P_{NO}$ are satisfied at 95% confidence levels for freespan indications and margins of $1.43\Delta P_{SLB}$ are satisfied at 95% confidence for indications dominantly within the TSP. The presence of the TSP would prevent rupture of indications within the TSP under severe accident conditions such as a Station Blackout. The average depth repair limit for freespan indications is about 40% which is consistent with the development basis for current Technical Specifications and deterministically satisfies the $3\Delta P_{NO}$ burst requirement with additional margin. It is therefore concluded that the proposed depth based repair limits provide the same risk for rupture under severe accident conditions as current Technical Specifications which have been considered to be acceptable.

The 40% maximum depth repair limit for freespan indications provides a very low likelihood of freespan leakage under design basis or severe accident conditions. The condition monitoring requirements for freespan indications limit leakage to 1 gpm summed over all freespan degradation mechanisms. Leakage for indications within the TSP is limited by the constraint of the TSP even under severe accident conditions and leakage behavior in a severe accident would be similar to that found acceptable for axial ODSCC at TSP intersections. Leakage tests for dented TSP intersections show very low or no leakage for throughwall indications inside the TSP. In addition, the constraint provided by the dented TSP intersection reduces leak rates even for throughwall indications extending outside the TSP. Even under severe accident conditions, the potential for significant leakage would be expected to be small and not significantly different than for other degradation mechanisms repaired to 40% depth limits. It is concluded that application of the depth based repair limits of this report result in negligible differences from current 40% repair limits relative to risk of a tube rupture or large leakage event under design basis or severe accident conditions.

2.1.6 NRC Reporting Requirements

In the event that condition monitoring requirements are not satisfied, the results shall be reported to the NRC in accordance with NEI 97-06 and time frames specified in 10 CFR 50.72/73. The results of the condition monitoring and operational assessments shall be reported to the NRC within 120 days following the return to power from the inservice inspection. The report shall include tabulations of indications found in the inspection and growth rate distributions for indications found in the inspection as well as the growth distributions used to establish the tube repair limits. Any corrective actions found to be necessary in the event that condition monitoring requirements are not met shall be identified in the report.

2.2 Summary

2.2.1 Pulled Tube and Laboratory Specimen Database

An extensive database of laboratory specimens with axial PWSCC at dented TSP intersections has been developed to supplement pulled tube data. The database for NDE qualification has been described in the NDE report of Reference 8-1 that supports this report.

2.2.2   NDE Qualification

Qualification of NDE techniques for detection and sizing of PWSCC in dented TSPs requires the assembly of a sample tube population with real or simulated cases of axial cracks. The specimen database described in this report constitutes a valid population on which to demonstrate the adequacy of candidate NDE techniques, specifically bobbin probe and +Point rotating probe analyses. Guidelines for the evaluation of bobbin and +Point data were developed by building on existing qualified techniques documented in the EPRI Performance demonstration database. The program employed had three phases: 1) Blind Analyses by selected senior NDE specialists; 2) Appendix H Peer Review and Qualification; and 3) NDE Performance Test. An NDE Performance Test Plan was performed using a bobbin and + Point detection PWSCC database for POD determination and for determination of +Point sizing NDE uncertainties. The NDE program through Appendix H qualification has been documented in Reference 8-1 and the results of the NDE Performance Test are documented in this report. The performance test preparation and scope includes the application of the NDE techniques in field equivalent procedures, preparation of a test population database from which POD and uncertainty parameters could be derived, a training program in which industry QDAs were given orientation and training specific for analysis of dented TSP/PWSCC ECT data and the testing of the field analysts against the PWSCC database.

2.2.3   Burst Correlation

The burst pressure of cracks extending partially through the tube wall is usually expressed as a function of the burst pressure of the uncracked portion of the tube. The analysis of partial depth cracks is practically based on consideration of an equivalent uniform depth rectangular shaped crack. Because of the irregular nature of the crack profiles, the burst pressure for shorter and deeper portions of the crack may be less than that for the overall crack. This means that a thin ligament could rupture and tearing could take place at the ends of the portion of the crack located in the section with the narrowest radial ligament without the rupture occurring over the entire crack length. Therefore, the evaluation of the burst pressure for an indication consists of estimating the burst pressure of every continuous subsection that can be formed from the individual, and contiguous, discrete crack profile sections. Westinghouse refers to the implementation of this approach as the "Weak Link" model. Other vendors refer to the same process as finding the structurally significant or structural minimum portion of the crack. For example, a crack may have an overall length of 0.9", but, because of the depth profile the central 0.5" may be predicted to have the lowest burst pressure. Hence, that section is the *weak link* in resisting burst. There are differences in the models used for the estimating the burst pressure of the discrete rectangular shapes, e.g., some expressions are aimed at estimating the burst pressure of the tube while others are aimed at estimating the pressure for tearing of the remaining ligament. The linear interpolation model has been found to correlate reasonably well with measured burst pressures, however, the associated error is greater, and tends to become non-conservative, for indications with the lowest burst pressures.

Regression analyses of measured burst pressures correlated with two theory-based lower bound models are developed in this report for predicting the burst pressure of SG tubes with axial indications. The results of the analysis are used to determine combinations of length and depth that would be expected to exhibit acceptable margin against burst during normal and accident operating conditions, thus satisfying the applicable performance criteria.

2.2.4   SLB Leakage Model

For a number of years, leak rates for free span cracks have been calculated using the CRACKFLO Code. This code calculates a crack opening area based on the primary to secondary pressure acting on a tube with a given crack length and material properties. Fluid mechanics relations are applied to the pressure opened crack and assumed crack surface geometry such as roughness and tortuosity of the crack flow path. Leak rates are a function of the primary pressure and temperature. Secondary pressure also affects the flow if choking does not occur.

The available crack leak rate data base has been used to correlate measure leak rates with CRACKFLO calculated values at steam line break conditions. This approach permits the development of statistical analyses of measured crack leak rates at SLB conditions with CRACKFLO Code predictions. The resulting correlation of measured leak rates with predictions is used to determine the leak rate and associated uncertainties for throughwall indications. Leak rates are based on throughwall crack lengths determined by applying the ANL ligament tearing model to the crack depth profiles obtained with appropriate adjustments for NDE uncertainties and growth.

3.0 PULLED TUBE AND LABORATORY SPECIMEN DATABASE

3.1 Introduction

The pulled tube and laboratory database supporting the NDE database for axial PWSCC at dented TSP intersections is described in the supporting NDE report of Reference 8-1. UT circumferential profile plots for the pulled tubes are provided in Reference 8-1 as well as length versus depth profile plots comparing the as reported NDE depths against destructive exam data. These data are summarized in this section for continuity of this report although graphics are not repeated in this report.

The pulled tube database for axially oriented PWSCC at dented TSPs is comprised of 3 tubes and 4 intersections from Diablo Canyon Unit 1, and one tube and one intersection from Sequoyah Unit 1.

Several sets of laboratory specimens were also prepared. It is necessary to employ laboratory created specimens due to the limited number of pulled tubes and the high cost of removing tubes from operating steam generators. The use of laboratory specimens permits a wider range of tube degradation to be prepared for testing and permits more extensive NDE examination. The laboratory samples were selected to be representative of the operational steam generator samples. To produce the desired samples, a combination of mechanical denting and an accelerated corrosion process was employed. Laboratory specimens were fabricated using mill annealed Alloy 600 tubing.

3.2 Pulled Tubes

Table 3-1 presents a summary of the flaw physical observations for each of the pulled tubes.

3.2.1 Sequoyah Unit 1

Tube R21C64 was removed from SG 3 of Sequoyah-1 in 1993 for an axial PWSCC indication at TSP 1. The bobbin dent voltage for this indication was about 13.9 volts. The maximum diametrical ovalization of 0.025" (0.893" major axis OD, 0.868" minor axis OD) based on the destructive examination occurred just above the top of the TSP. The RPC response (80 mil pancake coil) for this indication shows one well-defined axial indication and a small indication about 180° from the larger indication. Laboratory test found no leakage for this indication up to SLB conditions and the burst pressure was 8161 psi. As the flaw was pulled through the dented intersection, this action would have further opened the crack face during pulling and therefore would have increased the leakage potential, however, no leakage was observed during lab testing. The destructive examination identified the burst crack as 0.32" long, 58.6% average depth and 96% maximum depth. The bottom edge of the flaw was coincident with the top of the TSP and the flaw extended into the freespan region. No uncorroded ligaments were found in the burst crack. Two additional short (0.07" to 0.08" long) but deep axial flaws were located approximately in line with the burst flaw but were separated by non-degraded ligament sections. The maximum depth of the indications 180° from the burst crack was 50%. The ID cracks were found at the minor axes of the ovalized tube. Dimensional inspection of the tube in the lab following tube pull showed that the tube was deformed for approximately 4" above the TSP, indicating that the pulling operation affected the tube for a significant length as it was pulled through the intersection. This also lends credence to the physical composition of the TSP oxidation product as it retained significant homogeneity during the tube pulling operation. If the oxidation product were easily broken, the tube would not have been deformed above the TSP for such a significant length.

3.2.2   Diablo Canyon Unit 1

Three tubes with axial PWSCC indications at dented TSP intersections were removed from Diablo Canyon Unit 1 in 1995; R10C22, R12C32, and R21C43. R10C22 TSP 1H and 2H, R12C32 TSP 2H, and R21C43 TSP 1H and 2H were destructively examined in 1996. R12C32 TSP 1H was originally archived, but later destructively examined in 1998 as part of this program.

3.2.2.1   R10C22, TSP 1H

There was no reported dent voltage at this elevation. Field bobbin and +Point data was NDD. Destructive examination showed no SCC.

3.2.2.2   R10C22, TSP 2H

Field bobbin and +Point inspection produced indications at this elevation. The dent voltage was 2.4 volts. The field call using the +Point probe was a 0.31" long SAI. Reevaluated field +Point data shows a flaw length of 0.07" and 50% depth. Ovalization limits based on field UT data indicate a dent magnitude of 5.1 mils radial, at both quadrants of the minor axis. The axial cracks were seen at the minor axis of the ovalized tube which is typical of axial PWSCC at dented TSP intersections. Burst pressure was reported as 12437 psi. Destructive examination identified the burst crack as 0.122" long, 38% maximum depth, 23% average depth. The flaw extended from 0.358" below the top of the TSP to 0.480" below the top of the TSP, or slightly below the centerline of the TSP. No uncorroded ligaments were found in the burst crack. No secondary flaws were observed in the destructive examination. The non-degraded freespan burst pressure for the tube was 12554 psi. Based on the difference between the flawed and unflawed burst pressures of only 0.93%, it is judged that the degradation present had virtually no effect upon the burst pressure. R10C22 TSP 2H would represent a flaw near the lower bound of detectable indications based on the available pulled tube results.

3.2.2.3   R12C32 TSP 1H

Field bobbin and +Point inspection produced indications at this elevation. The dent voltage for this indication was 1.07 volts. The field call using the +Point probe was a 0.75" long SAI, which was reevaluated as 0.67" long and 74% deep. Ovalization limits based on field UT indicate a maximum denting extent of 7.3 mils, with a denting extent of 1.6 mils at the opposite quadrant of the minor axis. Elevated temperature laboratory leak testing was performed at 616° F, and pressure differentials up to 2555 psi. No leakage was reported. Burst pressure was reported at 7940 psi. Destructive examination identified the burst crack as 0.702" long, 97% maximum depth, 58% average depth. At the maximum depth region, >90% deep degradation was reported for approximately 0.10". As no leakage was reported during the leak testing, the non-degraded portions did not tear during the freespan leakage testing. The crack extended from the top edge of the TSP down to 0.702" below the top of the TSP. The macrocrack was comprised of 7 intergranular microcracks that were parallel and aligned in a narrow axial band. Of the 6 ligaments separating these 7 microcracks, 4 had ductile features, that is, they were determined to be torn during the burst test.

3.2.2.4   R21C43, TSP 1H

Field bobbin and +Point inspection produced indications at this elevation. The dent voltage was 3.9 volts. The field call using the +Point probe was a MAI, with crack lengths of 0.35" and 0.97". Reevaluated field +Point data shows flaw lengths of 0.0.30" and 0.98", with depths of 49% and 83%.

Ovalization limits based on field UT indicate a maximum denting extent of 5.9 mils, with a denting extent of 3.0 mils at the opposite quadrant of the minor axis. Burst pressure was reported as 7837 psi. Destructive examination of the burst crack indicated a macrocrack length of 0.991", 98% maximum depth, 50% average depth. The indication was > 85% deep only over about 0.15" length, and the maximum depth of 98% extended for 0.048". The second indication about 180° from the burst opening was found by destructive exam to be 0.277" long, 39.4% average depth and 50% maximum depth. Depth versus length profiles for these two indications were obtained from the destructive exam and are provided in Reference 8-1. Four uncorroded ligaments totaling 0.033" wide were found in the burst crack and two ligaments totaling 0.022" wide were found in the secondary crack. These ligaments are a small fraction of the corrosion lengths and adjustments to the average depths for the ligaments would be only about 1%. The burst crack corrosion extended from 0.14" above the TSP to 0.101" below the TSP.

The destructive examination measured a 4 mil radial dent. Field UT measured a radial dent of 5.9 mils at this intersection. In some tube pulls at dented intersections, the pulling operations distort the field dent due to the high pull forces through the dent and the hard magnetite may act to distort the original dent profile. Thus, it can only be concluded that the dent was likely between 4 and 6 mils. The PWSCC axial cracks at dented intersections tend to form at the minor axis of tubes ovalized by denting. This is shown by the UT inspection results which show the two axial indications about 180° apart at the minor axis of the tube. The two macrocracks were identified with no additional degradation at the TSP intersection.

3.2.3 PWSCC Crack Morphology for Pulled Tubes

The pulled tube results for axial PWSCC at dented TSP intersections show a common crack morphology. The indications form as one or two macrocracks about 180° apart. The microcracks forming the macrocrack are most commonly well aligned axially such that circumferential ledges or ligaments between microcracks forming the macrocrack are short. The narrow bands of microcracks indicate a process that is more stress driven than initiation of ODSCC which shows bands of microcrack initiation sites distributed extensively around the tube circumference. The indications are found at the minor axis of dent ovalized tubes where the ID hoop stresses are a maximum. Only two of the four macrocracks depth profiled were found to have remaining uncorroded ligaments and these ligaments were a small fraction of the macrocrack length.

In summary, the crack morphology for PWSCC at dented intersections is that of one or two macrocracks well aligned axially with only a few uncorroded ligaments and little or no other ID axial cracking at the intersection. This relatively simple morphology is conducive to obtaining good accuracy in NDE sizing of these indications.

3.3 Laboratory Specimens – Mechanically Dented

An essential part of this program was the design and preparation of the desired number of samples in the required configuration to replicate the defect conditions historically observed in degraded, dented tubes removed from operational steam generators. These samples were key to the program because not only were they the source of the defects used in the eddy current probe assessment during the NDE data acquisition phase, but they were subjected to subsequent mechanical testing to establish the burst characteristics of the defect including final fractographic examination of the fracture face.

To assure that the sample configuration replicated steam generator conditions for eddy current testing, it was necessary to include a tube support plate simulant on all of the test samples. Mill annealed Alloy

600 tubing and carbon steel TSP simulant collars were utilized. The TSP was also used during the burst testing of some of these samples to restrain bursting of that part of the crack under the support plate. Therefore the TSP, while specified to be the design thickness of the support plate, was of greater thickness to prevent deformation of the TSP during the applied burst pressure. It is necessary to employ laboratory created specimens due to the limited number of pulled tubes and the high cost of removing tubes from operating steam generators. The use of laboratory specimens permits a wider range of tube degradation to be prepared for testing and permits more extensive NDE examination. The laboratory samples were selected to be representative of the operational steam generator samples. To produce the desired samples, a combination of mechanical denting and an accelerated corrosion process was employed.

The key feature of the samples is the inclusion of axially oriented, ID initiated defects within the dented portion of the tube. While absolute control of the length and depth of the crack produced during the defect generation phase was not possible, the range of sizes finally obtained bound (lengths of 0.13 to 2.6 inches, average depths of 30% to 97%) those typically seen in operating steam generators. This assured that the results obtained and the conclusions reached as a result of the program were directly applicable to operational environments. Additional emphasis was placed on obtaining large PWSCC cracks challenging structural integrity to support NDE uncertainty assessments of potentially limiting indications.

Two sets of mechanically dented laboratory specimens were prepared; a set produced in 1996 for which a prefix P is applied to the sample number, and a second set produced in 1997 which used set screws to produce the denting force.

3.3.1 1996 Dented Laboratory Specimens

A total of 22 specimens were produced and exposed to the cracking environment, however, only seven dented TSP samples developed axial PWSCC. As a consequence of the dent geometry produced during preparation of the samples, each sample tube contained at least 2 defects approximately 180° apart located on the minor axis of the dent plane. Tube sections were approximately 15" long and the sample identification was Vibrotooled on one end. A short 0° orientation line was Vibrotooled next to the identification to preserve sample orientation throughout the testing. Details of the material used in the preparation of the samples including material certifications, and mechanical test data are contained in Appendix F of Reference 8-1 for information.

3.3.1.1 Preparation of 1996 Dented Laboratory Specimens

The geometric guidelines for the dents employed in this program were based on a series of dent profiles obtained from UT inspection of dented TSP indications in operating steam generators. UT profilometry provides the quantified shape of the dent and the location of the crack within the dent. As seen from the figures provided in Reference 8-1, ovalized tubes with one minor axis flatter than the other, or slightly indented are typical of the field experience with ID cracks.

The starting dents in the sample tubes were created using two mechanical processes developed specifically for this program. While corrosion induced dents are desirable for prototypicality, the laboratory techniques typically associated with producing the desired dent profiles involve heated crevice testing, require extensive time periods to obtain dented specimens, and lead to dent results that are not predictable. To produce samples in the large quantities to support NDE qualification, it is necessary to mechanically dent the tubes. The dent shape is similar to that obtained from the field UT

data.

The approach used to produce realistic flaws consisted of applying a predefined state of stress on a prototypic geometry of Alloy 600 steam generator tubing material with an accelerated aqueous corrosion environment that produced specifically desired flaws. The purpose of pre-stressing is to aid local initiation and axial growth of cracks. The stresses encountered in service were duplicated for both the active pressure stresses and the deformation-related residual stresses.

Twenty two specimens were prepared and exposed to the steam environment. For 16 specimens, the residual stress was introduced by mild deformation between a simulated split tube support plate. The deformation was introduced in two directions 90 degrees apart. The first deformation ovalized the tubes in compression just past the yield point (OD ~0.013 inch). A second deformation operation was then introduced 90 degrees away to obtain ovalities typical of field experience. The second deformation reduced ovalities from the first deformation that exceeded the desired values to simulate the field experience. The residual stresses remained highest at the initial deformation and the major cracks occurred at these locations. The result should be two locations within the deformed region with residual stresses approaching yield stresses on the ID 180 degrees apart.

Some of the samples were pre-stressed prior to autoclave exposure by compressing the sample diameter at the appropriate axial location between two flat steel lands. SCC was impeded outside the zones of desired cracking by peening with glass beads.

The tubes were then placed in the accelerated high temperature steam environment with sufficiently aggressive environmental conditions to produce SCC typically in a 25 to 500 hour exposure time depending on the tubing conditions and other experimental factors. Two stainless steel autoclaves were prepared to accommodate testing batches of six samples at 750°F steam raised from water containing sodium salts. This steam was mixed with hydrogen. Most specimens were tested with active pressure stressing to promote the SCC by pressurizing the ID of the tubes with the doped steam + hydrogen at 750°F and 3000 psig environment and maintaining the OD environment at 1500 psig pure steam without hydrogen. TSP collars were not applied to the specimens during the cracking phase of the program.

A through-wall crack is signaled by loss of differential pressure. The test is shut down and the specimens leak checked to determine which specimen is leaking. All of the specimens in the test assembly are inspected by NDE to determine which ones, if any, meet the specified crack morphologies. Specimens removed from test are replaced by fresh specimens.

3.3.1.2 Dent Profiles

In order to measure the degree of deformation in a length of steam generator tubing, laser profilometry was performed on a number of specimens. Laser profilometry is based on a shadow method. The cylindrical object is placed in front of a rastered laser beam and this blocks the path to the beam receptor. The diameter of the blocked beam is measured as well as an edge measurement. This method can be used directly to analyze objects where the radial cuts are convex. A geometrical construction is needed using a series of diameter and edge measurements to calculate more complex shapes.

Laser profilometry measurements can be made either on the OD surface of a tube or on a replica mold pulled from the tube ID. Most of the measurements conducted for this program, were conducted directly on the OD surface of the tubes. The region where the tube was deformed was rotated and translated

through the laser beam using a rotation and translation stepping motor positioning system. Diameter and edge measurements were made using a laser micrometer with a resolution of 0.00001 inch. Diameter and edge measurements were taken typically every 15 degrees and every 0.05 inch over the ovalized region or the region where SCC cracks were located.

3.3.1.3 Simulation of Packed TSP Crevices

To enhance the protypicality of the samples for the NDE probe evaluation phase and the burst testing, TSP collars were added to the samples. As an additional step in trying to achieve a representative TSP sample, the tube/TSP gap was packed with a magnetite material representative of the material composition found in steam generators.

The packing of the tube/TSP gap is accomplished in the following manner. The ID of the TSP collar simulants were machined to the maximum tolerance dimension of 0.900 inches to provide maximum clearance between the tube OD and the TSP ID. The TSP collar was positioned on the tube on a case by case basis as a function of a review of the defect position. The collar was held in position using an O-Ring and Teflon tape. With the collar positioned, the gap between the tube and TSP collar was vibration filled with a mixture of magnetite, $CuSO_4$, and $ZnSO_4$ in an alkaline silicate solution. Comparative weight measurements of the sample before packing and as the packing progresses verifies that the crevice has been filled during the vibration process. As a final step following the packing of the sample, the packed sample is placed in a protective atmosphere furnace and the sample baked to consolidate the crevice material.

Table 3-2 provides a summary of the crack lengths outside of the TSP collar, as the samples were presented for the NDE phase of the program. It should be noted that with the exception of sample number P13 where the tube was centered within the collar, all of the collars were deliberately offset in specific directions to vary the crack lengths outside the TSP and thereby vary the burst pressure.

3.3.1.4 NDE Data Collection

To provide the desired database, the laboratory dented samples were subjected to extensive NDE examination during the course of this program. The data was acquired using a TC-6700 eddy current system coupled with several different types of probes through a 50 foot length of cable. Data was collected for the following coils: two mid-range + point, mag biased + point, high frequency + point, gimbaled + point, 80mil high frequency pancake, and 115 mil pancake. The length of cable was utilized to maintain compliance with the requirements of Appendix H of the EPRI ISI guidelines during the data acquisition phase.

In addition to the utilization of a variety of Eddy Current probes, the data was acquired using both ANSER and EDDYNET software to obtain a broad data base and facilitate evaluation of the sensitivity of NDE sizing uncertainties to the software system. NDE analysis results are given in Section 4. Additional NDE analyses comparing results for the different coils are given in Reference 8-4.

3.3.1.5 Burst Test Procedure and Results

Procedure

Following the NDE data acquisition phase of the project, the samples were subjected to burst testing. All burst testing under this program was conducted with procedures for burst testing written to be in compliance with EPRI guidelines on leak and burst testing. As noted in Table 3-2, some of the samples were tested with and some of the samples were tested without the simulated tube support plate in place. Also noted in Table 3-2, in some instances, the TSP was displaced axially along the tube from its original position when the defects were generated to expose more or less of the predefined limiting crack based on NDE analysis. The object of repositioning the TSP prior to burst testing was to provide a more varied set of burst test conditions thereby providing a broader data base applicability. In addition to displacing the TSP axially, the TSPs were also offset radially to place the maximum amount of packing material under the longitudinal axis of what was considered to be the most limiting defect.

The burst testing operation follows a number of discrete steps to assure consistency of results. The sample is carefully examined to locate the most limiting defect based on the NDE evaluation data. The location of the top of the TSP is scribed on the tube to assure the establishment of a reference point which can be used to relate the burst test results with the comparable NDE data.

The burst testing apparatus incorporates a pressure intensifier to translate the hydraulic oil pressure at 2000 psi (maximum) to water pressure at 30,000 psi (maximum). The unit is operated under pressure control mode to maintain a sample pressurization rate of 2000 psi/sec (water) within the elastic range.

Precautions must be taken with the samples in their preparation to assure consistent test results. Each sample is lined full length with Tygon tubing prior to burst testing. Additionally, a shim patch is lubricated and placed between the Tygon tubing OD surface and the tube ID surface in the area of the limiting defect. The shim is fabricated from 0.006 inch brass stock and is cut to be approximately 0.25 inches larger than the limiting defect in all directions. The sample is then capped off using Swagelok fittings and attached to the pressure source. The sample undergoes a prefill wherein the fluid is pressurized to approximately 300 psi and bled down to assure that all air is removed from the system prior to the commencement of the test.

In addition to the burst test data, representative samples of the tube material used to fabricate the test pieces are subjected to tensile testing to obtain the yield and tensile properties of the samples. This information is used in conjunction with other test data to calculate the burst pressure of the degraded tube. Corrosion specimens P7 to P12 were fabricated from heat NX-8161. Specimen LC-1A, also identified as specimen P13 in this report, was fabricated from heat NX-3330-19B.

Test Results

The results of the burst testing are developed graphically in the form of pressure versus time plots showing the maximum pressure at failure. Additionally, post burst test photographs of each sample showing the condition of the tube following rupture were obtained. Pressure versus time plots were obtained for all of the samples during burst testing. Table 3-2 summarizes the burst test data obtained for the samples used in this program.

3.3.1.6   Destructive Examination Results

Following burst testing, the burst defect as well as other major defects in the sample as defined through review of the NDE results are subjected to a detailed fractographic examination. In the fractographic evaluation, the faces of the burst defect as well as the faces of the major defects at other locations in the sample are viewed to locate key features which influence the samples performance during burst testing. Tabulations of the depth profiles from the fractographic examinations are given in Reference 8-1. The examination provides the overall configuration of the defect by indicating the length versus depth profile from a specific reference point to the crack tip. The initial reference point is based on the location of the TSP either during the burst test or placement prior to removal in those cases where the sample is burst without a support plate.

Using optical or SEM microscopy, the length vs. depth profile of the defect, and the ligaments within the crack are identified. Estimates are made with regard to the orientation of the ligaments as well as the length and width from which ligament areas can be calculated. The area of the crack is then adjusted to account for the effect of the ligaments on the average crack depth.

3.3.1.7   PWSCC Crack Morphology

As described above, the laboratory specimens were prepared by mechanically denting the tubes. This process results in ovalized tubes with minor diameters about 180° apart. The resulting SCC cracks are typically confined to two bands with the cracks confined to the deformation region. When the stressing fixture remains in place during the testing to produce cracking, the cracks can grow long and will typically branch after they reach a sufficient length. The RPC inspection results for these specimens show one indication or two axial PWSCC indications approximately 180° apart. This section describes the crack morphology for the laboratory specimens and compares with that found for the pulled tubes as described in Section 3.2.

Laboratory specimens P7 through P12 were found to have axial indications formed as narrow bands of microcracks. There are essentially no microcracks around the tube except immediately adjacent to the dominant macrocrack. Non-corroded ligaments were sized and found to have a small area compared to the crack area. This crack morphology is typical of specimens P7 to P12 and is essentially the same as found for the pulled tubes described in Section 3.2.

The cracking in specimen P13 (also identified as specimen LC1A) is different from that found in the other specimens and the pulled tubes. The cracking is present as a large array of short, generally isolated shallow cracks present in about 4 bands. Two bands of cracks about 180° apart were located above the TSP and another two bands were located below the TSP. All cracking was located outside the region of the tubing where the deformation was introduced. Laser profilometry revealed that the maximum permanent deformation was located within the TSP region but no cracking occurring at the largest deformation. This unusual crack morphology for ID indications is most likely due to the crack initiation being more "corrosion" than "stress" driven. A large number of crack initiation events occurred over the six months of testing. However, the residual plus active stress was apparently insufficient to cause those cracks to link up and propagate. Additional detail on the morphology for this specimen is given in Reference 8-2. It is concluded that the crack morphology for laboratory specimens P7 to P12 is common to that for indications pulled from operating steam generators for PWSCC at dented TSP intersections. These laboratory specimens are thus appropriate simulations of pulled tubes

for the NDE sizing qualification objective of this report. Laboratory specimen P13 has a distinctly different crack morphology and is not an appropriate simulation of pulled tube morphology.

3.3.2 1997 Mechanically Dented Specimens

The largest laboratory specimen data base was developed from mechanically deformed samples which used a localized deformation process. In these samples, 18" long, mill annealed Alloy 600 tube sections had 5 TSP simulant collars positioned at 3" center to center spacings on the tube. The collars at the ends were located at 3" from the end of the tube to the center of the collars. A screw thread was machined into the TSP collar at the midpoint of the collar, oriented perpendicular to the axis of the tube, prior to assembly. Varying sized screw threads from a #6 (0.112" major thread diameter) to a 5/16" thread diameter were applied through the thickness of the TSP simulant collars. Once located on the tube, a set screw was inserted and by application of varying torques, varying denting levels were produced in the tubes. Denting levels were checked by bobbin to produce dent voltages of 1.5 to 3 volts. UT profilometry traces for several of these samples are provided in Reference 8-1. The UT profilometry data for these tubes shows that less ovalization, and more localized denting patterns developed for the smaller set screw samples. For all samples in which ovalization data was acquired, the localized ovalization (relative to nominal) due to the set screw interaction exceeded the ovalization (relative to nominal) at 180° from the set screw. For the samples which used a smaller diameter set screw, the localized ovalization at the screw was often several times larger than the opposite side ovalization. For the samples which used larger diameter sized set screws, the difference between the ovalizations was reduced considerably, with the local ovalization at the screw still greater than the opposite side. More significant ovalization patterns were developed in the samples using larger sized set screws. Following denting, the crevices were packed as described above, and the samples subjected to the high temperature doped steam environment on the ID to initiate PWSCC flaws. A detailed breakdown of the screw thread sizes, applied torques, and localized dent levels for each of the specimens is provided in Table 3-3.

Essentially all of the set screw samples developed at least one crack. For the samples that developed only 1 crack, the flaw was located azimuthally within the bounds of the set screw location. Approximately 40% of this group of samples developed a second flaw, roughly 180° from the set screw, at the minor axis of the ovalized shape. Of the samples which developed two flaws located approximately 180° apart, the set screw diameters were 0.19" (#10-32), 0.25" and 0.31" (5/16).

Flaw morphologies of the samples is similar to the pulled tubes except that the band width containing the flaws is somewhat more extensive than the pulled tubes. The Set B samples typically contain more non-degraded ligaments compared to the pulled tubes.

The 1997 specimens were processed in the same manner as the 1996 specimens. The discussions of Sections 3.4.1.2 to 3.4.1.6 relative to dent profiles, simulation of packed TSP crevices, NDE data collection, burst testing and destructive examination also apply to the 1997 specimens. In addition, nine of the 1997 specimens were leak tested at room temperature. The destructive examination results, burst pressures and leak test results are given in Table 3-3. Tabulations of the destructive examination depth profiles for these specimens are given in Reference 8-1.

3.4   Burst Test Results

The pulled tubes and laboratory specimens were burst tested to develop a database in support of the burst pressure correlation described in Section 5. The burst pressures for the pulled tubes are given in Table 3-1. Tables 3-2 and 3-3 provide the burst pressures for the mechanically dented laboratory specimens.

3.5   Prototypicality of Laboratory Dented PWSCC Specimens for Simulating Field Data

The laboratory specimen NDE data and crack morphology were reviewed to ensure that the signals observed were consistent with flaw signals observed in the field and that the crack morphology was similar to that found for the pulled tubes. This comparison of the laboratory specimen and pulled tube data is documented in the NDE report of Reference 8-1. It was concluded that the laboratory specimens are very good simulations of the field indications and adequate for NDE, leak and burst testing.

3.6   Applications of Pulled Tube and Laboratory Specimens

Table 3-4 provides a summary of the pulled tube and laboratory specimen data including the application of each specimen to evaluations in this report. Possible applications include burst correlation, NDE Performance Test or Appendix H qualification for bobbin and/or +Point detection and/or +Point sizing, and NDE analyst training for bobbin or +Point. Notes 7 to 9 identify invalid burst pressure data per the data exclusion Criterion 1a of Appendix C. Invalid tests include specimens that burst away from the flaw, and pressurized second indications that were cut from the tube after burst testing to open the larger crack and then retested. In addition, the reported burst pressures of >11 ksi (near that of undegraded tubing) for specimens 9-5H and 10-3H would be physically impossible for cracks of the reported size, and these indications are excluded from the burst correlation. Specimen 10-3H also burst at a welded connection away from the crack indication. Additional evaluations for selection of burst pressure data for the burst pressure correlation are described in Section 5. None of the pulled tubes were found to leak and only one of the laboratory specimens (11-3H, Crack 1) was found to leak. This data point was not included in the leak rate correlation of Section 6 as the correlation development was completed prior to the availability of the test results.

Some mechanically dented specimens were cracked in doped steam and NDE data were obtained, but no destructive exam was performed. In general, these specimens had deep depths that duplicated other specimens or no detectable degradation. These specimens were available for analyst training where expert analysis results can be used for comparisons with the trainee's results. Specimens included in this category of training specimens include: 1-1, 1-2, 1-5, 2-2, 3-1, 3-2, 3-5, 4-1, 4-2, 4-3, 4-5, 5-2, 5-3, 5-4, 5-5, 7-2, 7-4, 7-5, 8-4, 8-5, 10-1, 10-2, 10-5, 11-1, 11-5, 12-1, 12-5, 13-1,13-2, 13-4 and 13-5.

Table 3-1
Dented TSP Pulled Tube Burst Flaw Geometries

Tube	Total Macrocrack Length	Length Outside TSP	Maximum Depth	Average Depth	Bobbin Dent Voltage	Ovalization (inch)	Burst Pressure (psi)	Flow Strength (Ksi)
R21C64-1H	0.32"	0.32"	96%	59%	13.9	0.025"	8161	99.65
R10C22-2H	0.122"	0"	38%	23%	2.4	0.008"	12437	85.63
R12C32-1H	0.702"	0"	97%	58%	1.07	0.007" (by UT)	7940	90.11
R21C43-1H	0.991"	0.14" above 0.101"below	98%	50%	3.9	0.016" (by UT)	7837	101.5
Crack 2	0.277"	0"	50%	39.4%				

Table 3-2
Positioning of Collars on 1996 Dented TSP Samples and Burst Pressure Information

Sample	Burst Pressure (psi)	Length of Crack Outside of TSP (inch)	Flow Stress (Ksi)	Collar Radial Offset	Burst Test Configuration	
					with TSP	w/o TSP
P7	2700	0.87	80.6	N/A		X
P8	2720	0.96	80.6	.025 @ 0°	X	
P9	4150	0.87	80.6	.025 @ 180°	X	
P10	2740	0.97	80.6	.025 @ 180°	X	
P11	3250	0.69	80.6	N/A		X
P12	3220	1.29	80.6	N/A		X
P13	8360		72.35	N/A		X

Sample	Set Screw Size	Torque (in-lb)	OD	ID	Wall	Length (inch)	Local Max. Depth	Avg. Depth Lig. Corr.	Burst Pressure (psi)	Leak Rate (gpm) ΔP = 1610 psi	ΔP = 2560 psi	ΔP = 2840 psi
R10 C22-1H										not tested	not tested	not tested
R12 C32-1H										0	0	0
R12 C32-2H							Data given in Table 3-1.			not tested	not tested	not tested
R21 C43-1H										not tested	not tested	not tested
R21 C43-2H										not tested	not tested	not tested
R21 C64-1H										0	0	0
1-3	6-32	10	0.8711	0.7670	0.0521	0.660	56%	39.4%	8900 (5)	0	0	0
1-4	6-32	10	0.8711	0.7670	0.0521	0.708	68%	36.7%	9230 (4)			
2-1	10-32	18	0.8691	0.7660	0.0516	0.876	48%	21.7%	11025 (5)			
2-3	10-32	14	0.8691	0.7660	0.0516	0.472	32%	15.2%	>11500 (1)			
2-4	10-32	15	0.8691	0.7660	0.0516	0.580	53%	29.0%	11300 (5)			
2-5	10-32	15	0.8691	0.7660	0.0516	0.860	41%	18.3%	10970 (4)			
3-3	1/4	16	0.8698	0.7672	0.0513	0.188	35%	23.4%	>12425 (1)			
3-4	1/4	16	0.8693	0.7672	0.0511	0.183	16%	6.4%	12400 (5)			
4-4	5/16	29	0.8698	0.7658	0.0520	0.551	28%	9.6%	>11300 (1,5)			
5-1	5/16	30	0.8720	0.7640	0.0540	0.294	42%		>11300 (1,5)			
6-1	5/16	27	0.8723	0.7660	0.0532	0.772	89%	60.5%	7100 (4)	0	0	0
6-2	5/16	29	0.8723	0.7660	0.0532	0.692	80%	59.1%	6500 (5)	0	0	0
6-3	1/4	17	0.8723	0.7660	0.0532	0.588	74%	56.1%	8500 (5)	0	0	0
6-4	10-32	15	0.8723	0.7660	0.0532	0.416	75%	49.4%	9380 (4)			
6-5	10-32	17	0.8723	0.7660	0.0532	0.604	85%	54.1%	9100 (5)			
7-1	5/26	38	0.8725	0.7661	0.0532	0.598	39%	20.1%	11700 (5)			
7-3	1/4	24	0.8730	0.7661	0.0535	0.560	45%	25.0%	11800 (4)			
8-1	10-32	14	0.8724	0.7684	0.0520	0.420	58%	40.7%	10560 (4)			
8-2	1/4	16	0.8724	0.7684	0.0520	0.380	55%	37.1%	10900 (4)			
8-3	1/4	16	0.8724	0.7684	0.0520	0.460	50%	31.8%	11060 (4)			
9-1	1/4	15	0.8722	0.7672	0.0525	0.424	49%	30.9%	11220 (4)			
9-2	14	15	0.8722	0.7672	0.0525	1.010	97%	67.4%	3940 (4)			

Table 3-3. Pulled Tube and Laboratory Specimen Burst Pressure and Leak Rate Data

Sample	Set Screw Size	Torque (in-lb)	OD	ID	Wall	Length (inch)	Local Max. Depth	Avg. Depth Lig. Corr.	Burst Pressure (psi)	Leak Rate (gpm)		
										ΔP = 1610 psi	ΔP = 2560 psi	ΔP = 2840 psi
9-3 Crack 1	1/4	16	0.8722	0.7672	0.0525	0.850	89%	60.9%	5700 (5)	0	0	0
9-3 Crack 2			0.8722	0.7672	0.0525	0.717	66%	40.8%	8600 (5,7)	0	0	0
9-4 Crack 1	1/4	15	0.8722	0.7672	0.0525	0.840	82%	56.4%	7100 (4)	0	0	0
9-4 Crack 2			0.8722	0.7672	0.0525	0.328	36%		>11300 (1,5,7)	0	0	0
9-5 Crack 1	1/4	14	0.8722	0.7672	0.0525	0.632	86%	57.5%	11400(5)	0	0	0
9-5 Crack 2			0.8722	0.7672	0.0525	0.120	38%	26.8%	>11300 (1,5,6)	0	0	0
10-3 Crack 1	10-32	15	0.8725	0.7672	0.0525	0.760	99.4%	73.2%	>11300(1,5)			
10-3 Crack 2			0.8725	0.7662	0.0532	0.490	48%	31.7%	10400 (2,6)			
10-4	10-32	14	0.8725	0.7662	0.0531	0.698	89%	63.6%	7400 (5)	0	0	0
11-2	5/16	25	0.8724	0.7668	0.0528	0.837	99%	81.4%	4470 (4)			
11-3 Crack 1	5/16	27	0.8724	0.7668	0.0528	1.072	99.5%	68.4%	4900 (5)	0.00046	2.14	2.25
11-3 Crack 2			0.8724	0.7668	0.0528	0.563	55%	38.2%	>11300 (1,5,6)			
11-4	5/16	25	0.8724	0.7668	0.0528	1.009	98%	68.7%	4160 (4)			
12-2	1/4	18	0.8723	0.7662	0.0531	0.242	34%	20.8%	>10700 (1,3)			
12-3	10-32	14	0.8723	0.7662	0.0531	0.129	23%	16.0%	13000 (5)			
12-4	5/16	24	0.8723	0.7662	0.0531	0.360	33%	20.2%	13170 (4)			
13-3	5/16	26				0.336	46%	27.3%	10930 (4)			

Notes:
1. Invalid burst test. Sample burst in extension tube away from flaw.
2. Burst tested without use of bladder or foil.
3. Weld tube extension failed at 10700 psi. Sample retested, flaw burst at 7000 psi on second attempt. Flaw did not burst on first attempt at 10700 psi, therefore, 10700 psi recorded as lower bound burst pressure.
4. Burst using bladder and 0.006" thick lubricated brass shim
5. Burst using bladder only, in situ testing equipment at Waltz Mill
6. Invalid burst test. Specimen pressurized to open second crack for destructive exam after crack one was burst. Specimen was cut and welded into another tube.

For set screw samples, YS = 61 ksi, US = 103 Ksi, FS = 82 Ksi

Table 3-4. Application of Pulled Tube and Laboratory Specimen Test Results												
			NDE Performance Test			App. H Qualification		Destructive Exam Results				
Sample	Burst Corr.	Dent Volts[3]	Bobbin Det.	+Point Det.	+Point Sizing	Bobbin Det.	+Point Det. & Sizing	Length (inch)	Local Max. Depth	Avg. Depth Lig. Corr.	Burst Pressure (psi)	Leak Rate (gpm) ΔP = 2560 psi
R10 C22-2H[1]	NO	2.4	YES	YES	YES	YES	YES	0.122	38.0%	23.2%	12437	not tested
R12 C32-1H[1]	YES	1.07	YES	YES	YES	YES	YES	0.702	97%	57.5%	7940	0
R21 C43-1H Crack 1[1]	YES	3.89	YES	YES	YES	YES	YES	0.991	98%	49.2%	7837	not tested
R21 C43 –1H Crack 2[1]	NA	3.9	NA	YES	YES	NO	YES	0.277	50%	39.6%	not tested	not tested
R21 C64-1H	YES	13.9	Training	NO	Training	YES	NO	0.320	96%	60.4%	8161	0
1-3	YES	2.63	YES	YES	YES	YES	NO	0.660	56%	39.4%	8900	0
1-4	YES	2.32	YES	YES	YES	YES	YES	0.708	68%	36.7%	9230	not tested
2-1	YES	3.87	YES	YES	YES	YES	NO	0.876	48%	21.8%	11025	not tested
2-3	NO	2.21	YES	YES	YES	YES	YES	0.472	32%	15.2%	Note 8	not tested
2-4	YES	1.84	YES	YES	YES	YES	NO	0.580	53%	29.0%	11300	not tested
2-5	YES	2.32	YES	YES	YES	YES	NO	0.860	41%	18.3%	10970	not tested
3-3	NO	5.68	YES	YES	YES	NO	NO	0.188	35%	23.4%	Note 8	not tested
3-4	YES	4.62	YES	YES	YES	NO	NO	0.183	16%	6.4%	12400	not tested
4-4	NO	5.14	YES	YES	YES	NO	NO	0.551	28%	9.6%	Note 8	not tested
5-1	NO	2.42	YES	YES	Training	NO	NO	0.294	42%	20-30%[6]	Note 8	not tested
6-1	YES	2.03	YES	YES	YES	YES	NO	0.772	89%	60.5%	7100	0
6-2	YES	1.89	YES	YES	YES	YES	YES	0.692	80%	59.1%	6500	0
6-3	YES	2.24	YES	YES	YES	YES	YES	0.588	74%	56.1%	8500	0
6-4	YES	2.18	YES	YES	YES	YES	YES	0.416	75%	49.4%	9380	not tested
6-5	YES	1.98	YES	YES	YES	YES	NO	0.604	85%	54.1%	9100	not tested
7-1	YES	5.03	YES	YES	YES	YES	YES	0.598	39%	20.1%	11700	not tested
7-3	YES	4.28	YES	YES	YES	YES	YES	0.560	45%	25.0%	11800	not tested
8-1	YES	1.42	YES	YES	YES	YES	YES	0.420	58%	40.7%	10560	not tested
8-2	YES	1.52	YES	YES	YES	YES	NO	0.380	55%	37.1%	10900	not tested
8-3	YES	1.61	YES	YES	YES	YES	YES	0.460	50%	31.8%	11060	not tested

Sample	Burst Corr.	Dent Volts[3]	NDE Performance Test			App. H Qualification		Destructive Exam Results				
			Bobbin Det.	+Point Det.	+Point Sizing	Bobbin Det.	+Point Det. & Sizing	Length (inch)	Local Max. Depth	Avg. Depth Lig. Corr.	Burst Pressure (psi)	Leak Rate (gpm) $\Delta P = 2560$ psi
9-1 Crack 1	YES	1.34	YES	YES	Training	YES	NO	0.424	49%	30.9%	11220	not tested
9-1 Crack 2	NA	1.34	NA	YES	Training	YES	NO	Not Deter-mined	25.4%	25.4	not tested	not tested
9-2 Crack 1	YES	1.24	YES	YES	YES	YES	NO	1.010	97%	67.4%	3940	not tested
9-2 Crack 2	NA	1.24	NA	YES	YES	YES	YES	0.786	61.5%	35.6%	not tested	not tested
9-3 Crack 1	YES	1.23	YES	YES	YES	YES	NO	0.850	89%	60.9%	5700	0
9-3 Crack 2	NO	1.23	NA	YES	YES	YES	NO	0.717	66%	40.8%	Note 7	0
9-4 Crack 1	YES	1.21	YES	YES	Training	YES	NO	0.840	82%	56.4%	7100	0
9-4 Crack 2	NO	1.21	NA	YES	Training	NO	NO	0.328	36%	23.14[6]	Note 7	0
9-5 Crack 1	NA	1.41	YES	YES	YES	YES	NO	0.632	86%	57.5%	Note 9	0
9-5 Crack 2	NO	1.41	NA	YES	YES	NO	NO	0.120	38%	26.8%	Note 7	0
10-3 Crack 1	NA	1.28	YES	YES	YES	YES	NO	0.760	99.4%	73.2%	Note 9	not tested
10-3 Crack 2	NO	1.28	NA	YES	YES	NO	NO	0.490	48%	31.7%	Note 7	not tested
10-4	YES	1.70	YES	YES	YES	YES	NO	0.698	89%	63.6%	7400	0
11-2 Crack 1	YES	1.49	YES	YES	YES	YES	NO	0.837	99%	81.4%	4470	not tested
11-2 Crack 2	NA	1.49	NA	YES	YES	YES	YES	0.160	43%	32.8%	not tested	not tested
11-3 Crack 1	YES	1.34	YES	YES	YES	YES	NO	1.072	99.5%	68.4%	4900	2.14
11-3 Crack 2	NO	1.34	NA	YES[2]	YES	YES	NO	0.563	55%	38.2%	Note 7	not tested
11-4 Crack 1	YES	1.95	YES	YES	YES	YES	NO	1.009	98%	68.7%	4160	not tested
11-4 Crack 2	NA	1.95	NA	YES	YES	YES	NO	0.790	46%	36.6%	not tested	not tested
12-2	NO	1.38	YES	YES	YES	NO	NO	0.242	34%	20.8%	Note 8	not tested
12-3	YES	1.22	YES	YES	YES	YES	YES	0.129	23%	16.0%	13000	not tested
12-4	YES	1.39	YES	YES	YES	YES	YES	0.360	33%	20.2%	13170	not tested
13-3	YES	1.19	YES	YES	YES	YES	YES	0.336	46%	27.3%	10930	not tested
P7 Crack 1	YES	NM[4]	YES	YES	YES	NO	YES	0.870	100%	94.3%	2700	not tested
P7 Crack 2	NA		NA	YES	YES	NO	YES	0.658	100%	82.5%	not tested	not tested
P8 Crack 1	NO	NM	YES	YES	YES	NO	YES	2.664	100%	84.8%	2720[5]	not tested
P8 Crack 2	NA		NA	YES	YES	NO	YES	2.452	100%	79.4%	not tested	not tested
P9 Crack 1	NO	12.82	YES	YES	YES	NO	YES	1.868	100%	75.3%	4150[5]	not tested

Table 3-4. Application of Pulled Tube and Laboratory Specimen Test Results

Sample	Burst Corr.	Dent Volts[3]	NDE Performance Test			App. H Qualification		Destructive Exam Results				
			Bobbin Det.	+Point Det.	+Point Sizing	Bobbin Det.	+Point Det. & Sizing	Length (inch)	Local Max. Depth	Avg. Depth Lig. Corr.	Burst Pressure (psi)	Leak Rate (gpm) ΔP = 2560 psi
P9 Crack 2	NA		NA	YES	YES	NO	YES	1.589	100%	86.6%	not tested	not tested
P10 Crack 1	NO	NM	YES	YES	YES	NO	YES	2.563	100%	88.7%	2740[5]	not tested
P10 Crack 2	NA		NA	YES	YES	NO	YES	2.146	100%	69.0%	not tested	not tested
P11 Crack 1	YES	NM	YES	YES	YES	NO	YES	0.675	100%	95.6%	3250	not tested
P11 Crack 2	NA		NA	YES	YES	NO	YES	0.568	95.8%	74.6%	not tested	not tested
P12 Crack 1	YES	NM	Training	Training	Training	NO	YES	1.286	100%	77.3%	3220	not tested
P12 Crack 2	NA		NA	Training	Training	NO	YES	0.548	82.8%	29.9%	not tested	not tested
P12 Crack 5	NA		NA	Training	Training	NO	YES	0.181	90.2%	69.4%	not tested	not tested

Table 3-4. Application of Pulled Tube and Laboratory Specimen Test Results

Notes:
1. These samples were included twice in the performance test using different data collection runs with different assigned tube numbers.
2. Detection results inadvertently, but conservatively, not included in + Point POD evaluation of Section 4. Indication was detected by all analysts
3. Dent volts are values prior to cracking for laboratory specimens. Pulled tube values are based on analysis of field data as given in Table 3-1. Dent volts after cracking based on the NDE Performance Test analyses are used in Section 4.
4. NM = not measured. Dent volts not measured prior to cracking and crack voltages too large to permit measurement of dent volts after cracking. The physical dent sizes are similar to those of the other mechanically induced dents although dominantly ovalization for these specimens.
5. Invalid burst test per Appendix C, Criterion 1b. Specimen burst with TSP present. Burst pressure corresponds to crack extension outside TSP. Data not appropriate for inclusion in burst pressure correlation of this report.
6. Specimen has incomplete destructive exam depth profile. Range estimated from available data.
7. Invalid burst test per Appendix C, Criterion 1b. Specimen pressurized to open second crack for destructive exam after the larger crack was burst. Specimen was cut and welded into another tube.
8. Invalid burst test per Appendix C, Criterion 1b. Specimen burst in area away from flaw.
9. Invalid burst test per Appendix C, Criterion 1b. It is physically impossible for these large indications to correspond to the reported burst pressures of >11 ksi, and the indications are excluded from the burst correlation. In addition, specimen 10-3H burst at a welded connection away from the flaw.

4.0   NDE DEVELOPMENT

4.1   Introduction

Qualification of NDE techniques for detection and sizing of PWSCC in dented TSPs requires the assembly of a sample tube population with real or simulated cases of axial cracks. The specimen database described in Section 3 constitutes a valid population on which to demonstrate the adequacy of candidate NDE techniques, specifically bobbin probe and +Point rotating probe analyses. Guidelines for the evaluation of bobbin and +Point data were developed by building on existing qualified techniques documented in the EPRI Performance demonstration database. The program employed had two phases:

      1) Blind Analyses by selected senior NDE specialists
      2) Appendix H Peer Review and Qualification

After the techniques were qualified in accordance with Appendix H, an NDE Performance Test Plan was devised to secure the application of the techniques in field equivalent procedures, to prepare a test population from which POD and uncertainty parameters could be derived, and to institute a training program in which industry QDAs could be given orientation specific to analysis of dented TSP/PWSCC ECT data.

This section describes the NDE analysis guidelines, results of the blind analyses, results of the Appendix H qualification, results of the NDE Performance Test and PWSCC growth rates. The NDE Performance Test results are used to develop PODs as a function of maximum and average depth and NDE uncertainties on length, average depth and maximum depth for bobbin and +Point coils. The sizing analysts used in the performance test also developed axial PWSCC growth rate data for the Sequoyah and Diablo Canyon SGs.

4.2 NDE Analysis Guidelines

4.2.1   NDE Analysis Guidelines

The bobbin NDE guidelines developed in this program were provided in draft form to 4 senior NDE specialists, two (W.Junker and A.Sagar) from Westinghouse and 2 from the utility sponsors (C.Webber –TVA, Joon Kang – PG&E) of the program. From the comments of the senior analysts, as well as those from the technical leads for Westinghouse, the utilities, and the EPRI NDE Center, the NDE guidelines used for the blind analyses were finalized. After completion of the blind analyses by the 4 senior NDE specialists, who confirmed the capability of the techniques, additional revisions were made to the technique guidelines; these changes reflected the subtleties that experience had indicated would enhance the performance of subsequent users. Appendix A of the NDE report (Reference 8-1) contains the guidelines, as well as the procedures into which they were incorporated.

The +Point analysis guidelines prepared for the blind analyses incorporated length and depth adjustment guidelines. The EPRI Peer Review activity was performed without the depth adjustment procedure using the then current +Point guidelines for detection of PWSCC in dented TSPs, ETSS#96703, because time constraints did not permit the updating of the procedure concurrently with the qualification of the bobbin technique. Therefore the +Point Peer Review was dedicated to extending and firming the previously qualified depth range and establishing maximum depth as a qualified NDE parameter. The

final versions of the guidelines as qualified by EPRI were posted as ETSS#96012 for the bobbin technique and a revision to ETSS#96703 for the +Point coil. Both were included in the EPRI Performance Demonstration Database effective April 18, 1998.

The +Point sizing guidelines permit limited flexibility for implementation in field procedures. The +Point sizing analyses are limited to use of the 720 mil probe, mid-range coil evaluated at 300 kHz. The phase rotation will be set at 15° for the 40% EDM notch in the calibration standard, which results in about 40° for a 100% notch. A minimum of three points is to be used to establish the depth versus phase calibration curve with the points including the 40% and 100% notches. Additional points can include 0% or other EDM notch depths. The ETSSs for bobbin and + Point analyses given in Appendix A from the NDE Performance Test or Appendix H qualification can be applied provided these constraints are included in the field requirements. Variations in parameters such as cable length between ETSSs are acceptable provided equivalence testing following the EPRI ISI guidelines has been performed. Setups for channels other than 300 kHz may vary between guidelines.

4.2.2 NDE Length and Depth Adjustment Procedures

A data processing code (PWSCC ARC) was developed to provide length and depth adjustments to the NDE data and to provide an option to perform an adjustment to the critical length of the crack that results in the lowest burst pressure. The length adjustments correct the ends of the NDE depth profile for coil lead-in and lead-out effects (also referred to as look-ahead and look-behind) associated with the pancake or +Point coil response to the crack prior to entering the crack and after leaving the crack. As shown in Reference 8-1, the coil lead-in and lead-out effects result in increasing phase angles with corresponding depth increases at low voltages. In some cases, the phase angle increases are large enough to increase the ID phase response to an OD response. These increases in depth and potential OD phase responses provide the basis for the length adjustment procedure. It is found that the +Point response for throughwall indications is frequently in the 90% to 100% depth range. PWSCC indications having maximum voltages greater than about 4.5 volts have a high probability of being throughwall. A depth adjustment is provided such that the NDE depth profiles for indications with greater than 4.5 maximum volts are adjusted to a maximum depth of 100%. Low voltage indications tend to have a relatively poor signal to noise ratio. This condition tends to result in over estimates of the depth as the voltage decreases. For these low voltage signals, the most reliable depth estimate is that at maximum voltage. Indications with less than a one volt response are used to define a low voltage signal. For indications less than or equal to one volt, the depth profile is adjusted to define the maximum depth as that found at the maximum voltage location of the depth profile. The procedures applied for these adjustments are described below.

For some phase angle responses for the depth profile, the phase response is separated between the entrance and exit signals. When this occurs, the NDE analysis guidelines recommend that the phase angle and depth be entered in the depth profile for both the entrance and exit signals at the same elevation or within 0.01 inch of each other. The guidelines recommend that the two depths at approximately the same elevation be averaged to obtain the crack depth. Comparisons of this averaging process with destructive examination results has shown that averaging the split phase signals results in better agreement with destructive exam data than either the larger or smaller depth for the individual phase angles. The averaging of multiple depths at locations within 0.01 inch of each other is performed in the PWSCC ARC data processing code. Voltages and elevations are also averaged. This averaging of duplicate depth locations is performed prior to performing the length and depth adjustments described below. However, in cases for which the +Point data is collected at very slow speeds such that the

spacing between data points is about 0.01 inch, the PWSCC ARC code provides an option to omit averaging of closely spaced data entries.

Length and Depth Profile Adjustment Procedure

This procedure provides a length adjustment for coil lead-in and lead-out effects (i.e., the +Point coil provides a signal response prior to entering the beginning and after leaving the end of the crack) and depth adjustments for very low and very high voltage indications. The length adjustment procedure is based upon the fact that coil responses show an increase in the phase angle as the coil approaches or leaves the crack. This increasing phase angle leads to sharply increasing depths at the low voltage tails of the NDE crack profile and the PWSCC phase angles sometimes increase to OD phase angles. The requirements for this procedure are:

1.   Length Adjustment

NDE data points satisfying the requirements given below are deleted from the ends of the crack. The maximum length reduction for the length correction applied to either end of the original NDE profile shall not exceed 0.2". The adjustment shall not reduce the length of the crack to less than 0.05" with at least 3 data points remaining to define the crack. Data points are progressively checked against the requirements starting at the end of the crack and proceeding 0.2" or up to approximately the center of the crack.

   a) Adjustments for OD phase angles at each end of crack (phase angle > value at 100% depth)

   - If the data point has an OD phase angle, cut off the data point from the profile if the voltage is ≤ 40% of the maximum voltage or if the depth is > 75% with the voltage < 1.0 volt. Data points are cut off from the crack tip (first or last reading) to the point at which the phase angles change from ID to OD. The depth at the point of the phase change is reset to 0% to define the new end of the crack.
   - This adjustment is not applied if the crack exhibits primarily OD phase angles over the length of the crack.
   - When progressing from one end of the crack, the adjustments are terminated for that end of the crack if a data point having a voltage exceeding the above cut off thresholds is found. This limits the length adjustment to the low voltage tail of the NDE profile.

   b) Adjustments for increasing depth points at the end of the crack

   - If the data point has a depth increase of ≥ 10% relative to the next innermost 0.05" of the crack such that it reverses a decreasing or near constant depth trend and the voltage is ≤ 35% of the maximum voltage or ≤ 0.35 volt as well as < 75% of the maximum voltage, the data point shall be ignored and the point of the ≥ 10% depth increase is set to 0% depth to define the new end of the crack.
   - When progressing from the one end of the crack, the adjustments are terminated for that end of the crack if a data point having a voltage exceeding the above cut off thresholds is found.

2. Depth Adjustments for Maximum Volts ≤ 1.0 or ≥ 4.5

NDE cracks satisfying the voltage requirements given below have depth adjustments applied to the NDE depths. For shallow cracks with low signal to noise ratio, the most reliable depth call is expected to be the depth at the maximum voltage response for the crack. The depth adjustment for cracks with a maximum voltage ≤ 1.0 is based on this consideration. When the maximum voltage is ≥ 4.5, there is a high probability that the crack has throughwall penetration and the depth adjustment given below reflects this consideration. These depth adjustments are applied after the length adjustment described above.

   a) Maximum Depth Adjustment Only if the Maximum Voltage is ≥ 4.5 Volt

- Adjust all depths by the ratio of 100% to the maximum depth from phase analyses ($D_{\Phi max.}$) in the NDE depth profile. That is, $D_{i, adj.} = D_i \times (100\%/D_{\Phi max.})$.

   b) Low Voltage Adjustment Only if the Maximum Voltage is ≤ 1.0 Volt
- Adjust all depths by the ratio of the depth at maximum volts (D_{Vmax}) for the crack to the maximum depth from phase analyses ($D_{\Phi max.}$) in the NDE depth profile. That is, $D_{i, adj.} = D_i \times (D_{Vmax}/D_{\Phi max.})$ where D_{Vmax} is the larger of D_{Vmax} and 20%. The latter conservatively establishes that the maximum depth of the indication is not less than 20%.

4.3   NDE Technique Qualification

4.3.1 "Blind" NDE Analyses

The analyses of the dented TSP PWSCC laboratory specimens and pulled tube intersections that constituted the qualification sample population were performed by four senior NDE specialists. Details of the results of the "blind" analyses are given in NDE report for PWSCC axial cracks in Reference 8-1. These analyses were performed prior to the completion of the destructive analyses for the laboratory samples prepared in 1997 and, to the extent possible, without reference to or refreshed recollections of the 1995 pulled tube and the 1996 laboratory specimens. The blind analysis results were used to select the laboratory specimens destructively examined in order to obtain a distribution of crack depths spanning shallow to deep indications. The detection statistics and the sizing estimates obtained were analyzed to establish the basis for qualification of the technique. It was demonstrated by the senior NDE specialist's results that the techniques yielded satisfactory POD values as well as sizing uncertainties. Table 4-1 summarizes the NDE uncertainties given as the mean and standard deviation from the blind analyses. For these analyses the length and depth adjustments referred to in Section 4.2.2 were implemented; therefore some improvements over the uncertainties obtained in the Appendix H qualification were realized. The Table 4-1 results for maximum depth include the effective coil field average (0.16 inch) maximum depth and the local or point maximum depth from the destructive examination. Appendix H recommends use of destructive examination results averaged over the effective coil field and this definition is used for the NDE uncertainties applied in this report. The comparisons of the blind analyses with the Appendix H results and the NDE Performance Test results are further discussed in Section 4.3.2 below.

4.3.2 Appendix H Qualification

In conjunction with the convening of the industry peer review team, Westinghouse submitted to the EPRI NDE Center a qualification data package. The qualification package included the opticals containing the raw ECT data for the pulled tube and laboratory specimen database, the detailed hardcopy documentation of the NDE and destructive examination results, the NDE guidelines, and various spreadsheet analyses illustrating the impact of the adjustment routines on the NDE uncertainties. This package documented the work Westinghouse had completed to establish the basis for qualification of both the bobbin and +Point techniques.

Five QDAs were invited by EPRI to examine the data package and to evaluate the EC test data. Under EPRI auspices a Westinghouse representative and the Level III analysts from the sponsoring utilities explained the guidelines to the participating reviewers. The results of the Industry Peer Review established that the POD satisfied the detection criteria for Appendix H criteria, i.e., ≥ 80% at the 90% confidence level, for both bobbin and +Point coil detection techniques. The bobbin technique POD (89% @ 90% confidence for maximum depths > 34%) was established as meeting the Appendix H detection criteria for PWSCC flaws in dented TSP intersections with dent amplitudes up to 2 volts and for flaws ≥ 34% throughwall depth; this result is documented in ETSS#96012. The +Point technique POD (89% @ 90% confidence for maximum depths > 34%) also satisfied the Appendix H detection criteria for PWSCC flaws in dented TSP; this result is documented in ETSS#96703.

Sizing parameters for the +Point technique were evaluated and the results were found to be acceptable. A revision to the previous qualification (ETSS#96703) was issued in April 1998 for the +Point technique, extending the range for average depth determination to shallow flaws, qualifying the maximum depth parameter, and re-qualifying the length determination parameter. Due to time constraints in conducting the peer review, not all of the laboratory specimens with destructive exam data were included in the sizing analyses. RMSE errors established for these parameters, found in ETSS#96703 November 1998 editorial Revision 3, were as follows: average depth = 10.52%, length = 0.13" and maximum depth = 15.13%. Some of the destructive exam results were finalized after the Appendix H review was completed although differences in the results are small. In addition, it is desirable to develop the Appendix H sizing results as the mean and standard deviation for comparisons with the results from the "blind" analyses and the NDE Performance Test.

Table 4-1 provides a comparison of the mean and standard deviation NDE uncertainties between the "blind" analyses, Appendix H analyses and the NDE Performance Test results (Section 4.7). The blind and performance test results include the results of multiple analysts and thus include analyst variability while the Appendix H results are a single analysis representing NDE technique uncertainty. The Appendix H results include the length adjustment but do not include the depth adjustment procedure of Section 4.2.2. The omission of the depth adjustment is the primary reason that the maximum depth NDE uncertainty for the Appendix H results is larger than found for the blind and performance test results. Good agreement is found between all three analyses for length and average depth uncertainties. As demonstrated in the NDE report of Reference 8-1, multiple analysts agree very well on the depth profiles for axial PWSCC at dented TSP intersections, particularly for indications having maximum voltages above about 1.0 volt. This is also shown for examples from the NDE Performance Test in Section 4.7. As a result of the good agreement between analysts for the depth profiles, the contribution of analyst variability to the NDE uncertainties is small. Thus, the differences are small for length and average depth uncertainties between the NDE technique uncertainties of Appendix H and the blind or performance test uncertainties, which include both technique uncertainty and analyst variability.

4.4   NDE Performance Test Plan for Validating NDE Techniques

To establish the acceptability of the techniques to support the proposed ARC for PWSCC in dented TSPs, it was necessary, in accordance with Draft Reg. Guide 1074, to confirm that acceptable POD and sizing uncertainty values could be realized by production analysts using field procedures consistent with the Appendix H techniques. To satisfy DG-1074 guidance for the development of PODs and NDE uncertainties, the sponsoring utilities and Westinghouse designed a test plan to obtain performance data based on statistically robust sample populations of well-characterized dented TSP intersections.

4.4.1   NDE Performance Test Plan

The overall plan consisted of the following major activities:
   1. Preparation for NDE Performance Testing Procedures
   2. Preparation of the NDE Performance Test Database
   3. NDE Performance Test Training
   4. NDE Performance Test Data Processing Code Development
   5. NDE Performance Testing

Craig Bowser- Level III, QDA (Corestar), was designated the trainer, by the sponsoring utilities, since he had intimate familiarity with the condition of the SG tubing inspection results at both Sequoyah and Diablo Canyon. Mr. Bowser was given an orientation on the newly qualified bobbin and +Point techniques prior to the beginning of the NDE Performance Test. He subsequently participated in the preparation of the field procedures and the assembly of the test database. His duties also included the actual conduct of the NDE Performance Test training of the participating analysts.

4.4.2   NDE Performance Test Procedures

By joint agreement, the field analysis guidelines for the Diablo Canyon site, as adapted to conform to the requirements of the Appendix H techniques qualified for PWSCC in dented TSPs (i.e., ETSS #'s 96012 and 96703), were used as the basis for the test procedures. This work was performed cooperatively among G.P.Pierini (WELCO), C.M.Bowser (Corestar), and J.Kang (PG&E). The completed procedures were subjected to internal Westinghouse NSD QA review procedures. D.D.Malinowski performed the Engineering review on behalf of Westinghouse NSD.

The completed, signed off procedures were designated as follows:

1. DAT-PWSCC-1-Rev.0	Examination Procedure for Bobbin Detection of PWSCC in Dented Intersections
2. DAT-PWSCC-2-Rev.0	Examination Procedure for Plus Point Detection and Sizing of Axial PWSCC in Dented Intersections

Each procedure defines the scope intended and specifies the personnel qualifications and responsibilities. Directions are given for calibration, reporting requirements, and resolution of discrepancies. Flaw detection and sizing criteria are provided along with setup specifications, analysis instructions, and numerous examples of standard and typical field data behavior. Since ETSS#96012 represents substantially new analysis guidance, it was adopted in its entirety for evaluation of bobbin data from

dented TSP intersections. The elements of ETSS#96703 were integrated into a field procedure that also treats the evaluation of circumferential PWSCC detection and sizing as well as NDE analyses for TSP integrity from rotating probe data. A copy of the pertinent EPRI ETSS was appended to each of the procedures, which are included in Appendix A of the NDE report (Reference 8-1).

4.4.3 NDE Performance Test Database

Performance testing for validation of field application of qualified NDE techniques requires that the analysts demonstrate their capabilities to realize the expected technique PODs. Analyst performance demonstrations are typically conducted in accordance with Appendix G of the EPRI guidelines. This requires that the ground truth specimens used to assess the analysts' performance be supplemented with about 2x their number with specimens which are free from apparent flaw signals. In this application, dented TSP intersections known to be free from cracks were used to satisfy this condition.
While the typical bobbin field analysis is performed on full-length tube records, including 14 TSP intersections each, such a ground truth specimen is not available. Typically 1-3 intersections are included on pulled tube specimens, but only three such tubes with dented intersections are available. The cost of preparing laboratory simulations of full-length tubes is prohibitive. Therefore, for the purposes of assembling a database of specimens, it was resolved that all specimens, whether of bobbin or rotating probe data origin, would be comprised of the data segment representing about 6" length centered on a single TSP intersection. The laboratory ECT data was acquired for tubes fitted with 5 TSP simulants at which cracks could be induced. The intersections were sampled by cutting data segments from the digital record, using the ANSER system software. The segment cutting process resulted in 10 specimens per laboratory tube, 5 from the pre-cracked specimen ECT, and 5 from the post-cracked specimen ECT. Similar segments were extracted from the field ECT data, which typically consisted of full tube lengths for bobbin data and variable lengths (1 or more TSPs) for +Point data.

Each of the specimens was then placed into an individual CAL group along with the ECT data for the appropriate calibration standard that governed the original data acquisition setup for that tube. Approximately 1000 such CAL groups were created. All the ground truth specimens, a small population of field flaw results, and sufficient numbers of unflawed (NDD) intersections to satisfy Appendix G concerns were then identified for inclusion in the NDE Performance test database. In all cases, where ground truth characterization was not available, the pedigree of the specimen depended on +Point characterization. Laboratory pre-cracked ECT specimens were accorded de facto NDD status. Field ECT specimens designated as unflawed were NDD to both bobbin and +Point analyses. Each of the specimens and its CAL group was renamed with a fictional ID and converted to EDDYNET format. The selected ECT specimens were then randomized and copied to the testing opticals. Specimens used for training, with few exceptions, were similarly made anonymous. Both the training and testing were conducted using the EDDYNET analysis tools.

Table 4-2 provides a summary of the specimens used in the NDE Performance Test and the maximum depths of specimens destructively examined. Specimens used for training are also described in the table. Table 4-3 shows the distributions of the specimens relative to maximum depth, average depth, length and dent voltage. It is seen that the specimens are well distributed in terms of depths and lengths. The laboratory specimen dent voltages are principally low voltage dents as support for qualification of bobbin detection in low voltage dents was a major objective in preparation of the laboratory specimens.

4.4.4 NDE Performance Test Training

Analyst Teams: To provide test conditions that closely simulated the field experience, analyst teams were specified so that for bobbin data analysis, exclusively a detection function, each team consisted of a Primary (PRI), a Secondary (SEC), and a Resolution (RESO) analyst. Two teams were established to include analyst variability in the results. A utility Level III analyst was available to review Resolution decisions to delete a potential flaw call. A similar process was used for the detection (POD) phase of the +Point testing. For +Point sizing analysis, 3 teams were established to include analyst variability and increase the statistical validity of the performance test results. Each team employed an analyst and an Independent Technical Reviewer (ITR) whose task it was to verify that gross errors had not occurred in the evaluation of flaw data. As for the detection activity, a Utility level III was available in the event that the analyst and the ITR were in conflict as to the correct characterization of a flaw indication.

The production analysts who staffed the POD phases of the performance test were required to be QDAs, with at least Level IIA status. Zetec, FTI, and Westinghouse provided the participating analysts for both the bobbin and the +Point performance tests. To optimize the benefits of conducting this program, Resolution Analysts (2) and designated ITRs (3) were experienced Level III's. For the POD phase, the Resolution Analysts represented FTI and Westinghouse. For the sizing phase of the program, each of the 3 vendors provided one of the ITRs. Clayton Webber (TVA) and/or Joon Kang (PG&E) filled the utility Level III role in both performance testing phases. The detection testing resulted in 2 independent sets of resolved data, since both teams analyzed all the data.

The Phase 1a analysts completed the +Point detection performance data deployed as two analyst teams, each consisting of at least 1 Level III Resolution Analyst and 2 Primary/Secondary analysts qualified at least to Level IIA; their identities are given below:

Phase 1a: Detection (POD) with +Point Techniques

Function	Team 1	Team 2
Primary	WELCO (W.J.Spence)	ZETEC (P.L.Notch)
Secondary	ZETEC (E.J.Emery)	FTI (N.J.DeFillippis)
Resolution	FTI (D.M.Chambers)	WELCO (W.F.Stock)

After the evaluation of the Phase 1a bobbin results, which did not satisfy the Appendix H qualification criteria, the training program was revised as described below. A second set of analysts was employed for the bobbin data analysis. The Phase 1b bobbin analysis teams are identified below:

Phase 1b (2nd analysis): Detection (POD) Teams (Bobbin only)

Function	Team 1	Team 2
Primary	WELCO (J.V.Krasnevich)	FTI (D.J.Torres)
Secondary	Zetec (A.J.Horochiwsky)	Zetec (D.J.Schaible)
Resolution	FTI (D.E.Shibley Jr.)	WELCO (T.E.Gootz)

Three analyst teams, each consisting of 1 Level III Independent Technical Reviewer (ITR) and 1 sizing analyst who is experienced and qualified at least to Level IIA, were assigned to the task of developing sizing information. Three independent sets of measurements were obtained. The +Point sizing analysis teams are identified below:

Phase 2: +Point Sizing

Function	Team 1	Team 2	Team 3
Sizing	FTI (J.D.Sordini)	ZETEC (G.L.Webb)	WELCO (R.J. Pocratsky)
ITR	Zetec (J.L.Darragh)	WELCO (S.H.Taylor)	FTI (M.M.Story)

Analyst Training – Bobbin Phase 1a: All analysts were provided with a general orientation concerning the objectives of the program, i.e., validating the detection and sizing capabilities of the Appendix H-qualified techniques for PWSCC in dented TSP intersections. The field procedures referenced in Section 4.4.2 (NDE Performance Test Procedures) were then distributed and explained by the trainer (C.Bowser). Graphical examples of typical examples of dented intersections with flaws and without (NDD) flaws were presented and discussed. For each phase of the training, the analysts were provided a training optical containing representative dented TSP specimens prepared in the single intersection fashion described above (Section 4.4.3: NDE Performance Test Database). In the initial bobbin training exercise, the data on the training opticals were identified to the analysts as flawed or unflawed, as they practiced the evaluation techniques. The trainer and the Utility Level III's were available on a continuous basis for consultation during the practice sessions. After several hours of practice, the analysts commenced the performance testing.

It became apparent after completion of the first attempt to validate the bobbin detection POD (Phase 1a), that more intense briefing and extended practice time were needed to communicate the guidance given in the bobbin detection technique guidelines. This experience illuminates the hazards inherent in extending the normal range of analysis practice without thorough explanation of the changes needed to effect the desired result. The prevailing set of evaluation rules common to the industry's analyst community, without specific instruction, would not be expected to identify small flaw components in dented TSP composite signals.

Analyst Training – Bobbin Phase 1b: A second set of analysts was committed to the bobbin detection performance test. Daily or twice daily debriefing sessions were conducted with the participating analysts to facilitate communication and shared experience during the training exercises. The specific correct interpretation of the training examples were provided to this group of analysts in the form of printed graphics, which identified the segment of the specimen EC trace that represented the flaw. Additionally, the bobbin training program was modified to incorporate a practice test using the training specimens. This approach was successful in validating the POD values obtained in the Appendix H Peer Review. The false call rate encountered indicates that the conservative flaw identification guidelines incorporated in ETSS#96012 will result in a relatively large population of intersections to be +Point tested based on bobbin probe screening.

Analyst Training – +Point: As expected, no difficulties were encountered in validating the +Point technique POD in the Phase 1 effort, since the rotating coil techniques are especially suited for reducing the interference presented by the dent signals. The 3 sets of results provided a basis for determining measurement uncertainties that could be used in support of tube integrity assessments.

4.4.5 NDE Performance Test Data Processing

To facilitate evaluation of sizing data from +Point analyses, the PWSCC ARC data processing code as described in Section 4.2.2 was written. The code plots the reported depth profile and applies end effect corrections to determine the flaw length. Depth profile corrections are performed per the procedures described in Section 4.2.2. Average depth calculations are performed on the basis of the corrected length and depth profiles. One further set of optional calculations is also performed to determine a burst-related average depth and length that results in the crack length within the total crack length that yields the lowest burst pressure. This method removes shallow depth profile tails that could result in low average depths and high burst pressures calculated from the average depths. The EDDYNET data files (ASCII) containing the line by line profile analyses for a specimen are accessed via FTP from the ECT local area network (LAN); the data processing are performed on a PC.

It is intended that the results from the data processing code be reviewed against the sizing analyses for potential unintended errors (e.g., point changes in depth) or data omissions (incomplete crack profile). In addition, the results of the data processing code should be reviewed for potential irrational data adjustments that could occur from automated data adjustments when the profile is much different from that used for the code validation. For the NDE Performance Test, results of the data processing code were only available after the analyses were completed. The ITR reviews of the results led to only a few changes in the original NDE profiles. All evaluations of the NDE Performance Test results are based on the profiles obtained from the processing code.

4.5 Average Probability of Detection (POD)

4.5.1 Average Bobbin Coil POD

A summary of the bobbin detection results from the NDE Performance Test is given in Table 4-4. More detailed detection results are given in Appendix A. For each specimen included in the test, the dent volts, destructive exam data and bobbin detection results are given. The detection results are given as the fraction detected (0/2, 1/2, 2/2) for resolution analysts 1 and 2. The POD for bobbin detection with +Point confirmation of the flaw is also of interest. The +Point detection results are summarized in Table 4-5 and discussed in more detail in Section 4.5.2. The bobbin detection column of Table 4-4 also includes entries for +Point detection when the flaws were not detected by both of the +Point resolution analysts. Flaws in two specimens (5-1H and 12-3H) were detected by only 1 of the 2 +Point resolution analysts. The combined fraction of bobbin detection with +Point confirmation for these two specimens is then obtained as the product of the fractions detected by bobbin and by +Point analyses. Since all other specimens were detected by both +Point resolution analyses, the combined fraction detected is the same as for bobbin detection.

Specimens without flaws were also included in the detection phases of the NDE Performance Test. This NDD database included laboratory specimens with the NDE data collected prior to cracking of the specimens and field dented TSP intersections from Sequoyah and Diablo Canyon SGs that were NDD by both bobbin coil and +Point inspections. These specimens were included in the NDE Performance Test to assess false call rates for the analyst teams. Details of the test results for these NDD specimens are given in Appendix A. For bobbin detection, the false call rates[1] for the two resolution teams were [67%

---

[1] The false call rate is defined as the number of false calls divided by the number of non-degraded intersections examined.

and 86%] [g]. The high false call rates are partly attributable to the laboratory specimen flaws being somewhat more difficult to detect than field flaws, since the laboratory generated flaws tended to coincide with the dent signals more often than found in typical field data. In addition, the test specimens were cut into single TSP intersections which eliminates the analyst's capability to compare one TSP intersection with others to help separate flaw signals from more typical dented TSP signals.

Consequently, lower false call rates are expected in field applications. The EOC-9 Seqouyah-1 inspection using similar analysis guidelines resulted in a low (about 8%) +Point confirmation rate[2]. If the false call rate was significantly higher, the confirmation rate would have been significantly lower. Overall, the high false call rates are acceptable for the intended bobbin inspection of < 2 volt dents since the total extent of +Point inspection of these TSP intersections is significantly reduced by performing the bobbin inspection of small dents. However, the false call rate found in the EOC-9 Seqouyah-1 inspection was about 1% of the dented TSP intersections which is much lower than found in the NDE Performance Test. The much lower false call rate in the field experience may be due to the increased difficulties in separating flaws from undegraded dented intersections for the laboratory specimens than for the field intersections as discussed above. However, the cause for the large difference in the false call rate between the performance test and field experience cannot be clearly defined. Until this issue is resolved, the bobbin detection results from the performance test are not considered appropriate for developing a detailed POD as a function of depth. Only the average results of the performance test are reported herein as described below. As a consequence, a POD distribution is not available for inclusion in operational assessments for tube degradation.

In Table 4-4, the specimens are binned into 10% intervals of average depth and maximum depth. The fraction detected and percent detected for the specimens in each bin are also given in the table. The percent detected can be considered to be the mean POD for each depth bin since no statistical confidence values are assigned to the data. The mean PODs for bobbin detection as a function of maximum depth and average depth are plotted in Figures 4-1 and 4-2, respectively. POD points are also shown for bobbin detection with +Point confirmation for the two bins where this POD differs from the bobbin POD alone. It is seen that the mean POD as a function of maximum depth approaches [unity at > 40% depth and is close to one in the range of 30% to 40% depths. The mean POD for average depth approaches unity at > 30% depth.][g] The mean bobbin PODs can be compared with the corresponding +Point mean PODs plotted in Figures 4-3 and 4-4.

It is seen in Figures 4-1 and 4-2 that bobbin detection with +Point confirmation results in [slightly lower PODs between 10% and 30% average depths. The combined POD is the same as the bobbin POD for depths > 30% average depth or > 40% maximum depth.][g] The POD reductions result from indications detected by the bobbin coil but not confirmed by the +Point coil analyses. The POD for bobbin detection with +Point confirmation is of primary interest for this report since bobbin detection will be used for inspection of dents < 2 volts. Confirmation by +Point provides a basis for tube repair decisions.

The performance test POD results can be compared with the EPRI Appendix H results discussed in Section 4.3.2 by evaluating the effective POD at 90% confidence for maximum depths > 34%. For this comparison, the Appendix H results are reevaluated to adjust for a few depth differences from the Appendix H ETSS. The resulting maximum depth PODs are given below:

Evaluation	POD - Coil Field Average	POD - Local Maximum Depth

---

[2] The confirmation rate is the number of indications confirmed by +Point divided by the number of bobbin identified locations.

Bobbin: App. H ETSS 96012   0.887 (32/33 calls)   0.859 (34/36 calls)
+Point: App. H ETSS 96703   0.915 (26/26 calls)   0.924 (29/29 calls)
Bobbin: NDE Performance Test   0.947 (65/66 calls)   0.942 (71/72 calls)
+Point: NDE Performance Test   0.954 (83/84 calls)   0.897 (94/100 calls)
Bobbin with +Point Confirmation   0.921 (64/66 calls)   0.842 (65/72 calls)

The number of calls differ between the Appendix H and performance test evaluations since two analysis teams were used in the performance test. Also, the local maximum depth evaluation includes more specimens above 34% depth than found for the coil field averaged maximum depth. The higher bobbin coil PODs from the performance test are a consequence of more calls affecting the 90% confidence value and the more conservative detection calls emphasized in the NDE Performance Test.

4.5.2 Average +Point Coil (POD)

A summary of the +Point coil detection results from the NDE Performance Test is given in Table 4-5. More detailed detection results are given in Appendix A. For each specimen included in the test, the dent volts, destructive exam data and +Point detection results are given in Table 4-5. The detection results are given as the fraction detected (0/2, 1/2, 2/2) for resolution analysts 1 and 2.

Specimens without flaws were also included in the detection phases of the NDE Performance Test. This NDD database included laboratory specimens with the NDE data collected prior to cracking of the specimens and from field dented TSP intersections from Sequoyah and Diablo Canyon SGs that were NDD by both bobbin coil and +Point inspections. These specimens were included in the NDE Performance Test, providing 118 unflawed grading units, to assess false call rates for the analyst teams; the Team #1 and Team #2 resolution results were [0.7% (1 false call) and 1.4% (2 false calls)][g] respectively. Details of the test results for these NDD specimens are given in Appendix A. The low false call rates are acceptable for the intended +Point inspections of dents > 2 volts and satisfy the EPRI NDE guidelines, Appendix G objectives for a 10% false call rate. The low false call rate found for +Point detection supports development of a detailed POD distribution as a function of depth. The detailed +Point POD is included in Revision 1 of this report, but is excluded in this revision due to the absence of an acceptable bobbin coil POD.

In Table 4-5, the specimens are binned into 10% intervals of average depth and maximum depth. The fraction detected and percent detected for the specimens in each bin are also given in the table. The mean PODs for +Point detection as a function of maximum depth and average depth are plotted in Figures 4-3 and 4-4, respectively. It is seen that the mean POD as a function of maximum depth approaches [unity at > 40% depth and is > 70% in the range of 10% to 40% depths. The mean POD for average depth approaches unity at > 40% depth and is near 90% in the 20% to 40% depth range.][g]

The following discussion provides a review of detection capability relative to the significance of undetected indications for tube integrity and ARC considerations.

All three pulled tube intersections with < 5 volt dents were detected by bobbin and + Point coils by all analysts in the NDE Performance Test. This includes the smallest Diablo Canyon pulled tube R10C22 with an average depth of 23% (local maximum depth of 38%), a length of only 0.122 inch and a burst pressure of 12437 psi. This indication had also been detected in the field inspection prior to the tube pull. The largest indication not detected by bobbin in the NDE Performance Test (Table 4-4) was specimen 2-4H with an average depth of 29%, maximum depth of 47.6%, length of 0.58 inch and a burst pressure of 11300 psi. The next largest indication not detected in dents < 5 volts was specimen 12-4H

with an average depth of 20.8%, maximum depth of 23.4%, length of 0.242 inch and a burst pressure of 13170 psi. Non-detection of these indications by the bobbin coil is clearly insignificant relative to tube integrity considerations. The largest indication not detected by +Point in the NDE Performance Test (Table 4-5) was specimen 11-2H Crack 2 with an average depth of 32.8%, local maximum depth of 43% and a length of 0.16 inch. This specimen burst at the larger Crack 1 so that a burst pressure is not available for Crack 2, but the burst pressure would be expected to exceed 10000 psi. The next largest indication not detected by +Point was specimen 12-4H with an average depth of < 30%, local maximum depth of 42%, length of 0.242 inch and a burst pressure of > 11300 psi (burst away from flaw). Non-detection of these indications by the +Point coil is also clearly insignificant relative to tube integrity considerations.

The PODs of Figures 4-1 to 4-4 can also be used to demonstrate the adequacy of flaw detection for ARC applications. These figures indicate PODs approaching unity for average depths of about 40% and maximum depths of about 50%. Growth rates per cycle at 95% probability are about 20% for average depth and 24% for maximum depth. The EOC average depth assuming about a 5% probability of missing the indication at 40% average depth combined with a 5% probability growth rate would be about 60%. The burst pressure of a very long flaw (> 1.4") with an average depth of 60% would exceed $3\Delta P_{NO}$ burst capability at 95%/95% confidence on variability in the burst correlation and material properties. The maximum depth for such a low probability indication would be about 70% that would not leak or breakthrough the remaining ligament at SLB conditions. Thus, undetected indications having a very low probability of occurrence would not challenge tube integrity at the next EOC.

Overall, this review of potentially undetected indications based on the NDE Performance Test results and on low probability undetected indications based on the POD trends demonstrate that the undetected indications are insignificant for tube integrity considerations.

4.6   +Point NDE Sizing Uncertainties

This section describes an evaluation carried out to examine the +Point NDE sizing uncertainties obtained from the NDE performance tests. The uncertainties were obtained by comparing NDE data directly with destructive examination data for the tube specimens. Specifically, the crack length, average depth and maximum depth values obtained from the analysis of +Point signals were compared against the corresponding results from destructive examination. The method of least squares regression analysis was used to examine the degree of covariability between the crack size parameters obtained by +Point sizing and the "truth" from the destructive examination of the tube specimens, and correlations between the two sets crack size parameters were established. Also, uncertainties in the true crack size predicted from the correlations for a given value from NDE sizing were determined by establishing confidence limits for the predicted value and the standard deviation for the predictions.

The results of the NDE Performance Test for +Point sizing are given in Table 4-6. Graphical results giving comparisons of the NDE and destructive exam results for one analyst, as an example, are given in Appendix D. The NDE results for each sizing team are given in Table 4-6 for length, maximum depth, average depth and maximum volts. NDE results are given for the unadjusted data, the adjusted NDE data including the length and depth adjustments described in Section 4.2.2. Destructive exam results are also given in the table although no adjustments are made to the destructive exam data. Differences between the destructive exam and NDE results are included in the table. The arithmetic mean, standard deviation and 95% uncertainty values obtained from the DE-NDE differences are given at the end of Table 4-6. These

values were included in Table 4-6 for comparison with the "blind" and Appendix H results as given in Table 4-1. However, the NDE uncertainties recommended for repair limit development and tube integrity assessments are the results of the regression analyses given in this section. The data exclusion criteria of Appendix C are applied to the destructive examination data. The criteria include Criterion 4C, which eliminates very shallow tails from the destructive exam data prior to comparisons with NDE results.

Regression Analysis

The method of least squares was used to examine for a correlation between the crack size parameters inferred from sizing +Point data with the true crack size determined directly from destructive examination. Since the crack size parameters obtained from +Point sizing and destructive examination are independent of each other, either may be treated as the predictor and the other as the response. Herein, crack size parameters (crack length, average depth and maximum depth) derived from the NDE data were treated as regressor variables so that the correlations can be used to estimate the true crack size, within limits of uncertainty, based on the value inferred from +Point sizing.

The correlations based on a linear relationship between the size parameters from +Point sizing and destructive examination yield high values for the correlation coefficient (better than 75% for all the data examined) indicating that a linear relationship provides a good representation. Also, the p-values for the slope parameter in the correlations are very small indicating a good correlation. Therefore, no other relationship form (such as logarithmic or a combination of linear and logarithmic functions) was considered.

The following relationship form was used to relate the NDE-based crack size parameters with those from destructive examination:

$$X_{de} = b_0 + b_1 \times X_{nde}$$

where X denotes crack size parameter and subscripts 'de' and 'nde' respectively identify destructive examination (the "truth") and NDE (+Point) data. The values for coefficients b_0 and b_1 in above equation and the standard deviation for the estimated X value were obtained using the least squares method. In addition, confidence limits for the regression line which specify the band within which the average of the future true values of X for a given value X_{nde} at a certain confidence level is expected to lie were also obtained. The 95% confidence interval and the standard deviation for the predicted X_{de} represent uncertainties in the X_{nde} obtained from NDE sizing.

Residual Analysis

In performing the regression analysis and establishing the confidence limits for the predicted variable (true crack size X), the difference between the predicted and measured value of the variable, called as regression residual or error, is assumed to be normally distributed with a mean value of zero and a variance that is uniform over the range of interest. An analysis of the regression residuals was performed to check if the above assumptions are valid. A plot of the residual value against the predicted value was prepared for each correlation examined. Such a plot should be nondescript since residual should not be correlated with the predicted values. Such results indicate that the variance is approximately constant (as assumed), that there is no systematic departure from the regression curve, and that the number of terms in the regression equation is adequate.

If the frequency distribution of the residual values is similar to a normal distribution, then a plot of the ordered residuals on normal probability paper should approximate a straight line. To prepare a

cumulative normal probability plot, the residuals were sorted in ascending order and then plotted against an ordinate representing cumulative percent value for a variable given by:

$$100 \times \frac{(i - \frac{1}{2})}{n}$$

where n is the number of data points used in the regression and i is an index ranging from 1 to n. The data should fall approximately on a straight line if the residuals are normally distributed.

Results of the regression analysis and residual analysis for each correlation examined are discussed in the following sections for each of the 3 crack size parameters considered. Uncertainties are established separately for the crack length, crack depth and maximum depth values.

4.6.1 NDE Sizing Uncertainties

This section describes estimation of uncertainties in the NDE crack profiles for which length and depth adjustment have been made per the procedure of Section 4.2.2. The NDE uncertainties are established by relating the NDE data to the "truth" from destructive examination data by linear regression analysis and determining the limits that include the mean of future values at a 95% confidence level and the upper bound at 95% confidence level for an individual future value.

Qualification of the +Point coil for detection was not an objective of this program since detection had previously been qualified per Appendix H of the EPRI ISI guidelines, and this program focused primarily on +Point sizing development. The +Point coils are spring loaded to achieve surface riding coils. Dents have relatively smoothly varying diameter changes as compared to expansion transitions. The ovalization from denting typically spans the TSP thickness and frequently extends outside the TSP. Local indentations that may be superimposed on the ovalized tube are generally short spanning a few tenths of an inch or less. Based on profilometry results, local indentations tend to be a few mils while ovalization tends to dominate the reduction in the tube diameter due to denting. Responses of the surface riding coils are not strongly influenced by the modest rate of diameter change for the ovalized tubes, particularly at the minor axes where PWSCC is found. The local indentations, which might have more influence on the coil response due to liftoff effects, tend to be short in length and would not be expected to be a strong function of dent size. For the specimens used to develop the sizing uncertainties about 2/3 of the specimens were less than 2 volts and the remaining 1/3 spanned the range of 2 to 6.3 volts. As expected, the +Point sizing results show no apparent dependence upon dent size for these specimens. A review of the sizing results of Table 4-6 for indications in dents < 2 volts and dents > 2 volts indicates that the depth mean errors are smaller and the standard deviations slightly larger (about 1.5% depth change) for the population > 2 volts. It is concluded that there is no significant difference in the NDE uncertainties between these groups. Due to the surface riding coils and the expected similarities of local indentations across varying dent sizes, the +Point sizing uncertainties should not be significantly dependent upon dent size.

The specimens used for sizing included 3 specimens with lengths between 1.0 and 1.5 inch and 6 specimens between 1.5 and 2.6 inches (See Table 4-8). These indications are longer than found in the field and are believed to provide an adequate sample of long indications. The longer cracks were principally part of the first phase of this program (Reference 8-4) which emphasized sizing of

structurally challenging indications. The first phase indications have a prefix P for the specimen labels of this report.

The axial PWSCC morphology found at dented TSP intersections is that of a single crack or two cracks typically about 180° apart at the minor axes. Minor microcracking is sometimes found adjacent to the dominant axial indication. MAIs 180° apart have no affect on +Point sizing of the individual indications. The minor microcracks are present in some of the laboratory specimens as well as pulled tubes with no apparent affect on sizing accuracy.

Based on the above considerations, no limits are placed on +Point sizing for dent voltages, crack lengths or MAI versus SAI. For leaving indications in service based upon +Point sizing, flaw locations are limited to dented TSP intersections although the sizing uncertainties are expected to apply to all axial PWSCC locations except potentially hardroll expansion transitions. No limits are placed on flaw locations within or adjacent to TSP intersections.

4.6.1.1 Crack Length NDE Uncertainty

Results from the regression analysis for the adjusted crack length are shown in Figure 4-5. Crack length based on the +Point signal sizing adjusted per the procedure of Section 4.2.2 is used as the regressor and the regression correlation predicts the "true" crack length. The correlation coefficient (r^2 value) for the regression line is 94%, which indicates that a good correlation exists. The p-value for the slope parameter gin the correlation is 1.4×10^{-99} which also suggest a good correlation. The standard error for the "true" crack length estimate from the correlation is [0.139 inch] [g]. The correlation line is given by:

$$[\, l_{true} \; = \; 1.008 \times l_{nde} \; + \; 0.010 \;]^{g}$$

where l represents the crack length.

The residuals plot for the crack length is shown in Figure 4-6 and the data show random scatter without suggesting any type of correlation. Thus, the data in Figure 4-6 verify that a correlation does not exist between the residuals and the predicted values, and that the variance of the residuals is approximately uniform. It is also evident from Figure 4-7 that the residuals for the correlation are approximately a straight line indicating they follow that expected for a normal distribution. Hence, it is concluded that the assumptions inherent in the least square analysis are verified for the crack length regression.

Figure 4-5 also shows 95% confidence bound for the mean of the true crack lengths predicted with the correlation. The upper prediction bound at 95% confidence level for an individual future value of crack length predicted with the correlation is also shown in Figure 4-5.

4.6.1.2 Maximum Crack Depth NDE Uncertainty

Results from the regression analysis for the adjusted maximum crack depth are shown in Figure 4-8. Maximum crack depth based on the +Point signal sizing adjusted per the procedure of Section 4.2.2 is used as the regressor and the regression correlation predicts the "true" maximum crack depth. The correlation coefficient (r^2 value) for the regression line is 75%, which indicates that a good correlation exists. The p-value for the slope parameter in the correlation is 6.5×10^{-51} which also suggest a good correlation. The standard error for the "true" crack maximum depth estimate from the correlation is $[14.2\%]^g$. The correlation line is given by:

$$[d_{max,true} = 0.939 \times d_{max,nde} - 0.923]^g$$

where d_{max} represents the maximum crack depth.

The residuals plot for the maximum depth is shown in Figure 4-9 and the data show random scatter without suggesting any type of correlation. Thus, the data in Figure 4-9 verify that a correlation does not exist between the residuals and the predicted values, and that the variance of the residuals is approximately uniform. It is also evident from Figure 4-10 that the residuals for the correlation approximate a straight line indicating they follow approximately a normal distribution. Hence, it is concluded that the assumptions inherent in the least square analysis are verified for the regression for the maximum crack depth.

Figure 4-8 also shows 95% confidence bound for the mean of the true crack maximum depths predicted with the correlation. The upper bound at 95% confidence level for an individual future value of maximum depth predicted with the correlation is also shown in Figure 4-8.

4.6.1.3 Average Crack Depth NDE Uncertainty

Results from the regression analysis for the adjusted average crack depth are shown in Figure 4-11. Average crack depth based on the +Point signal sizing adjusted per the procedure of Section 4.2.2 is used as the regressor and the regression correlation predicts the "true" average crack depth. The correlation coefficient (r^2 value) for the regression line is 89%, which indicates that a good correlation exists. The p-value for the slope parameter in the correlation is 4.9×10^{-81} which also suggest a good correlation. The standard error for the "true" crack average depth estimate from the correlation is $[7.8\%]^g$. The correlation line is given by

$$[d_{avg,true} = 0.914 \times d_{avg,nde} + 0.687]^g$$

where d_{avg} represents the average crack depth.

The residuals plot for the average depth is shown in Figure 4-12 and the data show random scatter without suggesting any type of correlation. Thus, the data in Figure 4-12 verify that a correlation does not exist between the residuals and the predicted values, and that the variance of the residuals is approximately uniform. It is also evident from Figure 4-13 that the residuals for the correlation approximate a straight line indicating they follow approximately a normal distribution. Hence, it is concluded that the assumptions inherent in the least square analysis are verified for the regression for the average crack depth.

Figure 4-11 also shows 95% confidence bound for the mean of the true crack average depths predicted with the correlation. The upper bound at 95% confidence level for an individual future value of average depth predicted with the correlation is also shown in Figure 4-11.

4.6.2 Conclusions

The NDE uncertainties resulting from the performance test are expressed as linear correlations with associated standard deviations. Uncertainties have been obtained for length, average depth and maximum depth for the adjusted NDE data. The resulting NDE uncertainties are given below.

Length

$$\left[\, l_{true} \;=\; 1.008 \times l_{nde} \;+\; 0.010 \,\right]^g$$

$$\left[\, \sigma \;=\; 0.139 \text{ inch} \,\right]^g$$

Uncertainty at 95% confidence for crack length of about [0.6 inch = 0.244 inch and for crack length of about 1 inch = 0.247 inch]^g

Average Depth

$$\left[\, d_{avg,true} \;=\; 0.914 \times d_{avg,nde} \;+\; 0.687 \,\right]^g$$

$$\left[\, \sigma \;=\; 7.8\% \,\right]^g$$

Uncertainty at 95% confidence for average depth of about 40% = [10.1%]^g

Maximum Depth

$$\left[\, d_{max,true} \;=\; 0.939 \times d_{max,nde} \;-\; 0.923 \,\right]^g$$

$$\left[\, \sigma \;=\; 14.2\% \,\right]^g$$

Uncertainty at 95% confidence for maximum depth of about 55% = [19.1%]^g

4.7 Axial PWSCC Growth Rates

This section describes the methods applied for development of growth rates for axial PWSCC at dented TSP intersections. Growth rate values are obtained for indication length, maximum depth, and average depth.

4.7.1 Methods Applied for Growth Analyses

In order to develop applicable growth rates, inspection results from two successive outages are required. Based on the current plugging philosophies employed by the industry, crack-like indications are repaired upon detection. As a consequence, previous inspection data must be "forced" in some cases, based on the low relative signal strength for the previous cycle data. The analysts who participated in the NDE

Performance Test performed analyses of the NDE profiles for growth data except as described below. The same analyst evaluated the data from both inspections to obtain the growth rates. The NDE adjustment procedure described in Section 4.2.2 is applied to the profiles to obtain the growth rates. Growth data are obtained from Sequoyah-1 Cycles 8 and 9 and from Cycle 8 for both Diablo Canyon Units 1 and 2. A growth data point is defined only when the indication can be sized for both cycles. In some cases, the prior cycle indication was too small to be detected or sized. When the later cycle indication was large, the prior cycle data could be sized so that omitting the data with no prior cycle indication does not affect the large growth rate tail of the growth distribution. The growth rates are developed on a per EFPY basis. The cycle lengths for Sequoyah-1 Cycle 8 was 1.236 EFPY and Cycle 9 was 1.293 EFPY. The cycle length for Cycle 8 of Diablo Canyon-1 was 1.284 EFPY and for Diablo Canyon-2 was 1.622 EFPY.

The NDE data from the two plants are temperature corrected to combine the data sets. T_{hot} for both cycles of Seqouyah-1 was 611°F and for both Diablo Canyon Units was 603°F. The Arrhenius equation used for the temperature adjustment is given by:

$$\text{Rate proportional to: } \exp(-Q/RT)$$

where Q is commonly described as the "Activation Energy". The Arrhenius equation is commonly used for both crack initiation and growth with Q values for initiation higher than for growth. A propagation Q value of 32.5 kcal/mole for PWSCC crack growth in mill annealed Alloy 600 tubing is applied for the temperature correction. The 32.5 kcal/mole value is an average of an unpublished Westinghouse evaluation of 32 kcal/mole and an unpublished French evaluation of 33 kcal/mole. Laboratory measurements of the crack propagation rate in Alloy 600 have been reported in the EPRI report of Reference 8-31. The Q value developed in this report is 32.4 kcal/mole, which is consistent with the 32.5 value used in this report. Applying the Arrhenius equation with Q = 32.5 kcal/mole for a temperature increase from 603 to 611°F results in a PWSCC growth rate increase of 22%.

For the Cycle 8 data, growth rates were developed as part of the NDE Performance Test. Sequoyah Unit 1 Cycle 9 depth profiles were provided separately by TVA. NDE analysts trained on the analysis guidelines of this report were used for the Cycle 9 analyses and the NDE data were processed using the adjustment procedures of Section 4.2.2. Evaluation of the growth rates was then performed for each applicable plant individually, and then combined. Growth rates are developed on an effective full power year (EFPY) basis so that the combined growth rate data set can be applied to either applicable plant by multiplying the EFPY growth rates times the cycle length in EFPY. Growth allowances used in operational assessments are taken from histograms, which provide the number of indications in each growth bin and the cumulative probability distribution functions for the Sequoyah and Diablo Canyon growth data sets. Sequoyah will apply Sequoyah specific growth data and Diablo Canyon will apply combined growth data until 200 growth data points are obtained from Diablo Canyon SGs. In preparing the cumulative probability distributions, negative growths are set to zero.

4.7.2 Sequoyah PWSCC Growth Rates

The largest portion of the combined plant growth database is obtained for Sequoyah Unit 1. Growth rates per EFPY as a cumulative probability distribution function for the combined Sequoyah Unit 1 Cycle 8 and Cycle 9 dataset at 611°F are graphically displayed in Figure 4-14. Average and 95% cumulative probability growth rates for Sequoyah Unit 1 with a T_{hot} of 611 °F are provided in Table 4-7 as well as adjusted growth values based on a T_{hot} of 603 °F. Growth distributions for axial length,

maximum depth, average depth and voltage are provided. Voltage data are provided for information only as they are not used in the depth based analyses of this report. The individual intersection growth data were adjusted by the cycle length to obtain growth values on an EFPY basis. The growth data, as shown in Figure 4-14, have a large contribution of negative and zero growth values with the negative growths applied as zero growth for the cumulative probability distributions. In general, the indications are small and the NDE sizing tends to overestimate the depths (including after the adjustments) for small indications. As a result, very small growth may become negative in the growth evaluations. All applications of the growth rates apply zero growth for negative growth indications.

4.7.3   Diablo Canyon PWSCC Growth Rates

The growth rates for both Diablo Canyon Units 1 and 2 were combined into a single set of Diablo Canyon growth data. The individual intersection growth data were adjusted by the cycle length to obtain growth values on an EFPY basis. The cumulative probability distribution function for the Diablo Canyon dataset at 603°F and adjusted to 611°F are shown in Figures 4-15 and 4-16. Average and 95% cumulative probability growth rates for Diablo Canyon with a T_{hot} of 603 °F are provided in Table 4-7 as well as adjusted growth values based on a T_{hot} of 611°F. The average values for growth in depth are negative for Diablo Canyon, which reflects the smaller indications due to the lower operating temperatures and the tendency to overestimate depths for the smaller indications.

4.7.4   Comparison of the Data Bases

A set of simple statistical tests were performed based on the assumption of normality of the data. The length data from Diablo Canyon does not appear to satisfy this assumption, but it is apparent that no more refined tests would change the conclusions regarding the mean and variance, and standard deviation, of the underlying population. The data from the two plant sites were compared for equality of means and equality of variances. The results are summarized in the following table.

Comparison of the Sequoyah & Diablo Plants' Data					
Type Test	Probability Result	Length	Average Depth	Maximum Depth	Maximum Volts
t - Test	$Pr(\mu_S = \mu_D)$	0.23%	1.28%	2.31%	9.12%
F - Test	$Pr(\sigma_S = \sigma_D)$	0.001%	88.6%	25.7%	2.68%

In summary, the null hypothesis that the means, μ_S for Sequoyah and μ_D for Diablo Canyon, of the populations from which the data were drawn would be rejected at a 5% level for the geometry comparisons, but not the maximum volts. In addition, the hypothesis that the variances of the populations from which the data were drawn would be rejected for the length and maximum volts. This means combining of the growth data from each plant is not justified on mathematical grounds. The use of the combined data would be conservative for Diablo Canyon, but the growth rates for use at Sequoyah should be based only on the Sequoyah data. The cumulative distribution functions for the data are illustrated on Figures 4-17 through 4-20. The same conclusions could be drawn by inspection of the data, for which the variances of the depth growth are similar, but the means are not.

4.7.5   Combined Sequoyah and Diablo Canyon PWSCC Growth Rates

Due to the modest number of +Point indications that can be sized to obtain growth rates, it is desirable to combine the growth data from Sequoyah and Diablo Canyon SGs, particularly for application to the Diablo Canyon SGs. There are a total of 131 indications, including 96 values for Sequoyah SGs and 35 values for Diablo Canyon SGs, which can be applied to develop the combined data set. Normalization of data for temperature differences is necessary for PWSCC indications. For PWSCC, corrosion and growth data can generally be acceptably combined for plants with the same SG design and tube material as discussed below. However, as shown in Section 4.7.4, the available data cannot be statistically shown to be samples from the same population. Therefore, the data are not combined for Sequoyah applications. Due to the lower growth rates found in Diablo Canyon, the combined data set is applied for Diablo Canyon to obtain conservative growth distributions and compensate for the smaller dataset. For ODSCC degradation, significant variation in growth rates can occur between plants due to differences in secondary chemistry. Primary side chemistry does not significantly vary from plant to plant and PWSCC growth rate differences are primarily dependent upon stress and temperature. Denting provides the stress for PWSCC at TSP intersections. While denting spans a range of sizes, the characteristics of denting are local indentations with ovalization and ovalization with negligible indentation. Profilometry of the dents in Sequoyah and Diablo Canyon SGs have shown predominantly local indentations with ovalization and this geometry was the basis for the laboratory simulations of the field indications prepared in this program. Due to the similarities of the dent geometries and dent sizes between the Sequoyah and Diablo Canyon SGs, the stress ranges at dented intersections can be expected to be similar between these two plants. The primary difference between growth rates at the dented intersections would be due to temperature. The Arrhenius equation can then be applied to normalize the growth rates between the Sequoyah and Diablo Canyon SGs. The similarity of dent ranges between these plants and the ability to adjust growth rates for temperature differences would generally provide the basis for combining the two plant's growth rate data. The strong similarity of PWSCC growth rates between similarly stressed regions has been demonstrated for axial PWSCC in tubesheet expansion transitions as shown by European ARC experience. The EPRI report of Reference 8-19 for an expansion zone ARC also recommends application of a common growth distribution for axial PWSCC. However, the combined data set is applied only for Diablo Canyon SGs for which the combined data increases conservatism. For Sequoyah, only the Sequoyah growth data are applied as this dataset is slightly more conservative than the combined data set.

Since Sequoyah Unit 1 and Diablo Canyon Units 1 and 2 operate at significantly different reactor coolant hot leg temperatures (T_{hot}), the growths must be adjusted to account for temperature effects in order to combine the data sets. The T_{hot} value for Sequoyah Unit 1 is 611°F, while the T_{hot} value for Diablo Canyon Units 1 and 2 is 603°F. The difference in hot leg temperatures is expected to influence the growth rates by approximately 22% for an 8 degree hot leg temperature difference as discussed in Section 4.7.1. Therefore, in the combined growth rate data set for a hot leg temperature of 603°F, the Sequoyah Unit 1 growth rate values were reduced by 22%. In the combined data set for a hot leg temperature of 611°F, the Diablo Canyon growth rates were increased by 22%. The combined growth per EFPY data set at 611°F is given in Table 4-8. Average and 95% cumulative probability growth rates for the combined Sequoyah and Diablo Canyon data set for 603°F and 611°F are provided in Table 4-8 and the cumulative probability distributions are shown in Figures 4-21 and 4-22. Growth distributions for axial length, maximum depth, average depth and voltage are provided.

It is seen from the data of Table 4-7 that the Sequoyah and Diablo Canyon growth data are in reasonably good agreement for the 95% values when adjusted to the same T_{hot}. The growth values from Sequoyah

are slightly larger than for Diablo Canyon when adjusted to the same T_{hot}. The small differences may be attributable to the larger population of indications from the Sequoyah SGs. In particular, the Diablo Canyon growth data only has three indications with lengths ≥ 0.4 inch while the Sequoyah data have 19 indications in this range. Combining the data results in application of the large growth rate tail to the distribution for Diablo Canyon. The combined data increases the depth growth rates at 95% probability by about 3% for Diablo Canyon.

The Sequoyah and the combined growth distributions are used in the Monte Carlo operational assessments for Sequoyah and Diablo Canyon, respectively, as described in Section 7 to determine the need for tube repair.

Table 4-1. Comparison of NDE Uncertainties for "Blind", Appendix H and NDE Performance Test Analyses			
NDE Analysis and Parameters	Mean Error (DE – NDE)	Standard Deviation	NDE Error at 95% Confidence
"Blind" Analyses[1]			
• Length	-0.04"	0.11"	0.14"
• Average Depth	-3.36%	7.25%	8.60%
• Maximum Depth Averaged over Coil Field (0.16")	-4.98%	11.95%	14.75%
• Local Maximum Depth	2.86%	11.46%	21.77%
"Blind" Analyses Without Adjustments			
• Length	-	-	-
• Average Depth	-5.61%	8.83%	8.97%
• Maximum Depth Averaged over Coil Field (0.16")	-9.02%	15.73%	16.95%
• Local Maximum Depth	-1.18%	15.02%	23.61%
Appendix H Peer Review Analyses[2]			
• Length	0.04"	0.14"	0.25"
• Average Depth	-4.66%	8.65%	9.61%
• Maximum Depth Averaged over Coil Field (0.16")	-6.87%	13.9%	16.1%
• Local Maximum Depth	0.70%	13.9%	21.9%
NDE Performance Test Analyses[1]			
• Length			
• Average Depth			
• Maximum Depth Averaged over Coil Field (0.16")			
• Local Maximum Depth			
NDE Performance Test Analyses Without Adjustments			
• Length			
• Average Depth			
• Maximum Depth Averaged over Coil Field (0.16")			
• Local Maximum Depth			

g

Notes:
1. Analyses include results for multiple analysts (up to 4 for "blind" analyses and 3 for NDE Performance Test) and a larger number of specimens than the Appendix H review
2. Analyses include length adjustment but not depth adjustments of Section 4.2.2. Results are for a single consensus analysis of the peer review group.

Table 4-2a	
Summary of Specimens and Maximum Depths for NDE Performance Test	
Bobbin Detection (244 units)	**+Point Detection and Sizing (203 units)**

3 Pulled Tube Specimens
  10/22-2H (38.0%), 12/32-1H (91.1%),
  21/43-1H (90.5%)

39 Laboratory Specimens
  > 0 < 30%: 3-4H (7.7%), 4-4H (15.0%),
    12-3H (22.7%), 2-3H (23.2%),
    12-2H (23.4%), 12-4H (26.3%),
    3-3H (29.1%)
  30 < 40%: 7-1H(30.1%), 2-1H (33.5%),
    7-3H (34.8%), 2-5H (35.5%),
    13-3H (37.3%), 5-1H (35.0%)
  40 < 50%: 9-1H (43.7%), 8-3H (44.2%),
    8-2H (45.8%), 2-4H (47.6%),
    1-3H (47.9%)
  50 < 60%: 8-1H (52.2%), 1-4H (54.3%)
  60 < 70%: 6-4H (64.3%), 6-3H (67.3%)
  70 < 80%: 9-4H (71.7%), 6-2H (73.7%),
    9-5H (74.6%), 6-5H (77.9%)
  80 < 90%: 10-4H (81.8%), 6-1H (83.7%),
    9-3H (84.6%)
  90 ≤100%:11-3H (91.3%), 11-4H (95.3%),
    9-2H (95.1%), 10-3H (96.2%),
    11-2H (96.87%), P9 (99.4%),
    P7 (99.8%), P8 (99.7%),
    P10 (100%), P11 (100%)

30 Diablo Canyon Indications
    14/69-1H,2H,3H; 21/43-2H,3H;
    12/32-2H, 3H; 10/22-1H, 3H; 13/24-4H;
    29/24-2H; 26/22-4H; 29/22-2H; 27/36-3H
    24/15-2H; 10/20-2H; 11/20-2H;
    Repeat 10/22-2H; 9/30-1H;
    Repeat 12/32-1; Repeat 12/32-1H;
    31/32-3H; 21/37-4H; 9/38-2H; 25/38-2H;
    21/43-1H; Repeat 21/43-1H; 13/44-1H;
    9/45-1H; Repeat 14/69-2H

20 Sequoyah Indications
    10/3-2H; 15/3-3H; 12/6-2H; 7/7-3H;
    15/12-2H; 17/14-2H; 19/32-1H; 20/36-1H
    21/40-2H; 7/44-4H; 44/44-1H; 15/55-2H;
    24/60-1H; 14/65-1H; 23/67-1H; 6/70-1H;
    11/70-1H; 26/72-1H; 14/74-2H; 15/77-1H

152 NDD TSP Intersections (Dented)
    Laboratory Specimens:
  a. 65 original intersections (pre-exposure)
  b. 35 original intersections (duplicates)
  c. 52 Field intersections
      1. 10 TVA
      2. 42 PGE

---

4 Pulled Tube Specimens
  10/22-2H (38.0%), 21/43-1H-C2 (45.5%),
  21/43-1H-C1 (90.5%), 12/32-1H (91.1%)

52 Laboratory Specimens
  0 < 30%: 3-4H-1 (7.7%), 12-3H-1 (22.7%),
    4-4H-1 (15.0%), 9-4H-2 (23.1%),
    2-3H-1 (23.2%), 12-2H-1 (23.4%),
    9-1H-2 (25.4%), 12-4H-1 (26.3%),
    3-3H-1 (29.1%)
  30 < 40%: 7-1H-1 (30.1%), 2-1H-1 (33.5%),
    7-3H-1 (34.8%), 5-1H-1 (35.0%),
    2-5H-1 (35.5%), 13-3H (37.3%),
    9-5H-2 (38.0%), 10-3H-2 (39.8%)
  40 < 50%: 11-2H-2 (43.0%), 9-1H-1 (43.7%),
    11-4H-2 (44.0%), 8-3H-1 (44.2.0%),
    8-2H-1 (45.8%), 9-2H-2 (46.3%),
    2-4H-1 (47.6%), 1-3H-1 (47.9%)
  50 < 60%: 8-1H (52.2%), 9-3H-2 (54.1%),
    1-4H-1 (54.3%)
  60 < 70%: 6-4H-1 (64.3%), 6-3H-1 (67.3%)
  70 < 80%: 9-4H-1 (71.7%), 6-2H-1 (73.7%),
    9-5H-1 (74.6%), 6-5H-1 (77.9%),
  80 < 90%: 10-4H (81.8%), 6-1H-1 (83.7%),
    9-3H-1 (84.6%), P7-2 (89.7%),
  90 ≤100%: P10-2 (90.9%), P11-2 (90.3%),
    11-3H-1 (91.3%), 9-2H-1 (95.1%),
    11-4H-1 (95.3%), 10-3H-1 (96.2%),
    11-2H-1 (96.8%), P9-1 (99.4%),
    P9-2 (99.4%), P8-1 (99.6%),
    P8-2 (99.7%), P7-1 (99.8%),
    P10-1 (100%), P11-1 (100%)

3 Diablo Canyon Indications
  Repeat 10/22-2 (38.0%), 21/64-1 (83.8%),
  Repeat 21/43-1 (90.5%),

144 NDD TSP Intersections (Dented)
  Laboratory Specimens
    a. 65 original intersections (pre-exposure)
    b. 35 original intersections (duplicates)
    c. 44 Field (PGE) intersections

Table 4-2b Summary of Specimens and Maximum Depths for NDE Training	
Bobbin	**+Point**
156 Specimens Used for Training	Sizing Training
1 Pulled Tube Specimen TVA 21/64-1H (96%)	**1 Pulled Tube Specimen** TVA 21/64-1H (96%)
1 Laboratory Specimens with Destructive Data P12 (100%)	**8 Laboratory Specimens with Destructive Data** P12-1(100%), P12-2 (95.8%), P12-5 (90.3%), 5/1H (42.0%), 9/1H-1 (38.8%) ,9/1H-2 (34.5%), 9/4H-1 (70.2%),9/4H-2 (65.0%)
32 Laboratory Specimens without Destructive Data (All Specimens had DDI indications) 1/1H, 1/2H, 1/5H, 2/2H, 3/1H, 3/2H, 3/5H, 4/1H, 4/2H, 4/3H, 4/4H, 4/5H, 5/2H, 5/3H, 5/4H, 5/5H, 7/2H, 7/4H, 7/5H, 8/4H, 8/5H, 10/1H, 10/2H, 10/5H, 11/1H, 11/5H, 12/1H, 12/5H, 13/1H, 13/2H, 13/4H, 13/5H	**31 Laboratory Specimens without Destructive Data** (Sizing based on expert opinion, supported by ID dye penetrant results) 1/1H, 1/2H, 1/5H, 2/2H, 3/1H, 3/2H, 3/5H, 4/1H, 4/2H, 4/3H, 4/5H, 5/2H, 5/3H, 5/4H, 5/5H, 7/2H, 7/4H, 7/5H, 8/4H, 8/5H, 10/1H, 10/2H, 10/5H, 11/1H, 11/5H, 12/1H, 12/5H, 13/1H, 13/2H, 13/4H, 13/5H
62 PGE Field Intersections 27 - 4/97 (1R7) intersections 35 - 10/98 (1R8) intersections	
61 TVA (1C8) Field Intersections 10 NDD 50 SAI (RPC-confirmed bobbin distorted dent indications)	**Detection Training** **31 Laboratory Specimens without Destructive Data** (Same as Sizing Population) **60 Field Intersections** 30 PGE Intersections 30 TVA Intersections

Table 4-3. Distribution of Specimen Crack Depths, Lengths and Dent Volts						
Crack Depth - % Throughwall						
0-20%	20-30%	30-40%	40-50%	50-60%	60-80%	80-100%
Average Maximum Depth (Coil Field Average – 0.16")						
3-4H, 4-4H, 12-3H	10/22, 2-3H, 3-3H, 9-1H-2, 9-5H-2, 12-2H, 12-4H, 9-4H-2	2-1H, 2-5H, 5-1H, 7-1H, 7-3H, 9-1H-1, 10-3H-2, 11-2H-2, 13-3H	21/43-2, P7-3, 1-3H, 2-4H, 8-2H, 8-3H, 9-2H-2, 11-3H-2, 11-4H-2	1-4H, 8-1H, 9-3H-2,	6-2H, 6-3H, 6-4H, 6-5H, 9-3H-2, 9-4H-1, P12-2, P12-5, 9-5H-1	21/43-1, 12/32, P7-1, P7-2, P8-1, P8-2, P9-1, P9-2, P10-1, P10-2, P11-1, P11-2, P12-1, 6-1H, 9-2H-1, 9-3H-1, 10-3H-1, 10-4H-1, 11-2H-1, 11-3H-1, 11-4H-1
Local Maximum Depth						
3-4H-1	9-5H-3, 12-3H-1, 4-4H-1	10/22, 2-3H-1, 3-3H-1, 7-1H-1, 9-1H-2, 9-5H-2, 12-2H-1, 12-4H-1, 9-4H-2	21/43-2, 2-1H-1, 2-5H-1, 5-1H, 7-3H-1, 8-3H-1, 9-1H-1, 10-3H-2, 11-2H-2, 11-4H-2, 13-3H-1	1-3H-1, 2-4H-1, 8-1H-1, 8-2H-1, 11-3H-2	P7-3-1, 1-4H-1, 6-3H-1, 6-4H-1, 9-2H-2, 9-3H-2	21/43-1, P10-1, P10-2, P11-1, P11-2, P12-1, P12-2, P12-5, P7-1, P7-2, P8-1, P8-2, P9-1, P9-2, 9-2H-1, 9-4H-1, 11-2H-1, 11-4H-1, 11-3H-1, 6-1H-1, 6-5H-1, 9-3H-1, 6-2H-1, 9-5H-1, 10-4H-1, 10-3H-1, 21/64, 12/32
Average Depth						
2-3H-1, 2-5H-1, 3-4H-1, 9-5H-3, 12-3H-1, 4-4H-1	10/22, 2-11H-1, 2-4H-1, 3-3H-1, 7-1H-1, 7-3H-1, 9-5H-2, 9-1H-2, 12-2H, 12-4H, 13-3H, P12-2	21/43-2, 1-3H, 1-4H, 8-2H, 8-3H, 9-1H-1, 9-2H-2, 10-3H-2, 11-2H-2, 11-4H-2, 11-3H-2	21/43-1, 8-1H-1, 9-3H-2, 9-4H-2, P7-3, 6-4H-1	6-3H, 6-5H, 9-4H-1, 9-5H-1, 12/32-1, 8-2H-1	P8-2, P9-1, P10-2, P11-2, P12-1, P12-5, 9-3H-1, 10-3H-1, 10-4H-1, 11-3H, 11-4H-1, 6-1H-1, 9-2H-1, 21/64-1	P7-1, P7-2, P8-1, P9-2, P10-1, P11-1, 11-2H-1
Total Crack Length						
0-0.3"	>0.3-0.4"	>0.4-0.5"	>0.5-0.7"	>0.7-1.0"	>1.0-1.5"	>1.5"
10/22, 21/43-2, P7-3, P12-5, 3-3H, 3-4H, 5-1H, 9-5H-2, 9-5H-3, 11-2H-2, 12-2H, 12-3H	8-2H, 9-4H-2, 12-4H, 13-3H	2-3H, 6-4H, 8-1H, 8-3H, 9-1H-1, 10-3H-2	12/32, P7-2, P11-1, P11-2, P12-2, 1-3H, 2-4H, 6-2H, 6-3H, 6-5H, 7-1H, 7-3H, 9-5H-1, 10-4H	21/43-1, P7-1, 1-4H, 2-1H, 2-5H, 6-1H, 9-2H-2, 9-3H-1, 9-3H-2, 9-4H-1, 10-3H-1, 11-2H-1, 11-4H-2	P12-1, 9-2H-1, 11-3H, 11-4H-1	P8-1, P8-2, P9-1, P9-2, P10-1, P10-2

Table 4-3. Distribution of Specimen Crack Depths, Lengths and Dent Volts						
Bobbin Dent Voltage						
< 2	>2-3	>3-4	Estimated < 3 v[1]	>4-5	>5-10	> 10
12/32, 2-4H, 6-2H, 6-5H, 8-1H, 8-2H, 8-3H, 8-5H, 9-1H, 9-2H, 9-3H, 9-4H, 9-5H, 10-3H, 10-4H, 11-2H, 11-3H, 11-4H, 12-2H, 12-3H, 12-4H, 13-3H	10/22, 1-3H, 1-4H, 2-3H, 2-5H, 5-1H, 6-1H, 6-3H, 6-4H,	21/43, 2-1H	P-7, P-8, P-9, P-10, P-11, P-12	7-3H	3-3H, 3-4H, 7-1H	

Notes:

1. The 1996 specimens designated with a P prefix did not have dent voltages measured prior to cracking. The specimens were prepared by tube ovalization and have diameter reductions (< 4 mils radial) similar to those found for dents < 3 volts. It is reasonable to assign < 3 volt dents to these indications for bobbin detection considerations.

Table 4-4. Summary of Bobbin Detection Results from NDE Performance Test

Specimen (Largest Crack Applied)	TSP	Dent Volts[1]	Max. Depth Lig. Corr. (%)	Avg, Depth Lig. Corr. (%)	Resolution Analysts 1 & 2 Bobbin Calls
3	4H	5.22	7.7	6.4	
4	4H	6.29	15.0	9.6	
2	3H	2.16	21.5	15.2	
12	3H	1.32	16.0	16.0	
2	5H	2.88	35.5	18.3	
12	4H	1.18	26.3	20.2	
7	1H	4.40	30.1	20.1	
12	2H	1.54	23.4	20.8	
2	1H	3.73	33.4	21.8	
10/22	2H	2.39	23.2	23.2	
3	3H	6.17	29.1	23.4	
7	3H	3.70	34.4	25.0	
13	3H	0.91	37.3	27.3	
2	4H	1.30	47.6	29.0	
5	1H	2.28	30-35 [3]	20-30 [3]	
9	1H	1.34	38.8	30.9	
8	3H	1.61	44.2	31.8	
8	2H	0.93	45.8	37.1	
1	4H	1.84	54.3	36.7	
1	3H	2.78	47.9	39.4	
8	1H	1.42	52.2	40.7	
21/43	1H	3.87	45.5	49.3	
6	4H	1.12	64.3	49.4	
6	5H	1.06	77.9	54.1	

g

Average Depth

Depth Range	Number Specimen Dents <4.5 Volts	Number Detected Sum of Reso 1&2	Fraction Detected (Note 2)	Percent Detected	Bobbin with RPC Confirmation
0-10%	0				
10-20%	3				
20-30%	9				
30-40%	5				
40-50%	3				
50-60%	6				
60-70%	6				
70-80%	2				
80-90%	3				
90-100%	2				
Sum	39				
Sum >20%	36				

Table 4-4. Summary of Bobbin Detection Results from NDE Performance Test

Specimen (Largest Crack Applied)	TSP	Dent Volts[1]	Max. Depth Lig. Corr. (%)	Avg, Depth Lig. Corr. (%)	Resolution Analysts 1 & 2 Bobbin Calls	Number Detected Sum of Reso 1&2	Fraction Detected (Note 2)	Percent Detected	Bobbin with RPC Confirmation
6	3H	2.24	67.3	56.1					
9	4H	1.2	70.2	56.4					
12/32	1H	1.21	88.9	57.5					
9	5H	0.93	74.6	57.5					
6	2H	1.84	73.7	59.1					
6	1H	1.05	83.7	60.5					
9	3H	1.23	84.6	60.9					
9	2H	1.24	95.1	67.4					
10	4H	0.95	81.8	63.6					
11	3H	1.34	91.3	68.4					
11	4H	2.49	95.3	68.7					
10	3H	0.74	96.2	73.2					
P9	1H		99.5	75.3					
11	2H	0.78	96.8	81.4					
P8	1H		99.6	84.8					
P10	1H		100.0	88.7					
P7	1H		99.8	94.3					
P11	1H		100.0	95.6					

Depth Range	Number Specimen Dents <4.5 Volts
0-10%	0
10-20%	1
20-30%	5
30-40%	7
40-50%	3
50-60%	2
60-70%	2
70-80%	4
80-90%	4
90-100%	11
Sum	39
Sum >20%	38

Notes:
1. Dent volts based on average of post-cracking sizing analyses from NDE Performance Test or pre-cracked dent voltage when data not available from the performance test.
2. Fraction detected based on sum of both resolution analyses divided by twice the number of test specimens.
3. Respective values of 35% and 30% were used in the regression analyses.
4. Detection results from + Point analyses shown in parentheses. All other indications were confirmed by + Point inspection.

Table 4-5. Summary of + Point Detection Results from NDE Performance Test											
Specimen	TSP	Crack No.	Dent Volts[1]	Maximum Depth Lig. Corr. (%)	Average Depth Lig. Corr. (%)	Resolution Analysts 1 & 2 +Point Calls	Depth Range	Number Test Specimens	Number Detected Sum of Reso 1&2	Fraction Detected (Note 2)	Percent Detected
3	4H	1	5.22	7.7	6.4				Average Depth		
4	4H	1	6.29	15.0	9.6		0-10%				
2	3H	1	2.16	21.5	15.2		10-20%				
12	3H	1	1.32	16.0	16.0		20-30%				
2	5H	1	2.88	35.5	18.3		30-40%				
9[3]	4H	2	1.2	23.1	10-20		40-50%				
12	4H	1	1.18	26.3	20.2		50-60%				
7	1H	1	4.40	30.1	20.1		60-70%				
12	2H	1	1.54	23.4	20.8		70-80%				
2	1H	1	3.73	33.4	21.8		80-90%				
10/22	2H	1	2.39	23.2	23.2		90-100%				
3	3H	1	6.17	29.1	23.24		Sum				
7	3H	1	3.70	34.4	25.0		Sum >20%				
9	1H	2	1.34	25.4	25.4						
9	5H	2	0.93	26.7	26.8						
13	3H	1	0.91	37.3	27.3						
2	4H	1	1.3	47.6	29.0						
5	1H	1	2.28	30-35[4]	20-30[4]						
8	3H	1	1.61	44.2	31.8						
9	1H	1	1.31	38.8	30.9						
10	3H	2	0.74	38.0	31.7						
11	2H	2	0.78	32.8	32.8						
9	2H	2	1.24	46.3	35.6						

Table 4-5. Summary of + Point Detection Results from NDE Performance Test

Specimen	TSP	Crack No.	Dent Volts[1]	Maximum Depth Lig. Corr. (%)	Average Depth Lig. Corr. (%)	Resolution Analysts 1 & 2 +Point Calls	Depth Range	Number Test Specimens	Number Detected Sum of Reso 1&2	Fraction Detected (Note 2)	Percent Detected
11	4H	2	2.49	44.0	36.6						
8	2H	1	0.93	45.8	37.1		0-10%				
1	4H	1	1.84	54.32	36.7		10-20%				
1	3H	1	2.78	47.9	39.4		20-30%				
21/43	1H	2	3.82	45.5	39.6		30-40%				
8	1H	1	1.42	52.2	40.7		40-50%				
9	3H	2	1.23	54.1	40.8		50-60%				
21/43	1H	1	3.87	90.5	49.3		60-70%				
6	4H	1	1.12	64.3	49.4		70-80%				
6	5H	1	1.06	77.9	54.1		80-90%				
6	3H	1	2.24	67.3	56.1		90-100%				
9	4H	1	1.2	70.2	56.4		Sum				
12/32	1H	1	1.21	88.9	57.5		Sum >20%				
9	5H	1	0.93	74.6	57.5						
6	2H	1	1.84	73.7	59.1						
6	1H	1	1.05	83.7	60.5						
9	3H	1	1.23	84.6	60.9						
10	4H	1	0.95	81.8	63.6						
9	2H	1	1.24	95.1	67.4						
11	3H	1	1.34	91.3	68.4						
11	4H	1	2.49	95.3	68.7						
P10	1H	2		90.9	69.0						
10	3H	1	0.74	96.2	73.2						
P11	1H	2		90.3	74.6						
P9	1H	1		99.5	75.3						
P8	1H	2		99.7	79.4						

(Right-hand summary block is headed "Maximum Depth" spanning the Number Detected / Fraction / Percent columns.)

Table 4-5. Summary of + Point Detection Results from NDE Performance Test											
Specimen	TSP	Crack No.	Dent Volts[1]	Maximum Depth Lig. Corr. (%)	Average Depth Lig. Corr. (%)	Resolution Analysts 1 & 2 +Point Calls	Depth Range	Number Test Specimens	Number Detected Sum of Reso 1&2	Fraction Detected (Note 2)	Percent Detected
11	2H	1	0.78	96.8	81.4		g				
P7	1H	2		89.7	82.5						
P8	1H	1		99.6	84.8						
P9	1H	2		99.4	86.6						
P10	1H	1		100.0	88.7						
P7	1H	1		99.8	94.3						
P11	1H	1		100.0	95.6						

Notes:

1. Dent volts based on average of post-cracking sizing analyses from NDE Performance Test or pre-cracked dent voltage when data not available from the performance test.

2. Fraction detected based on sum of both resolution analyses divided by twice the number of test specimens.

3. Although the total crack profile was not measured in destructive exam, the average depth can be reasonably estimated at about 19% for use in the POD evaluation.

4. Respective values of 35% and 30% were used in the regression analyses.

Table 4-6
NDE Performance Test +Point Sizing
Summary of Analysts Results

Ins. Year	Row	Column	Location	Crack No.	Analyst	Unadjusted NDE				Adjusted NDE				EXAM Unadjusted DE		
						Length (in.)	Max. Depth (%)	Avg. Depth (%)	Max. Volts	Length (in.)	Max. Depth (%)	Avg. Depth (%)	Max. Volts	Length (in.)	Max. Depth (%)	Avg. Depth (%)
1998	1	85	01H	1	D9674											
1998	1	85	01H	1	S4373											
1998	1	85	01H	1	T9093											
1998	1	91	01H	1	D9674											
1998	1	91	01H	1	S4373											
1998	1	91	01H	1	T9093											
1998	1	91	01H	2	D9674											
1998	1	91	01H	2	S4373											
1998	1	91	01H	2	T9093											
1998	2	66	01H	1	D9674											
1998	2	66	01H	1	S4373											
1998	2	66	01H	1	T9093											
1998	2	66	01H	2	D9674											
1998	2	66	01H	2	S4373											
1998	2	66	01H	2	T9093											
1998	5	18	01H	1	D9674											
1998	5	18	01H	1	S4373											
1998	5	18	01H	1	T9093											
1998	5	18	01H	2	D9674											
1998	5	18	01H	2	S4373											
1998	5	18	01H	2	T9093											
1998	6	24	01H	1	D9674											
1998	6	24	01H	1	S4373											
1998	6	24	01H	1	T9093											
1998	6	31	01H	1	D9674											
1998	6	31	01H	1	S4373											
1998	6	31	01H	1	T9093											
1998	6	31	01H	2	D9674											
1998	6	31	01H	2	S4373											
1998	6	31	01H	2	T9093											
1998	6	64	01H	1	D9674											
1998	6	64	01H	1	S4373											
1998	6	64	01H	1	T9093											
1998	6	64	01H	2	D9674											
1998	6	64	01H	2	S4373											
1998	6	64	01H	2	T9093											
1998	9	7	01H	1	D9674											
1998	9	7	01H	1	S4373											
1998	9	7	01H	1	T9093											
1998	9	7	01H	2	D9674											
1998	9	7	01H	2	S4373											
1998	9	7	01H	2	T9093											
1998	9	19	01H	1	D9674											
1998	9	19	01H	1	S4373											
1998	9	19	01H	1	T9093											
1998	9	19	01H	2	D9674											
1998	9	19	01H	2	S4373											
1998	9	19	01H	2	T9093											

Table 4-6
NDE Performance Test +Point Sizing
Summary of Analysts Results

Ins. Year	Row	Column	Location	Crack No.	Analyst	Unadjusted NDE Length (in.)	Unadjusted NDE Max. Depth (%)	Unadjusted NDE Avg. Depth (%)	Unadjusted NDE Max. Volts	Adjusted NDE Length (in.)	Adjusted NDE Max. Depth (%)	Adjusted NDE Avg. Depth (%)	Adjusted NDE Max. Volts	EXAM Unadjusted DE Length (in.)	EXAM Unadjusted DE Max. Depth (%)	EXAM Unadjusted DE Avg. Depth (%)
1998	9	37	01H	1	D9674											
1998	9	37	01H	1	S4373											
1998	9	37	01H	1	T9093											
1998	9	64	01H	1	D9674											
1998	9	64	01H	1	S4373											
1998	9	64	01H	1	T9093											
1998	13	7	01H	1	D9674											
1998	13	7	01H	1	S4373											
1998	13	7	01H	1	T9093											
1998	13	16	01H	1	D9674											
1998	13	16	01H	1	S4373											
1998	13	16	01H	1	T9093											
1998	13	16	01H	2	D9674											
1998	13	16	01H	2	S4373											
1998	13	16	01H	2	T9093											
1998	13	34	01H	1	D9674											
1998	13	34	01H	1	S4373											
1998	13	34	01H	1	T9093											
1998	13	59	01H	1	D9674											
1998	13	59	01H	1	S4373											
1998	13	59	01H	1	T9093											
1998	13	85	01H	1	D9674											
1998	13	85	01H	1	S4373											
1998	13	85	01H	1	T9093											
1998	17	43	01H	1	D9674											
1998	17	43	01H	1	S4373											
1998	17	43	01H	1	T9093											
1998	17	58	01H	1	D9674											
1998	17	58	01H	1	S4373											
1998	17	58	01H	1	T9093											
1998	19	38	01H	1	D9674											
1998	19	38	01H	1	S4373											
1998	19	38	01H	1	T9093											
1998	19	38	01H	2	D9674											
1998	19	38	01H	2	S4373											
1998	19	38	01H	2	T9093											
1998	21	13	01H	1	D9674											
1998	21	13	01H	1	S4373											
1998	21	13	01H	1	T9093											
1998	21	13	01H	2	D9674											
1998	21	13	01H	2	S4373											
1998	21	13	01H	2	T9093											
1998	21	28	01H	1	D9674											
1998	21	28	01H	1	S4373											
1998	21	28	01H	1	T9093											
1998	21	31	01H	1	D9674											
1998	21	31	01H	1	S4373											
1998	21	31	01H	1	T9093											
1998	21	31	01H	2	D9674											
1998	21	31	01H	2	S4373											
1998	21	31	01H	2	T9093											

Table 4-6
NDE Performance Test +Point Sizing
Summary of Analysts Results

Ins. Year	Row	Column	Location	Crack No.	Analyst	Unadjusted NDE				Adjusted NDE				EXAM Unadjusted DE		
						Length (in.)	Max. Depth (%)	Avg. Depth (%)	Max. Volts	Length (in.)	Max. Depth (%)	Avg. Depth (%)	Max. Volts	Length (in.)	Max. Depth (%)	Avg. Depth (%)
1998	21	73	01H	1	D9674											
1998	21	73	01H	1	S4373											
1998	21	73	01H	1	T9093											
1998	21	79	01H	1	D9674											
1998	21	79	01H	1	S4373											
1998	21	79	01H	1	T9093											
1998	21	85	01H	1	D9674											
1998	21	85	01H	1	S4373											
1998	21	85	01H	1	T9093											
1998	23	15	01H	1	D9674											
1998	23	15	01H	1	S4373											
1998	23	15	01H	1	T9093											
1998	25	40	01H	1	D9674											
1998	25	40	01H	1	S4373											
1998	25	40	01H	1	T9093											
1998	25	52	01H	1	D9674											
1998	25	52	01H	1	S4373											
1998	25	52	01H	1	T9093											
1998	25	79	01H	1	D9674											
1998	25	79	01H	1	S4373											
1998	25	79	01H	1	T9093											
1998	27	77	01H	1	D9674											
1998	27	77	01H	1	S4373											
1998	27	77	01H	1	T9093											
1998	29	16	01H	1	D9674											
1998	29	16	01H	1	S4373											
1998	29	16	01H	1	T9093											
1998	29	34	01H	1	D9674											
1998	29	34	01H	1	S4373											
1998	29	34	01H	1	T9093											
1998	29	41	01H	1	D9674											
1998	29	41	01H	1	S4373											
1998	29	41	01H	1	T9093											
1998	29	41	01H	2	D9674											
1998	29	41	01H	2	S4373											
1998	29	41	01H	2	T9093											
1998	29	67	01H	1	D9674											
1998	29	67	01H	1	S4373											
1998	29	67	01H	1	T9093											
1998	30	45	01H	1	D9674											
1998	30	45	01H	1	S4373											
1998	30	45	01H	1	T9093											
1998	30	45	01H	2	D9674											
1998	30	45	01H	2	S4373											
1998	30	45	01H	2	T9093											
1998	33	34	01H	1	D9674											
1998	33	34	01H	1	S4373											
1998	33	34	01H	1	T9093											
1998	33	58	01H	1	D9674											
1998	33	58	01H	1	S4373											
1998	33	58	01H	1	T9093											

Table 4-6
NDE Performance Test +Point Sizing
Summary of Analysts Results

Ins. Year	Row	Column	Location	Crack No.	Analyst		Unadjusted NDE				Adjusted NDE				EXAM Unadjusted DE		
							Length (in.)	Max. Depth (%)	Avg. Depth (%)	Max. Volts	Length (in.)	Max. Depth (%)	Avg. Depth (%)	Max. Volts	Length (in.)	Max. Depth (%)	Avg. Depth (%)
1998	37	31	01H	1	D9674												
1998	37	31	01H	1	S4373												
1998	37	31	01H	1	T9093												
1998	37	52	01H	1	D9674												
1998	37	52	01H	1	S4373												
1998	37	52	01H	1	T9093												
1998	39	28	01H	1	D9674												
1998	39	28	01H	1	T9093												
1998	39	28	01H	2	D9674												
1998	39	28	01H	2	T9093												
1998	41	64	01H	1	D9674												
1998	41	64	01H	1	S4373												
1998	41	64	01H	1	T9093												
1998	43	40	01H	1	D9674												
1998	43	40	01H	1	S4373												
1998	43	40	01H	1	T9093												

Table 4-6
NDE Performance Test +Point Sizing
Summary of Analysts Results

Ins. Year	Row	Column	Location	Crack No.	Analyst	EXAM - Unadjusted NDE Length (In.)	Max. Depth (%)	Avg. Depth (%)	EXAM - Adjusted NDE Length (In.)	Max. Depth (%)	Avg. Depth (%)
1998	1	85	01H	1	D9674						
1998	1	85	01H	1	S4373						
1998	1	85	01H	1	T9093						
1998	1	91	01H	1	D9674						
1998	1	91	01H	1	S4373						
1998	1	91	01H	1	T9093						
1998	1	91	01H	2	D9674						
1998	1	91	01H	2	S4373						
1998	1	91	01H	2	T9093						
1998	2	66	01H	1	D9674						
1998	2	66	01H	1	S4373						
1998	2	66	01H	1	T9093						
1998	2	66	01H	2	D9674						
1998	2	66	01H	2	S4373						
1998	2	66	01H	2	T9093						
1998	5	18	01H	1	D9674						
1998	5	18	01H	1	S4373						
1998	5	18	01H	1	T9093						
1998	5	18	01H	2	D9674						
1998	5	18	01H	2	S4373						
1998	5	18	01H	2	T9093						
1998	6	24	01H	1	D9674						
1998	6	24	01H	1	S4373						
1998	6	24	01H	1	T9093						
1998	6	31	01H	1	D9674						
1998	6	31	01H	1	S4373						
1998	6	31	01H	1	T9093						
1998	6	31	01H	2	D9674						
1998	6	31	01H	2	S4373						
1998	6	31	01H	2	T9093						
1998	6	64	01H	1	D9674						
1998	6	64	01H	1	S4373						
1998	6	64	01H	1	T9093						
1998	6	64	01H	2	D9674						
1998	6	64	01H	2	S4373						
1998	6	64	01H	2	T9093						
1998	9	7	01H	1	D9674						
1998	9	7	01H	1	S4373						
1998	9	7	01H	1	T9093						
1998	9	7	01H	2	D9674						
1998	9	7	01H	2	S4373						
1998	9	7	01H	2	T9093						
1998	9	19	01H	1	D9674						
1998	9	19	01H	1	S4373						
1998	9	19	01H	1	T9093						
1998	9	19	01H	2	D9674						
1998	9	19	01H	2	S4373						
1998	9	19	01H	2	T9093						

Table 4-6
NDE Performance Test +Point Sizing
Summary of Analysts Results

Ins. Year	Row	Column	Location	Crack No.	Analyst	EXAM - Unadjusted NDE Length (in.)	Max. Depth (%)	Avg. Depth (%)	EXAM - Adjusted NDE Length (in.)	Max. Depth (%)	Avg. Depth (%)	g
1998	9	37	01H	1	D9674							
1998	9	37	01H	1	S4373							
1998	9	37	01H	1	T9093							
1998	9	64	01H	1	D9674							
1998	9	64	01H	1	S4373							
1998	9	64	01H	1	T9093							
1998	13	7	01H	1	D9674							
1998	13	7	01H	1	S4373							
1998	13	7	01H	1	T9093							
1998	13	16	01H	1	D9674							
1998	13	16	01H	1	S4373							
1998	13	16	01H	1	T9093							
1998	13	16	01H	2	D9674							
1998	13	16	01H	2	S4373							
1998	13	16	01H	2	T9093							
1998	13	34	01H	1	D9674							
1998	13	34	01H	1	S4373							
1998	13	34	01H	1	T9093							
1998	13	59	01H	1	D9674							
1998	13	59	01H	1	S4373							
1998	13	59	01H	1	T9093							
1998	13	85	01H	1	D9674							
1998	13	85	01H	1	S4373							
1998	13	85	01H	1	T9093							
1998	17	43	01H	1	D9674							
1998	17	43	01H	1	S4373							
1998	17	43	01H	1	T9093							
1998	17	58	01H	1	D9674							
1998	17	58	01H	1	S4373							
1998	17	58	01H	1	T9093							
1998	19	38	01H	1	D9674							
1998	19	38	01H	1	S4373							
1998	19	38	01H	1	T9093							
1998	19	38	01H	2	D9674							
1998	19	38	01H	2	S4373							
1998	19	38	01H	2	T9093							
1998	21	13	01H	1	D9674							
1998	21	13	01H	1	S4373							
1998	21	13	01H	1	T9093							
1998	21	13	01H	2	D9674							
1998	21	13	01H	2	S4373							
1998	21	13	01H	2	T9093							
1998	21	28	01H	1	D9674							
1998	21	28	01H	1	S4373							
1998	21	28	01H	1	T9093							
1998	21	31	01H	1	D9674							
1998	21	31	01H	1	S4373							
1998	21	31	01H	1	T9093							
1998	21	31	01H	2	D9674							
1998	21	31	01H	2	S4373							
1998	21	31	01H	2	T9093							

Table 4-6
NDE Performance Test +Point Sizing
Summary of Analysts Results

Ins. Year	Row	Column	Location	Crack No.	Analyst	EXAM - Unadjusted NDE Length (in.)	Max. Depth (%)	Avg. Depth (%)	EXAM - Adjusted NDE Length (in.)	Max. Depth (%)	Avg. Depth (%)
1998	21	73	01H	1	D9674						
1998	21	73	01H	1	S4373						
1998	21	73	01H	1	T9093						
1998	21	79	01H	1	D9674						
1998	21	79	01H	1	S4373						
1998	21	79	01H	1	T9093						
1998	21	85	01H	1	D9674						
1998	21	85	01H	1	S4373						
1998	21	85	01H	1	T9093						
1998	23	15	01H	1	D9674						
1998	23	15	01H	1	S4373						
1998	23	15	01H	1	T9093						
1998	25	40	01H	1	D9674						
1998	25	40	01H	1	S4373						
1998	25	40	01H	1	T9093						
1998	25	52	01H	1	D9674						
1998	25	52	01H	1	S4373						
1998	25	52	01H	1	T9093						
1998	25	79	01H	1	D9674						
1998	25	79	01H	1	S4373						
1998	25	79	01H	1	T9093						
1998	27	77	01H	1	D9674						
1998	27	77	01H	1	S4373						
1998	27	77	01H	1	T9093						
1998	29	16	01H	1	D9674						
1998	29	16	01H	1	S4373						
1998	29	16	01H	1	T9093						
1998	29	34	01H	1	D9674						
1998	29	34	01H	1	S4373						
1998	29	34	01H	1	T9093						
1998	29	41	01H	1	D9674						
1998	29	41	01H	1	S4373						
1998	29	41	01H	1	T9093						
1998	29	41	01H	2	D9674						
1998	29	41	01H	2	S4373						
1998	29	41	01H	2	T9093						
1998	29	67	01H	1	D9674						
1998	29	67	01H	1	S4373						
1998	29	67	01H	1	T9093						
1998	30	45	01H	1	D9674						
1998	30	45	01H	1	S4373						
1998	30	45	01H	1	T9093						
1998	30	45	01H	2	D9674						
1998	30	45	01H	2	S4373						
1998	30	45	01H	2	T9093						
1998	33	34	01H	1	D9674						
1998	33	34	01H	1	S4373						
1998	33	34	01H	1	T9093						
1998	33	58	01H	1	D9674						
1998	33	58	01H	1	S4373						
1998	33	58	01H	1	T9093						

Table 4-6
NDE Performance Test +Point Sizing
Summary of Analysts Results

Ins. Year	Row	Column	Location	Crack No.	Analyst	EXAM - Unadjusted NDE			EXAM - Adjusted NDE			
						Length (in.)	Max. Depth (%)	Avg. Depth (%)	Length (in.)	Max. Depth (%)	Avg. Depth (%)	9
1998	37	31	01H	1	D9674							
1998	37	31	01H	1	S4373							
1998	37	31	01H	1	T9093							
1998	37	52	01H	1	D9674							
1998	37	52	01H	1	S4373							
1998	37	52	01H	1	T9093							
1998	39	28	01H	1	D9674							
1998	39	28	01H	1	T9093							
1998	39	28	01H	2	D9674							
1998	39	28	01H	2	T9093							
1998	41	64	01H	1	D9674							
1998	41	64	01H	1	S4373							
1998	41	64	01H	1	T9093							
1998	43	40	01H	1	D9674							
1998	43	40	01H	1	S4373							
1998	43	40	01H	1	T9093							

Table 4-7 Sequoyah Unit 1 and Diablo Canyon Units 1 and 2 Growth Rate per EFPY				
Plant and Growth Parameter	**Length (inch)**	**Max. Depth (%TW)**	**Avg. Depth (%TW)**	**Volts**
Sequoyah Data				
Average Growth Rate				
Growth at 95% Cum. Prob.				
Diablo Canyon Data				
Average Growth Rate				
Growth at 95% Cum. Prob.				
Combined Data				
Average Growth Rate				
Growth at 95% Cum. Prob.				
Sequoyah Data				
Average Growth Rate				
Growth at 95% Cum. Prob.				
Diablo Canyon Data				
Average Growth Rate				
Growth at 95% Cum. Prob.				
Combined Data				
Average Growth Rate				
Growth at 95% Cum. Prob.				
Note: Applicable data for Sequoyah are Sequoyah data at 611°F and for Diablo Canyon are combined data at 603°F.				

g

Table 4-8
Combined Sequoyah and Diablo Canyon
Growth Rate per EFPY Database at 611° F

Plant	SG	Row	Col	Loc	Crack No.	First Inspection Adjusted NDE Length (in.)	Max. Depth (%)	Avg. Depth (%)	Max. Volts	Second Inspection Adjusted NDE Length (in.)	Max. Depth (%)	Avg. Depth (%)	Max. Volts
TVA	1	2	40	01H	1								
TVA	1	4	72	01H	1								
TVA	1	6	94	02H	1								
TVA	1	30	83	01H	1								
TVA	2	4	32	01H	1								
TVA	3	2	52	01H	1								
TVA	3	2	59	01H	1								
TVA	3	2	64	01H	1								
TVA	3	4	12	01H	1								
TVA	3	6	78	01H	1								
TVA	3	8	88	01H	1								
TVA	3	9	66	01H	1								
TVA	3	9	78	01H	1								
TVA	3	10	79	01H	1								
TVA	3	11	59	01H	1								
TVA	3	12	85	01H	1								
TVA	3	14	73	01H	1								
TVA	3	14	81	01H	1								
TVA	3	15	55	01H	1								
TVA	3	15	55	01H	2								
TVA	3	15	92	01H	1								
TVA	3	16	83	01H	1								
TVA	3	17	14	01H	1								
TVA	3	19	32	01H	1								
TVA	3	22	36	01H	1								
TVA	3	24	86	01H	1								
TVA	3	26	79	01H	1								
TVA	3	27	41	01H	1								
TVA	3	27	71	01H	2								
TVA	3	35	60	01H	1								
TVA	3	44	44	01H	1								
TVA	4	1	21	01H	1								
TVA	4	1	23	01H	1								
TVA	4	1	46	01H	1								
TVA	4	2	28	03H	1								
TVA	4	3	45	01H	1								
TVA	4	3	49	01H	1								
TVA	4	3	83	04H	1								
TVA	4	3	84	01H	1								
TVA	4	4	29	01H	1								
TVA	4	5	39	01H	1								
TVA	4	5	40	01H	1								
TVA	4	6	31	01H	1								
TVA	4	9	27	03H	1								
TVA	4	9	27	03H	2								
TVA	4	9	54	01H	1								
TVA	4	10	32	03H	1								
TVA	4	11	41	01H	1								

g

Table 4-8
Combined Sequoyah and Diablo Canyon
Growth Rate per EFPY Database at 611° F

Plant	SG	Row	Col	Loc	Crack No.	First Inspection Adjusted NDE				Second Inspection Adjusted NDE			
						Length (in.)	Max. Depth (%)	Avg. Depth (%)	Max. Volts	Length (in.)	Max. Depth (%)	Avg. Depth (%)	Max. Volts
TVA	4	11	41	01H	2								
TVA	4	11	86	01H	1								
TVA	4	11	86	02H	1								
TVA	4	12	38	03H	1								
TVA	4	12	43	04H	1								
TVA	4	13	91	01H	1								
TVA	4	13	91	03H	1								
TVA	4	14	50	01H	1								
TVA	4	14	63	02H	1								
TVA	4	17	45	01H	1								
TVA	4	20	41	01H	1								
TVA	4	23	28	01H	1								
TVA	4	24	12	01H	1								
TVA	4	26	11	01H	1								
TVA	4	26	15	02H	1								
TVA	4	27	41	01H	1								
TVA	4	29	16	01H	1								
TVA	4	30	30	03H	1								
TVA	4	31	17	01H	1								
TVA	4	34	24	03H	1								
TVA	4	35	48	01H	1								
TVA	4	36	26	01H	1								
TVA	4	36	48	01H	1								
TVA	4	37	44	01H	1								
TVA	4	37	44	01H	2								
TVA	4	38	23	01H	1								
TVA	4	38	53	01H	1								
TVA	4	39	56	01H	1								
TVA	4	39	56	03H	1								
TVA	2	8	32	H01	1								
TVA	3	6	45	H03	1								
TVA	3	6	74	H01	1								
TVA	3	6	74	H01	3								
TVA	3	7	76	H02	1								
TVA	3	9	67	H02	1								
TVA	3	14	84	H01	1								
TVA	3	18	74	H01	1								
TVA	3	18	74	H01	2								
TVA	3	24	80	02H	1								
TVA	3	33	79	H01	1								
TVA	3	34	52	H01	1								
TVA	4	2	56	H01	1								
TVA	4	11	35	H02	1								
TVA	4	11	35	H04	1								
TVA	4	13	61	H03	1								
TVA	4	23	43	H01	1								
TVA	4	23	43	H01	2								
TVA	4	28	52	H01	1								
PGE	1	17	39	01H	1								

g

Table 4-8
Combined Sequoyah and Diablo Canyon
Growth Rate per EFPY Database at 611° F

| | | | | | | First Inspection | | | | Second Inspection | | | |
| | | | | | | Adjusted NDE | | | | Adjusted NDE | | | |
Plant	SG	Row	Col	Loc	Crack No.	Length (in.)	Max. Depth (%)	Avg. Depth (%)	Max. Volts	Length (in.)	Max. Depth (%)	Avg. Depth (%)	Max. Volts
PGE	1	18	64	01H	1								
PGE	1	18	64	03H	1								
PGE	1	21	42	01H	1								
PGE	1	21	44	01H	1								
PGE	2	5	66	02H	1								
PGE	2	7	68	03H	1								
PGE	2	13	81	01H	1								
PGE	2	14	72	02H	1								
PGE	2	14	74	01H	1								
PGE	2	16	73	01H	1								
PGE	2	16	82	01H	1								
PGE	2	26	43	02H	1								
PGE	2	35	56	02H	1								
PGE	2	35	67	03H	1								
PGE	2	35	77	01H	1								
PGE	2	35	77	01H	2								
PGE	2	43	49	03H	1								
PGE	3	32	47	03H	1								
PGE	4	38	27	01H	1								
PGE	4	39	58	01H	1								
PEG	2	2	2	01H	1								
PEG	2	4	28	01H	1								
PEG	2	6	24	01H	1								
PEG	2	12	28	01H	1								
PEG	2	14	15	01H	1								
PEG	2	14	29	01H	1								
PEG	2	15	42	01H	1								
PEG	2	17	36	01H	1								
PEG	2	18	16	01H	1								
PEG	2	18	44	01H	1								
PEG	2	19	15	01H	1								
PEG	2	22	45	01H	1								
PEG	4	4	37	01H	1								
PEG	4	34	34	01H	1								

g

Table 4-8
Combined Sequoyah and Diablo Canyon Growth Rate per EFPY Database at 611° F

Plant	SG	Row	Col	Loc	Crack No.		Length (in.)	Max. Depth (%)	Avg. Depth (%)	Max. Volts
							Second Minus First Inspection Growth Data			
							Adjusted NDE Growth Data			
TVA	1	2	40	01H	1					
TVA	1	4	72	01H	1					
TVA	1	6	94	02H	1					
TVA	1	30	83	01H	1					
TVA	2	4	32	01H	1					
TVA	3	2	52	01H	1					
TVA	3	2	59	01H	1					
TVA	3	2	64	01H	1					
TVA	3	4	12	01H	1					
TVA	3	6	78	01H	1					
TVA	3	8	88	01H	1					
TVA	3	9	66	01H	1					
TVA	3	9	78	01H	1					
TVA	3	10	79	01H	1					
TVA	3	11	59	01H	1					
TVA	3	12	85	01H	1					
TVA	3	14	73	01H	1					
TVA	3	14	81	01H	1					
TVA	3	15	55	01H	1					
TVA	3	15	55	01H	2					
TVA	3	15	92	01H	1					
TVA	3	16	83	01H	1					
TVA	3	17	14	01H	1					
TVA	3	19	32	01H	1					
TVA	3	22	36	01H	1					
TVA	3	24	86	01H	1					
TVA	3	26	79	01H	1					
TVA	3	27	41	01H	1					
TVA	3	27	71	01H	2					
TVA	3	35	60	01H	1					
TVA	3	44	44	01H	1					
TVA	4	1	21	01H	1					
TVA	4	1	23	01H	1					
TVA	4	1	46	01H	1					
TVA	4	2	28	03H	1					
TVA	4	3	45	01H	1					
TVA	4	3	49	01H	1					
TVA	4	3	83	04H	1					
TVA	4	3	84	01H	1					
TVA	4	4	29	01H	1					
TVA	4	5	39	01H	1					
TVA	4	5	40	01H	1					
TVA	4	6	31	01H	1					
TVA	4	9	27	03H	1					
TVA	4	9	27	03H	2					
TVA	4	9	54	01H	1					
TVA	4	10	32	03H	1					
TVA	4	11	41	01H	1					
TVA	4	11	41	01H	2					
TVA	4	11	86	01H	1					
TVA	4	11	86	02H	1					
TVA	4	12	38	03H	1					

g

Table 4-8
Combined Sequoyah and Diablo Canyon Growth Rate per EFPY Database at 611° F

Plant	SG	Row	Col	Loc	Crack No.	Length (in.)	Max. Depth (%)	Avg. Depth (%)	Max. Volts
TVA	4	12	43	04H	1				
TVA	4	13	91	01H	1				
TVA	4	13	91	03H	1				
TVA	4	14	50	01H	1				
TVA	4	14	63	02H	1				
TVA	4	17	45	01H	1				
TVA	4	20	41	01H	1				
TVA	4	23	28	01H	1				
TVA	4	24	12	01H	1				
TVA	4	26	11	01H	1				
TVA	4	26	15	02H	1				
TVA	4	27	41	01H	1				
TVA	4	29	16	01H	1				
TVA	4	30	30	03H	1				
TVA	4	31	17	01H	1				
TVA	4	34	24	03H	1				
TVA	4	35	48	01H	1				
TVA	4	36	26	01H	1				
TVA	4	36	48	01H	1				
TVA	4	37	44	01H	1				
TVA	4	37	44	01H	1				
TVA	4	38	23	01H	1				
TVA	4	38	53	01H	1				
TVA	4	39	56	01H	1				
TVA	4	39	56	03H	1				
TVA	2	8	32	H01	1				
TVA	3	6	45	H03	1				
TVA	3	6	74	H01	1				
TVA	3	6	74	H01	3				
TVA	3	7	76	H02	1				
TVA	3	9	67	H02	1				
TVA	3	14	84	H01	1				
TVA	3	18	74	H01	1				
TVA	3	18	74	H01	2				
TVA	3	24	80	02H	1				
TVA	3	33	79	H01	1				
TVA	3	34	52	H01	1				
TVA	4	2	56	H01	1				
TVA	4	11	35	H02	1				
TVA	4	11	35	H04	1				
TVA	4	13	61	H03	1				
TVA	4	23	43	H01	1				
TVA	4	23	43	H01	2				
TVA	4	28	52	H01	1				
PGE	1	17	39	01H	1				
PGE	1	18	64	01H	1				
PGE	1	18	64	03H	1				
PGE	1	21	42	01H	1				
PGE	1	21	44	01H	1				
PGE	2	5	66	02H	1				
PGE	2	7	68	03H	1				
PGE	2	13	81	01H	1				
PGE	2	14	72	02H	1				

Table 4-8
Combined Sequoyah and Diablo Canyon Growth Rate per EFPY Database at 611° F

Plant	SG	Row	Col	Loc	Crack No.	Length (in.)	Max. Depth (%)	Avg. Depth (%)	Max. Volts
							Second Minus First Inspection Growth Data		
							Adjusted NDE Growth Data		
PGE	2	14	74	01H	1				
PGE	2	16	73	01H	1				
PGE	2	16	82	01H	1				
PGE	2	26	43	02H	1				
PGE	2	35	56	02H	1				
PGE	2	35	67	03H	1				
PGE	2	35	77	01H	1				
PGE	2	35	77	01H	2				
PGE	2	43	49	03H	1				
PGE	3	32	47	03H	1				
PGE	4	38	27	01H	1				
PGE	4	39	58	01H	1				
PEG	2	2	2	01H	1				
PEG	2	4	28	01H	1				
PEG	2	6	24	01H	1				
PEG	2	12	28	01H	1				
PEG	2	14	15	01H	1				
PEG	2	14	29	01H	1				
PEG	2	15	42	01H	1				
PEG	2	17	36	01H	1				
PEG	2	18	16	01H	1				
PEG	2	18	44	01H	1				
PEG	2	19	15	01H	1				
PEG	2	22	45	01H	1				
PEG	4	4	37	01H	1				
PEG	4	34	34	01H	1				
				Max.					
				Average					
				95% Cum. Probability					

g

g
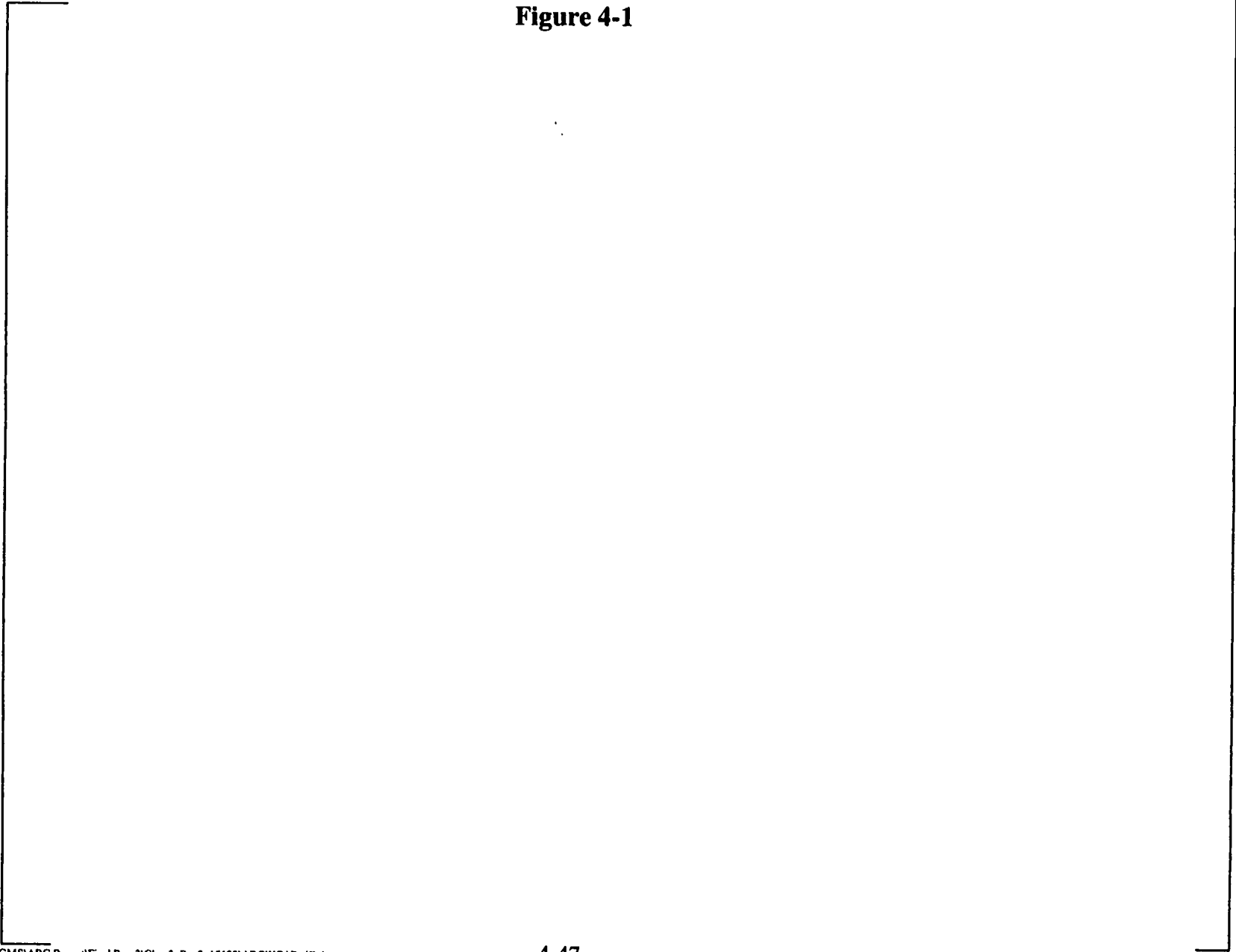
Figure 4-1

Figure 4-2

Figure 4-3

g
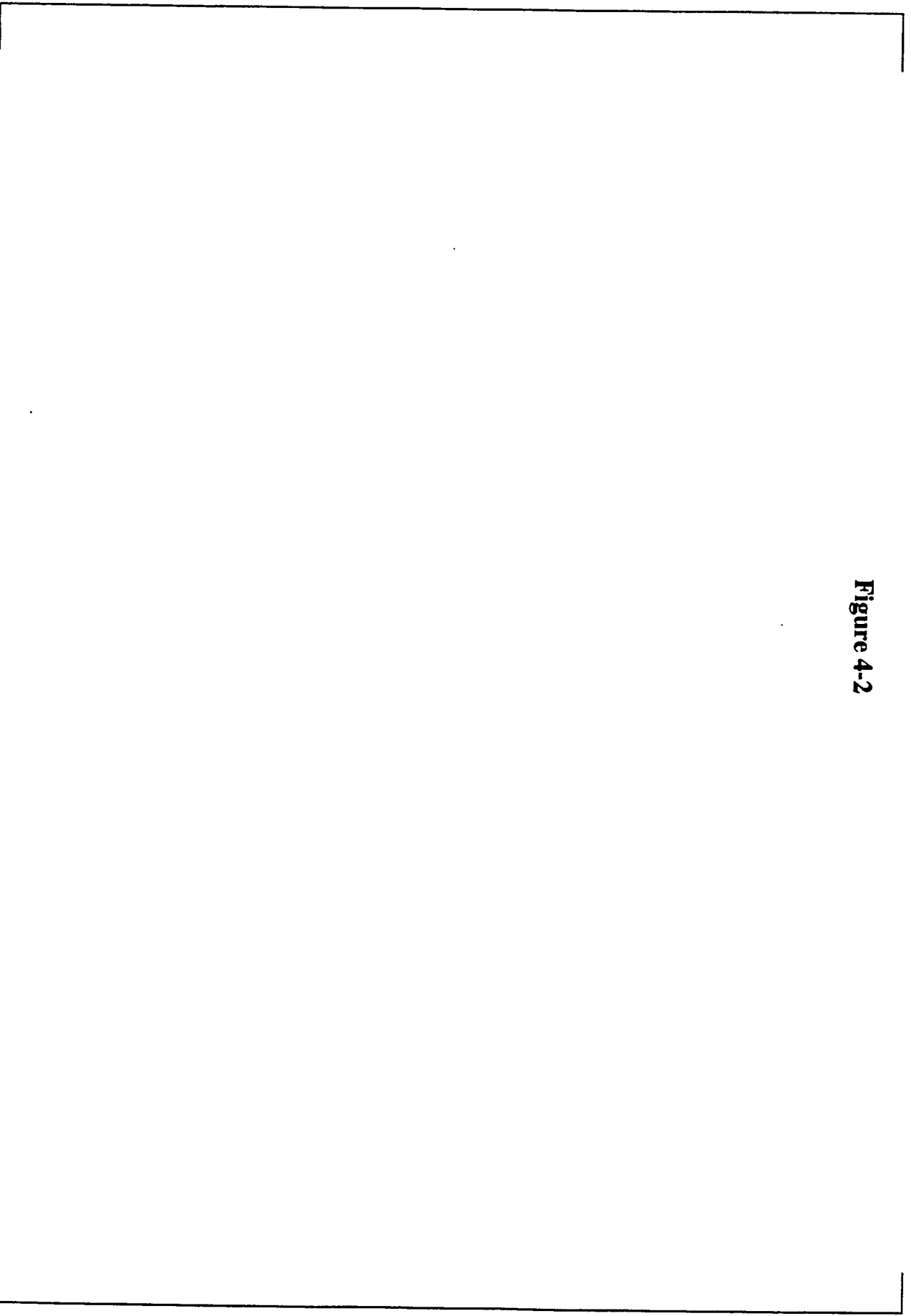
g
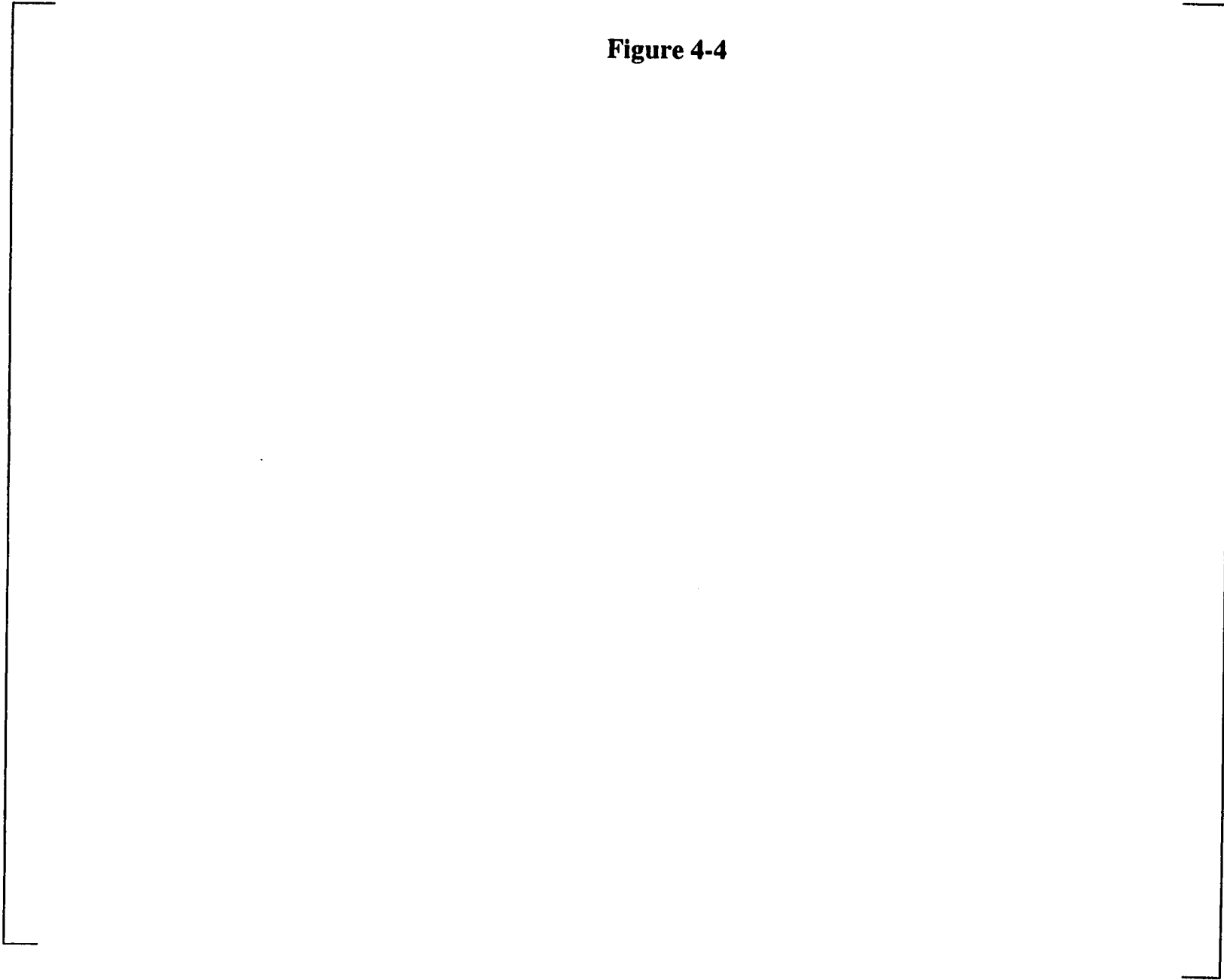
Figure 4-4

g

Figure 4-5
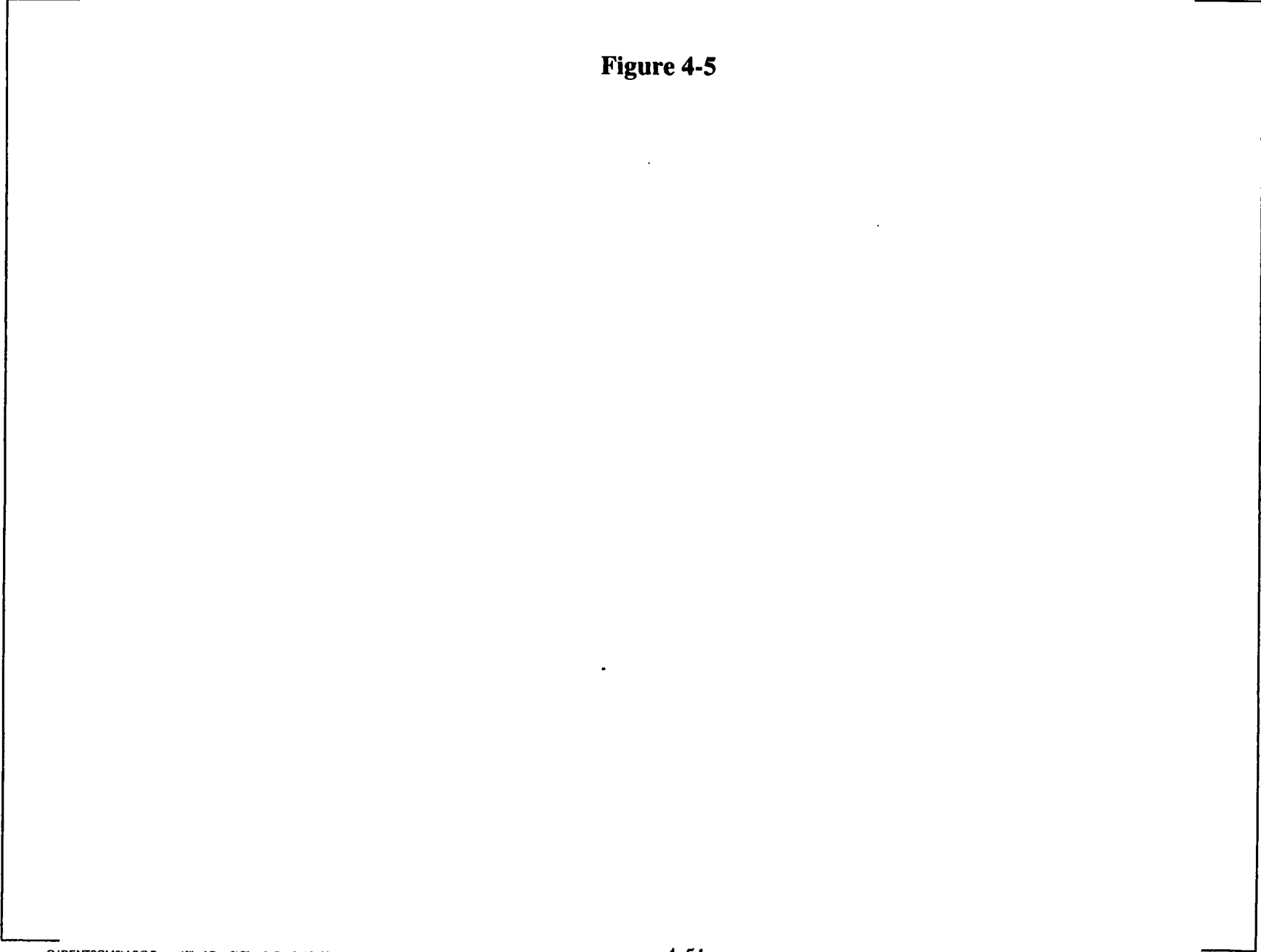
Figure 4-6

Dented TSP Axial PWSCC -- NDE Performance Test
Scatter Plot Of Residuals - Adjusted NDE, Length
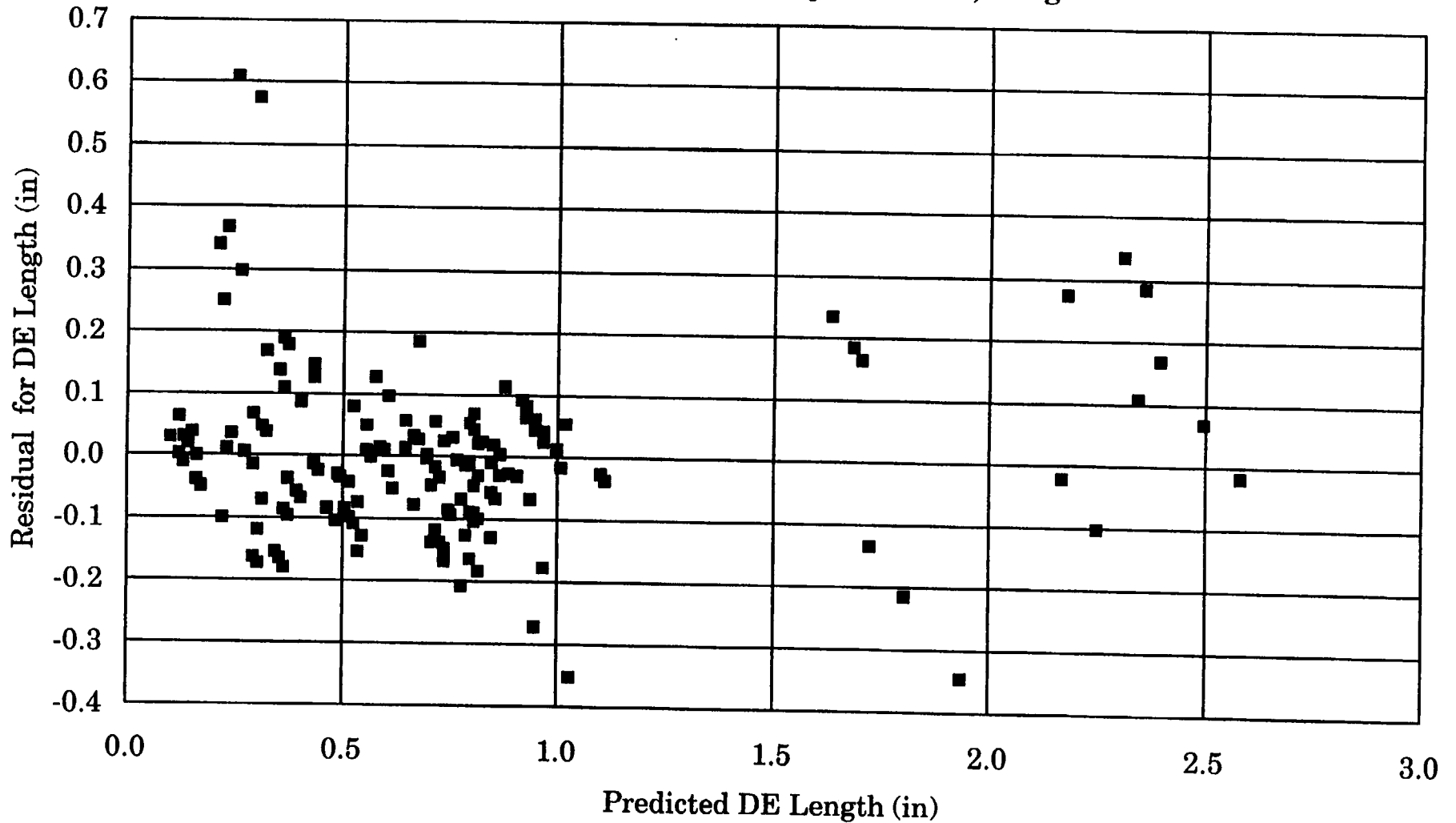
Figure 4-7

Dented TSP Axial PWSCC -- NDE Performance Test

Normal Plot Of Residuals - Adjusted NDE, Length
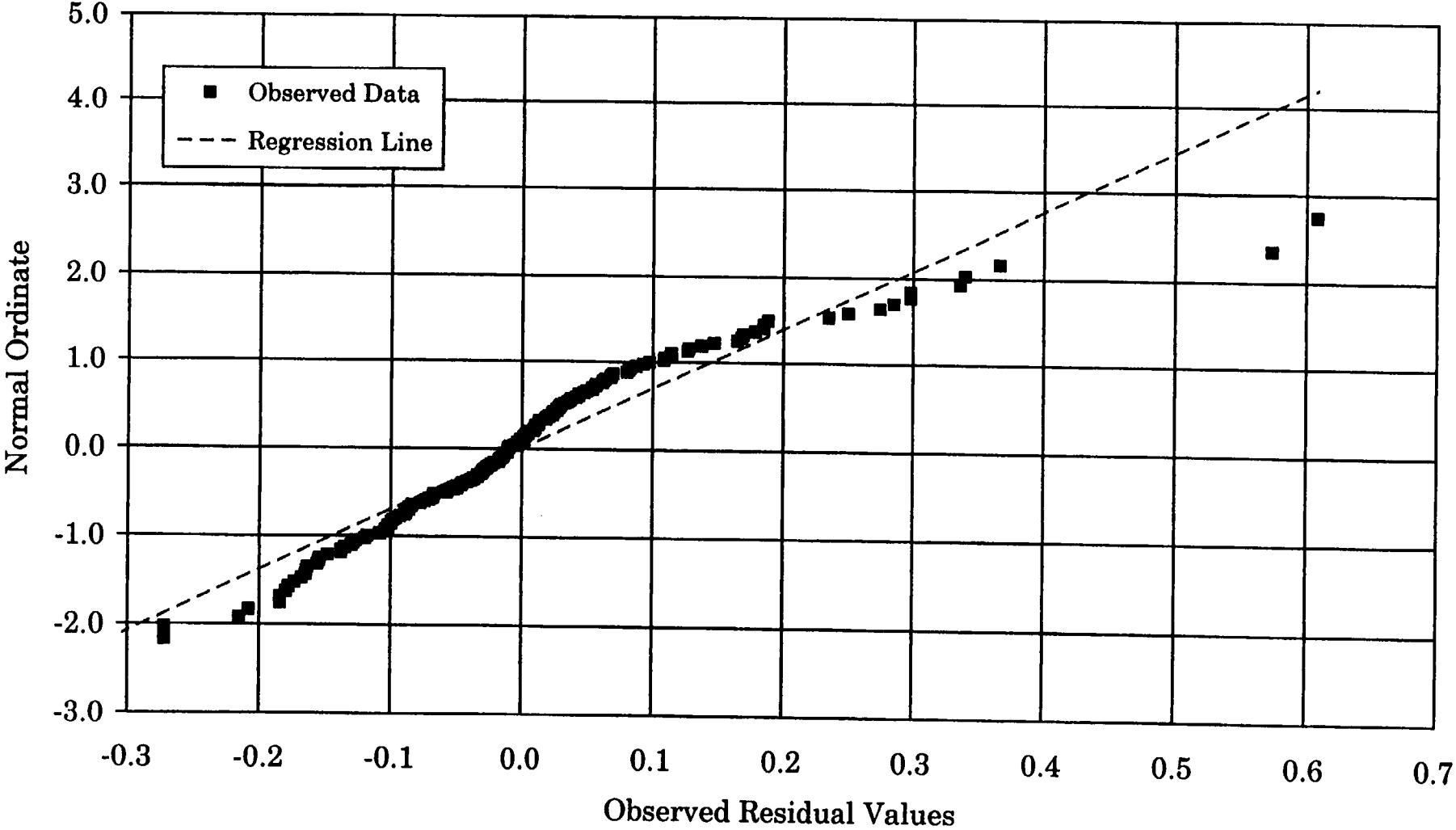
Figure 4-8
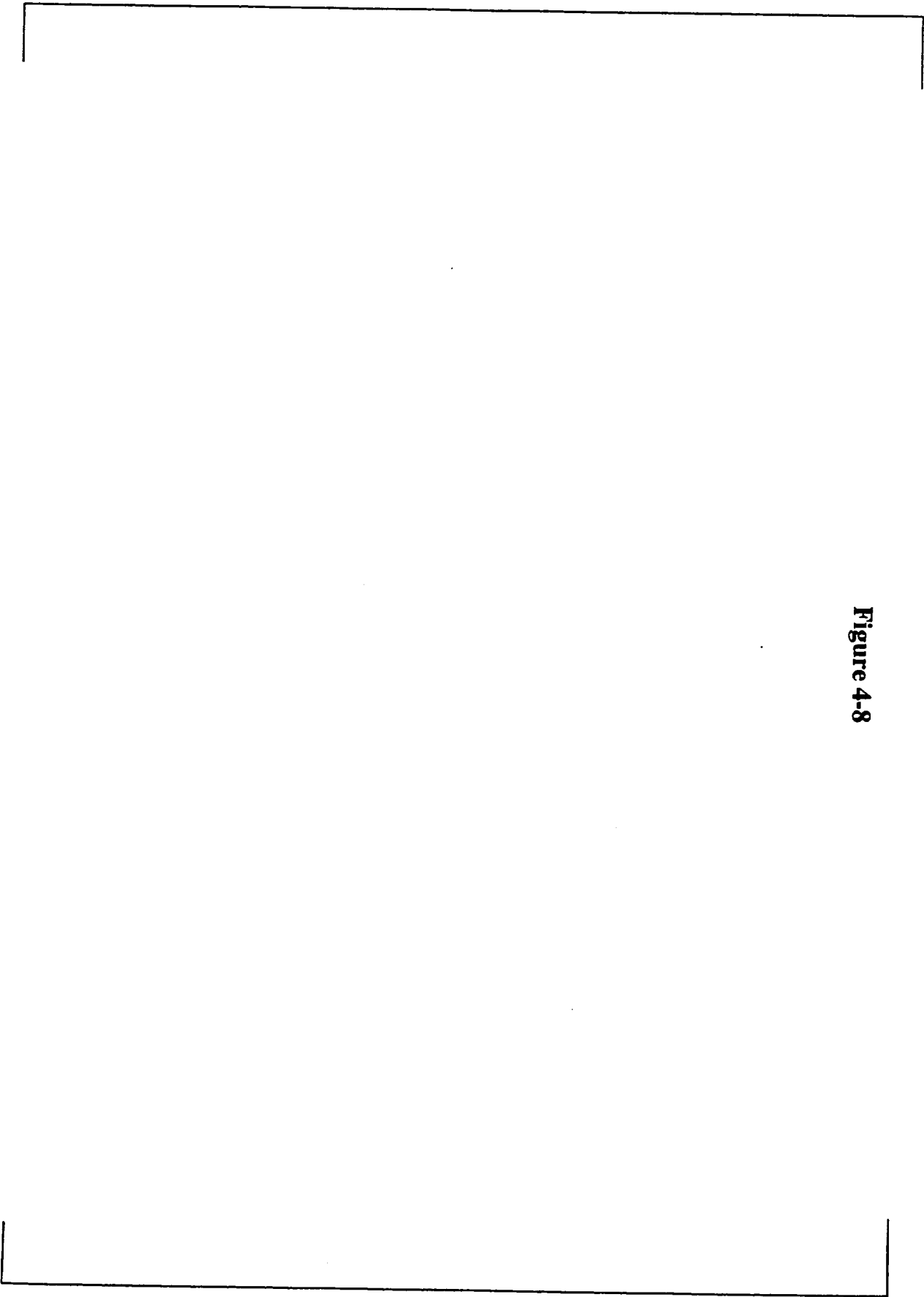
Figure 4-9
Dented TSP Axial PWSCC -- NDE Performance Test
Scatter Plot Of Residuals - Adjusted NDE, Maximum Depth
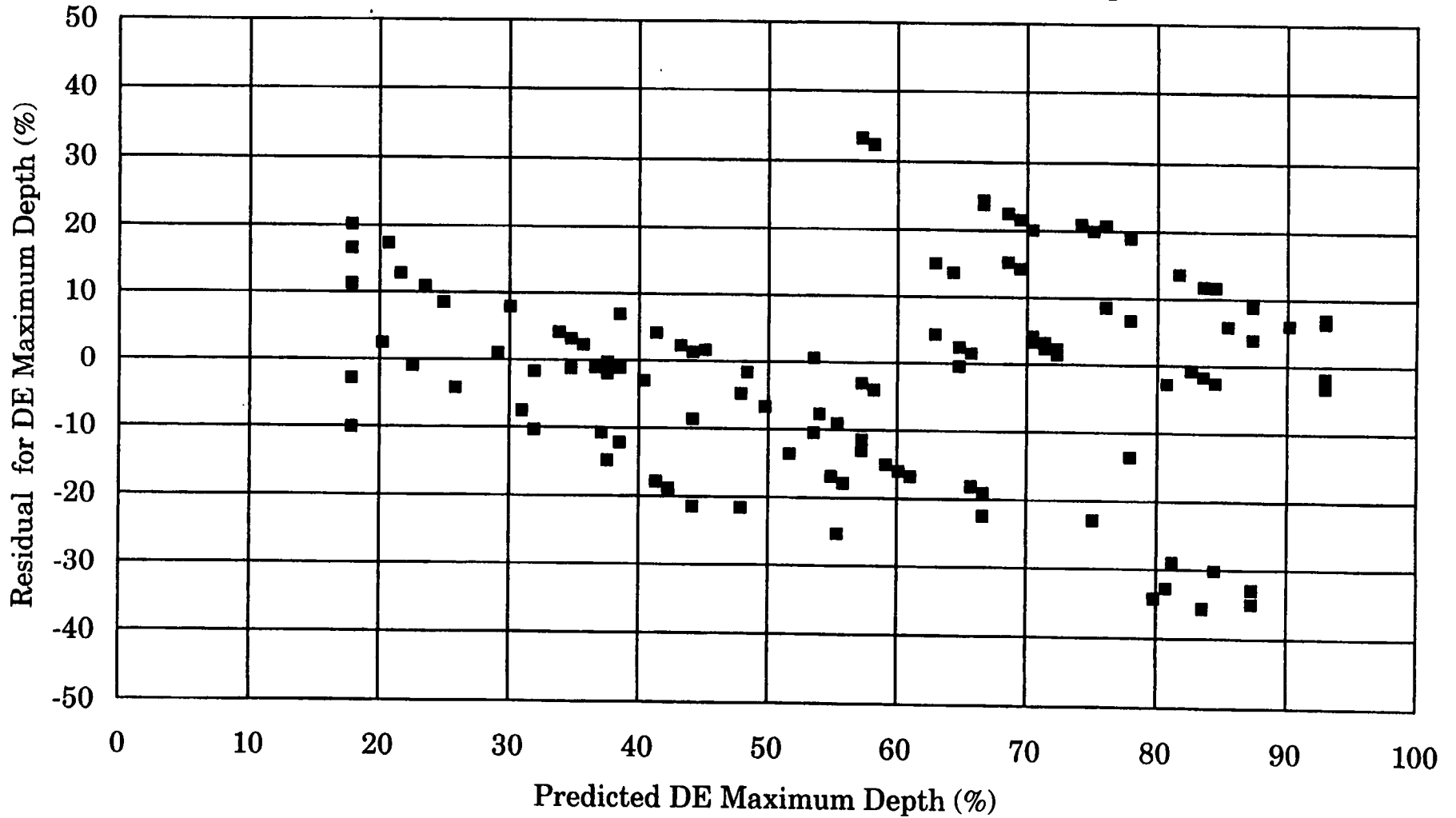
Figure 4-10

Dented TSP Axial PWSCC -- NDE Performance Test

Normal Plot Of Residuals - Adjusted NDE, Maximum Depth

g
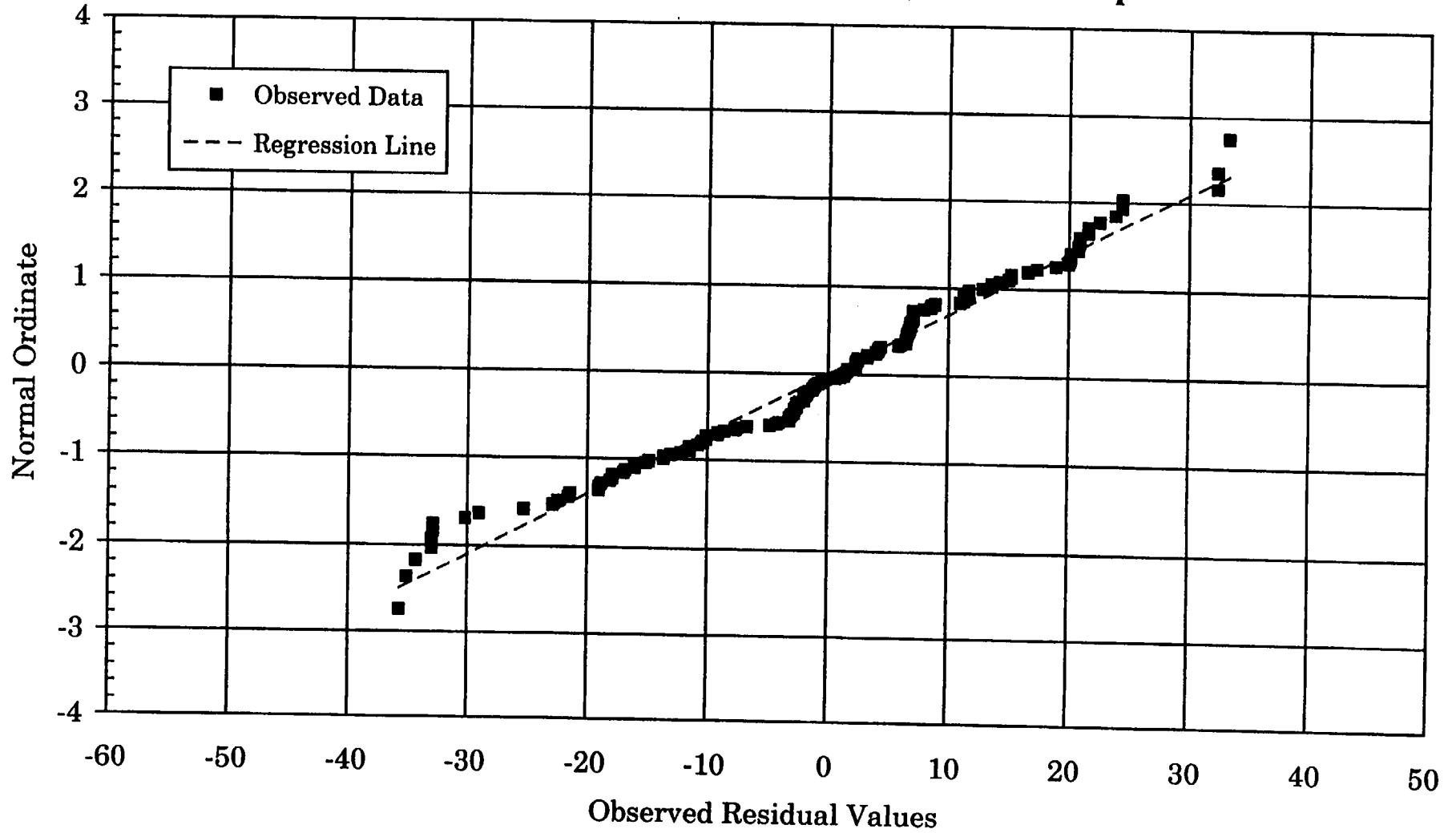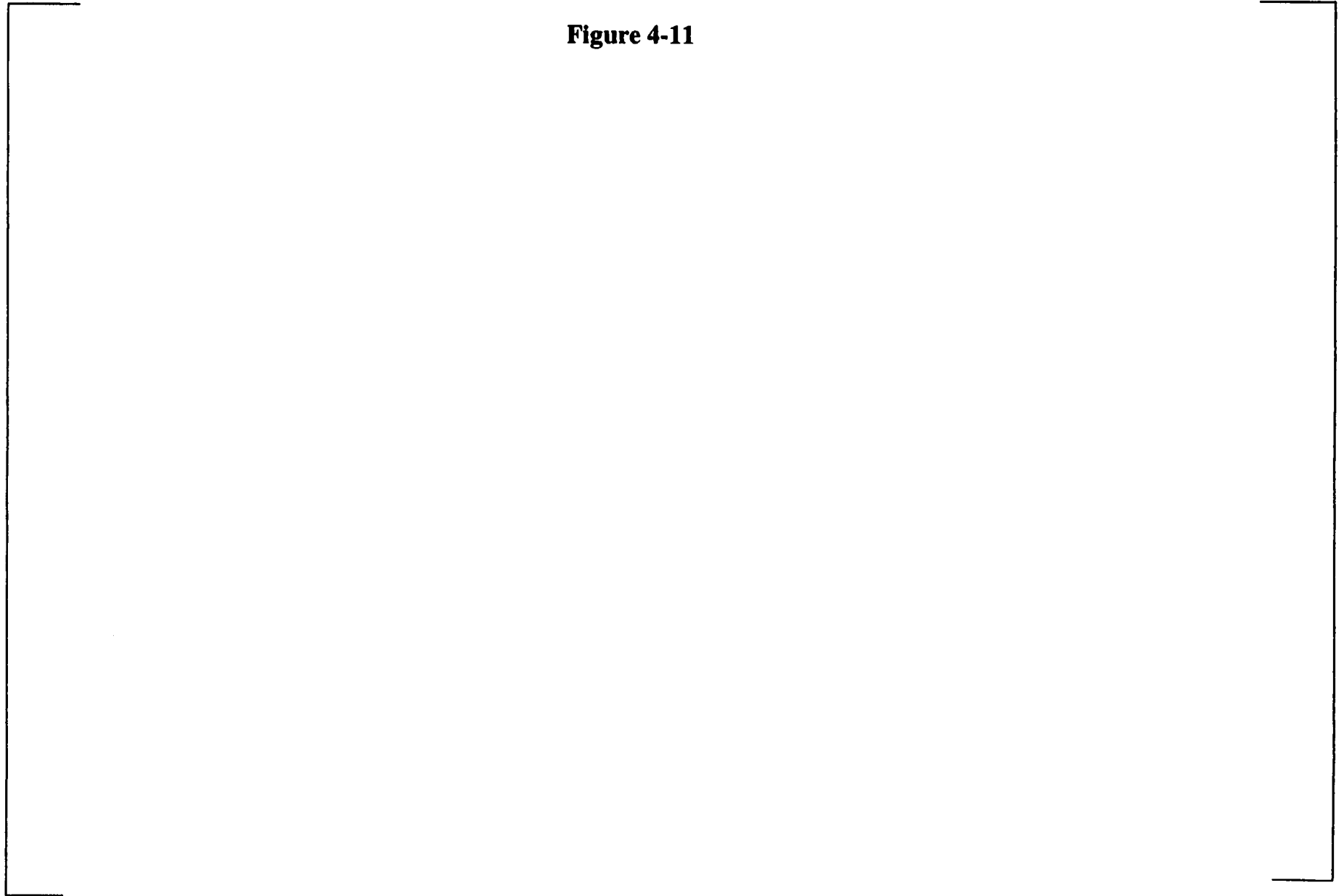
Figure 4-11

Figure 4-12

Dented TSP Axial PWSCC -- NDE Performance Test
Scatter Plot Of Residuals - Adjusted NDE, Average Depth
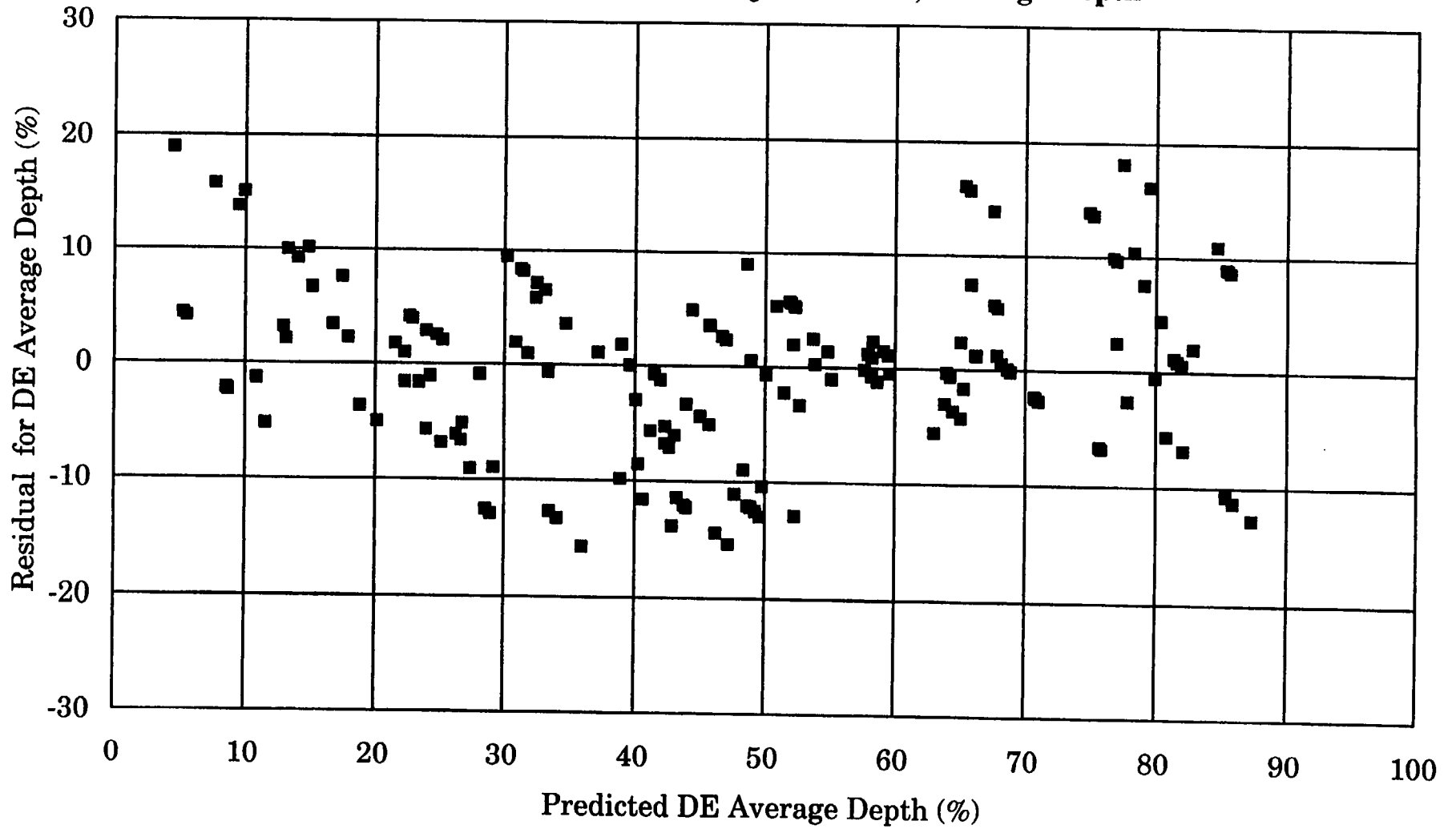
Figure 4-13
Dented TSP Axial PWSCC -- NDE Performance Test
Normal Plot Of Residuals - Adjusted NDE, Average Depth

Figure 4-14

g

Figure 4-15

g

g

Figure 4-16

g

g
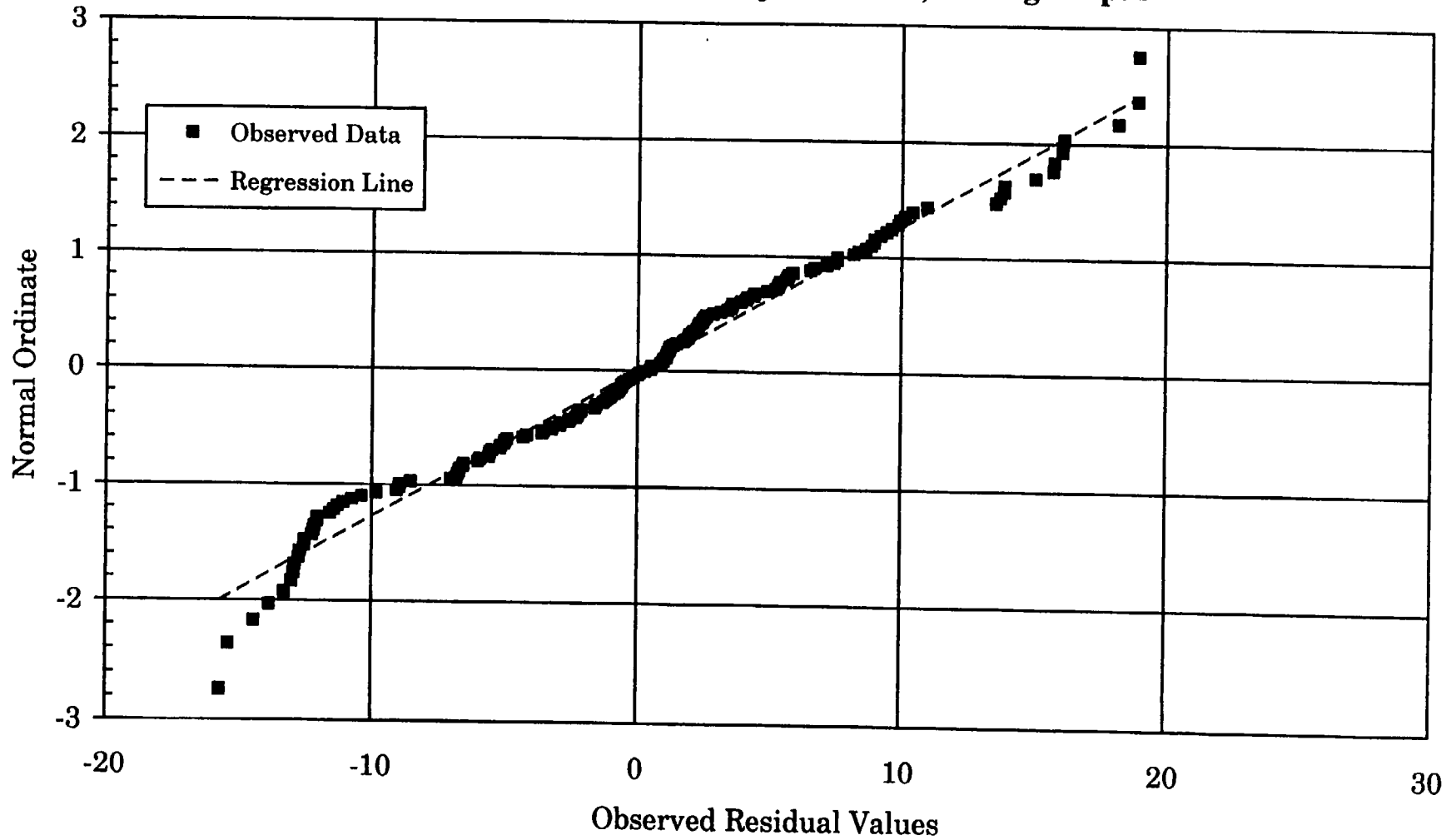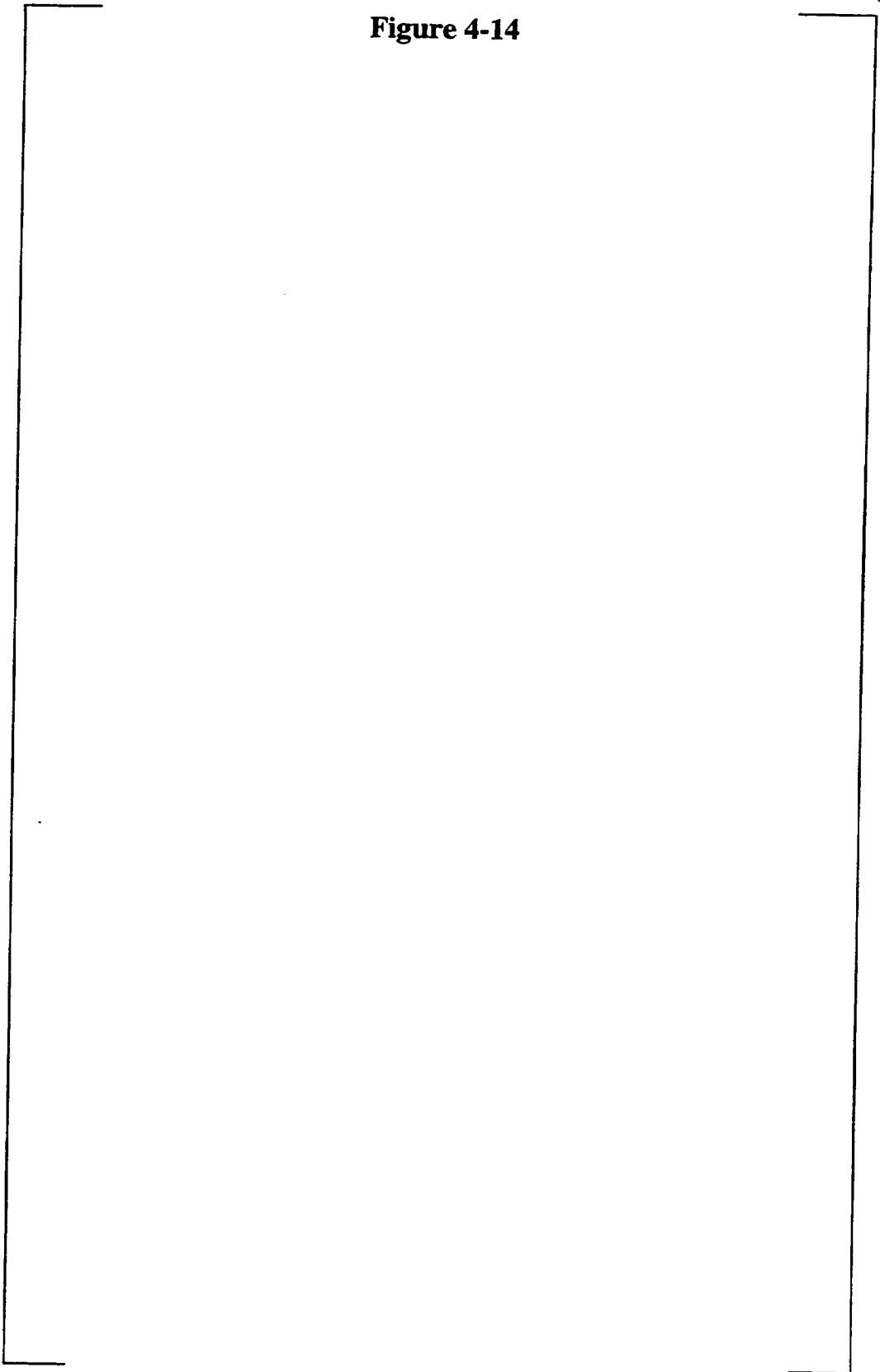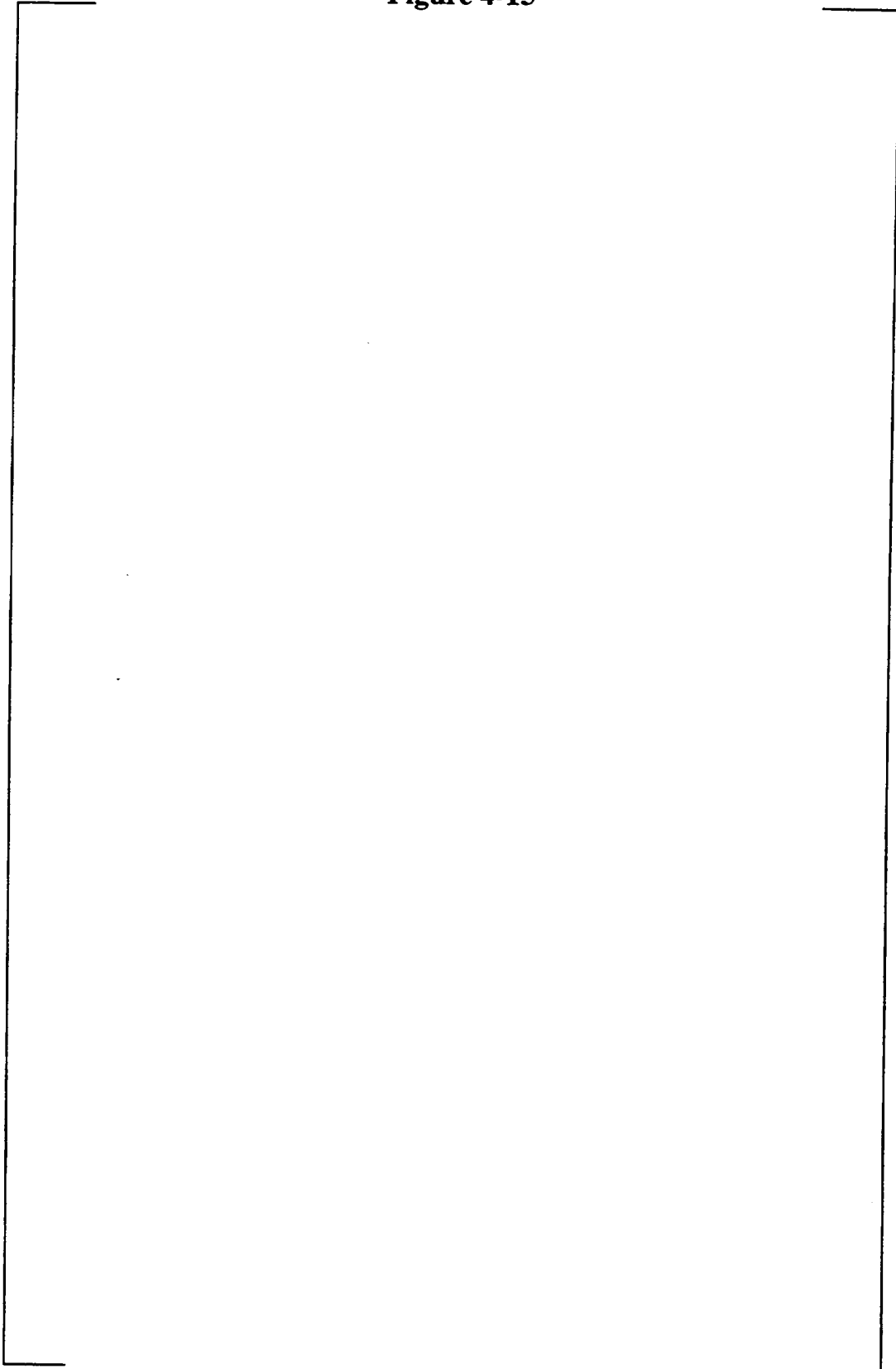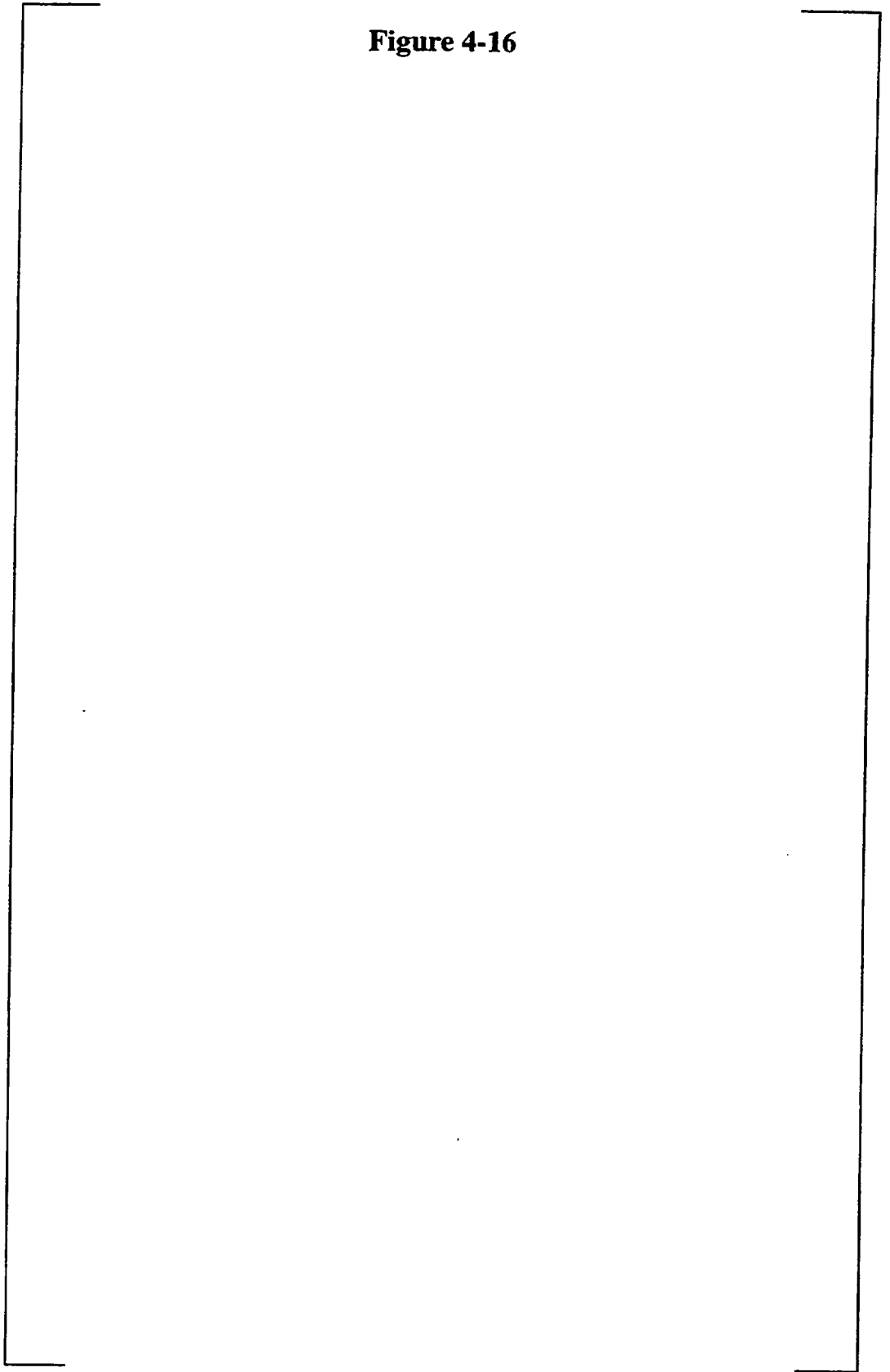
Figure 4-17

Figure 4-18

Figure 4-19

g

Figure 4-20

Figure 4-21

g

g
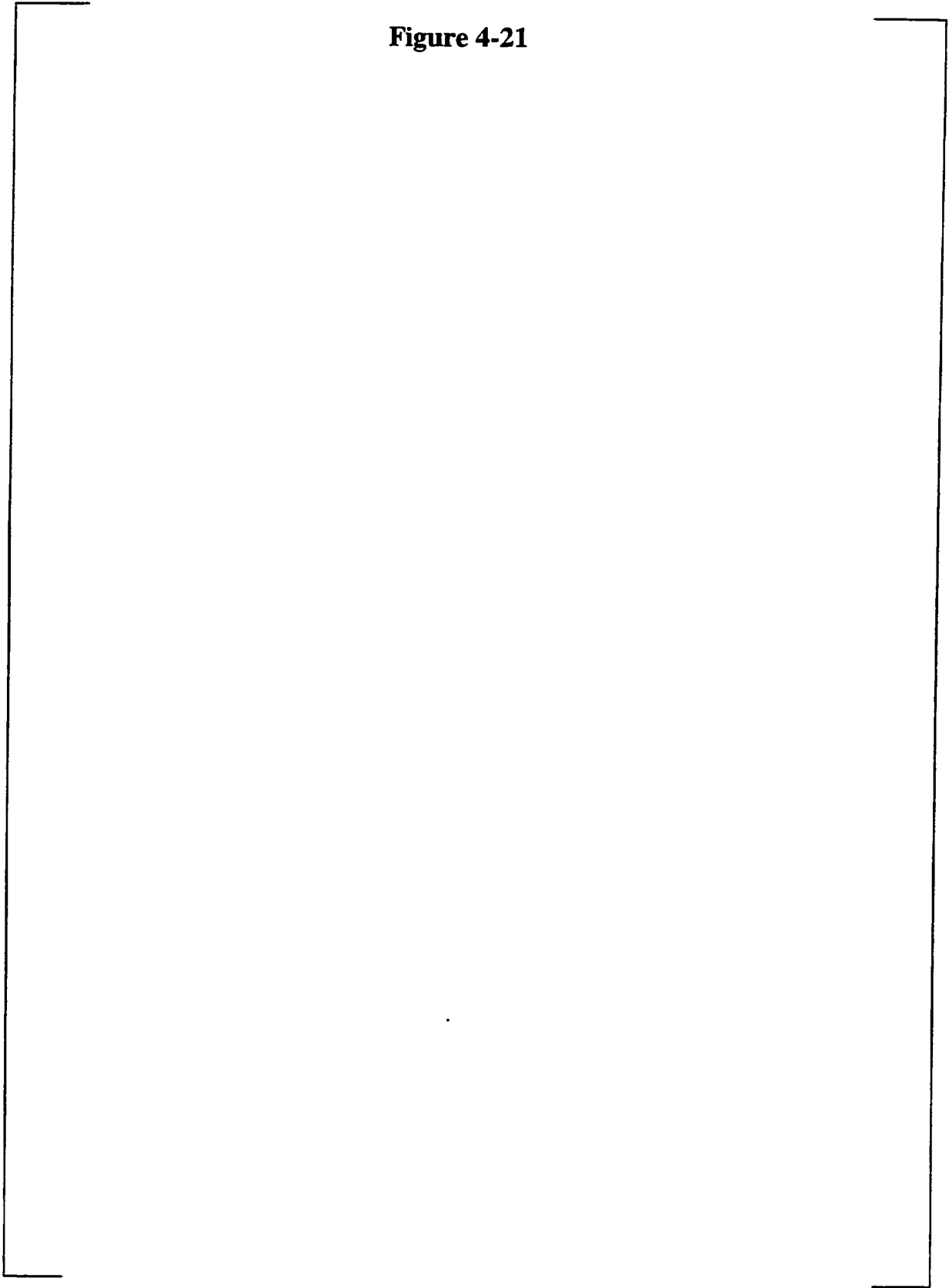
Figure 4-22
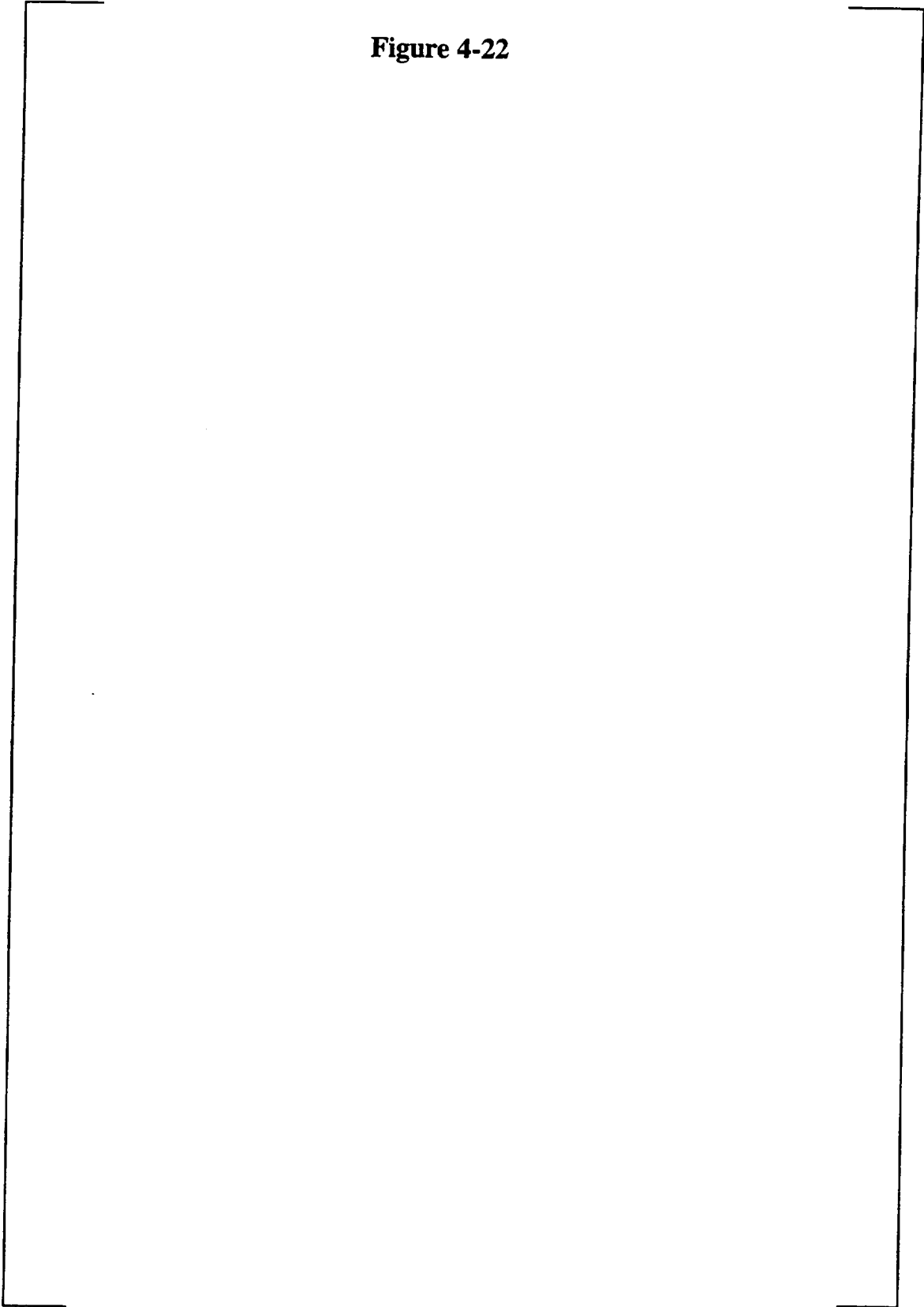
5.0 BURST PRESSURE ANALYSES

5.1 General Description of Burst Pressure Analyses

The development and description of the methodology to predict the burst pressure of SG tubes with axial, stress corrosion cracks which extend partly through the tube wall is presented in this section. Following the definition associated with throughwall cracks, the burst pressure corresponds to opening the crack to the extent that plastic tearing of the tube material at the ends of the crack occurs. In a SG tube in which the pressure is replenished the crack will continue to extend until the pressure is no longer maintained. The degradation morphology considered herein is that of primary water stress corrosion cracking (PWSCC), but may also be applied to outside diameter stress corrosion cracking (ODSCC) by omitting the consideration of pressure on the crack flanks. The PWSCC indications may be typified as being of irregular, or variable, depth along the length of the crack. The deepest location in the crack may or may not correspond to the midpoint of the crack. An idealization of a typical crack profile is illustrated on Figure 5-1(a). This corresponds to a profile to be analyzed and is derived from knowledge of the crack depth at discrete locations along the length. In practice, the depths may be measured after the crack is mechanically opened, e.g., by burst testing, or by nondestructive examination. The development of the evaluation models and methods in this section is based on measuring the corrosion crack depths after burst testing of the SG tubes. In general, the number of locations at which the depth is measured ranges from about 10 to 30, but may be significantly more. For NDE measurements, the discrete locations correspond to elevations at which the eddy current coil passes over the crack, e.g., about every 20 or 30 mils. Thus, a one inch long crack would be typified by about 30 to 50 measurements of the depth over the length of the crack. Because of the variability of the amount of uncracked radial ligament material along the length of the crack, the actual process of the tearing of the ligament and the eventual burst of the tube is a complex event. The intent of the development activity discussed herein was to obtain a relatively simple model that could be used to describe a more complex event with reasonable statistical error.

The burst pressure of cracks extending partially through the tube wall is usually expressed as a function of the burst pressure of the uncracked portion of the tube. The analysis of partial depth cracks is practically based on consideration of an equivalent uniform depth rectangular shaped crack. Usually, the overall crack length is maintained as a constant and the rectangle depth is calculated to maintain the crack area constant. This is the same as calculating the average depth of the crack accounting for the specific lengths of the segments making up the crack. There are two limiting pressures between which the burst pressure must lie, that for the non-degraded tube at the upper end and that for a tube with a 100% throughwall crack of the same overall length at the lower end. For degradation that is truly rectangular in shape the burst pressure appears to be a linearly decreasing function of depth up to about 80% of the thickness of the tube. Thus, initial model considerations tend to treat the remaining ligament area as uniformly contributing to the burst strength of the tube. The governing equation for the linear model is,

$$P_B = P_0 - h(P_0 - P_{TW}),$$ (5-1)

where P_B = the predicted burst pressure of the tube,

P_0 = the burst pressure of the non-degraded portion of the tube,

h = the ratio of the depth of the indication to the thickness of the tube, and

P_{TW} = the burst pressure of a 100% throughwall crack of the same length.

When h is zero the predicted burst pressure is the non-degraded burst pressure and when h is one the predicted burst pressure is the 100% throughwall burst pressure. Because of the irregular nature of the crack profiles, the burst pressure for a shorter and deeper portion of the crack may be less than that for the overall crack. This means that a thin ligament could rupture and tearing could take place at the ends of the portion of the crack located in the section with the narrowest radial ligament without the rupture occurring over the entire crack length. Therefore, the evaluation of the burst pressure for an indication consists of estimating the burst pressure of every continuous subsection that can be formed from the individual, and contiguous, discrete crack profile sections. Two examples of such subsections are illustrated on Figure 5-1(a). If there are N individual segments described by the eddy current depth measurements, the very first burst pressure calculation is for only the first segment. The second calculation involves the combined first and second segments. In this manner, the Nth profile evaluated is that of the entire crack. The $N+1^{st}$ profile considered consists of only the 2nd segment, etc. The very last profile for which a burst pressure is calculated consists of only the Nth segment. The minimum calculated burst pressure is then taken as the best prediction of the burst pressure of the tube. Westinghouse refers to the implementation of this approach as the "Weak Link" model. Other vendors refer to the same process as finding the structurally significant or effective or the structural minimum portion of the crack. For example, a crack may have an overall length of 0.9", but, because of the depth profile the central 0.5" length may be predicted to have the lowest burst pressure when the remaining portion of the crack is ignored. Hence, that section is the *weak link* in resisting burst. An illustration of the potential weak-link profile for a part-throughwall axial crack is illustrated on Figure 5-1(b). The rectangular shape is characterized as having a structurally effective length and depth. These may alternatively be referred using terms such as structural, effective, etc. There are differences in the models used for estimating the burst pressure of the discrete rectangular shapes, e.g., some expressions are aimed at estimating the burst pressure of the tube while others are aimed at estimating the pressure for tearing of the remaining ligament. The linear interpolation model has been found to correlate reasonably well with measured burst pressures, however, the associated error is greater, and tends to become non-conservative, for indications with the lowest burst pressures.

There are two features of the linear interpolation model that can lead to an over-prediction of the burst pressure. The first is in treating the flow strength of the material as being independent of depth, which essentially ignores the potential for the ligament to tear at a pressure lower than the actual burst pressure. In other words, the model always assumes that the ligament material will contribute to the overall burst pressure. The second feature is that the analysis model of the sub-crack does not consider that the adjacent ligament is thinner than the tube wall.

Experimental results from burst tests using rectangular EDM slits to simulate axial cracks in tubes indicates that the linear interpolation assumption appears reasonable for ligament thickness values greater than 20 to 25% of the tube wall. This result was also independently reported for results from burst tests performed in France. For smaller ligaments the increase in burst pressure above the throughwall value is less than expected using a linear model. This means that the remaining ligament area does not contribute uniformly to the burst strength of the tube. For a crack that has a very small remaining ligament, i.e., is almost throughwall, the ligament material is incapable of absorbing any significant plastic strain and the ligament would not be expected to contribute to the overall strength of the tube. In effect, the burst pressure of the tube without the ligament is greater than the internal pressure to tear of the ligament. A calculation model, which simply adds the ligament tearing pressure to the burst pressure without the ligament, would be expected to over-predict the burst pressure.

With regard to the second feature of the model that could lead to over-prediction of the burst pressure, consider an idealized crack with a total length of, say, 1.5 inches, and a depth of penetration 35% of the tube wall for the first 1/2", a depth of 85% over the next 1/2" and a depth of 35% for the final 1/2". The

center portion of the crack will likely dominate the estimation of the burst pressure, which is based on a depth of 85% in a tube with a full thickness adjacent ligament, not a tube where the adjacent ligament is 65% of the wall thickness. This is likely to be meaningfully less significant than the first feature because the diminished ligament thickness extends only over the width of the crack and some notch strengthening will be present, i.e., the situation is not like one in which the thickness of the remaining tube would be considered to be reduced. No specific refinements to the model have been postulated or planned to address the effect of the reduction in adjacent ligament thickness. The is not a significant omission since the end result of the development is a regression model with the distribution of prediction errors being well characterized by a normal distribution.

Two approaches were considered as the basis for the prediction methodology, modify an analysis model for predicting mean burst pressures and modify an analysis model for predicting lower bound burst pressures. Starting with the mean model, for example, the linear interpolation model, adjustments could be made to account for reduced ligament contribution to the strength of the tube, etc. Use of a lower bound model leads to the consideration that the actual burst strength should frequently exceed of the lower bound prediction. The use of both approaches was investigated. The lower bound model was found to be simpler, easier to develop, and more reliable in dealing with the complex profiles of part-throughwall cracks and was selected as the final methodology.

Most tube burst evaluation models consider the burst pressure to be a function of the tube dimensions and a material property referred to as the flow stress. The flow stress is used to evaluate an elastically calculated stress to failure of the material for ductile materials. For Alloy 600 and 690 the flow stress is taken as a fraction of the sum of the yield and ultimate tensile strengths of the material. For tubes with no degradation the nominal value of the fraction to relate the Tresca stress intensity to the burst pressure is 0.60. European (Belgian and French) practice has been to use a value of 0.58 and to express the burst pressure in terms of the hoop stress. The net result of a comparison of the two forms is that they are essentially equivalent, differing by less than 3%.

The selected approach to estimating the burst pressure, P_B, was evaluated using the work of Cochet, References 8-15 and 8-16, for predicting remaining ligament tearing of rectangular shaped axial crack profiles. For axial cracks there are essentially three analytic models depending on the depth of the crack. The first model applies to axial cracks with relative depths, h, in the range of 20 to 85%; the second for cracks greater than 85% deep; and the third for 100% throughwall indications. For cracks less than 20% deep, the burst pressure is not considered to be significantly degraded. The equation for predicting the lower bound burst pressure, that is, the ligament tearing pressure, for rectangular cracks with depths in the range of 20% to 85% is based on force equilibrium between the cracked and uncracked portions of the tube in the hoop direction. The radial ligament is postulated to tear when the ligament area, and an additional length of the tube, equal to the thickness of the tube, at the ends of the crack is at the flow stress of the material. Hence the force on the cracked area, F_C, at incipient tearing of the ligament is the flow stress, taken as 0.58 times the sum of the yield and ultimate tensile strengths, times the affected area, i.e.,

$$F_C = 0.58(S_Y + S_U)\left[L(t-d) + 2t^2\right],$$

where L = the length of the crack,
  t = the thickness of the tube,
  d = the depth of the crack,
  S_Y = the yield strength of the material, and
  S_U = the ultimate tensile strength of the material.

For an outside diameter crack, the hoop force, F_H, due to the burst pressure hoop stress acting on an area of like length away from the crack is,

$$F_H = \frac{P_B R_i}{t} t(L + 2t),$$

where: P_B = the predicted tube burst pressure, and

         R_i = the inside radius of the tube.

The two forces must be equal for equilibrium, so the final equation for the burst pressure becomes,

$$P_B = 0.58(S_Y + S_U)\frac{t}{R_i}\left[1 - \frac{L}{L + 2t}h\right], \tag{5-2}$$

where h = the ratio of the depth of the crack to the thickness of the tube.

The consideration that material beyond the tips of the crack must be at the flow stress leads to the $2t$ term in the denominator of the term in brackets. Both foreign and domestic experience using this failure equation with the weak-link calculation method leads to effective lower bound estimates of the burst pressure. This will become evident from the subsequent discussion of the final model and comparison of test data to predictions as illustrated on Figure 5-2. The main reason for this is that the burst pressure must be greater than or equal to the ligament tearing pressure. While the model is an effective model for the lower bound burst pressure of part-throughwall (PTW) cracks, a tube might not burst when the remaining ligament tears. Therefore, the above model must be considered in conjunction with a lower bound model for the burst pressure of tubes with 100% throughwall cracks. So, to complement the PTW model, a lower bound model for estimating the burst pressure of throughwall cracks was developed, i.e.,

$$P_B = 1.15(S_Y + S_U)\frac{t}{R_o}\left(\sqrt{4 + 1.61\frac{L^2}{R_m t}}\right)^{-1}, \tag{5-3}$$

from work performed to support limits contained in the ASME Code, Reference 8-17. Here, R_o and R_m are the outside and mean radius of the tube respectively. Results from predictions using this equation were compared to the data of Reference 8-13 to verify that it is an effective lower bound expression. The theoretical bases for the form and constants in the equation are provided in Reference 8-21.

For completeness, the French approach for indications with an average depth greater than 85% deep employs an expression for the tearing of the ligament based on empirical work performed at Battelle, Reference 8-18. When the depth of the indication is 100%, the tearing pressure is zero, hence, the model is more aimed at the prediction of onset of leakage instead of tube burst. Once the ligament has torn, however, the 100% depth expression could be used to determine if the crack would continue to run. For indications that are uniformly 100% deep, the burst pressure is considered to be related to the Tresca stress intensity associated with the flow stress divided by a bulging magnification factor. In conclusion, the French approach does support the contention that any ligament thickness of less than 15 to 20% of the tube wall thickness will likely tear in advance of the burst pressure of the subsequent throughwall crack.

As previously noted the final model selected for the analyses is composed of two parts, the limit tearing stress model for the remaining ligament, Equation 5-2, coupled with the throughwall equation from the

ASME Code, Equation 5-3. Because the ligament tearing model is based on estimating when leakage will occur and not when burst will occur, it is a lower bound model. Hence, it is coupled with a lower bound model for the burst pressure of throughwall indications. Both Equations 5-2 and 5-3 have their roots in the theoretical evaluation of the strength of the tubes and have no parametric uncertainties. For each of a number of combinations of crack profile and burst test results the estimated burst pressure of the tube was calculated. Regression analyses of the measured against the predicted burst pressures was then performed. The results from the regression analysis leads to a exponential model relating the measured to the calculated burst pressure. The regression results were then used to characterize the uncertainties associated with the prediction of the burst pressure.

5.2 The Database for Analysis

The database for the development of the model is presented in Section 3.0 of this report. However, not all of the data was utilized because the range of application of the model is really limited to measured burst pressures less than about 5000 psi (the largest $3 \cdot \Delta P_{NOp}$ requirement to comply with regulatory guidelines). Moreover, the main range of interest is probably more limited to less than about 4000 psi to comply with the $1.4 \cdot \Delta P_{SLB}$ requirement during a postulated steam line break event. For the analysis, it was decided to first consider all data for which the burst pressure was less than or equal to 10000 psi. The standard deviation of the model residuals would be expected to be on the order of 500 psi, therefore, the selection of 10000 psi provides a margin to the potential loading of about 11 standard deviations. The database used for the analysis is listed in Table 5-1 and depicted on Figure 5-2. Data were omitted from the regression analysis for two causes. The first being the predicted burst pressure being greater than 10000 psi. The data excluded from the regression analysis because of high predicted burst pressures are listed in Table 5-2 and also identified on the Figure 5-2.

5.3 Burst Pressure Correlation for Partial Depth Cracks

Examination of the data presented in Table 5-1 and on Figure 5-2 demonstrates that the models selected do indeed result in practical lower bound predictions of the burst pressure. Comparison of the data in Tables 5-2 and 5-3 does not lead toward any different conclusion. The only significant negative deviation (measured minus predicted) occurs for a specimen with a measured burst pressure of about 5.5 ksi. To perform the regression analysis, a *normalized* burst pressure, G_B, was defined as the ratio of the tube burst pressure to the sum of the yield and ultimate tensile strengths of the material, S_F, also referred to as twice the flow stress, S_f, i.e.,

$$G_B = \frac{P_B}{S_Y + S_U} = \frac{P_B}{S_F} = \frac{P_B}{2S_f}.$$ (5-4)

The P_B in the numerator of Equation 5-4 is the measured or calculated burst pressure. Note that the capital F subscript is used to denote a material strength of twice the flow stress. The subscript B is used to designate a quantity associated with the measured burst pressure, while the same quantity calculated from the mathematical model will have a subscript M. Thus, the PTW lower bound model becomes:

$$G_M = \frac{P_M}{(S_Y + S_U)} = 0.58 \frac{t}{R_i} \left(1 - \frac{L}{L + 2t} h\right),$$ (5-5)

from Equation 5-2, and the throughwall bounding model is,

$$G_M = \frac{P_M}{(S_Y + S_U)} = 1.15\frac{t}{R_o}\left(\sqrt{4 + 1.61\frac{L^2}{R_m t}}\right)^{-1}, \tag{5-6}$$

from Equation 5-3. The estimated normalized burst pressure is then obtained as the maximum of the two different calculations. The calculation returns the larger of the smallest estimate from the Equation 5-5 that is greater than the value from Equation 5-6 or the value from the Equation 5-6. The database for the regression analysis is depicted on Figure 5-3. The rationale for normalizing the data was that the distribution of material strength from the tested tubes would not be expected to be representative of that of the population of operating tubes. Using this approach, the distribution of actual burst strengths is then calculated as the product of the distribution of regression errors and the distribution of material strengths for the specific SG or tube size from a specific manufacturer.

A regression analysis of the normalized measured burst pressures on the model predicted normalized burst pressures was performed to obtain the final predictive equation,

$$\ln(G_B) = a_0 + a_1 \ln(G_M), \text{ i.e., } G_B = e^{a_0 + a_1 \ln(G_M)}. \tag{5-7}$$

The results from the regression analysis are summarized in Tables 5-4 and 5-5. Table 5-5 lists the index of determination values corresponding to linear and logarithmic scale factors for the coordinate axes. The linear-linear and log-log scale factor combinations have a slight advantage relative to the linear-log and log-linear combinations. The log-log pair of scale factors was selected based on the physical consideration that the burst pressure cannot be negative regardless of the magnitude of the theoretical prediction. The p value for the slope parameter is essentially zero, hence the regression is significant at an acceptable level. Moreover, the indices of determination for the various scale choices indicate that both scales should be linear or both should be logarithmic, with about equal preference. The analysis performed considered both scales to be linear. The regression line on Figures 5-3 and 5-4 illustrates the measured data relative to the final predictions made using the regression equation. The distribution of the residual values of G_B is shown on Figures 5-5 and 5-6. The scatter plot on Figure 5-5 illustrates that the residuals are not correlated to the predicted values of the normalized burst pressure. Finally, the normal probability plot on Figure 5-6 confirms that the residuals of the logarithm of the pressure do not contradict the assumption of being from a normal, i.e., Gaussian, distribution.

The test data used in the regression analysis were obtained from ODSCC specimens and from PWSCC specimens that were not necessarily pressurized on the crack flanks. The testing process for ID cracks frequently includes the use of a plastic liner to prevent premature loss of pressure if the cracks are suspected of being very deep. Therefore an adjustment to the predicted burst pressure, if it is governed by the PTW expression, must be made. The ligament tearing equation is derived for inside diameter cracks by adding the internal pressure force on the crack flanks to the hoop stress force. The resulting solution for the burst pressure for internally pressurized cracks can easily be shown to be a multiple of the solution for an external crack. The adjustment term calculated for the PTW burst prediction is,

$$P_{Bi} = P_{Bo}\left(1 + \frac{t}{R_i}h\frac{L}{L + 2t}\right)^{-1} \text{ where } P_{Bo} = G_B(S_Y + S_U), \tag{5-8}$$

and the subscript P_{Bi} stands for the burst pressure of an ID crack, e.g., PWSCC, and P_{Bo} stands for the burst pressure of an OD crack. The inverse relationship with some typical numbers for 7/8" diameter

tubes indicates that the burst pressure for ID cracks will usually be on the order of 6% lower than the burst pressure for OD cracks.

5.4 Calculation of Burst Pressures and Probability of Burst by Simulation

The development of the probabilities of burst during a postulated SLB event as reported in Section 7 of this report are based on Monte Carlo simulation of the contributing factors of the analysis, e.g., length, depth, growth, etc., along with the uncertainties associated with those factors. For example, the measurements of the depth profile of an indication have an associated random error or uncertainty. The same is true for the measurement of the length of the indication. The basic simulation process for one indication would be to calculate the burst pressure many times, say 5,000 or 10,000, and record the number of times the calculated burst pressure is less than a specified limit, e.g., the SLB predicted pressure. The nominal probability of burst is the number of times the calculated pressure is less than or equal to the criterion pressure divided by the number of simulations performed. The distribution of results is dichotomous, the calculated pressure either exceeds the criterion value or it doesn't. Hence, binomial distribution characteristics may then be used to adjust the nominal probability to establish a new value with a specified level of confidence. This is the same methodology endorsed by the staff in Generic Letter 95-05.

The variables associated with the calculation of the burst pressure are the initial length and depth profile of the indication, the future growth of the profile, the predicted normalized burst pressure for the future profile, and the material strength of the tube. The Monte Carlo simulation proceeds as follows:

1. A nondestructive examination length and depth profile of an indication is selected in the order of a listing of all of the active, not plugged, indications present in the SG. This is done after the creation of indications that are representative of missed indications based on the POD.

2. The length values of the profile are adjusted to account for a random error associated with the length measurement where the distribution parameters are given in Section 4 of this report. For example, assume that the random length error is positive, meaning that the measured length is expected by chance to be shorter than the actual length. The axial location value of the tip of the crack farthest from the centerline of the TSP is increased by the amount of the error. Profile locations or nodes within a distance from the end equal to the error are adjusted proportionately. For example, if the error was 0.060" and the spacing of the profile nodes was 0.030", the tip and the 1st inboard nodes would be adjusted by 0.060" and 0.030" respectively to achieve a net lengthening of the overall crack. The 2nd inboard node would not be adjusted.

3. The depth values of the profile are adjusted to account for a random error associated with the measurement of the average depth. Each depth value in the profile is adjusted by the same error, creating a self-similar profile at a different average depth. The distribution of depth uncertainties is given in Section 4 of this report.

4. The length values are adjusted further to account for a random growth of the crack in the axial direction. Each individual point of the profile is proportionately adjusted for the total projected growth of the indication. The adjustment proceeds in each direction from the axial center of the crack. A uniform random number is selected to represent a random value of the CDF probability of the growth. The random CDF value is then used to enter the growth distribution to obtain a corresponding value of the growth to be applied.

5. The depth values are adjusted further to account for a random growth in the thickness direction. All points of the profile are adjusted by the same absolute value of the average depth growth, creating a self-similar profile at the final average depth. Final depth values greater than the thickness of the tube are assigned a depth equal to the thickness of the tube.

6. The final length and depth profile is then used as input to the *Weak Link* algorithm to calculate the mean predicted value of the normalized burst pressure, G_B. A random relational error is then added to the predicted pressure. The relational error is calculated as a Student's t deviate times the effective standard deviation associated with establishing a prediction bound for a single occurrence of the independent variable. A random uniform distribution value (between zero and one) is used to obtain a random variate from the inverse relation for the Student's t distribution.

7. A random, normal distribution value of the material strength is calculated using the mean material strength and the reported standard deviation for the material strength. The normalized burst pressure of the previous step is multiplied by the material strength to obtain a random value of the expected burst strength of the indication.

8. The burst strength value is then compared to the criterion limit value. If it is greater than the criterion value the tube is predicted to not burst during a postulated SLB event and vice versa.

9. All of the preceding steps are performed for each indication in the SG. The calculated burst pressures are stored along with the number estimated tube bursts.

10. All of the preceding steps are performed to effect many simulations of the combined effect of all of the indications present in the SG. The results of the simulations are then evaluated to estimate the probability of a predicted burst pressure being less than the criterion pressure.

The final solution for the probabilities of burst, i.e., probability of a single burst of more than one burst, are developed using binomial distribution probabilities. The solution is a probability value at a 95% upper level of confidence. In other words, the likelihood of the probability of burst being less than the value reported is 0.95.

5.5 Estimated Burst Pressures and Probability of Burst

The burst pressure for a given value of the yield plus ultimate stress, S_F, or equivalently twice the flow stress, S_f, is then given by,

$$P_B = G_B(S_Y + S_U) = G_B S_F \tag{5-9}$$

As before, G_B is obtained from the maximum value of G_M corresponding to the physical dimensions of the tube and the crack profile. The results of the regression analysis demonstrate that the distribution of $\log(G_B)$ may be considered to be normal about the predicted, or mean, value of $\log(G_B)$ from Equation 5-7. This is the same as saying that the distribution of residual values, the actual value minus the equation prediction, may be considered to be normally distributed about Equation 5-7 predictions. Because the axes for the regression analysis were log-log, the distribution of G_B about the regression predictions will be lognormal. Although the indices of determination from the linear-linear and log-log regression analyses are about the same, see Table 5.5, the log-log expression was selected on the basis that it appeared to provide better predictions when the burst pressures were low, i.e., in the range less than about 4500 psi.

The main difference between the normal and log-normal distributions about the mean regression line is that the log-normal distribution has a zero probability of predicting a zero or negative normalized burst pressure, G_B, from the residuals of the regression equation. Mathematically, the same is not true if a normal distribution were used. However, the mean predictions of interest are several multiples of the standard deviation greater than zero in the linear case so that the probabilities of burst (POB) obtained from either equation are similar. This means that probability distribution function (PDF) plots of either solution would look very similar except in the extreme lower tail region, and the discussion of the following paragraph would not be materially affected by the difference.

The interest in using the regression analysis results is in predicting the actual burst pressure, P_B, which is the product of the normalized burst pressure and the material strength, i.e., $G_B \cdot S_F$. It is standard practice to consider the distribution of S_F to be from a normally distributed population having a mean and standard deviation which depend on the tubing size and the vendor of the tubing. Difficulties arise with the above estimation scheme because the value of interest is the product of a lognormal distribution and a normal distribution. Determining the statistical characteristics of the distribution of the product, i.e., of P_b, is algebraically difficult, but may be easily performed using Monte Carlo simulation techniques, the technique used in the PWSCC simulation code.

For comparative purposes, algebraic estimates of the POB can be made based on some simplified calculations. It is known that the product of the two normal distributions does not itself follow a normal distribution. However, the distribution of the product is skewed right and lower bound statistics may be conservatively estimated by using a normal distribution with a mean equal to the product of the regression equation value for G_B and the mean material strength, S_F. As previously noted, the evaluation of the residuals from the regression model indicated they could be equally well represented as being a sample from a normal distribution, hence, it was decided to use the normal distribution properties in a deterministic analysis to estimate the POB as a function of G_B.

The mean value of the product of two distributions is the same as the product of the means of the two distributions. Hence, the mean actual burst pressure is the product of the regression line prediction of G_B and the mean value of the material strength, S_F. The unbiased estimate of the standard deviation, s_B, of the product $G_B S_F$ is given by,

$$s_B = \sqrt{\overline{G}_B^2 \, V(S_F) + \overline{S}_F^2 \, V(G_B) - V(S_F) V(G_B)} \ .$$

Here, V represents the variance of a variate, e.g., the variance of the residuals about the regression line, and the overbar denotes the mean value of the variable. The calculation of the probability of burst then proceeds as follows:

1. The normalized burst pressure is calculated as the maximum from the ligament tearing and ASME throughwall burst models.

2. The expected burst pressure is calculated using the material strength of the tube.

3. The number of multiples, t, of the standard deviation of the predicted burst pressure, P_B, from a specified performance criterion pressure, P_{SLB}, is then calculated as,

$$t = \frac{P_B - P_{SLB}}{s_B} \ .$$

4. The value of t follows a Student's t distribution because the test data were obtained from a sample of tubes and not the entire population of tubes. The Student's t distribution is similar to a normal distribution with the same mean, but has a larger variance and is more spread out. The probability of the burst pressure being less than the criterion value is the same as the probability of t being less than the calculated value from a Student's t distribution.

Estimated values of the probability of burst for a single indication are illustrated on Figure 5-7 as a function of the predicted normalized burst pressure values (the linear-linear relationship was used for ease of calculation and introduces insignificant error). The predicted normalized values of the burst pressure may be converted to burst pressure by multiplying by the mean value of the flow stress of the material in question. For Alloy 600 MA SG tubes in Westinghouse plants the mean value of the sum of the yield and ultimate stresses is about 138 ksi at 650°F. Thus, an indication with a predicted burst pressure of about 4.500 ksi has an average normalized burst pressure of 0.033 and an estimated PoB during a postulated SLB event on the order of 10^{-3}.

5.6 Additional Statistical Investigations

Additional statistics of the data were examined to determine if the predictions from the model could be improved based on correlations between descriptive features of the indications. The model calculated effective depth is correlated to the overall average depth, but the maximum depth is only weakly correlated to the average depth. Neither the average nor the maximum depth were found to be correlated to the total length of the cracks. Finally, the effective length was weakly correlated to the total length with significant dependence of the variance on the total length. In addition, the residual burst pressures were compared to the maximum depth to average depth ratio and to the actual indication length. The burst pressure residuals do not appear to be correlated to either parameter. The burst pressure residuals were also compared to the length-to-depth aspect ratios for average and maximum depths respectively. Again, there is no apparent trend or correlation of the residuals to either parameter. The results from the statistical evaluations and the secondary comparisons indicate that the model is sufficient for the prediction of burst pressures without including additional parameters.

5.7 Alternative Models

As an alternate to performing the regression analysis, the distribution of the errors from the theoretical prediction model were compared to several theoretical distributions. Since the prediction model is based on theoretical considerations instead of strictly empirical considerations, it is not unreasonable to expect the distribution of the residuals from the predictions should be other than normal. Several distributions were considered with regard to describing the dispersion of the data. The distribution of the residual values of the burst pressure, taken as the measured value minus the predicted value, as well as the distribution of the ratio of the observed to predicted burst pressure were considered for evaluation. The actual burst pressure cannot be less than zero, so zero is a lower bound for the distribution of the residuals and ratios. Skewed right distribution functions, e.g., lognormal, were considered first. It was found that some of the extreme value distributions, e.g., Gumbel & Weibull, can be used to provide a reasonable description of the data. This approach was not pursued further because of difficulties expected in establishing mean values of the burst pressure and estimating POB values. In addition, the tests performed indicate that there should be a significant level of confidence in the fitted model. Finally, further evaluations would likely not result in improving the correlation, but would be expected to result in a reduction of the variance of the residuals about the model, thereby reducing some of the conservatism of the analyses.

5.8 Development of 95%/95% Confidence Limits

An important result of the evaluations performed regarding the strength of axially cracked tubes is the identification of allowable EOC degradation which complies with the structural performance criteria. There are essentially two objectives relative to the actual strength of the tube. The first is that the likelihood of a free-span indication having a burst pressure less than $3 \cdot \Delta P_{NOp}$ must be small. The second objective is that the likelihood that an indication that becomes exposed during a postulated SLB event has a burst pressure less than $1.43 \cdot \Delta P_{SLB}$ must also be small. For the EOC case, the criteria must have a probability of 0.95 of being met at a confidence level of 95%. Alternatively, the probability of an indication having a burst pressure less than the performance criterion must be less than 5% at a 95% confidence level.

The computation of critical dimensions of the cracks is best performed numerically, i.e., as a Monte Carlo simulation. The results of such computations utilizing the Excel® spreadsheet program are illustrated on Figure 5-8 as the critical depth corresponding to a known length and structural criterion. Results for four pressures ranging from 3.657 to 4.300 ksi are illustrated. For each value of the pressure and length, a series of simplified Monte Carlo evaluations were performed until the depth was found that corresponded to the input pressure being the 95%/95% value of the simulation distribution.

The calculations performed to develop the information presented on Figure 5-8 treated the NDE depth and length errors as being normally distributed using the relationships presented in Section 4.6 of this report. The process for effecting a calculation of the burst pressure for a specified length of an indication was as follows:

1. A specified burst pressure, e.g., 4.100 ksi, was selected as the goal for the calculations.

2. A depth of the indication was postulated as an independent variable and a random, normally distributed error was added to the postulated depth. Normally distributed random numbers, or deviates, are calculated as the inverse of a standardized normal distribution using uniformly distributed random numbers as cumulative probability input values.

3. A random, normally distributed measurement error was added to the postulated length.

4. A mean normalized value of the burst pressure, G_B, was calculated from the length and depth resulting from steps 2 and 3 using the final regression relationship. A random, normally distributed error based on the regression residuals was added to the calculated mean value.

5. The normalized burst pressure, G_B, was multiplied by a random, normally distributed value for the material strength, S_F.

6. The calculation was repeated 1000 times and the burst pressure from each calculation was stored for an evaluation of the array. The random numbers were generated using a variance reduction technique to improve the accuracy of the predictions.

7. The array was sorted in ascending order and the 38th entry was selected for reporting as the 5th percentile (95th percentile lower bound) with 95% confidence. The 50th entry represents the 5th percentile with 50% confidence. Binomial distribution statistics, which, conservatively, do not account for the use of simulation variance reduction techniques, were used to identify the number of the entry associated with the specified confidence level.

8. The reported value was compared with the selected value of step 1. Steps 2 through 7 were repeated until a match of the 95th percentile lower bound burst pressure with the target burst pressure was obtained.

The simulation process was repeated many times for several different combinations of indication length and target burst pressure. The results of the calculations are illustrated on Figure 5-8.

Since the curves of Figure 5-8 include uncertainties in the burst correlation, material properties and NDE sizing, the curves are typical of an acceptance limit for condition monitoring assessments. Because of the large number of data for both the burst pressure and material strength, the residuals about the regression line and the residuals about the mean value of the material strength were also treated as normally distributed. In essence, it is assumed that the uncertainties in the parameters of the estimated distributions will not significantly affect the results. For 117 degrees of freedom, the average value of the inverse of the chi-squared distribution differs by about 1 to 1.5% from the inverse of the degrees of freedom. Hence, the effect of simulating the variation in the standard deviation and equation coefficients would be expected to be small. This is more likely to be true for the variation in the material properties because the larger number of data (360) used to describe the distribution indicate a variation of the mean standard deviation of about three parts in a thousand. It is also noted that these arguments relative to the lack of significance relative to the results of the analysis are also based on the consideration that the 95th percentile is being quantified. If the requirement were for the 99th percentile, the variation of the parameters of the distributions would likely become significant. This is because the multiplier for the standard deviation at 99% is about 1.5 times that at 95%.

From Figure 5-8, the results of the analysis indicate that for a measured 0.8" long indication with a depth of about 65.5%, the probability of burst at 3.657 ksi would be 5% at a 95% confidence level. This essentially means that the probability of violating the margin requirement, i.e., performance criterion, for SLB is 5%. Likewise, if the depth of the indication were 60.7%, the probability of violating a $3 \cdot \Delta P_{NOp}$ requirement of 4.100 ksi would be 5%.

5.9 Summary & Conclusions

A regression equation, i.e., Equation 5-7, was established for predicting the burst pressure of a SG tube as a function of the prediction based on two theory-based lower bound models. The lower bound analysis calculates the maximum of the ligament tearing pressure or the 100% throughwall crack burst pressure. The result is correlated to test data from a significant database using a linear regression equation. The residuals from the regression analysis were demonstrated to be independent of the test data and to be well characterized by a Gaussian or normal distribution. The equations presented may be used to simulate the burst pressure of axially cracked SG tubes using the standard error of the normalized predicted burst pressures as a normally distributed stochastic variable, i.e., $G_B \sim N(G_M, s)$ where s is the standard deviation of the regression errors.

Table 5-1 :Axial SCC Database, Part-Throughwall Crack Burst Pressure Prediction Model														
Plant Name	Year	Tube Identification	O.D. (inch)	Thick (inch)	Yield + Ultimate (ksi)	Model Burst (ksi)	Test Burst (ksi)	Effective Tip (inch)	Effective Length (inch)	Effective Depth (%TW)	Total Length (inch)	Avg. Depth (%TW)	Max. Depth (%TW)	Calc Mode

b,c

Plant Name	Year	Tube Identification	O.D. (inch)	Thick (inch)	Yield + Ultimate (ksi)	Model Burst (ksi)	Test Burst (ksi)	Effective Tip (inch)	Effective Length (inch)	Effective Depth (%TW)	Total Length (inch)	Avg. Depth (%TW)	Max. Depth (%TW)	Calc Mode

Table 5-1 : Axial SCC Database, Part-Throughwall Crack Burst Pressure Prediction Model

b,c

Table 5-1 :Axial SCC Database, Part-Throughwall Crack Burst Pressure Prediction Model														
Plant Name	Year	Tube Identification	O.D. (inch)	Thick (inch)	Yield + Ultimate (ksi)	Model Burst (ksi)	Test Burst (ksi)	Effective Tip (inch)	Effective Length (inch)	Effective Depth (%TW)	Total Length (inch)	Avg. Depth (%TW)	Max. Depth (%TW)	Calc Mode

b,c

Table 5-1 : Axial SCC Database, Part-Throughwall Crack Burst Pressure Prediction Model															
Plant Name	Year	Tube Identification	O.D. (inch)	Thick (inch)	Yield + Ultimate (ksi)	Model Burst (ksi)	Test Burst (ksi)	Effective Tip (inch)	Effective Length (inch)	Effective Depth (%TW)	Total Length (inch)	Avg. Depth (%TW)	Max. Depth (%TW)	Calc Mode

b,c

Plant Name	Year	Tube Identification	O.D. (inch)	Thick (inch)	Yield + Ultimate (ksi)	Model Burst (ksi)	Test Burst (ksi)	Effective Tip (inch)	Effective Length (inch)	Effective Depth (%TW)	Total Length (inch)	Avg. Depth (%TW)	Max. Depth (%TW)	Calc Mode
Table 5-2 : Axial SCC Database, Part-Throughwall Crack Burst Pressure Prediction Model															b,c
Data omitted from the regression on the basis of Model Predicted Burst > 10.0 ksi.															

Table 5-4: Regression Parameters of the Normalized Burst Pressure as a Function of the Model Normalized Burst Pressure $\ln(G_B) = a_0 + a_1 \ln(G_M)$		
Parameter	**Value**	**Standard Error**
Intercept, a_0	b,c	b,c
Slope, a_1		
Standard Error, SG		
Degrees of Freedom, DoF		
Number of Data, N		
Index of Determination, r^2		
Slope p Value		
Mean $\ln(G_M)$		
Corrected SS $\ln(G_M)$		

Table 5-5: Comparison of Axes Scales		
Model Burst Variate, G_M	**Measured Burst Variate, G_B**	
	Linear	**Logarithmic**
Linear	b,c	
Logarithmic		

Tube ID

Tube OD   Evaluated Sub-Cracks
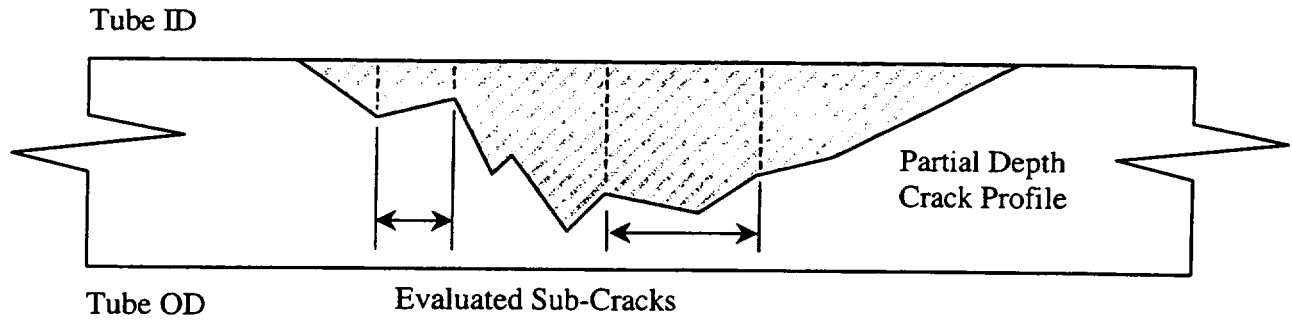
Figure 5-1(a): Representative part-throughwall axial crack profile.

Tube ID

Tube OD
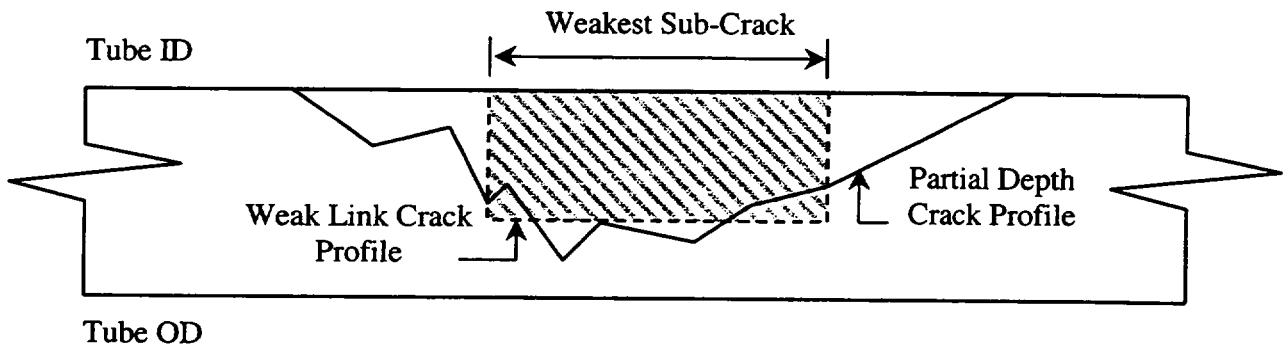
Figure 5-1(b): Representative part-throughwall axial crack profile with
the Weak Link (weakest sub-crack) profile shown.

Figure 5-2

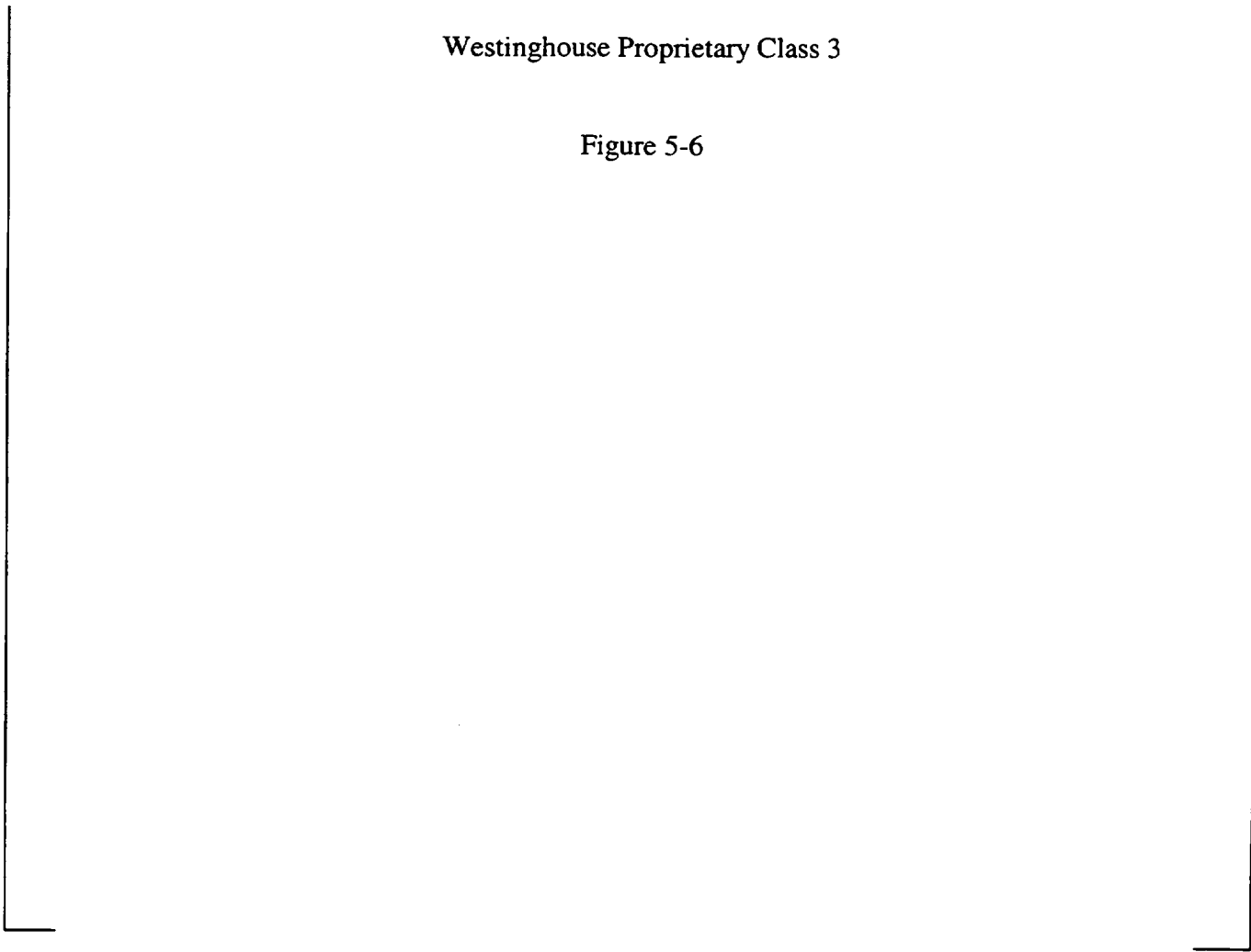Figure 5-3

b,c

Figure 5-4

Figure 5-5

Westinghouse Proprietary Class 3

Figure 5-6

Figure 5-7

Figure 5-8

6.0   SLB LEAK RATE ANALYSIS

This section develops a correlation between measured leak rates and leak rates calculated using the CRACKFLO code. The resulting leak rate correlation is then used to support condition monitoring and operational assessment leak rate analyses. The CRACKFLO code and alternate correlations of measured to calculated leak rates are described in Section 6.2. Section 6.3 provides the correlation applied for leak rate analyses in support of this report. Since the CRACKFLO leak rates are correlated to measured leak rates, the leak rates predicted with the correlation are not strongly dependent upon the specific use of the CRACKFLO code, although the uncertainties in the correlation can be dependent upon the analytical model used to develop the correlation. The ligament tearing model used to predict the throughwall length resulting from breakthrough of wall thickness ligaments is described in Section 6.4.

6.1   Leak Rate Calculation Methodology

For a number of years, leak rates for free span cracks have been calculated using the CRACKFLO Code. This code calculates a crack opening area based on the primary to secondary pressure differential acting on a tube with a given crack length and material properties. Fluid mechanics relations are applied to the pressure opened crack and assumed crack surface geometry such as roughness and tortuosity of the crack flow path. Leak rates are a function of the primary pressure and temperature. Secondary pressure also affects the flow if choking does not occur.

6.2   Leak Rates for Free Span Cracks

In this section, the available crack leak rate database is used to validate the CRACKFLO Code at steam line break conditions. The data base will also be used to assess the effect of various CRACKFLO user specified input parameters. The validation approach will be to develop a correlation including uncertainties between measured crack leak rates (i.e., "truth") and CRACKFLO Code predictions at SLB conditions. SLB leak rates with defined uncertainties can then be determined from the correlation using the CRACKFLO leak rates and a measured crack depth profile. Thus the correlation can support both deterministic and probabilistic leak rate analyses.

6.2.1   CRACKFLO Code Model Description

Crack Leakage Model

The crack leakage model assumes one-dimensional flow and accounts for crack entrance pressure losses, tube wall friction and flashing. The flow experiences a sudden contraction on entering from the primary side. The flashing of liquid to vapor generates an acceleration pressure drop while surface roughness and number of flow path turns along the flow path (tortuosity) result in a friction loss. The total pressure drop is the sum or these pressure losses, determining the pressure at the exit of the crack. For non-critical flow the crack exit pressure will equal the secondary side pressure of the steam generator, while for critical flow, this pressure will be higher than the secondary pressure.

Critical flow is evaluated according to Henry's non-equilibrium model, References 8-22 & 8-23. This method accounts for non-equilibrium effects due to finite flashing rates. This is expected to be particularly important for flow through large cracks where the fluid transit time is short.

The governing equation for flow through an axial crack is the one-dimensional momentum equation for a homogeneous two-phase fluid.

$$\frac{dP}{dy} = \frac{1}{A_c}\frac{d}{dy}\left(\frac{G^2 A_c}{\rho}\right) + \frac{f}{2D}\frac{G^2}{\rho} \qquad \text{6-1}$$

where

$P =$ Static pressure
$y =$ Flow coordinate
$A_c =$ Crack opening area
$G =$ Mass flux
$\rho =$ Fluid density
$D =$ Flow path hydraulic diameter
$f =$ Friction Factor

The first term on the right hand side of equation 6-1 is the is the acceleration pressure drop, while the second term represents friction pressure drop. The acceleration pressure drop can be expanded into component drops due to area and phase change. Assuming isenthalpic conditions, Equation 6-1 can be integrated analytically to give the pressure drop components:

Entrance
$$\Delta P_e = \frac{G_c^2 v_{fo}}{2C_D^2}\left(\frac{A_c}{A_o}\right)^2 \qquad \text{6-2}$$

Phase change
$$\Delta P_{ae} = G_c^2\left(\frac{A_c}{A_i}\right)\left[v_{fc} + x_c\left(v_{gc} - v_{fc}\right) - v_{fo}\right] \qquad \text{6-3}$$

Area change
$$\Delta P_{aa} = \frac{G_c^2 v_{fo}}{2}\left\{\left(\frac{A_c}{A_i}\right)^2 - \left(\frac{A_c}{A_o}\right)^2\right\} + \frac{G_c^2\left[\overline{v_f + x\left(\overline{v_g - v_f}\right)}\right]}{2}\left\{1 - \left(\frac{A_c}{A_i}\right)^2\right\} \qquad \text{6-4}$$

Friction

$$\Delta P_f = \left(\frac{12f}{2}\right)\left(\frac{G_c^2 A_c^2 v_{fo}}{A_o A_i}\right) + \frac{f}{2}\left(\frac{L}{D}-12\right)\frac{G_c^2 A_c}{A_i}\left[\overline{v_f}+\overline{x}\left(\overline{v_g}-\overline{v_f}\right)\right] \qquad 6\text{-}5$$

where

L = Crack depth
v = Specific volume
x = Steam quality
C_D = Orifice discharge coefficient

Subscripts f & g refer to liquid and vapor phases while o, i & c refer to crack inlet, L/D = 12 (limit of non-equilibrium flow) and crack exit. The overbar indicates average property values.

For tight cracks, short lengths and or low pressure difference, the wall thickness can comprise a large number of L/D's, often in excess of 100. For these cracks friction loss, consisting of wall shear and flow path tortuosity, predominates. Tortuosity is treated using a method proposed by Shrock (Reference 8-24), in which it is represented by a number of fluid expansions, contractions and bends. The equivalent friction factor is given by

$$f = f_p + D\sum_i n_i k_i \qquad 6\text{-}6$$

where pipe friction, f_p, is given by the modified von Karman relation

$$f_p = \left(2\log\frac{D}{2\varepsilon}+1.74\right)^{-2} \qquad 6\text{-}7$$

and also

n = Number of turns, contractions or expansions
k = Loss coefficient for turns, contractions or expansions
ε = Crack surface roughness

Critical Flow Model

For crack leakage flows, critical flow is possible. When it occurs, the rate of discharge has a maximum value, for a given crack opening, dependent on primary side conditions. Due to its importance in accident analysis, two-phase critical flow has been studied extensively. Theoretical models can be divided into two general categories: 1) equilibrium models which assume thermodynamic equilibrium between both phases throughout the discharge and 2) models which account for non-equilibrium between the phases. Equilibrium models accurately predict the critical mass flow rate in long channels, L/D > 100, where there is sufficient time for thermodynamic equilibrium to be established and the interphase forces are sufficiently developed to maintain relative motion between the phases. For shorter channels, L/D < 20-30, there is insufficient time for the vapor formation to proceed to equilibrium. In this case, non-equilibrium models provide a better predictive tool for mass flow rate. Since crack geometry comprises both short and long flow channels, both equilibrium and non-equilibrium models

are appropriate. A good representation of both flow regimes is provided by Henry's critical flow model, References 8-22 & 8-23. According to Henry, the critical mass flow is given by

$$G_c^2 = -\left(\left(v_g - v_{fo}\right)N \cdot \frac{dx_E}{dP}\right)_t^{-1}$$

6-8

for wall thickness to hydraulic diameter ratios less than 12 and

$$G_c^2 = -\left(\frac{xv_g}{P} - \left(v_g - v_{fo}\right)N * \frac{dx_E}{dP}\right)_t^{-1}$$

6-9

for wall thickness to hydraulic diameter ratios greater than 12, where

G_c = Critical mass flux
x = Non-equilibrium quality
x_E = Equilibrium quality
N = Henry's non-equilibrium parameter

The subscript t on the large brackets in these equations refers to the throat or choking plane at the exit to the crack. The parameter N accounts for non-equilibrium effects due to finite evaporation rates. This is expected to be particularly important in flow through flow through large cracks, where the fluid transit time is short. For small cracks, characterized by a large wall thickness to hydraulic diameter ratio, non-equilibrium effects are not as important and Henry's model reduces to the equilibrium model.

Crack Opening Area Model
Crack opening area is determined from equations presented by Paris and Tada in Reference 8-25. For a tube subject to differential pressure, ΔP, the elastic crack opening area is given by

$$A_c = \frac{\sigma}{E}(2\pi R t_w)G(\lambda)$$

6-10

where $G(\lambda)$ is evaluated as

a,c

6-11a

6-11b

for λ greater than or equal to 1. The crack geometric parameter, λ, is given by

$$\lambda = \frac{a}{\sqrt{R t_w}}$$

6-12

and,

σ = Hoop stress
E = Young's modulus
R = Mean tube wall radius
t_w = Wall thickness
a = Crack half length

The effect of yielding near the crack tips is incorporated by the customary method of plastic zone corrections in which a and λ are replaced by a_{eff} and λ_{eff}, respectively. In essence, the size of the plastic zone ahead of the crack is a function of the applied stress intensity factor. However, the stress intensity factor is a function of the size of the crack. Hence, the initial stress intensity factor is used to estimate the size of the plastic zone ahead of the crack tip, which is then added to the crack length to calculate an effect length for the structural and leak rate analysis. The relationship between a_{eff} and λ_{eff} is as follows

$$a_{eff} = a + \left(\frac{1}{2\pi}\right)\left(\frac{K_I}{\sigma_f}\right)^2 \qquad \text{6-13a}$$

and,

$$\lambda_{eff} = \frac{a_{eff}}{\sqrt{Rt_w}} \qquad \text{6-13b}$$

where

K_I = Applied stress intensity factor
σ_f = Flow stress

The flow stress is the average of the yield and ultimate stresses. It is apparent from Equation 6-13a that the lower the flow stress the greater the plastic zone adjustment and the greater the predicted leak rate. The stress intensity factor is a function of the hoop stress, the crack half length and geometry parameter. It is given by

a,c

6-14a

6-14b

for λ greater than or equal to 1.

6.2.2 Leak Rate Data Base

The primary validation of CRACKFLO calculated leak rates is empirical. The six sets of crack leak rate data available are listed in Table 6-1. Of these, five have leak rates measured at SLB conditions, and were the ones used for this CRACKFLO validation. Sets 1, 3 & 6 were PWSCC cracks and Sets 4 & 5 were ODSCC. For Set 2, the fatigue cracks, no leak rates were measured at SLB conditions and these data are not used in the correlations of this report.

The data sets listed in Table 6-1 provide leak rates at specified primary and secondary side operating conditions. Crack lengths are defined for tube ID and OD or as maximum and through wall lengths. Tube material properties, principally flow stress, were sometimes available; otherwise, mean properties from Reference 8-26 were used for the Inconel 600 tube in question. Tube ID & OD were of course given for each data set.

Mean material properties were used for the leakage analyses when the specific tube material properties were not reported since the leak rates have only a modest sensitivity to material properties and the affect of high or low material properties on the correlation cannot be predicted prior to completing the work. The sensitivity of leak rates to flow stress is shown in Figure 6-8 and tabulated in Table 6-5 for mean properties and for the upper/lower 95%/95% confidence on the flow stress. The effect of flow stress is insignificant for throughwall crack lengths less than 0.2 inch and a modest effect for lengths greater than about 0.3 inch. A 0.5 inch throughwall crack bounds most of the data in the leak rate database, and would be expected to bound any field indication. From Table 6-5 for a 0.5 inch crack, the lower 95%/95% on flow stress results in an increased leak rate by 37% and the upper confidence results in a decreased leak rate by 20%. About 75% of the data used in the leak rate correlation has a throughwall length less than about 0.35 inch for which the flow stress effect is bounded by about 20% for the lower confidence on flow stress. These effects are small compared to the differences frequently found between measured and predicted leak rates. Before the predicted and experimental leak rates are quantitatively compared for each data point, it is not known whether a higher or lower flow stress will improve or reduce the agreement between test and calculation. Conceptually, knowledge of the flow stress for each specimen would reduce the difference between test and analysis, and, thereby, reduce uncertainty in the correlation. However, the differences between test and calculation are more influenced by variability in the test and analysis methods than by variations in flow stress about the mean value. Overall, it is concluded that the use of the mean flow stress in the analysis, when the actual flow stress is unknown, does not significantly influence the test versus calculation leak rate correlation.

For the data sources used in this evaluation as given in Table 6-1, all of the data used in the SLB leak rate correlation are for corrosion cracks since the fatigue data does not include SLB leak rates. The database for the SLB correlation is for pulled tubes and laboratory corrosion specimens included in 5 of the 6 data sets noted in the table. Data sets 4 and 5 were obtained from the EPRI ODSCC database used for the NRC GL 95-05 ARC and are comprised of laboratory specimens. The laboratory specimens were shown in the referenced reports to have corrosion cracks representative of ODSCC pulled tubes. The PWSCC laboratory specimens from Set 1 of Table 6-1 were generated in doped steam tests, for which this report and other work have shown crack morphologies typical of pulled tube specimens. The leakage correlation is based on throughwall crack length, which reduces the sensitivity of the correlation to crack morphology. The differences between PWSCC and ODSCC cracks are primarily due to increased tortuosity for ODSCC compared to PWSCC and some tendency for ODSCC to have more uncorroded ligaments in the crack face. Increased tortuosity factors are included for ODSCC in the correlation as described below in Section 6.2.3. The throughwall crack lengths used for the leakage specimens ignore small uncorroded ligaments between microcracks which would be expected to result in increased differences between analytical predictions and test results. Due to the relatively large crack openings for the longer cracks, the leak rates for long cracks (about > 0.4 inch) are not strongly sensitive to crack morphology (surface roughness, tortuosity) or the differences between PWSCC and ODSCC cracks. As a result, the differences between PWSCC and ODSCC are even less significant than for shorter cracks. In summary, the database used for the correlation is comprised of pulled tube and lab specimens prototypic of pulled tube crack morphologies. Thus, the leak rate data is consistent with flaws found in service.

The distribution of throughwall crack lengths for the specimens used in the correlation of test results to CRACKFLO predictions ranges from 0.03 to 0.6 inch. A number of the PWSCC specimens include more than one throughwall crack. These secondary cracks were dominantly 0.1 inch with a few up to 0.15 inch. The leak rate calculations sum the leak rate from all throughwall cracks for comparison with the test results.

6.2.3 Methodology for Predicting Measured Leak Rates

For calculation, the CRACKFLO Code requires input of a single crack length. Since the data sets provide ID & OD or maximum & through wall crack lengths, there is an option to input either the through wall or a mean value. There are two additional, user specified parameters which are not available with the data sets, crack surface roughness and tortuosity. In the CRACKFLO Code, tortuosity is assumed to be the number of 45° turns along the flow path. Selection of these parameters provides additional options when comparing predicted and measured leak rates.

The following three sets of CRACKFLO Code input assumptions, with respect to crack length, surface roughness and tortuosity, were tested against the data base.

> Case 1: Mean crack length, CRACKFLO Code default roughness and tortuosity
>
> Case 2: Mean crack length, increased roughness and tortuosity.
>
> Case 3: Through wall crack length, increased roughness and tortuosity.

The choices above will significantly affect the relationship between predicted and measured values. However, as long as the selected choice is used for both the development of the correlation and the application of the correlation for field prediction, any of the choices can be used.

Crack Length Choice

Choosing either a mean length or a through wall length, as input into the CRACKFLO Code for comparison with a measured result, is a choice which significantly affects the predicted value. Often, the two measured lengths for a given crack are quite different, especially for short cracks.

Crack Roughness and Tortuosity Choice

The character of the crack surfaces and the tortuosity of the crack along the flow path through the tube wall are not measured for the available data but CRACKFLO input parameters for them are required. The default value for roughness is 0.0002 inches which is somewhat rougher than a smooth pipe. Tortuosity is input as the number of 45° turns in the flow path and the default value is zero. Both these values are conservative in the sense that they would yield higher predicted values than more realistic assumptions.

The input values for the three sets of assumptions listed above are defined in Table 6-2. The values for roughness are somewhat arbitrary. [

]^{a,c} Table 6-3 displays the roughness values used in relation to values found in Schrock, Reference 8-24, and a standard fluids text, Streeter, Reference 8-20.

The tortuosity is defined here as the number of 45° turns along the flow path. Schrock, Reference 8-24, based on studies with IGSCC cracks in a weld affected region of stainless steel pipe, gives the following relation for this number:

$$[\qquad\qquad\qquad\qquad]^{a,c} \quad 6\text{-}15$$

where, in the present application,

t_w = tube wall thickness - in.

δ = crack opening width - in.

The formula in equation 6-15 is assumed to give the tortuosity for ODSCC cracks. Because PWSCC cracks are less tortuous, an intermediate value between equation 6-15 and no tortuosity is used, given by Equation 6-16.

$$[\qquad\qquad\qquad\qquad]^{a,c} \quad 6\text{-}16$$

The above values and relations for crack surface roughness and tortuosity are reasonable for determining the impact of these parameters on CRACKFLO Code predictions in relation to the conservative default values used by the code.

6.2.4 Comparisons of Predicted and Measured Leak Rates

CRACKFLO Code predictions were made for each measured leak rate available in the data sets listed in Table 6-1. Three different predictions were made, corresponding to the 3 cases of CRACKFLO Code assumptions listed in Table 6-2.

Insofar as possible, all required CRACKFLO Code input not listed in Table 6-2, including geometry, operating conditions and material properties were take from the test data sheets and supporting materials. In some cases, material properties were not provided with the test data and were derived from Reference 8-26. The material property most important for calculating leak rate is flow stress; the best estimate value from Reference 8-26 was used. Young's modulus, which has a minimal effect on leak rate, used the ASME Code value.

Some leak tests using pulled tubes contained a number of cracks. For these cases, predictions for each crack were made and summed for comparison with the single measured leak rate.

Comparison Results

Figures 6-1 through 6-3 present comparisons of the crack the measured values with predicted leak rates for the corresponding test. Case 1 CRACKFLO assumptions, Figure 6-1, results in consistent over prediction of measured leak rates though the slope of the regression line is close to the slope of the predicted = measured line. The 95% confidence prediction upper bound follows the predicted = measured line closely. Adding more realistic roughness and tortuosity, Figure 6-2, reduces the degree of over prediction by CRACKFLO but at the same time increases the scatter of the data about the regression line. The slope of the regression continues to be close to the slope of the predicted = measured line. Using the through wall crack length for the predictions, Figure 6-3, further reduces the over prediction of the regression line, but also changes the slope to a value significantly different from

the slope of the predicted = measured line and tends to further increase the scatter of the data in relation to the regression line.

In summary, Figure 6-4 presents the three regression lines in relation to the predicted = measured line. Using the Case 2 & 3 CRACKFLO assumptions increases flow resistance and/or reduces flow area. These effects reduce, as expected, the over prediction of the Case 1 conservative assumptions. Both these assumptions tend to reduce leak rate more for short cracks (low measured leak rates) than long cracks (high measured leak rates), explaining the decrease of the regression line slope for the Case 2 & 3 assumptions. The surface roughness contributes more significantly to leak rate reduction in short cracks with small opening width because the friction losses constitute a large part of the total pressure drop for these cracks. Similarly for tortuosity, the same turns on a crack surface contribute more to turn losses when the matching crack surfaces are close together, short cracks, than when they are farther apart. The Schrock relation for Number of 45° turns reflects this since the number is inversely proportional to crack opening width, Equations 6-15 & 6-16. With respect to the assumption of through wall crack length rather than the mean length, the effect is also larger for short cracks since the ratio of maximum length to through wall length is larger for these cracks. As cracks grow deeper, the ratio of maximum crack length to through wall length tends toward unity.

6.3 SLB Leak Rate Correlation

In this section the SLB measured leak rate data sets, reported in section 6.2, are used to define a leak rate correlation for calculating SLB leak rates for throughwall cracks. The throughwall crack model as used in this analysis can be easily applied in deterministic or Monte Carlo analyses using crack depth profiles. Given a crack profile, the throughwall (applied at less than throughwall to allow for radial ligament tearing) crack length can be readily determined for input to the leak rate calculation. The radial ligament breakthrough model applied for the leakage analysis is described in Section 6.4. Based on the statistical correlation given in Figure 6-3, the measured or "truth" leak rates can be obtained from the CRACKFLO Code calculated leak rates and developed to account for uncertainties. The predicted leak rates can be obtained at any confidence level from the correlation parameters for any given throughwall crack.

6.3.1 SLB Through Wall Crack Leak Rate and Confidence Bounds

Figure 6-3 shows the regression line or median leak rate, the arithmetic average leak rate from the regression analysis (for a log correlation, the average leak rate is not the regression correlation) and the 95% confidence prediction bounds for the measured leak rates at any given calculated leak rate. For any leak rate calculated by CRACKFLO (on the abscissa), the 95% confidence prediction upper bound line represents the conservative upper bound leak rate for that calculated value. CRACKFLO leak rates are calculated as a function of the throughwall crack length for standard SLB conditions. The correlation is then applied to obtain the predicted or "truth" leak rate from the CRACKFLO leak rate. The correlation is linear in the logarithms and given by:

$$[\qquad\qquad\qquad\qquad\qquad\qquad]^{a,c} \qquad\qquad 6\text{-}18$$

The parameters for the correlation are given in Table 6-4. The correlation parameters of Table 6-4 can be used in Monte Carlo analyses for SLB leak rates as discussed in Section 7. The p-value for the slope

of the correlation is seen to be on the order of 10^{-22} and readily satisfies statistical guidance for use of a correlation.

The distribution of the residual values of Q_{truth} is shown on Figures 6-5 and 6-6. The scatter plot on Figure 6-5 illustrates that the residuals are not correlated to the predicted values of leak rates. Finally, the normal probability plot on Figure 6-6 confirms that the residuals of the logarithm of the leak rate do not contradict the assumption of being from a normal, i.e., Gaussian, distribution.

6.3.2 CRACKFLO and Correlation SLB Leak Rates for PWSCC

The Steam Line Break conditions assumed for the leak rate calculation are as follows

Primary Temperature —	600°F
Primary Pressure —	2575 psia
Secondary Pressure —	15 psia

In addition, a 7/8" OD by 0.050" wall thickness tube with a mean flow stress from Reference 8-26 and Case 3 CRACKFLO assumptions for PWSCC from Table 6-2 are assumed. With these assumptions, a unique leak rate can be calculated as a function of throughwall crack length. The SLB leak rate calculated by CRACKFLO is tabulated in Table 6-5. Although the leak rates are calculated for operating temperature conditions, the resulting leak rates are converted to room temperature gpm for comparisons with acceptance limits given as room temperature values. Table 6-5 also includes the corresponding correlation nominal leak rate from the regression equation and the upper 95% confidence on the predicted leak rate for "truth". The correlation nominal leak rate is the regression line for the correlation of measured ("truth") and CRACKFLO leak rates and represents the regression median value or 50% probability at 50% confidence.

The correlation nominal, regression or arithmetic average and upper 95% SLB leak rates as a function of throughwall crack length given in Figure 6-7 to graphically illustrate the uncertainty levels associated with the correlation. As described in Section 7, condition monitoring and operational assessment analyses for SLB leak rates are expected to be performed by Monte Carlo analyses using the CRACKFLO leak rates of Table 6-5 and the correlation parameters of Table 6-4. A correction for flow stress, as described in the following section, is applied to the CRACKFLO leak rates of Table 6-5.

6.3.3 Leak Rate Correction for Material Flow Stress

The calculations in the previous section assumed a mean flow stress of 68.8 ksi for a 7/8" OD, mill annealed, Inconel 600 tube at 650°F (Reference 8-26). From the same reference, the lower tolerance limit (LTL) for flow stress is 63.0, 9.2% lower. Assuming an upper limit 9.2% above the mean results in a flow stress of 75.1 ksi. Flow stress values lower than the mean will result in higher leak rates than those defined in Figure 6-7 while higher values of flow stress will cause leak rates to be lower. Figure 6-8 shows the leak rate dependence on the LTL, mean and maximum flow stresses.

To use the values of leak rate plotted in Figure 6-7 for flow stress values different from the mean, a table of bounding correction factors has been developed using the results of Figure 6-8. These factors appear in Table 6-5, along with the numerical values of leak rate used to plot Figure 6-7. For small cracks, ≤ 0.2 inches, the correction factors are approximately inversely proportional to the flow stress. For this range the factor has been conservatively set to 1.0 for flow stresses larger than the mean and to the flow

stress ratio for flow stresses smaller than the mean. For cracks larger than 0.2 inches, the effect on leak rate is greater and the bounding factors listed in Table 6-5 were calculated using CRACKFLO results for different values of flow stress.

For Monte Carlo leak rate analyses, the flow stress correction of Table 6-5 is interpolated for the specific flow stress and throughwall crack length of each Monte Carlo sample and the correction is applied to the CRACKFLO calculated leak rate obtained from the function of Figure 6-7.

The values for parameters needed to perform the leak rate modeling are given in Tables 6-4 and 6-5. Additional parameters for ligament tearing are given in Section 6.4.2 below.

6.4 Monte Carlo Calculation of the Radial Ligament Breakthrough Length at SLB Conditions

6.4.1 Monte Carlo Leakage Analysis Method

A Monte Carlo simulation model is applied for estimating the leak rate through degraded tubes during a postulated steam line break (SLB) event. The Monte Carlo model uses the NDE crack profiles obtained for each indication including simulation sample adjustments for maximum depth and length NDE uncertainties for condition monitoring and maximum depth NDE uncertainties, length NDE uncertainties and maximum depth growth for operational assessments. Calculations may be performed to obtain the leakage distribution for a single indication or for the entire SG indication distribution. The Monte Carlo leakage model includes:

1. The crack profile is searched for the longest lengths that would be predicted to break through by ligament tearing at SLB conditions. The profile is evaluated three times. In general, the weakest ligament of the crack will be near the center of the crack. Once that torn length has been identified, the profile of the crack above and below the torn length is evaluated to determine if a second or third location is anticipated to tear.

2. The ANL (Argonne National Laboratories) model for ligament tearing is used to estimate the throughwall length(s) of the indication(s) (See Section 6.4.2 below).

3. CRACKFLO is used to calculate a model value of the leak rate using the throughwall length(s) from the ANL model.

4. The leak rate correlation is applied to calculate a random value of the leak rate distributed about the regression line.

5. The distribution of leak rates from each of the random samples is developed and evaluated at the required confidence level (See Section 7 for ARC requirements on confidence levels) for the analysis.

The combined use of a ligament tearing model and CRACKFLO leak rates results in a conservative overestimate of the leak rate. As described in Section 6.2.1, the CRACKFLO crack opening are model includes a calculation for crack extension at the crack tip, which is also effectively part of the ligament tearing effect. Leakage is therefore based on a longer length than that obtained only from the ligament

tearing model and the predicted leak rates are inherently conservative. In addition, PWSCC cracks are initiated as multiple microcracks which grow to link up with other microcracks to form the overall macrocrack. Crack depths vary significantly between microcracks such that non-throughwall depths vary sharply over short spans. As a consequence, leak tests of corrosion induced cracks rarely show ligament tearing for more than about 2% of the wall thickness where the depth is the largest. The ligament tearing models are based on uniform average depths and typically predict breakthrough at shallower depths and longer lengths than found in tests of corrosion cracks. This effect adds further conservatism to the predicted leak rates. That is, leak rates would be over-predicted due to the CRACKFLO crack extension beyond that of the ANO ligament tearing model and due to the analytical models predicting more ligament tearing than indicated by leak tests of corrosion cracks with non-uniform depth profiles.

6.4.2 Ligament Tearing (Breakthrough) Model

The ligament tearing model is based on the use of a hoop stress magnification factor approach as presented in Reference 8-27. For a single throughwall axial crack the pressure to cause burst of the tube, P_B, is given by,

$$P_B = \frac{P_0}{m},$$

6-19

where P_0 is the burst pressure of the non-degraded tube and m is referred to as the hoop stress or stress intensity (in the fracture mechanics sense) magnification factor. The factor m is also referred to as the bulging factor because it accounts for radial deformation of the crack flanks as a function of the crack length, L, the mean radius of the tube, R_m, and the thickness of the tube, t. Reference 8-27 reported m to be

$$m = 0.614 + 0.386\, e^{-1.25\lambda} + 0.481\lambda,$$

6-20

where λ is the normalized crack length given by,

$$\lambda = \frac{0.9089\, L}{\sqrt{R_m\, t}}.$$

6-21

The expression for m is the result of a regression analysis of data obtained from numerical solutions of theoretical models of axial cracks. Hence, it represents a theoretical solution to the problem of burst of axially cracked tubes. The constant in the numerator is a function of the Poisson's ratio of the material. Reference 8-28 reviewed several models for predicting the pressure required for tearing the remaining ligament based on modifying the above formulation to use a part-throughwall stress intensity magnification factor, m_p. The inverse of the stress intensity magnification factor is a failure pressure reduction factor, herein designated by ξ. Thus, the pressure required to tear the remaining radial ligament of a part-throughwall axial crack, P_T, is found as,

$$P_T = \frac{P_0}{m_p} = \xi P_0.$$

6-22

Reference 8-28 presented a review of various formulations for m_p and recommended a final expression for m_p as a function the relative depth of the crack, h (the ratio of the depth, d, to the thickness of the tube), and the throughwall axial crack magnification factor as,

$$m_p = \frac{1 - \alpha h/m}{1 - h}, \text{ where } \alpha = 1 + 0.85 h^2 \left(1 - \frac{1}{m}\right). \tag{6-23}$$

Reference 8-28 further designated this model as the ANL model. The coefficient of 0.85 used in equation 6-23 was originally reported as 0.9 in NUREG/CR-6511, Vol. 2. Subsequent examination of the original calculation revealed that some minor changes in the computation were required to account for temperature affects on the material properties (the tensile tests were performed at room temperature and the burst tests at 600°F), the radius used for the normalized crack length, the radius used for the non-degraded burst pressure, and the number of data for which ANL depth measurements were available. The revised coefficient was obtained via Reference 8-30. The non-degraded burst pressure is computed as,

$$P_0 = 0.595 \left(S_Y + S_U\right) \frac{t}{R_m}, \tag{6-24}$$

based on a large amount of Westinghouse and industry data, including the results used in the ANL computation, see Reference 8-13.

The limit of m_p as h goes to 1, i.e., corresponding to a throughwall crack, is infinity, and the ligament tearing pressure is then zero. Results obtained from the model for three different cracks lengths are illustrated on Figure 6-9. For very long cracks, say greater than 1.5", the model is linear between the non-degraded burst pressure for zero depth and zero for 100% depth. For shorter cracks the shape of the curve becomes more and more convex. As the length approaches zero, the location of the maximum rate of change of the slope, i.e., the *knee* of the curve, tends to the non-degraded burst pressure as the depth approaches 100%.

The critical crack length as a function of crack depth for the postulated SLB differential pressure for nominal and 95/95 lower tolerance limit (LTL) material properties is presented on Figure 6-10. A curve for the critical crack length under typical normal operating conditions is also presented. It may be concluded from the figure that the effect of material property variations is small for depths greater than about 90% throughwall.

The ligament tearing model was derived to predict the behavior of part-throughwall, rectangular shaped, axial cracks. The comments of Section 5 regarding the shape of real cracks also apply to the prediction of the ligament failure pressure. The approach used to predict the ligament tearing pressure is the same as that used to predict the tube burst pressure, with the exception that the ANL model is used. Since the intent is to predict ligament tearing, no calculations of the burst pressure of the resulting 100% throughwall axial crack are performed for the leak rate evaluations. Following the naming of the burst pressure algorithm, the leak rate algorithm was designated as the *weak leak* model.

The end goal of the weak leak model is different from that of the burst pressure model. In order to estimate the leak rate, the likely throughwall crack length for a given applied pressure must be known.

Hence, the model is applied to all possible sub-cracks from the original profile and the ligament tearing pressures are calculated. The length of the sub-crack with a ligament tearing pressure just less than (not more than) the SLB differential pressure may then be used for the leak rate calculation. Following identification of this longest throughwall length due to break through at SLB conditions, the crack profile is searched to identify the next two largest sub-lengths either above or below the longest throughwall length that would also be predicted to break through at SLB conditions. The lengths predicted to be throughwall are then included in the SLB leak rate analysis. Because the profile information is based on discrete increments, the appropriate sub-crack to evaluate is the one with the minimum tearing pressure that is greater than or equal to the given critical pressure. This means that the length returned is greater than or equal to that corresponding to the tearing pressure exactly matching the critical pressure. Because the leak rate from axial cracks varies approximately with the third to fourth power of the crack length, the subsequent leak rate calculation is conservative.

It is possible for multiple, distinct sub-cracks to exist with ligament tearing pressures equal to the SLB pressure. In this case the leak rate calculation would normally be performed for all such sub-cracks and the total leak rate found as the sum of the individual values. However, the presence of such cracks is judged to be a rare event although the model considers the longest and next two largest sub-cracks with a ligament tearing pressure nearest to, but greater than or equal to, the applied SLB pressure. For the rare case of two sub-cracks having the potential for ligament tearing, the longest sub-crack leak rate can be expected to be significantly higher than that of a shorter crack due to the leak rate dependence on throughwall crack length to a power of 3 to 4. Due to both low frequency of occurrence and lower leak rate of a second sub-crack with leakage, the leakage from a potential second sub-crack can be ignored. As discussed above in Section 6.4.1, the leakage model already incorporates conservative leak rate predictions and efforts to calculate the breakthrough length for a second, shorter sub-crack are not necessary, but is included in the analysis.

Additionally, there is a conservative shortcoming of the model associated with the representation of the crack as an equivalent rectangle. Consider the case where there is a 100% throughwall portion of the crack being evaluated. One of the crack segments analyzed will consist only of the 100% throughwall region (the ligament tearing pressure will be zero in this case). The next segment analyzed will consist of the 100% throughwall length plus the inspection increment at one end of that segment. To make a rectangular representation of the crack, the incremental material will be treated as being much narrower in order to extend it over the length of the rectangle while keeping the area of the crack constant. This means that the analysis will likely predict tearing of that incremental ligament even if it is quite wide. For example, consider a 7/8" by 0.050" SG tube with a 0.3" long throughwall axial crack segment, an inspection increment of 0.030", and an adjacent depth of 50%. The geometry of the throughwall portion and the next increment will be that of a rectangle with a length of 0.33" and a depth of 95%. It is likely that such a narrow ligament would be predicted to tear at a lower pressure than needed to actually extend the crack.

6.4.3 Simulation of the Torn Ligament Crack Length

The ANL ligament tearing relation involves the calculation of a constant in the expression for determining the bulging stress magnification factor, m_p. The evaluation of the test data indicate a mean error of –0.02 in predicting the inverse of the magnification factor. The error of the estimate, ε, is given by:

$$\varepsilon = \frac{\xi_t - \xi_c}{\xi_t} \quad \text{where} \quad \xi = \frac{1}{m_p}, \qquad\qquad 6\text{-}25$$

and the subscript t denotes the experimentally measured test failure pressure reduction factor and c denotes the predicted value from the empirical (ANL) equation. The negative value of the mean error indicates that the experimental failure pressure is usually slightly higher than the predicted failure pressure. The standard deviation of the error was calculated to be 0.05. Owing to the errors in the determination of ξ there will be an uncertainty associated with the value of m_p in the ligament tearing equation. The criterion for ligament tearing then becomes,

$$\frac{P_0}{m_p + \Delta m_p} \le P_{SLB} \quad \text{or,} \quad \frac{P_0}{m_p} \le \left[1 - \frac{\Delta\xi}{\xi}\right] P_{SLB}, \qquad\qquad 6\text{-}26$$

where $\Delta\xi$ is the uncertainty or error in determining $1/m_p$, and P_{SLB} is the primary-to-secondary differential pressure associated with a SLB event. The intent of the calculation is to account for the effect uncertainties associated with $1/m_p$ on the ligament tearing length from the ANL equation. The actual process of estimating the leak rate is to find the maximum length associated with any tearing pressure that is less than the critical accident pressure. The process is repeated for the remaining profile on either side of the initial maximum length to identify up to two additional maximum tearing lengths associated with the remainder of the profile. The relative error of $1/m_p$ is given in the square bracket of the above equation. Thus, uncertainties in $1/m_p$ may be translated to uncertainties in the length by adjusting the critical pressure for which the torn length is to be found. The simulation of the uncertainties in $1/m_p$ may be achieved by directly sampling (with replacement) the observed distribution of the errors. The observed relative errors, $\Delta\xi/\xi$, from the ANL data are listed in Table 6-6. The errors are approximately normally distributed as shown on Figure 6-11 and the errors are independent of the calculated value of $1/m_p$ as shown on Figure 6-12. This means that the simulation of the errors may be performed independent of the value of $1/m_p$ calculated.

For example, if the relative error of $1/m_p$ is negative, then the calculated tearing pressure, P_T, must be compared to a larger critical pressure to determine if ligament tearing occurs. The length of the torn ligament is calculated from the value of P_0/m_p that just satisfies or exceeds the criterion. Hence, increasing the criterion pressure results in the calculation of a longer crack length. This occurs when the error in ξ is negative. The converse is also true, if the relative error of ξ is positive, then the criterion pressure is reduced, consequently the applicable ligament tearing pressure is reduced as is the corresponding torn length.

In practice, a random error in ξ is selected for each indication in the SG. The critical pressure for ligament tearing is calculated as the right hand side of Equation 6-26. As the *WeakLeak* model calculation is performed, the ligament associated with the sub-crack with the minimum burst pressure that is still greater than the critical pressure is assumed to tear and the length used for the leak rate calculation. If no sub-cracks have ligament tearing pressures less than the critical value, the crack is assumed to not leak during a postulated SLB event.

6.4.4 Simulation of the Actual Leak Rate

Table 6-4 presents the results of performing a regression analysis of the measured leak rate on the leak

rate predicted by the Westinghouse code CRACKFLO. The leak rate values simulated by the Monte Carlo code are predictions based on using the effective standard deviation of the log, i.e., logarithm, of the leak rate and the Student's t distribution. The method includes simulation of the uncertainties of the regression parameters.

Information presented in Section 6.3 documented the development of a regression model to be used for predicting the expected actual leak rate, Q_a, from a throughwall axial crack as a function of the leak rate predicted by the Westinghouse computer code CRACKFLO, Q_c. The regression equation is linear in the logarithms of the respective variables, i.e.,

$$\log(Q_a) = b_0 + b_1 \log(Q_c), \qquad\qquad 6\text{-}27$$

where b_0 and b_1 are the coefficients of the equation obtained from the regression analysis. The values of the coefficients are listed in Table 6-4. The available data are only a sample of some infinite population of pairs of leak rates. Therefore, the solution coefficients, and the standard deviation, s_r, of the residuals from the regression analysis, are estimates of the parameters of some "true" equation that would be obtained if the entire population of all possible leak rates were analyzed. If these were the true coefficients and standard deviation of the residuals, the parameters of the "true" relation, the distribution of a large number, N, of future values of the logarithm of the actual as a function of a predicted leak rate could be calculated as,

$$\log(Q_{a,i}) = b_0 + b_1 \log(Q_c) + Z_i\, s_r \ ; i = 1,...,N, \qquad\qquad 6\text{-}28$$

where the subscript i indicates some i^{th} value, and the Z_i are random numbers from the standard normal distribution (mean of zero and standard deviation of one). However, the coefficients and standard deviation are obtained from the analysis of sample data. Therefore, the simulation must account for the potential statistical errors arising from the use of the sample data to estimate the population parameters.

One approach that has been approved by the staff for simulating the total leak rate from multiple indications is documented in Reference 8-10. The simulation proceeds as follows:

1. For each simulation of the indications in the SG in toto, a random value of the population standard deviation, σ, is estimated from the regression standard deviation, s_r, using a random value from the Chi-Square distribution (the distribution of variances of samples drawn from a normal population).

2. The population σ is then used to estimate a random value of the population intercept regression coefficient, β_0, corresponding to the sample estimate, b_0, as following a normal distribution with the known population standard deviation divided by the square root of the number of test values used in the correlation.

3. The population σ and β_0 are then used to estimate a random value of the population slope coefficient, β_1, corresponding to the sample estimates, b_1. The values of β_0 and β_1 follow a bivariate normal distribution, hence the sampling of each value is not independent of the other.

4. A random value of the log of each leak rate for each indication in the SG is then calculated as,

$$\log(Q_j) = \beta_0 + \beta_1 \log(Q_{c,j}) + Z_{R,j}\,\sigma \qquad \text{6-29}$$

where the $Z_{R,j}$ are independent random values from the standard normal distribution, and j varies from one to the number of indications.

5. The total leak rate from the simulation of all of the indications in the SG is then calculated and retained as the estimate from a single simulation.

6. The process is repeated many times, say 10,000, and the distribution of total leak rates characterized, mean, standard deviation, etc. A selected percentile, e.g., 95th, of the distribution of leak rates is then used to estimate the potential leakage that could occur during a postulated SLB event.

If that estimate exceeds a plant specific allowable value, additional tubes are removed from service until the 95th percentile prediction is less than the allowable. This approach simulates the uncertainties associated with estimating the regression parameters from the sample data. The approach using equation 6-29 is rigorous in accounting for all possible uncertainties associated with the prediction as long as the assumption of normally distributed residuals is valid.

If the number of data is large and the variance of the predictions small, the omission of the simulation of the uncertainties associated with the calculation of the parameters (the coefficients and the standard deviation of the residuals) may not significantly affect the simulation of the total leak rate. However, this has not been demonstrated to be the case for this problem and simulation of the uncertainties of the parameters was performed as part of the Monte Carlo analysis.

6.4.5 Conclusions

Monte Carlo simulations à la Equation 6-29 are performed to simulate the total leak rate from the SG. Due to the complexity of the equation for ligament tearing, the error in the predicted tearing pressure reduction factor is simulated using the actual distribution of errors associated with the qualification of the model, i.e., just as the growth rate is simulated.

6.5 Uncertainties in SLB Leak Rate Analyses

The following items address methods and uncertainties used in the SLB leak rate analyses relative to their increasing or decreasing the conservatism in the leakage analyses.

1. Leak rates based on calculated ligament tearing breakthrough length
   - Very conservative methodology for leak rate analysis based on leak rate correlation
   - Effects of ligament tearing are already included in leak rate correlation as the difference between test and calculation since calculations are based only on the corrosion throughwall crack length with no breakthrough allowance. Net effect on correlation is to increase uncertainty since difference between test and calculation would increase if ligament tearing was significant.

- Calculated TW length will always equal or exceed corrosion TW length, thus uniformly increasing predicted leak rate.
- If ligament tearing was included in the correlation development, the calculated leak rates would increase, the mean regression correction to test results would decrease, and the uncertainty in the correlation would conceptually decrease. However, crack depth profiles are not available for more than 50% of the database and these data could not be used in a correlation based upon ligament tearing analyses.

2. Inclusion of uncertainties in the ligament tearing model

- Conservative methodology
- Further increases the larger leak rate predictions above the conservatism resulting from Item 1 above.

3. Inclusion of POD = 0.6 in leakage operational assessment

- Very conservative methodology
- Indications large enough to leak in the subsequent operating cycle can are expected to be detected with a POD much higher than 0.6 and likely approaching unity. This expectation is supported by the absence of any leaking PWSCC indications at dented TSP intersections in Sequoyah and Diablo Canyon SGs.
- Based upon the POD adjustment applied as 1/POD to define the BOC indications, the effect of applying a POD = 0.6 is to increase the leak rate for indications left in service by 67%.
- The 0.6 POD leaves in service 0.67 of an indication for each repaired indication. For depth based tube integrity assessments, this effect is excessively conservative and can lead to repaired indications leading to unacceptable leakage in the operational assessment. For example, if a few indications satisfy all condition monitoring requirements but are very close to throughwall or have negligible leakage, the addition of growth to 0.67 indication for each of these repaired indications could lead to exceeding the operational leakage limit for plugged tubes. In this case, repair of all indications would still lead to exceeding operational assessment limits.

4. Crack depth profiles are adjusted to 100% depth for indications with maximum amplitudes > 4.5 volts based on application of the data adjustment procedures

- Conservative methodology intended to improve nominal leak rate predictions
- PWSCC indications with finite throughwall lengths are expected to exceed 4.5 +Point volts as supported by the database of this report.
- Addition of NDE uncertainties then increases the throughwall length and associated leakage
- Further calculation of ligament tearing length will further increase throughwall length and leakage

5. Finite +Point coil resolution (0.16") tends to reduce very short maximum depths

- Modest non-conservatism for leak rate analyses
- Since the NDE uncertainties on maximum depth are also based on coil resolution averaging of destructive exam results, the NDE uncertainties do not adjust for this effect
- Local maximum depths < 0.16" would have small leak rates of < 0.005 gpm based on nominal leak rate correlation of Table 6-5.

- Since ligament tearing model is based upon average depths, the average depths for significant leakage of > 0.16" would not be affected by the finite coil resolution.

6. Use of mean flow stress in leak rate calculations when actual tube flow stress was not reported in leak test reports

    - Negligible effect on calculated leak rates
    - Calculated leak rates would be slightly lower or larger if the flow stress was higher or lower, respectively, than obtained using the mean stress. In general, knowledge of the flow stress would lead to improved agreement with the test value, such that use of the mean value would tend to conservatively increase the uncertainty in the leak rate correlation.
    - Additional discussion on the use of the mean flow stress is given in Section 6.2.2.

7. Use of ODSCC data in leak rate correlation applied for PWSCC leak rates

    - Minor conservatism
    - Use of throughwall length for leak rate correlation reduces the differences between ID and OD flaws in leak rate analyses. The principal difference between PWSCC and ODSCC is the more tortuous leak path for ODSCC, for which a correction is applied in the leak rate calculation
    - Specimens with the largest differences between test and calculation in the correlation are ODSCC indications, which increase the uncertainty in the correlation

The cumulative influence of the above methods and uncertainties on SLB leak rates is dominated by the conservatism of Items 1 and 3 above. Substantial conservatism results from incorporating a ligament tearing model in the analysis even though the effects of ligament tearing are incorporated in the uncertainties of the leak rate correlation as part of the difference between test and analysis. Incorporation of the ligament tearing model can be expected to increase all calculated leak rates even though the effects of ligament tearing are already indirectly included in the correlation. It would be more appropriate to include the ligament tearing model in the analyses used to develop the correlation. However, less than half of the leak rate data include the depth profiles necessary to calculate ligament tearing. As noted for item 3, the use of POD = 0.6 can lead to not satisfying operational assessment leakage limits even if all indications are plugged. The influence of Items 4 to 7 above have a negligible impact on the leak rate analyses compared to Items 1 to 3.

Table 6-1. Crack Leak Rate Data Sources

Data Set	Source/ Set #	Sample Type	Tube OD/wall	Crack Length Info		--- Operating Conditions ---		
						T_o °F	P_o psia	P_b psia
W-IGASCC (PWSCC)	(1)	Lab	.75x043.	ID &OD	NOP	616	2250	1000
					SLB	616	3000	350
W-Fatigue	(2)	Lab	Variable	Single Value	NOP	550	2250	1000
McGuire-PWSCC	(3)	Pulled Tubes	.75x.043	ID &OD	NOP	550	2650	1350
					SLB	550	2750	100
ODSCC@TSP1	(4)	Lab	.875x.05	Max & T. Wall	NOP	616	2250	1000
					SLB	616	3000	350
ODSCC@TSP1	(5)	Lab	.75x.043	Max & T. Wall	NOP	616	2250	750
					SLB	616	3000	350
Farley-PWSCC	(6)	Pulled Tubes	.875x.05	Max & T Wall	NOP	Variable		
					SLB	Variable		

Sources
1) Calc TH-90-43 Attachment IV ("Begley Data")
2) Calc TH-88-81. See also WCAP-9922, Rev. 1, Pt. 3
3) TH-90-43 Attachment V
4) EPRI Report NP-7480-L,"SGT ODSCC @ TSP's Database for ARC, V1, Table 5-12
5) EPRI Report NP-7480-L,"SGT ODSCC @ TSP's Database for ARC, V2, Table 5-6
6) Roll Transition, Farley Pulled Tubes, Cullen

Definitions
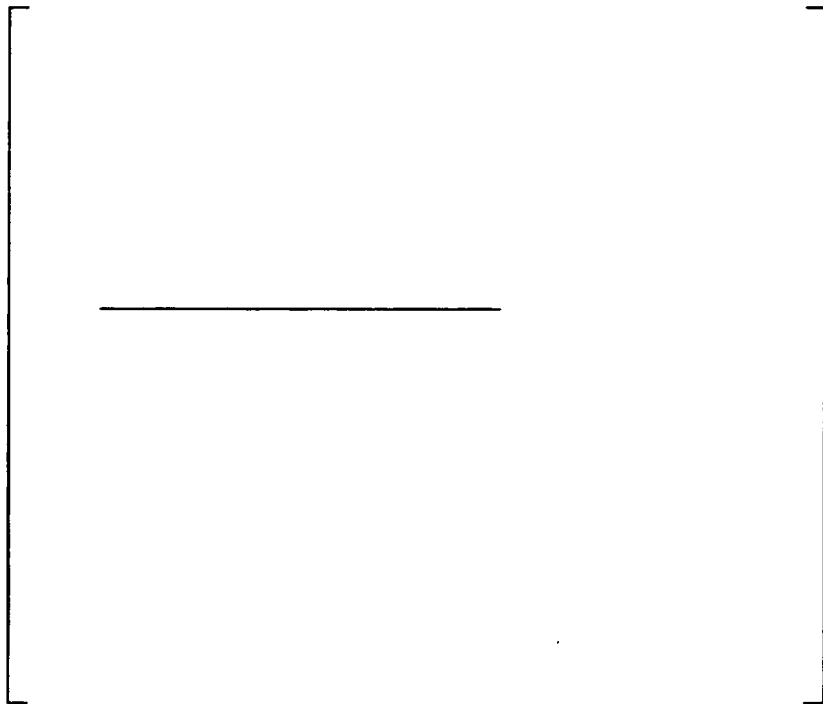NOP - Normal operating conditions
SLB - Steam line break conditions

a,c

* Reference 8-24

a,c

b,c

Table 6-4
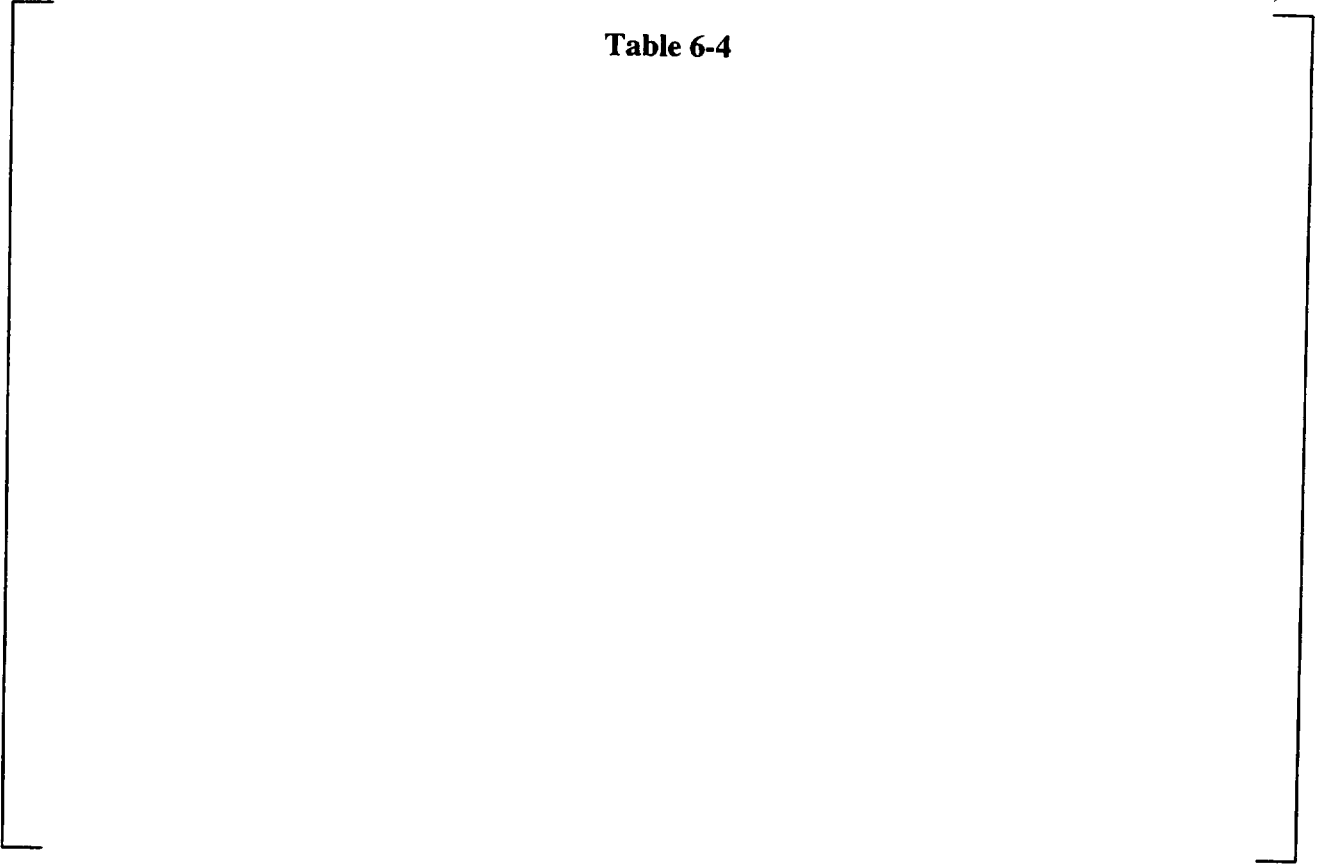
Table 6-5

b,c

Table 6-6: Distribution of Burst Reduction Factor Error (ANL Ligament Model)	
$1 / m_p$ Fractional Error	Median CDF
-0.2552	0.74%
-0.2308	1.80%
-0.1771	2.86%
-0.1633	3.92%
-0.1407	4.98%
-0.1379	6.04%
-0.1365	7.10%
-0.1192	8.16%
-0.1174	9.22%
-0.1117	10.28%
-0.1069	11.33%
-0.1051	12.39%
-0.1014	13.45%
-0.1002	14.51%
-0.0980	15.57%
-0.0970	16.63%
-0.0967	17.69%
-0.0931	18.75%
-0.0848	19.81%
-0.0825	20.87%
-0.0816	21.93%
-0.0794	22.99%
-0.0746	24.05%
-0.0733	25.11%
-0.0733	26.17%
-0.0729	27.22%
-0.0727	28.28%
-0.0698	29.34%
-0.0695	30.40%
-0.0680	31.46%
-0.0655	32.52%
-0.0646	33.58%
-0.0623	34.64%
-0.0589	35.70%
-0.0477	36.76%
-0.0452	37.82%
-0.0450	38.88%
-0.0434	39.94%
-0.0433	41.00%
-0.0425	42.06%
-0.0421	43.11%
-0.0406	44.17%
-0.0389	45.23%
-0.0381	46.29%
-0.0366	47.35%
-0.0337	48.41%
-0.0321	49.47%
-0.0310	50.53%
-0.0270	51.59%
-0.0175	52.65%
-0.0174	53.71%

Table 6-6: Distribution of Burst Reduction Factor Error (ANL Ligament Model)	
$1 / m_p$ Fractional Error	Median CDF
-0.0173	54.77%
-0.0172	55.83%
-0.0168	56.89%
-0.0147	57.94%
-0.0132	59.00%
-0.0106	60.06%
-0.0088	61.12%
-0.0073	62.18%
-0.0023	63.24%
0.0018	64.30%
0.0030	65.36%
0.0047	66.42%
0.0068	67.48%
0.0150	68.54%
0.0166	69.60%
0.0188	70.66%
0.0214	71.72%
0.0220	72.78%
0.0248	73.83%
0.0275	74.89%
0.0278	75.95%
0.0280	77.01%
0.0318	78.07%
0.0333	79.13%
0.0453	80.19%
0.0475	81.25%
0.0477	82.31%
0.0482	83.37%
0.0491	84.43%
0.0529	85.49%
0.0660	86.55%
0.0751	87.61%
0.0904	88.67%
0.1044	89.72%
0.1045	90.78%
0.1114	91.84%
0.1252	92.90%
0.1268	93.96%
0.1322	95.02%
0.1426	96.08%
0.1644	97.14%
0.1777	98.20%
0.2246	99.26%

Figure 6-1

b,c

Figure 6-2

b,c

b,c
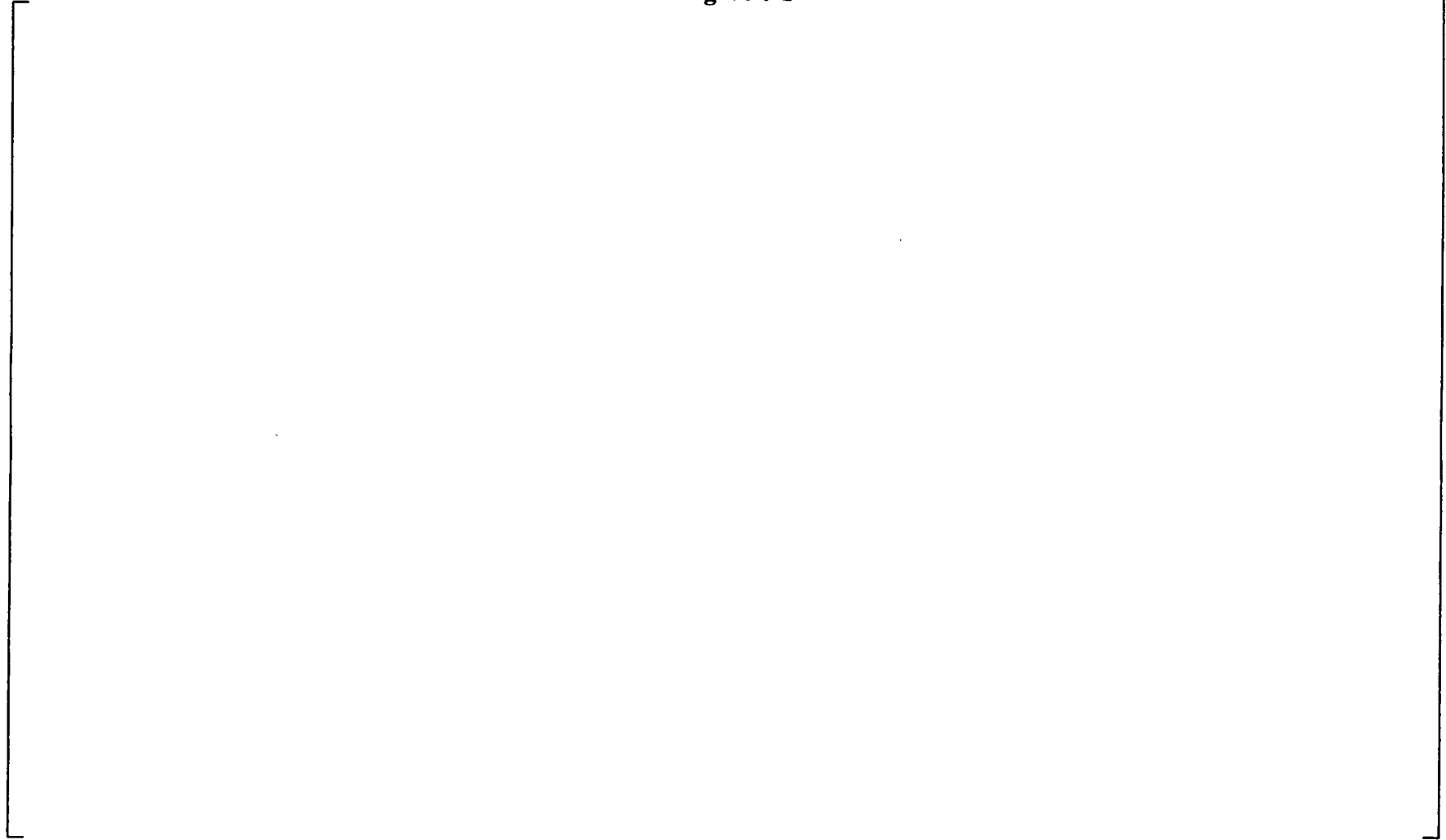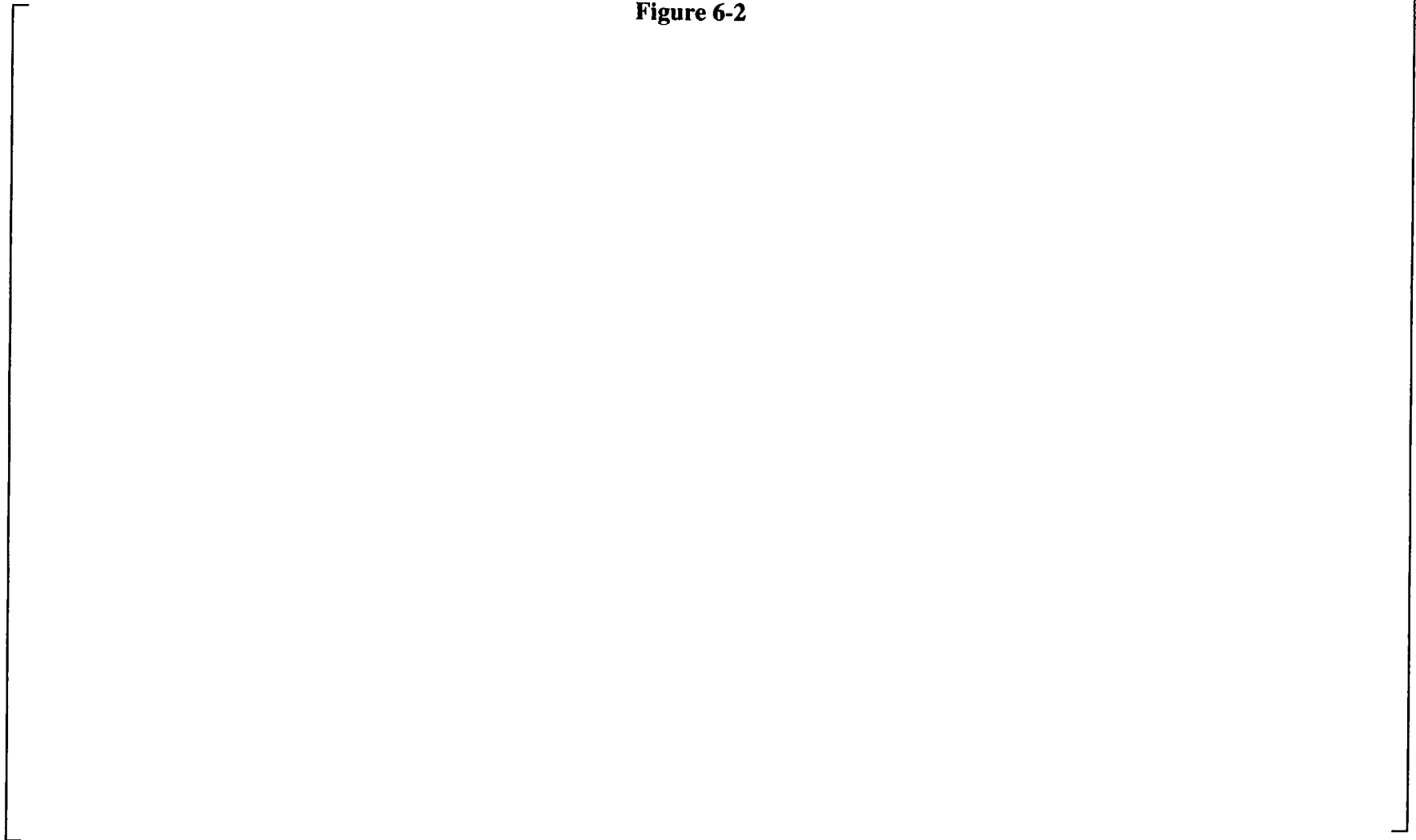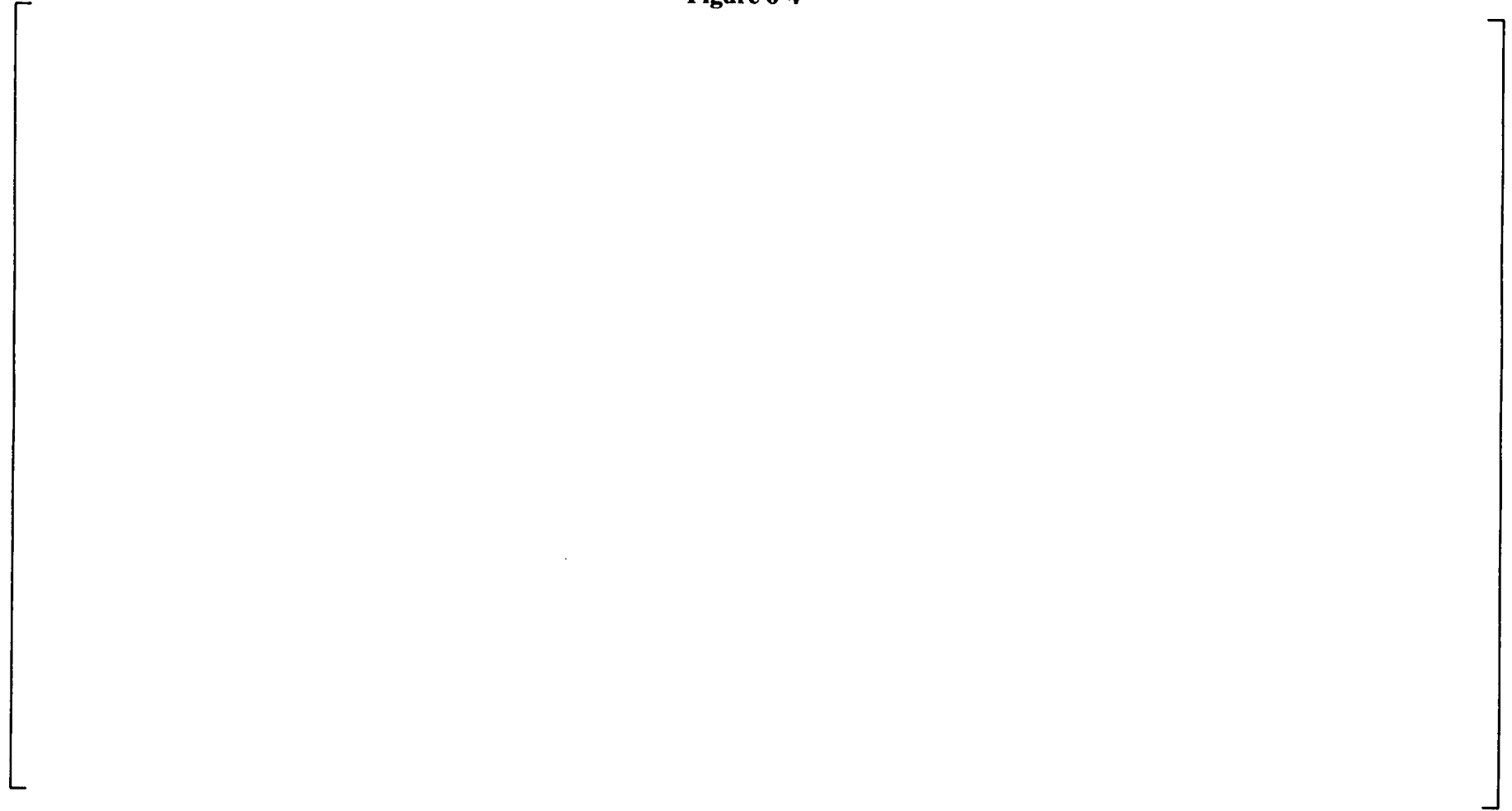
Figure 6-3

Scatter Plot of Regression Residuals vs. Predictions
Case 3 CRACKFLO Leak Rate Model
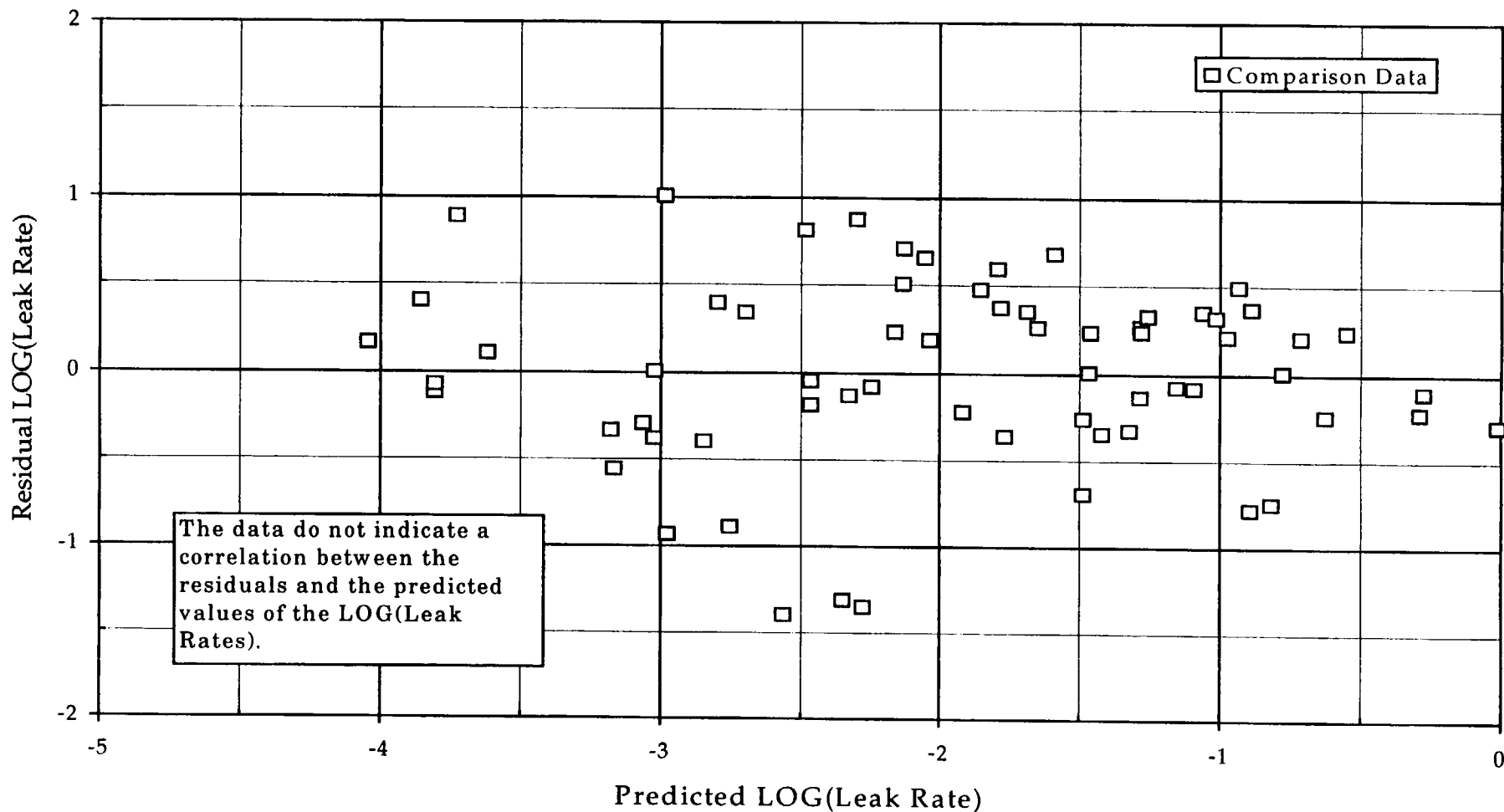
Figure 6-5. Scatter Plot of Regression Residuals versus Predictions

Normal Distribution Plot of Residual LOG(Leak Rates)
Case 3 CRACKFLO Assumptions
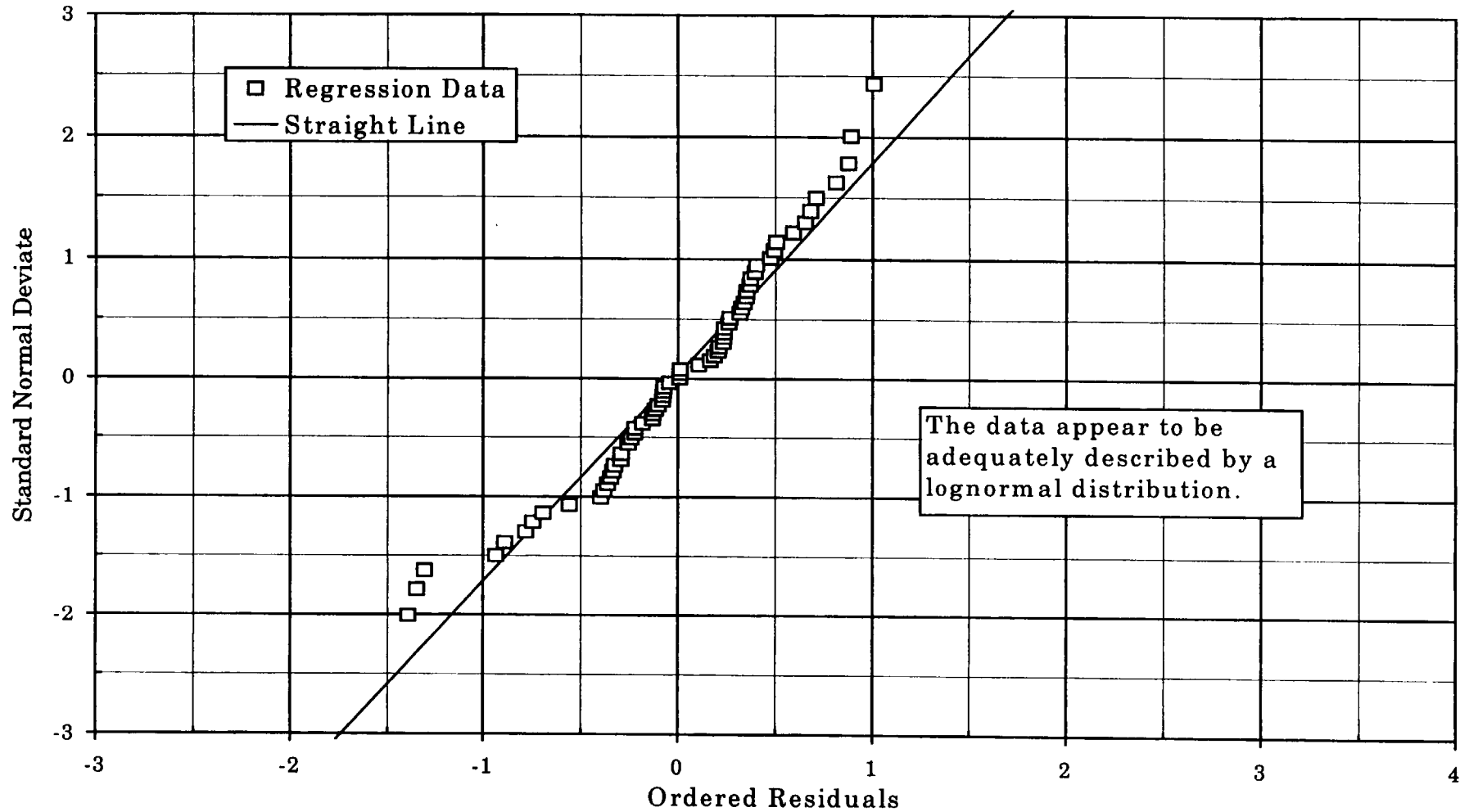
Figure 6-6. Normal Distribution of Residual Log of Leak Rates

b,c

Figure 6-7

Figure 6-8

b,c

Ligament Tearing Pressures vs. Crack Depth
Alloy 600 MA SG Tubes with Part-Throughwall Axial Cracks
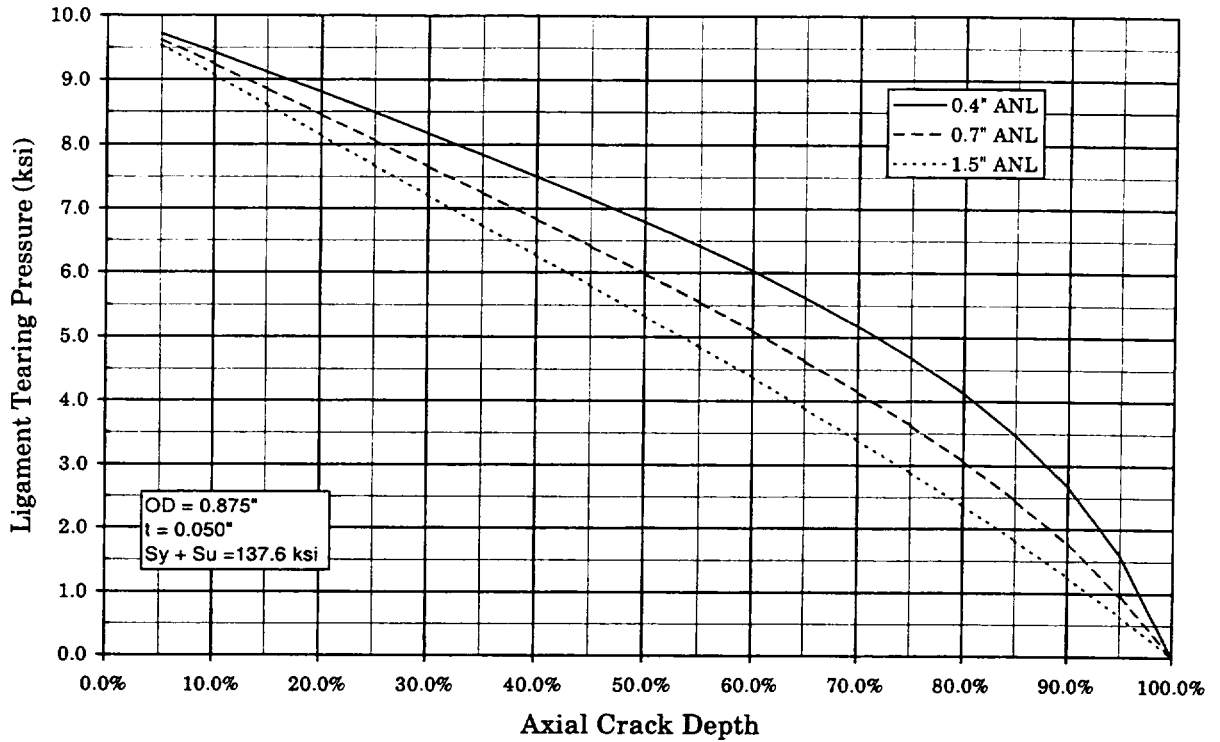
Figure 6-9

Critical Crack Length vs. Crack Depth
Alloy 600 MA SG Tubes with Part-Throughwall Axial Cracks
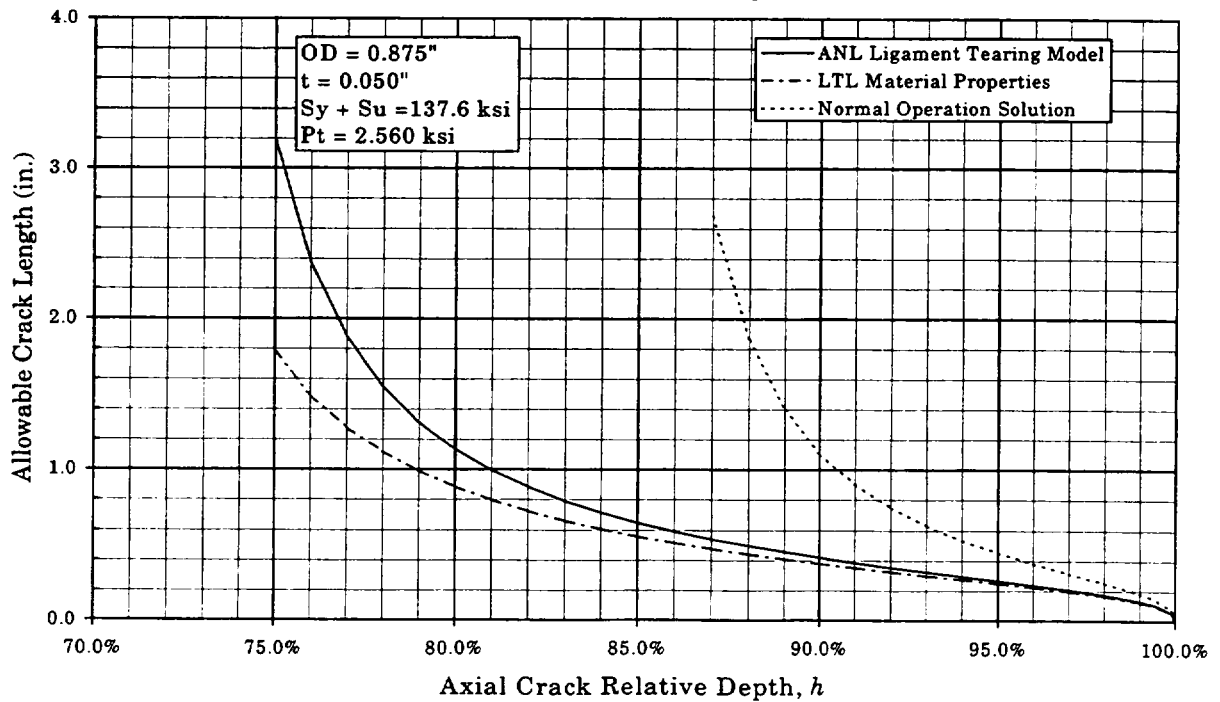
Figure 6-10

CDF of Ligament Failure Pressure Reduction Factor Errors
ANL Ligament Failure Equation - ANL Update 2/15/00

$$P_B = P_0 \frac{1}{m_p}$$
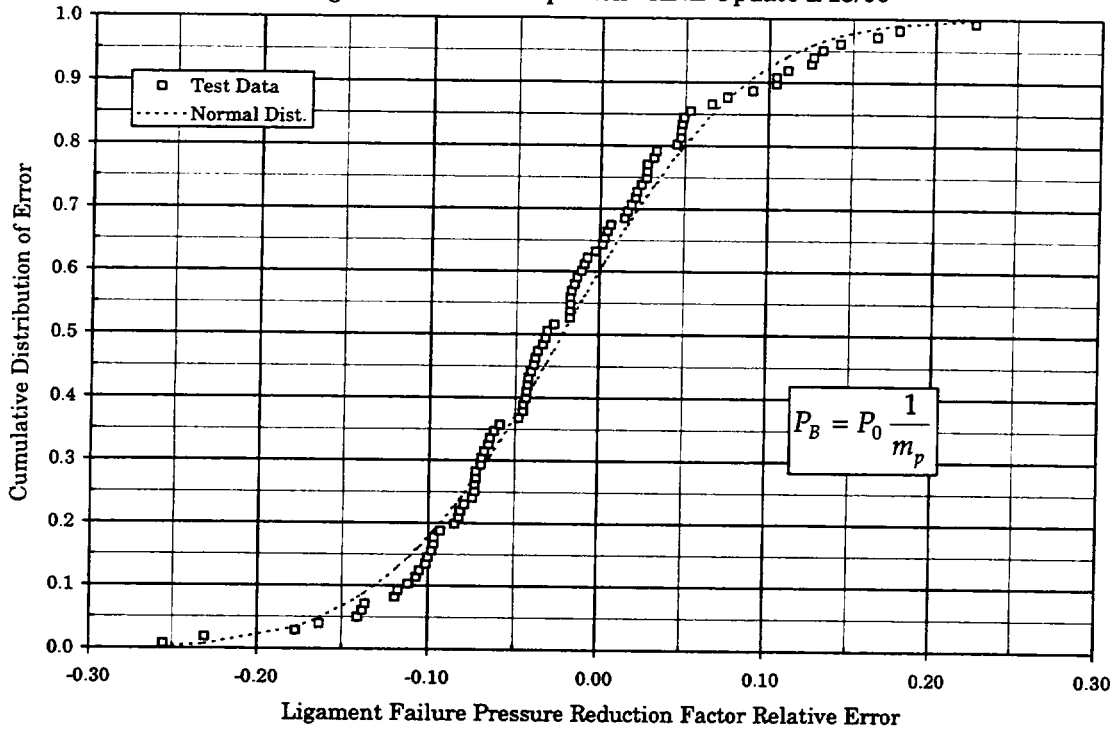
Figure 6-11

Scatter Plot of $1/m_p$ Errors
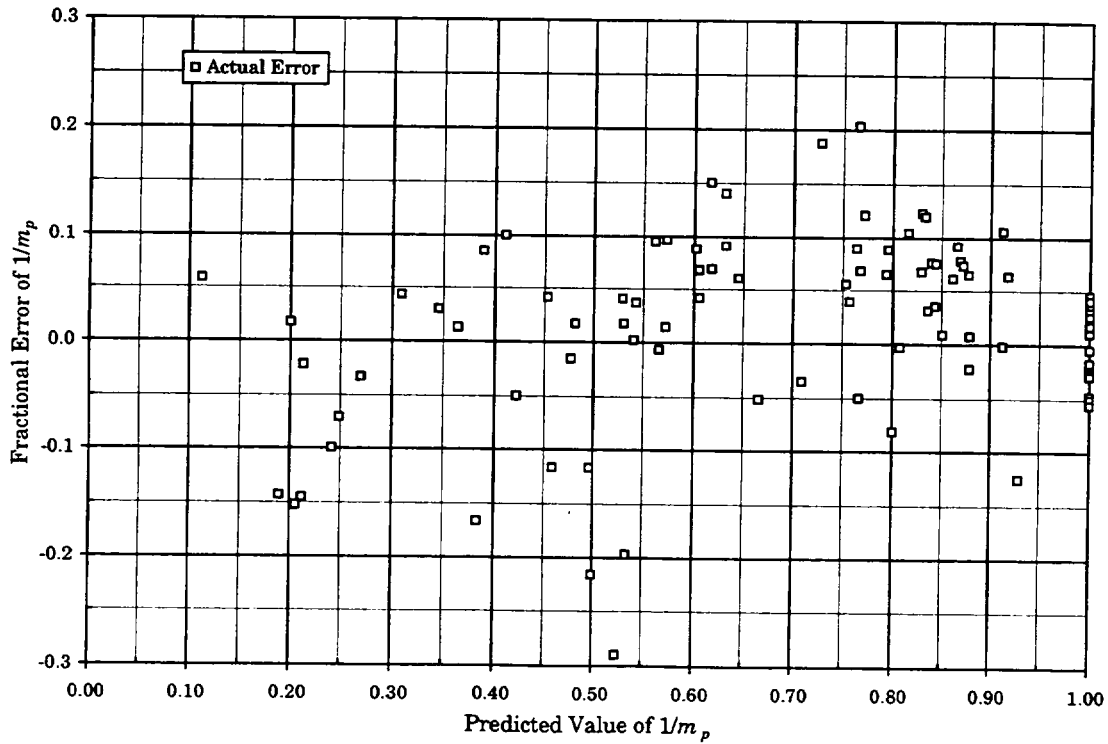
Figure 6-12

7.0 OVERVIEW OF ARC AND SUPPORTING ANALYSES FOR AXIAL PWSCC AT DENTED TSP INTERSECTIONS

This report provides the technical bases for a depth based ARC for axial PWSCC indications at dented TSP intersections. Repair limits are developed for indications within the dented TSP or with limited extension outside the TSP. The ARC repair limits of this report apply to axial PWSCC indications $\geq 40\%$ maximum depth. Indications $< 40\%$ maximum depth are left in service per the existing Technical Specification repair limit of 40% depth. The ARC and supporting requirements including inspection, burst analyses and leak rate analyses are described in this section. The ARC is conservatively based upon the assumption that the indications are freespan at SLB conditions and applies to axial indications that are located within or extending outside the TSP. However, crack extensions outside the TSP are required to be $< 40\%$ maximum depth. Requirements for including NDE uncertainties in the ARC analyses are also defined. The ARC satisfy steam generator tube integrity guidelines consistent with the requirements of NEI 97-06 (Reference 8-5), draft Regulatory Guide 1.121 (Reference 8-6) and the draft Regulatory Guide DG-1074 (Reference 8-7). The depth based repair limits are based upon establishing a high confidence that the indications will not burst or result in unacceptable leak rates under SLB conditions at the end of the operating cycle.

The ARC is based on the use of crack depth profiles obtained from a qualified and performance demonstrated +Point sizing technique. Burst pressures are calculated from the depth profiles by searching the total crack length for the partial length that results in the lowest burst pressure. The repair basis is obtained by projecting the crack profile to the end of the next operating cycle and determining if the burst pressure and SLB leakage for the projected profile satisfy acceptance requirements. If the projected EOC requirements are satisfied, the indication can be left in service. Thus, the repair basis assures that the operational assessment requirements are satisfied.

Applicable NDE uncertainties and growth rates are described in Sections 7.1 to 7.4. Repair limits for burst margins and potential leakage are developed in Section 7.5. The repair limits are based on single indication Monte Carlo analyses for the operational assessments to determine whether or not the projected EOC indications satisfy burst margin and leakage requirements. An option is provided to perform a total SG SLB leak rate operational assessment for comparison with the acceptance limits. Inspection requirements for application of the ARC are described in Section 7.6. Sections 7.7 and 7.8 describe supporting operational and condition monitoring assessment analysis methods for burst and leakage with an option for probabilistic condition monitoring analyses for indications dominantly within the TSP. Requirements for pulling tubes in support of the ARC are given in Section 7.9. Section 7.10 provides a risk assessment for the ARC and Section 7.11 identifies NRC reporting requirements.

7.1 Tube Burst Margin Requirements and Burst Pressure Correlation

The proposed ARC of this report assumes that the TSPs are not present in a SLB event such that all indications at dented TSP intersections are freespan at SLB conditions. The structural limit for indications within the TSP is based on the presence of the TSPs under normal operating conditions such that the $1.43\Delta P_{SLB}$ burst margin requirement is applicable for indications within the TSP and for the total crack length if extending outside the TSP. The structural limit for the length of an indication totally outside the TSP is based on satisfying $3\Delta P_{NO}$ burst margin requirements. In the case of a crack extending from inside to outside the TSP, the structural limit is based upon the more limiting of $1.43\Delta P_{SLB}$ for the total crack length or $3\Delta P_{NO}$ for the length outside the TSP.

The burst correlation for partial throughwall, axial cracks is developed in Section 5 and is applied for the Monte Carlo condition monitoring and operational assessments. The operational assessment burst margin analyses to determine the need for tube repair must be satisfied at 95% probability and 95% confidence given uncertainties in the burst correlation, material properties and NDE uncertainties on length and average depth. The condition monitoring burst margins must be satisfied at 95% probability and 50% confidence as further discussed in Section 7.8. These confidence level requirements are consistent with the guidance given in the draft NRC Regulatory Guide DG-1074 (Reference 8-7). Based upon the guidance of Draft DG-1074, the limiting indication must satisfy the burst margin requirements. This guidance is satisfied by performing single indication Monte Carlo analyses for each indication to compare the predicted burst pressure at the specified confidence level against the burst margin requirements.

The normal operating pressure differential, ΔP_{NO}, is based on normal full power operating conditions. This bounds other normal operating conditions such as hot standby or power level adjustments for Westinghouse SGs. The primary and secondary side pressures to be used for determining ΔP_{NO} are the pressures near the location of the tube degradation. For Westinghouse Model 51 SGs with a primary side pressure of 2250 psia at the pressurizer, the primary pressure at the inlet to the SG is slightly higher than 2250 psia and the pressure at the top of the tubesheet is very close to 2250 psia. As elevation in the tube increases above the tubesheet, the primary pressure decreases faster than the secondary side pressure decreases. Therefore, the maximum primary to secondary hot leg pressure differential under normal operating conditions occurs at the top of the tubesheet. Secondary side steam pressure used to determine ΔP_{NO} should therefore be that at the top of the tubesheet. Steam pressures are measured in the steam line and corrected to the SG but the location in the SG for the pressure correction may differ between plants. The reported location for Diablo Canyon SGs is at the elevation of the wide range level indicator (above primary separators) and the Sequoyah steam pressures are reported in the dome just inside the SG outlet nozzle. The adjustments of steam pressures to the top of the tubesheet are 17 psi for Sequoyah SGs and 14 psi for the Diablo Canyon SGs. The burst margin requirements are then $1.43\Delta P_{SLB} = 3657$ psi, $3\Delta P_{NO} = 4209$ for a Sequoyah steam pressure of 830 psia (in dome) and 4383 psi for a Diablo Canyon steam pressure of 775 psia (above primary separator).

7.2 SLB Leak Rate Requirements and Leak Rate Correlation

The SLB leak rate correlation and ligament tearing model developed in Section 6 are applied for the Monte Carlo condition monitoring and operational assessments. The operational assessment analyses performed to determine the need for tube repair must satisfy the allowable leakage limits at 95% probability and 95% confidence given uncertainties in the burst correlation, material properties and NDE uncertainties on length and depth. For condition monitoring, the allowable leak rate limits must be satisfied at 95% probability and 50% confidence as further discussed in Section 7.8. Leakage from the total crack length is constrained by the presence of the TSP except under the postulated SLB condition that the TSPs displace in a SLB event. The allowable limit for the total constrained leakage is the same as given in the licensing basis for the NRC GL 95-05 voltage based ARC. The total constrained leakage limit applies to the sum of leak rates from the PWSCC total crack length of this ARC, the GL 95-05 ARC for ODSCC at TSP intersections and indications within the tubesheet for application of the W* ARC. The allowable leakage limit for freespan indications is the 1 gpm limit included in FSAR evaluations which are a part of the licensing basis. The total freespan leakage limit applies to the sum of leak rates from the PWSCC ARC crack length outside the TSP and any other freespan leakage from the operational assessments for other degradation mechanisms. The tube repair basis for SLB leakage is defined in Section 7.5.4.

7.3 NDE Uncertainties

NDE uncertainties are required on maximum depth, average depth and length to support the repair criteria based upon the operational assessment. The NDE uncertainties on average depth and length are used for the burst pressure analyses, and uncertainties on maximum depth and length are applied in the leakage analyses. Validated +Point sizing techniques based on a NDE Performance Test to develop the NDE uncertainties are described in Section 4 and the NDE uncertainties are developed in Section 4.7. The NDE uncertainties are developed as correlations between "truth" based on destructive exam data and NDE measurements. The NDE correlations are applied in the Monte Carlo burst pressure and SLB leak rate analyses. The resulting correlations are given below with the 95% confidence values given as a specific example of the magnitude of the uncertainties.

Average Depth NDE Uncertainty

Correlation: y (truth) = $[0.914x + 0.687]^g$
Standard deviation = $[7.8\%]^g$

NDE Uncertainty at +95% confidence ($\Delta NDE_{AD95\%}$) = $[10.1\%$ for indication at $\approx 40\%$ average depth$]^g$

Maximum Depth NDE Uncertainty

Correlation: y (truth) = $[0.939x - 0.923]^g$

Standard deviation = $[14.2\%]^g$

NDE Uncertainty at +95% confidence ($\Delta NDE_{MD95\%}$) = $[19.1\%$ for indication at 55% maximum depth$]^g$

Length NDE Uncertainty

Correlation: y (truth) = $[1.008x + 0.010]^g$

Standard deviation = $[0.139$ inch$]^g$

NDE Uncertainty at +95% confidence ($\Delta NDE_{L95\%}$) = [approximately 0.25 inch for indications between 0.75 and 1.25 inch length$]^g$

7.4 Growth Rates

Growth rates for axial PWSCC at dented TSP intersections were developed in Section 4.8 based on data from Sequoyah and Diablo Canyon SGs. Analysts trained on +Point sizing as part of the NDE Performance Test or Sequoyah site specific training for NDE sizing performed the growth rate analyses. Cumulative probability distributions were developed for the growth rates. Separate growth rate distributions were developed for average depth, maximum depth and length on an EFPY basis. The growth rate distributions are used in the Monte Carlo analyses with length and average depth used in the burst pressure analyses and length and maximum depth used in the leak rate analyses. Separate growth rate distributions are given in Section 4.8 for Sequoyah and Diablo Canyon with plant specific data applied for Sequoyah SGs and a combined growth distribution applied for Diablo Canyon. The growth rates are temperature dependent with a hot leg temperature of 611°F applicable to the Sequoyah SGs and

603°F applicable to the Diablo Canyon SGs. As an example of the growth rate magnitudes, the 95% cumulative probability growth rates are (from Table 4-7):

Average depth growth at 95% probability ($\Delta G_{AD95\%}$) = [17.9% per EFPY at 611°F for Sequoyah and 13.2% per EFPY at 603°F for Diablo Canyon] [g]

Maximum depth growth at 95% probability ($\Delta G_{MD95\%}$) = [20.4% per EFPY at 611°F for Sequoyah and 15.5% per EFPY at 603°F for Diablo Canyon] [g]

Length growth at 95% probability ($\Delta G_{L95\%}$) = [0.21 inch per EFPY at 611°F for Sequoyah and 0.15 inch per EFPY at 603°F] [g]

Further discussion on updating the growth rate distributions is given in Section 7.5.5.

7.5   Tube Repair Limits

ARC tube repair limits are developed below for indications within the TSP, indications within and extending outside the TSP or at the edge of the TSP. Totally freespan indication repair limits are based on the Technical Specification repair limit of 40% maximum depth as described in Section 7.5.1. Similarly, indications < 40% maximum depth within the TSP or at the edge of the TSP are left in service per the existing Technical Specification repair limit of 40% depth and the additional ARC requirements for ≥ 40% depth indications are not applicable. Indications ≥40% maximum depth that can be left in service are limited to depths ≥40% only within the TSP. Separate repair bases are developed for burst and leakage considerations. Input to the repair limits are adjusted on an outage to outage basis as may be necessary to update growth rate distributions and steam pressures or account for changes in the cycle length or hot leg temperature from that used in the following development of the repair limits.

The ARC repair bases are limited to axial PWSCC at dented TSP intersections. If axial PWSCC is identified, a bobbin coil dent of any magnitude must be identifiable to leave the indication in service. NRC GL 95-05 would require repair of a TSP intersection found to have both PWSCC and ODSCC indications since the bobbin voltage response would not be limited to ODSCC indications.

7.5.1   Freespan Indication Repair Limits

The crack length outside the TSP will be repaired based on the current Technical Specification limit of 40% maximum depth. Although the 40% maximum depth repair limit is expected to result in acceptable conditions at the next EOC, the operational assessment performed to determine the potential need for tube repair evaluates the freespan length for acceptability as well as the total crack length.

The following is provided as a scoping demonstration of the acceptability of the 40% depth limit for freespan indications. Since NDE uncertainty on maximum depth is about 19% and growth at 95% is bounded by about 26%, the maximum depth at EOC would be about 85%. From Figure 6-9, a crack length of about 0.6 inch averaging 85% depth would be required for ligament tearing and potential leakage. Since 85% is the estimated maximum EOC depth, there is a low probability that a length of 0.6 inch averaging 85% depth would be present to permit ligament tearing and leakage. For a maximum depth of 40% and a typical maximum to average depth ratio of about 1.25, the average depth left in service would be on the order of 32%. With an average depth growth rate of about 20% at 95% confidence, the EOC average depth would be about 52%. For a $3\Delta P_{NO}$ burst margin including allowances

for NDE uncertainties, an EOC average depth of about 52% permits a very long crack length beyond a 1.4 inch length. Thus the 40% maximum depth limit provides large margins against burst and leakage.

For indications < 40% maximum depth that are dominantly within the TSP, the structural margins are even larger than for freespan indications since the $1.43\Delta P_{SLB}$ structural margin requirement is applicable. Consequently, the Technical Specification repair limit of 40% maximum depth can be applied to all axial PWSCC indications and the additional ARC requirements on location and length for indications $\geq$ 40% maximum depth are not necessary. The ARC requirements for $\geq$ 40% depth are developed in Sections 7.5.2 to 7.5.6.

In summary, axial PWSCC indications at dented TSP intersections with maximum depths < 40% can be left in service independent of length or position relative to the TSP. Indications $\geq$ 40% maximum depth outside the TSP will be repaired. The operational assessment of Section 7.5.3 is performed for these indications to further demonstrate acceptability of the Technical Specification 40% repair limit.

7.5.2   Crack Length Limit for $\geq$ 40% Maximum Depth

A crack length limit for $\geq$ 40% Maximum Depth is defined to limit the potential length of a deep crack outside the TSP at EOC conditions. The ARC repair limit is established to require repair of any indication having a maximum crack depth $\geq$ 40% outside the TSP. This limit is established to provide large margins against burst or leakage for freespan indications outside the TSP. As discussed in Section 7.5.1, the maximum EOC depth outside the TSP would be less than 85% deep, except for a short length at the TSP edge resulting from growth of the crack inside the TSP to possible extension outside the TSP as discussed in the following. Growth in length at 95% probability is given in Section 7.3 as $\Delta G_{L95\%}$ = [0.21"] ^{g} per EFPY at 611°F and [0.15"] ^{g} per EFPY at 603°F. For corresponding cycle lengths of 1.25 and 1.42 EFPY, the total growth in length would be [0.26 and 0.21 inch.] ^{g} The EOC length outside the TSP that could then be potentially more than about 85% depth would be about 0.26 inch under the conservative assumption that all growth occurred at the edge of the TSP. This potentially deeper, short length just outside the TSP together with the potentially longer length left in service at < 40% maximum depth would not challenge structural integrity at EOC conditions. Although no challenges to freespan burst margins at EOC conditions are expected, the operational assessment performed to identify repairable indications includes a burst pressure analysis for any crack length potentially extending outside the TSP.

Since crack positions are measured from the centerline of the TSP, the maximum allowable length that can be left in service at $\geq$ 40% maximum depth is 0.375 inch from the TSP centerline. This limit defines the edges of the TSP thickness of 0.75 inch for Model 51 SGs. It is acceptable for the crack to extend outside both edges of the TSP as long as the maximum depth of the crack outside the TSP is < 40% and burst margins at projected EOC conditions are acceptable per the structural assessment described in Section 7.5.3 below.

In summary, axial PWSCC indications at dented TSP intersections with $\geq$ 40% maximum depth at > 0.375 inch or < -0.375 from the TSP centerline will be repaired. Indications acceptable by this requirement are further evaluated against the burst pressure and SLB leakage repair bases of Sections 7.5.3 and 7.5.4.

7.5.3 Burst Pressure Repair Basis

The repair limit on maximum crack depth ($\geq 40\%$) for the potential length outside the TSP (length not within ± 0.375 inch of TSP centerline) is developed above in Section 7.5.2 and 7.5.3. If this limit is exceeded, the tube is repaired and the evaluation for tube repair described in this section is not required. However, an operational assessment will be performed for all PWSCC indications left in service at dented TSP intersections including indications with $< 40\%$ maximum depth within or extending outside the TSP. The crack profile must be evaluated to determine the partial length that results in the lowest burst pressure. Acceptability must be defined in terms of the projected EOC crack profile since growth in length and depth change the burst characteristics of the measured profile. Projecting the measured profile to the EOC is equivalent to performing an operational assessment for the indication. The measured profile is projected to EOC conditions by adding growth in length and growth in average depth. The projections to EOC conditions are performed using Monte Carlo analysis methods. Each simulated EOC profile is then searched for the lowest burst pressure using the burst correlation of Section 5. This process results in the effective length (partial length of total crack length) and associated average depth of the indication that results in the lowest burst pressure. This process is separately performed for the total crack length and for the length of the crack outside the TSP. The resulting Monte Carlo burst pressure distribution for the total crack length evaluation is compared to the $1.43\Delta P_{SLB}$ acceptance limits at 95% probability and 95% confidence on the distribution. The resulting burst pressure distribution obtained from the evaluation of the length outside the TSP is evaluated against the appropriate $3\Delta P_{NO}$ limits at 95% probability and 95% confidence on the distribution. If the burst pressures from both evaluations are less than their associated acceptance limits, the indication is left in service subject to the results of the leakage evaluation. If either burst pressure acceptance limit is exceeded, the indication must be repaired. The Monte Carlo methods for performing the operational assessment for burst pressures are described in Section 7.7.

In summary, the ARC repair limits, other than maximum depth outside the TSP, are established to satisfy structural limits at the projected EOC. This process is an operational assessment and no further operational assessment is required. The repair limits are dependent upon growth rates and cycle length with the freespan lengths also dependent upon steam pressure. These parameters must be updated for each inspection or it must be demonstrated that the prior cycle values remain acceptable.

7.5.4 SLB Leakage Repair Basis

The leakage repair basis applies a Monte Carlo, SG operational assessment for leakage to demonstrate that accident condition acceptance limits for leakage are not exceeded at the specified confidence levels. If the total SG leak rate is found to exceed acceptance limits, single indication leak rate analyses may be performed to identify the indications with the largest leak rates for potential repair. For conservatism, the total SG leak rate is evaluated assuming a constant POD of 0.6 for the analysis. The total SG leakage is evaluated at 95%/95% confidence for operational assessments. The PWSCC leakage for the total crack length, representing TSP constrained leakage, must be added to other degradation mechanisms with constrained leakage such as ODSCC at TSP intersections and W* indications within the tubesheet. The total constrained leak rate must be less than the licensing basis allowable leakage limit for the faulted SG per GL 95-05 guidelines. The freespan leakage must be added to potential contributions from other degradation mechanisms in the overall operational assessment and the total freespan leakage must be less than or equal to the allowable limit of 1 gpm. The constrained and freespan leak rates from the operational assessments must satisfy the allowable limits at 95% probability and 95% confidence. Contributions from separate degradation mechanisms may be individually evaluated at these confidence levels to satisfy the total leakage requirements. If either the constrained or freespan leakage limit is

exceeded, indications with the largest leak rates will be repaired until the leakage limit is satisfied. For the Sequoyah and Diablo Canyon SGs, the steamline break event (SLB) is the limiting accident condition for leakage. Any indications with known leakage will be repaired where known leakage may result from identification of the indication due to operational leakage or in situ testing.

The leakage model used in the Monte Carlo operational assessment is described in Section 6 of the report. The analyses are based on the use of crack depth profiles projected to EOC conditions. At SLB conditions, there is conceptually a potential that a near throughwall crack would "breakthrough" (ligament tearing) the remaining wall thickness ligament to result in a leak. No occurrences of breakthrough of more than a few percent wall thickness have been identified in available leak rate data for PWSCC cracks or the more extensive ODSCC database for indications at TSP intersections. However, the Monte Carlo analysis conservatively includes a ligament tearing analysis based on the ANL model including uncertainties as described in Section 6. Each simulated EOC profile for the total crack length is searched for the longest length that could potentially breakthrough at the SLB pressure differential of 2560 psi. If ligament tearing is predicted, the partial crack length estimated to tear through the remaining ligament is assumed to be throughwall in applying the SLB leak rate correlation described in Section 6. The resulting Monte Carlo SLB leak rate distribution for the indication is evaluated at the specified confidence level. A description of the Monte Carlo methods for the operational assessment is provided in Section 7.7.

The above formulations provide the basis for developing the need for tube repair based upon potential SLB leakage. The analyses are a function of growth rates, hot leg temperature and cycle length, which may have to be updated on an outage specific basis if changes occur in growth rates, hot leg temperature or cycle length.

7.5.5 Adjustments to Repair Limits for Changes in Operating Conditions

Prior to an inspection for which the depth based repair limits are to be applied, growth distributions are to be updated to include growth data from the previous inspection. In addition, changes in planned cycle lengths or steam pressure can change the repair limits. The updated growth rates, cycle lengths and steam pressures should be used to update the inputs to the Monte Carlo operational assessments per Sections 7.5.3 and 7.5.4 above for application during the inspection outage. Growth rates in average depth, maximum depth and length are developed for the indications found in the prior inspection. In addition, if the new growth data and deletion of the oldest cycle of growth data in the growth distribution result in a minimum of 200 growth points, the oldest cycle of growth data should be deleted from the growth distribution. However, data cannot be deleted from the last two cycles of growth data since it is necessary to utilize the largest growth distribution over the last two cycles of operation in the operational assessments.

The initial application of the ARC repair limits for axial PWSCC at dented TSP intersections is based on growth data combined from Sequoyah and Diablo Canyon SGs for application to the Diablo Canyon SGs and Sequoyah specific growth data for the Sequoyah SGs. When growth data from Diablo Canyon SGs exceed 200 data points, the plant specific growth distribution should be applied for the Diablo Canyon analyses. The guidance noted above for updating the growth distributions would then apply to the plant specific growth data. If the last two cycles of plant specific data each have 200 growth points, the most conservative growth distribution (largest growth at +95% confidence) from the last two cycles of operation should be used to define the updated repair limits. As a minimum, growth rates for large indications that could impact the upper tail of the growth distribution shall be evaluated during an inspection outage. If the growth data for new indications causes the growth distribution above 90%

probability to be more conservative, the new growth data shall be added to the growth distribution for the operational assessment.

7.5.6 Exclusion Zones for Application of the Alternate Repair Criteria

LOCA + SSE

For the combined LOCA + SSE loading condition, the potential exists for yielding of the tube support plate in the vicinity of wedge groups, accompanied by potential deformation of the tubes and subsequent postulated in-leakage if the tube has significant degradation. In-leakage may occur if deep axial cracks are present and propagate throughwall as tube deformation occurs. This deformation may also lead to opening of preexisting tight throughwall cracks. Significant deformation for this potential in-leakage applies to indications left in service exceeding the current Technical Specification 40% maximum depth repair limit. In-leakage is a potential concern as modest leakage could have an adverse effect on the FSAR safety analysis results. Any tubes that are defined to be potentially susceptible to significant deformation under LOCA + SSE loads are excluded from consideration of the ARC.

No tubes are calculated to be susceptible to significant deformation in the Sequoyah SGs as shown in documentation supporting the voltage based repair limits for ODSCC at TSP intersections; therefore, no tubes are excluded from the application of the ARC. For the Diablo Canyon SGs, tube locations susceptible to significant deformation are identified in the NRC submittal of Reference 8-29. Although the referenced exclusion zone submittal is for the TSP ODSCC ARC, the exclusion zones for Diablo Canyon SGs are applicable to both the voltage based repair limits for ODSCC at TSP intersections and the depth based repair limits of this report.

FLB or SLB + SSE

Since the TSPs provide lateral support to potential tube deformation that may occur during postulated accident conditions, tube bending stress can be induced at the TSP intersections. This bending stress is distributed around the circumference of the tube cross section, tension on one side of the tube, compression on the other side and is oriented in the axial direction of the tube. Axial cracks at the TSP intersection could experience either a tension stress that tends to close the crack or a compressive stress that tends to open the crack. The compressive stress has the potential to reduce the burst capability of the cracked tube due to the crack opening if the stress level is sufficiently large. Test results (Reference 8-14) have shown that an OD bending stress on the order of 34 ksi, which is very close to the yield strength of the tube material at 650°F, will not have a significant effect on the burst capability of a cracked tube. In the absence of test data for bending stresses above the tube yield strength, it is conservatively assumed that high bending stresses (above yield) could have a degrading effect on tube burst pressure. In general, the potential for bending stresses exceeding yield in Westinghouse SGs is significant only at plants with relatively large SSEs in the design basis.

No tubes have been identified to have bending stresses exceeding the yield strength in the Sequoyah SGs and, therefore, no tubes are excluded from the application of the ARC. For the Diablo Canyon SGs, tube locations susceptible to bending stresses exceeding about 34 ksi have been identified at the top TSP for a FLB + SSE event. These locations are conservatively excluded from application of the alternate repair limits. The tube locations are defined in the PG&E NRC submittal of Reference 8-29. These exclusion zones for Diablo Canyon SGs are applicable to both the voltage based repair limits for ODSCC at TSP intersections and the depth based repair limits of this report.

7.6 Inspection Requirements

To support the ARC for axial PWSCC at dented TSP intersections, inspection requirements are identified for the extent of inspection and NDE data analysis.

Extent of Inspection

The bobbin coil probe is applied for sizing of dent voltages and for detection of axial PWSCC indications at TSP intersections with less than or equal to 2.0 volt dents for which the bobbin probe qualification is described in Section 4. The +Point probe is applied for sizing of bobbin detected indications and for detection and sizing at intersections with greater than 2.0 volt dents. The extent of inspection required for the ARC is then:

- 100% bobbin coil inspection of all TSP intersections

- +Point coil inspection of all bobbin coil indications at dented TSP intersections

- +Point coil inspection of all prior PWSCC indications left in service.

- On a SG basis, +Point coil inspection of all TSP intersections having > 2.0 volt dents up to the highest TSP for which PWSCC has been detected in the prior and current inspection and 20% of dents > 2.0 volts at the next highest TSP

NDE Analysis Requirements

In addition to general reporting requirements such as tube location, TSP number and crack location relative to the center of the TSP, the following data are required from the inspection:

Bobbin Coil Probe

- Dent voltage if dented
  - When it is established that denting has been arrested and dents are not growing, dent voltages for TSP intersections can be established one time and applied for subsequent inspections. It is preferable that dent voltages be defined prior to the presence of an indication.
  - Dent voltages must be determined to at least a minimum of 2 volt dents in order to define the +Point inspection requirements.
  - If PWSCC is found at a TSP intersection for which no dent has previously been defined, the intersection must be reevaluated for denting. If no dent of any size is found in the reevaluation, the indication must be repaired.

- NDD or DSI (or equivalent code) if potential indication detected with associated bobbin flaw voltage

+Point Probe

- NDD, SAI or MAI for each dented intersection inspected

- Crack length versus depth and voltage profile with axial positions defined relative to the center of the TSP. The NDE profiles are adjusted for length and depth (if maximum voltage ≤ 1.0 or ≥ 4.5 volts) per the adjustment procedure given in Section 4.

- Identification of crack as ID or OD

- When PWSCC indications at dented TSP intersections are to be left in service, the +Point data shall be applied to evaluate the TSP for cracked ligaments. If cracked ligaments are detected, the PWSCC indication shall be repaired.

The NDE profile adjustment procedure of Section 4 has been applied to the +Point data used to develop NDE uncertainties and growth rates. The same procedure must therefore be applied to all field axial PWSCC indications for which the ARC of this report are applied. Tube repair limits are applied to the +Point sizing results.

7.7   Operational Assessments

The ARC operational assessment is performed to determine the indications requiring repair as described in Section 7.5. The analysis process for the operational assessment is outlined in this section utilizing flow charts to describe the methodology. Figures 7-1 to 7-4 show the flow charts outlining the operational assessment. All indications are conservatively assumed to be free span indications under SLB conditions for both the operational and condition monitoring assessments even if the indication is totally inside the TSP.

POD as a function of depth from the NDE Performance Tests discussed in Section 4 is not currently applicable for use in Monte Carlo analyses due to the high false call rate attained in the tests, and the need to confirm that field inspections will apply comparable calling criteria prior to application of PODs developed from the performance tests. The performance test results and field inspections following implementation of bobbin coil detection for axial PWSCC in dents support a conclusion that indications large enough to challenge structural integrity at the next inspection are being detected. The false call rate relates to calling indications at NDD intersections. A conservative objective of identifying small flaws detectable only as distorted dent signals was incorporated in the NDE analyst training. Flaws of significant length and depth tend to show a flaw phase response separable from the horizontal dent signal and do not require conservative calling criteria for detection. Bobbin detection for PWSCC in dents ≤ 2 volts has been implemented in Sequoyah-1 and results from subsequent inspections have been obtained. The inspection results show that no axial PWSCC indications were found at dented intersections that challenged structural or leakage integrity. This field inspection result demonstrates the adequacy of bobbin detection for significant flaws. Only about 8% of the bobbin indications reported in the last Sequoyah-1 inspection were confirmed as flaws by +Point inspection. Although the NDE evaluations and field experience show the adequacy of the bobbin inspection for small dents, a very conservative constant POD of 0.6 will be used for the SG Monte Carlo leak rate analyses. All burst pressure analyses to define the need for tube repair are based on single indication analyses for comparisons with the limiting indication burst margin requirements, and no SG analyses are applied for the structural assessment.

Preparations for the outage inspection and assessments are described in Figure 7-1. Growth rate distributions are updated to reflect growth data from the last inspections and for potential changes in the T_{hot} resulting from estimated tube repair or changes in operating conditions. The +Point inspection

requirements for dents greater than 2 volts are defined based on the dent population found in the prior inspection.

Figure 7-2 describes ARC implementation for the inspection, evaluation for exclusion zones and for the evaluation of each indication against the criterion for repair of indications $\geq$ 40% depth outside of the TSP thickness of 0.375 inch. The upper boxes of the figure reflect the inspection requirements of Section 7.6 to identify the PWSCC axial indications and size the indications using +Point depth profiling. Each indication is evaluated for potential repair due to being located in the zones excluded from ARC application as discussed in Section 7.5.6. The exclusion zones apply only to Diablo Canyon SGs and indications located in the exclusion zone are repaired and a condition monitoring assessment is performed for the indication if one or more of the additional repair criteria are exceeded. If the maximum depth of the indication is < 40%, the indication is left in service per the existing Technical Specification repair limits and evaluations against the ARC repair limits are not required as described in Section 7.5.1. Indications with maximum depth outside the TSP $\geq$ 40% are repaired and a condition monitoring assessment is performed for the indication. A Monte Carlo operational assessment is then performed for the indications $\geq$ 40% maximum depth within the TSP. In addition, an operational assessment is performed for indications < 40% maximum depth left in service.

The Monte Carlo burst pressure operational assessment for comparison with the burst margin requirements is described in Figure 7-3. The following describes the Monte Carlo processing of NDE uncertainties and growth to obtain the EOC crack profile, where the order of the calculations is not important since the individual components are additive:

- Average depth NDE uncertainties and growth are added to the NDE profile. Average depth values are used for burst pressure analyses due to the dominant dependence of burst pressure on average depth. Depth NDE uncertainties and growth are added to each point in the depth profile so that the adjustments yield the correct average depth for the profile.

- The NDE uncertainties on length occur only at the ends of the crack due to difficulties in detecting shallow tails of the crack and/or coil lead-in and lead-out effects. The length adjustment for NDE uncertainty is conservatively applied at the end of the crack farthest from the TSP centerline, which maximizes the potential length outside the TSP. When a sample length uncertainty is obtained in the Monte Carlo analysis, the end points of the NDE crack profile having a spacing just greater than the uncertainty are scaled to correct for the uncertainty.

- Growth in length is applied to the profile by scaling all point-to-point spacings in the profile to correct for the sample growth value. The center point of the crack is held at a fixed position so growth occurs in both directions relative to the center of the crack.

As described in Section 5, the burst pressure is obtained for the partial length of the crack that results in the lowest burst pressure, which is called the burst effective length or the weak link of the crack. Burst pressures are calculated for both the total crack length and the freespan length outside the plate when the crack extends from the TSP. The burst pressure distribution for total or constrained length is evaluated at 95%/95% confidence and compared to the $1.43\Delta P_{SLB}$ burst margin requirement as given in Section 7.1. If the burst pressure is less than the required margin, the indication is repaired and a condition monitoring assessment is performed for the indication. Similarly, if the freespan burst margin of $3\Delta P_{NO}$ is not satisfied, the indication is repaired and a condition monitoring assessment is performed. If the burst pressure exceeds the burst margin requirements, the indication is evaluated for leakage as described below.

The SLB leak rate operational assessment is described in Figure 7-4. A total SG leak rate analysis is required to compare total leakage against both constrained and freespan indication acceptance requirements. A conservative POD = 0.6 is used in the SG analysis. The Monte Carlo projection to obtain the EOC profile is the same as for burst pressure analyses except that maximum depth NDE uncertainties and growth are used in the leakage analysis. Maximum depth, rather than average depth, values are used to improve the projection of the deepest part of the crack for leakage analysis. As described in Sections 7.2 and 6.4, the projected EOC crack profile is searched for the longest length for which the remaining wall thickness ligament tears to throughwall at SLB pressure differentials. The partial crack length from the ligament tearing analysis is assumed to be throughwall for the leakage analysis. Based on available leak rate test data for non-throughwall corrosion cracks which show ligament tearing only over a few percent depth, the use of the ligament tearing model is expected to result in significant conservatism in the calculated leak rates. The total crack length and freespan lengths (if present) are separately evaluated for ligament tearing and leakage to develop distributions of the leak rates. The total length or constrained leakage and the freespan leak rate are evaluated at 95%/95% confidence to define the leak rate for the indication. The PWSCC leak rate from the total SG Monte Carlo analysis, must be added to other degradation mechanisms found in the overall operational assessment to have projected EOC leakage. For the constrained leak rates associated with the total PWSCC crack length leakage, the PWSCC leak rates would be summed with the leak rates from the TSP ODSCC ARC of GL95-05 and from the W* ARC indications. Freespan leak rates are summed with the potential leak rates found in the operational assessments for other degradation mechanisms. The total constrained and freespan indication leak rates are then compared with the acceptance limits (see Section 7.5.4). If the acceptance limits are exceeded, additional ARC indications with the largest leak rates, but otherwise acceptable for continued service, are repaired until the resulting leakage satisfies the acceptance limits. If additional indications are repaired, the total SG Monte Carlo analysis would be repeated to confirm that the leakage acceptance limits are satisfied.

Single indication Monte Carlo analyses are performed as the +Point sizing data is obtained. The single indication analyses identify leaking indications that may require repair if the total SG leakage limits are not satisfied. A condition monitoring assessment is then performed for any indications found to leak in the single indication operational assessment.

If the condition monitoring assessments performed per Section 7.8 satisfy burst and leakage requirements, no adjustments of the repair limits developed per Section 7.5 are required other than for the changes in operating conditions described in Section 7.5.5. If the condition monitoring requirements are not satisfied for burst and/or leakage, the causative factors for EOC indications exceeding the expected values should be evaluated. In general, it would be expected that larger than expected growth rates would be the cause of not satisfying condition monitoring requirements. If the growth rate update developed from this causative factor evaluation is applied for an analysis of the prior cycle and results in acceptable comparisons with EOC conditions, this update of the growth would be a basis for performing an additional operational assessment. This update assessment would identify indications requiring repair for the inspection found to exceed condition monitoring requirements. If this growth update does not result in acceptable EOC conditions, additional causative factor evaluation is required and the results should be documented in the reports identified in Section 7.11.

7.8   Condition Monitoring Assessments

The assessments described in Figures 7-2 to 7-4, and discussed above in Section 7.7, identify the indications requiring a condition monitoring assessment. Indications for which condition monitoring (CM) analyses will be performed include all indications with ≥ 40% maximum depth outside the TSP, indications requiring repair due to exceeding burst margins (CM burst analysis) and any indications found to have leakage in the operational assessment (CM leakage analysis). The condition monitoring analyses will also utilize Monte Carlo analyses, and Figures 7-5 and 7-6 show the logic diagrams for performing the analyses.

Figures 7-5 and 7-6 permit options for the use of a SG Monte Carlo analysis for the total crack length (constrained crack) burst probability and leak rate analyses. These condition monitoring SG analyses are performed assuming a POD of 1.0 on the basis that indications that could challenge structural and leakage integrity are detected in the inspection. This application of POD = 1.0 is consistent with NRC GL 95-05, Attachment 1, Section 2.c, Alternative Tube Integrity Calculation. This section of GL 95-05 requires that the actual indication distribution and NDE uncertainties be included in the calculation as well as uncertainties in the burst and leak rate analyses. The SG condition monitoring analyses of this report are consistent with these GL 95-05 requirements.

The logic followed for the condition monitoring burst pressure assessment is shown in Figure 7-5. The Monte Carlo analysis methods for condition monitoring are the same as for the operational assessment except that growth is not included in the analysis. The principal differences from the operational assessment are the actions required if an indication does not satisfy the burst margin requirements. If the total length burst margin of $1.43\Delta P_{SLB}$ is not satisfied at 95%/50% confidence for one or more indications, a total SG Monte Carlo analysis should be performed to determine the tube burst probability at SLB conditions. The acceptance limit for the SLB burst probability for PWSCC alone is 1.0×10^{-2} at 95%/50% confidence based on the guidance of NRC GL95-05 for ODSCC at TSP intersections and the guidance of draft Regulatory Guide DG-1074 for condition monitoring. If this burst probability limit is exceeded, the condition monitoring total length burst margin requirement is not satisfied and the results must be reported to the NRC. The application of the SLB burst probability criterion is limited to the total length, constrained crack evaluation and cannot be applied to the freespan indication evaluation. If the freespan burst margin of $3\Delta P_{NO}$ is not satisfied for any PWSCC indication, the indication should be in situ pressure and leak tested. This criterion for defining the need for in situ pressure testing can only be applied to the freespan indication length and is applied in lieu of the EPRI In Situ Test Guidelines based on the detailed analyses performed to determine the need for in situ testing. If the in situ pressure test does not demonstrate satisfaction of the burst margin requirement, the condition monitoring freespan burst margin requirement is not satisfied and the results must be reported to the NRC.

Figure 7-6 outlines the condition monitoring SLB leak rate assessment for axial PWSCC. The Monte Carlo leakage analysis methods are also the same as for the operational assessment other than growth is not included in the condition monitoring assessment. As performed for the operational assessment, the sum of PWSCC leakage for the total crack length is added to that from other ARCs for comparison with the acceptance limits. If the total constrained leakage is less than the allowable dose based limit in the licensing basis, the condition monitoring leakage requirements on accident condition leakage are satisfied for constrained indications (ARC applications). If the constrained leakage limit is exceeded, a total SG Monte Carlo analysis should be performed for the total length leakage. This analysis with total SG leakage evaluated at 95%/50% confidence is a more accurate calculation and less conservative than summing all indication leakage values at their individual confidence levels. The results of this total SG analysis are then added to the leakage from other constrained mechanisms and compared to the

acceptance limit. If the total constrained leakage limit is exceeded, condition monitoring leakage limits are not satisfied and the results must be reported to the NRC. In addition, a corrective action program must be initiated to identify the causative factors for exceeding the leakage limits. If any freespan leakage is predicted, the indication should be in situ pressure and leak tested. This requirement for in situ testing, which replaces application of the EPRI In Situ Guidelines for selection of indications for in situ testing, is applicable only to the freespan evaluation and cannot be applied to the total crack length evaluation. The sum of all freespan leak rates from analysis and in situ tests is added to the leakage from other freespan degradation mechanism condition monitoring assessments. If this limit exceeds 1 gpm, NRC reporting and a corrective action program are required.

If in situ testing is performed for free span indications, the results of the tests are used in place of any analytical results such as described above. The measured leak rate would be added to the calculated SLB leak rate from all other indications. In situ tests cannot be directly applied for the crack length inside the TSP due to the conservative ARC assumption that the TSPs are displaced in a SLB event.

7.9   Tube Removal Requirements for ARC Applications

The following define the requirements for pulling tubes in association with implementation of the alternate repair criteria of this report for axial PWSCC at dented TSP intersections.

- Plants shall pull a tube prior to or subsequent to implementing the PWSCC ARC to support +Point sizing of the indication and crack morphology consistent with the PWSCC database.
- When a tube pull is required to support +Point sizing, the tube selected for removal shall have a high probability of leaking in order to contribute to the leak rate database. The requirements for a tube removal to enhance the likelihood of finding a leaker are given below. The tube pull may be performed in the cycle following ARC implementation or later as necessary to obtain an indication satisfying the requirements for removal. No TSP intersection above the potentially leaking intersection should be removed due to the increased likelihood of damage to the desired intersection.
- The destructive exam for the removed tube shall include, as a minimum, a leak test at operating temperature, a burst test, fractography to obtain the depth profile of the burst crack and a second major crack if present and one or more transverse metallographic sections (cross sections of the tube) to characterize secondary cracking if present. If the tube section removed to obtain the potential leaking section includes a lower TSP with a PWSCC indication, this second intersection shall also be destructively examined.

Freespan indications that are predicted to leak at 95/50 confidence are required to be in situ tested as described in Section 7.8. If the indication leaks in an in situ test, the indication satisfies the requirements for tube removal. Selection of an indication within the TSP with a high probability of leaking can also be obtained from the condition monitoring evaluation. The single indication condition monitoring leakage analyses is performed for all indications predicted to leak in the operational assessment as described in Section 7.8. The Monte Carlo analyses provide a distribution of leak rates for the indication to permit selection of a leak rate at a specified probability of occurrence. To obtain a reasonable likelihood that the indication will leak, the indication selected for removal should be predicted to have a leak rate ≥ 0.01 gpm at 50% probability for the Monte Carlo leak rate distribution. For a 0.01 gpm calculated nominal leak rate, the ligament tearing breakthrough length would be predicted to be about 0.2 inch. The objective for a reasonable breakthrough length of at least 0.2 inch provides a better test of the leakage model than smaller leak rates for which local or specific depth points in the NDE profile may dominate the analysis. The use of the 50% probability value establishes a reasonable likelihood that the indication will leak in

contrast to the 95% leak rate which only assures a 5% likelihood of leakage since lower probability values could be zero or near zero.

In summary, the leakage based requirements that must be satisfied to pull a tube are:

1. The indication is found to leak in an in situ test, or
2. The indication has a predicted leak rate ≥ 0.01 gpm at 50% probability from the Monte Carlo leak rate distribution performed as part of the condition monitoring assessment

7.10 Risk Assessment

NRC draft Regulatory Guide DG-1074 requires that a risk assessment be performed to support an ARC submittal. This section provides this risk assessment for the depth based repair limits of this report. The depth based repair limits are conservatively established to provide deterministic margins against burst under normal operation and accident conditions. Burst margins of $3\Delta P_{NO}$ are satisfied at 95% confidence levels for freespan indications and margins of $1.43\Delta P_{SLB}$ are satisfied at 95% confidence for indications within the TSP. Indications within the TSP inherently satisfy the $3\Delta P_{NO}$ burst margin since the presence of the TSP prevents rupture under normal operation and accident conditions with the postulated exception of a SLB event. The presence of the TSP would also prevent rupture of indications within the TSP under severe accident conditions such as a Station Blackout. As noted in Section 7.5.3, the maximum depth repair limit for freespan indications is 40%, which is consistent with the current Technical Specifications and deterministically satisfies the $3\Delta P_{NO}$ burst requirement with additional margin. Freespan indications are required to satisfy the $3\Delta P_{NO}$ burst margin for condition monitoring assessments. It is therefore concluded that the proposed depth based repair limits provide the same risk for rupture under severe accident conditions as current Technical Specifications which have been considered to be acceptable.

The 40% maximum depth repair limit for freespan indications provides a very low likelihood of freespan leakage under design basis or severe accident conditions. In addition, it is required that the total leakage from all freespan indications including all degradation mechanisms must be less than 1 gpm at SLB conditions. The number of indications left in service for any one operating cycle is expected to be a few hundred or less and not numbers measured in the thousands. The modest population of indications left in service support a negligible freespan leakage potential under design basis conditions. Leakage from indications inside the TSP is limited by the constraint of the TSP even under severe accident conditions and leakage behavior in a severe accident would be similar to that found acceptable for axial ODSCC at TSP intersections. Leakage tests for dented TSP intersections show very low or no leakage for throughwall indications inside the TSP. In addition, the constraint provided by the dented TSP intersection reduces leak rates even for throughwall indications extending outside the TSP. Even under severe accident conditions, the potential for significant leakage would be expected to be small and not significantly different than for other degradation mechanisms repaired to 40% depth limits but with less well-defined growth rates and NDE uncertainties. It is concluded that application of the depth based repair limits of this report result in negligible differences from current 40% repair limits in risk of a tube rupture or large leakage event under design basis or severe accident conditions.

7.11 NRC Reporting Requirements

In the event that condition monitoring requirements as discussed in Section 7.7 are not satisfied, the results shall be reported to the NRC in accordance with NEI 97-06 and time frames specified in 10 CFR 50.72/73.

The results of the condition monitoring assessment and the operational assessment performed to define indications requiring repair shall be reported to the NRC within 120 days following the return to service from the inservice inspection. The report shall include tabulations of indications found in the inspection, the +Point confirmation rate for bobbin detected indications, indications repaired and growth rate distributions for indications found in the inspection as well as the growth distributions used to establish the tube repair limits. Any corrective actions found necessary in the event that condition monitoring requirements are not met shall be identified in the report.

7.12 ARC Summary

A summary of this section is provided in Section 2 of this report.

Figure 7-1. Preparation for Outage: Establish Operating Parameters, Growth Rates and Inspection Plan

Define ΔP_{NO}, T_{hot} and EFPY for Next Cycle

Update Growth Rate Database Incorporating Recent Inspection Results

Adjust Growth Rate Database for Expected T_{hot}. Define Maximum Depth, Average Depth and Length Distributions

Define the +Point Dent Inspection Plan

(e.g., highest TSP requiring + Point inspection based on results of last inspection)

1

Figure 7-2. ARC Implementation: Inspection and Evaluations for Exclusion Zones and Maximum Depth Outside the TSP

Figure 7-3. Burst Pressure Operational Assessment Repair Decision

Figure 7-4. SLB Leak Rate Operational Assessment.
Repair Decision

(3)

Perform single indication Monte Carlo leak rate analysis. Maximum depth and length NDE uncertainty & growth are added to the BOC NDE profile to project the EOC profile.

Complete inspection of dented TSP intersections and +Point size all indications.
Identify tubes with PWSCC indications requiring repair from PWSCC operational assessment and from other causes.

Calculate SLB leakage based on searching projected EOC profile for longest potential TW length resulting from ligament tearing. Develop distribution of leak rates for total and freespan length. Define total length and freespan SLB leak rates at 95/95 confidence levels.

Obtain SLB leak rates from a SG Monte Carlo operational assessment that includes all indications in the SG. Develop distribution of leak rates for total and freespan length. Define total length and freespan SLB leak rates at 95/95 confidence levels.
Add total length PWSCC leakage to that from other constrained ARCs (TSP ODSCC ARC and W*) to obtain total constrained leakage.
Add total PWSCC freespan leak rate to that from other freespan degradation mechanisms in overall operational assessment to obtain total freespan leakage.

Identify indications that leak for potential tube repair and for condition monitoring requirements.

Is total constrained leakage > acceptance limit (e.g., 8.2 gpm SQN)   no

Is total freespan leakage > acceptance limit (1 gpm)   no

Leakage limits satisfied

yes

yes

Perform condition monitoring leakage assessment on all indications with leakage.

(5)

Repair indications with the largest leak rates. Repeat SG leak rate analysis until the leakage acceptance limits are satisfied.

Figure 7-5. Condition Monitoring Burst Pressure Assessment
(only required for indications taken out of service)

(4)

Perform single tube Monte Carlo burst pressure
analyses including NDE uncertainties

Evaluate total length of the crack for that
portion with the lowest burst pressure.
Develop distribution of burst pressures.

Is the 95/50
total length
burst pressure
$<1.43\Delta P_{SLB}$

yes → Perform total SG Monte Carlo analysis for
burst probability at SLB conditions. Compare
burst probability with the acceptance limit of
1×10^{-2} at 95/50 confidence. If this limit is
exceeded, report to the NRC pursuant to CFR
50.72.

no

Evaluate crack length outside the TSP for
that portion with the lowest burst pressure.
Develop distribution of burst pressures.

Is the 95/50
freespan
burst pressure
$<3\Delta P_{NO}$

yes → Perform in situ pressure and leak test of
indication.
If $3\Delta P_{NO}$ burst pressure requirement not
satisfied by test, report to the NRC
pursuant to CFR 50.72 and perform corrective
action evaluation.

no

Condition monitoring
burst pressure analyses
complete.

Figure 7-6. Condition Monitoring SLB Leakage Assessment

8.0 REFERENCES

8-1. SG-99-01-004, "NDE Qualification of Bobbin Detection and + Point Detection/Sizing for Axial PWSCC at Dented TSP Intersections", Westinghouse Electric Company, February, 1999.

8-2. WCAP-14707, "Model 51 Steam Generator Limited Tube Support Plate Displacement Analysis for Dented or Packed Tube to Tube Support Plate Crevices", Westinghouse Electric Corporation, August, 1996.

8-3. EPRI Report, TR-107569-V1R5, "PWR Steam Generator Examination Guidelines: Revision 5 Volume 1: Requirements", September 1997.

8-4. SG-97-007, "Qualification of Rotating Coil Depth Sizing for Axial PWSCC at Dented TSP Intersections," Westinghouse Electric Corporation, December 1997.

8-5. NEI 97-06, "Steam Generator Program Guidelines," Nuclear Energy Institute, December 1997.

8-6. Draft Regulatory Guide 1.121, "Bases for Plugging Degraded PWR Steam Generator Tubes," September 1981.

8-7. Draft DG-1074, "Draft Regulatory Guide DG-1074 Steam Generator Tube Integrity", March 1998.

8-8. PG&E letter DCL-98-025 dated February 25, 1998, in response to the NRC RAI dated December 2, 1997.

8-9. EPRI NP-7480-L, Volume 1, Revision 2, and Volume 2, Revision 1, "Steam Generator Tubing Outside Diameter Stress Corrosion Cracking at Tube Support Plates – Database for Alternate Repair Limits," EPRI (August 1996).

8-10. WCAP-14277, Revision 1, "SLB Leak Rate and Tube Burst Probability Analysis Methods for ODSCC at TSP Intersections," Westinghouse Electric Company (December 1996).

8-11. Kunin, B., "A New Type of Extreme Value Distributions," *Engineering Fracture Mechanics*, Vol. 58, Nos. 5-6, pp. 557-570 (1997).

8-12. Kunin, Boris I., "An Extension of the List of Extreme Value Distributions," Submitted to *Advances in Applied Probability* (August 1998).

8-13. SG-95-03-010, "Burst Pressure Correlation for Steam Generator Tubes with Throughwall Axial Cracks," Westinghouse Electric Corporation for the Electric Power Research Institute (February, 1995). *Also EPRI TR-105505 (October 1998).*

8-14. WCAP-7832A, "Evaluation of Steam Generator Tube, Tubesheet, and Divider Plate Under Combined LOCA Plus SSE Conditions", April 1978 (Westinghouse Proprietary).

8-15. Cochet, B., and Flesch, B., "Crack Stability Criteria in Steam Generator Tubes," Transaction of the 9th International Conference on Structural Mechanics in Reactor Technology, Volume D, the American Association for Structural Mechanics in Reactor Technology, pp. 413-419 (1987).

8-16. Flesch, B., and Cochet, B., "Leak-Before-Break in Steam Generator Tubes," International Journal of Pressure Vessels and Piping, Vol. 43, pp. 165-179 (1990).

8-17. EPRI NP-4690-SR, "Evaluation of Flaws in Austenitic Steel Piping," Electric Power Research Institute, Palo Alto, CA (July 1986). Also in The Journal of Pressure Vessel Technology, Transactions of the ASME, Vol. 108 (August 1986).

8-18. BMI-1908, "Investigation of the Initiation and Extent of Ductile Pipe Rupture," Eiber, R. J., Maxey, W. A., Duffy, A. R., and Atterbury, T. J., Battelle Columbus Laboratories (June 1971).

8-19. EPRI Report NP-6864-L-Rev. 2, "PWR Steam Generator Tube Repair Limits: Technical Support Document for Expansion Zone PWSCC in Roll Transitions – Rev. 2", Draft Report, August 1993.

8-20. Streeter, "Fluid Mechanics," McGraw Hill, 1958.

8-21. ARL 64-174, "The Stresses in a Cylindrical Shell Containing an Axial Crack," E. Folias, Aerospace Research Laboratories (1964).

8-22. Henry, R. E., "The Two-phase Critical Discharge of Initially Saturated or Subcooled Liquid," Nuclear Science and Engineering, 41,336-342 (1970).

8-23. Henry, R. E., "The Two Phase Critical Flow of One-Component Mixtures in Nozzles, Orifices and Short Tubes," Journal of Heat Transfer, May 1971.

8-24. V. E. Schrock, et. al., "A Computational Model for Critical Flow through Intergranular Stress Corrosion Cracks, NUREG/CR-5133, November 1988.

8-25. Tada, Paris, & Irwin, The Stress Analysis for Cracks Handbook, Paris Productions and Del Research Corp., 1985.

8-26. J. A. Begley & J. L. Houtman, Inconel Alloy 600 Tubing Material Burst and Strength Properties, WCAP-12522, January 1990.

8-27. Erdogan, F., "Ductile Failure Theories for Pressurized Pipes and Containers," International Journal of Pressure Vessels & Piping, Vol. 4 (1976).

8-28. Majumdar, Saurin, "Predictions of Structural Integrity of Steam Generator Tubes Under Normal Operating, Accident, and Severe Accident Conditions," 24th Water Reactor Safety Meeting, October 21-26, 1996, Bethesda, MD (September 1996).

8-29. PG&E Letter DCL-99-165 to USNRC, "License Amendment Request 99-02, Exclusion Zone for Alternate Repair Criteria" (December 23, 1999).

8-30. Personal communications on the *ANL Ligament Tearing Model*, W. Shack, Argonne National Laboratory, and R. Keating, Westinghouse (February 15, 2000).

8-31. EPRI TR-109136, "Crack Growth and Microstructural Characterization of Nickel Alloy PWR Vessel Head Penetration Materials", EPRI, Palo Alto, CA

APPENDIX A

NDE Performance Test – Bobbin and + Point Detection Results

Table A-1: Bobbin Flaws with Destructive Exam Data for NDE Performance Test

Table A-2: +Point Flaws with Destructive Exam Data and NDE Performance Test +Point Results

Table A-3: False Call Rates for Detection of PWSCC in Dented TSP Intersections

Table A-4: Bobbin False Call Rates (Dents < 5 Volts)

Table A-5: +Point False Call Rates for NDD Intersections (All Dents)

Table A-1

Bobbin Flaws with Destructive Exam Data for NDE Performance Test

LAB SAMPLES Optical	Reel	Row	Column	Location	NEW REEL	New Row	New Column	Indication	Max. Depth	Resolution 1 Dent V	Flaw V	Call	Resolution 2 Dent V	Flaw V	Call	Reso POD	Analyst A1 Call	Analys B1 Call	Analyst A2 Call	Analyst B2 Call
ECLab	2	1	9	2H																
LAB	556	D-0	9	1H																
ECLab	14	1	12	3H																
ECLab	2	1	11	4H																
ECLab	2	1	2	3H																
ECLab	2	1	6	5H																
ECLab	323	1	4	4H																
LAB	556	D-0	8	1H																
ECLab	2	1	9	3H																
ECLab	2	1	1	4H																
PGE-SAG	225	12	32	1H																
ECLab	2	1	2	4H																
ECLab	2	1	6	1H																
ECLab	14	1	7	1H																
ECLab	14	1	7	3H																
ECLab	33	1	3	3H																
ECLab	2	1	8	2H																
ECLab	2	1	6	3H																
ECLab	2	1	10	4H																
ECLab	14	1	12	2H																
ECLab	2	1	10	3H																
ECLab	2	1	9	4H																
LAB	556	D-0	7	1H																
LAB	556	D-0	10	1H																
ECLab	14	1	12	4H																
ECLab	2	1	9	1H																
ECLab	2	1	11	2H																
ECLab	2	1	6	2H																
ECLab	2	1	2	5H																
ECLab	2	1	2	1H																
ECLab	2	1	8	1H																
ECLab	2	1	11	3H																
ECLab	2	1	6	4H																
PGE-SAG	225	21	43	1H																
ECLab	33	1	3	4H																
ECLab	2	1	8	3H																
ECLab	223	1	5	1H																
ECLab	2	1	9	5H																
PGE-SAG	225	10	22	2H																
ECLab	14	1	13	3H																
LAB	556	D-0	11	1H																
ECLab	2	1	1	3H																

Table A-2

LAB SAMPLES				
Optical	Reel	Row	Column	Location
ECLab	1	1	10	3H-1
ECLab	1	1	10	3H-2
ECLab	9	1	12	4H
ECLab	1	1	11	4H-1
ECLab	1	1	11	4H-2
PGE	127	10	22	2H
ECLab	1	1	11	3H
ECLab	1	1	6	3H
LAB	506	D-0	11	1H-1
LAB	506	D-0	11	1H-2
ECLab	1	1	9	2H-1
ECLab	1	1	9	2H-2
ECLab	1	1	2	5H
ECLab	1	1	2	4H
LAB	506	D-0	8	1H-1
LAB	506	D-0	8	1H-2
ECLab	1	1	9	5H-1
ECLab	1	1	9	5H-2
ECLab	1	1	9	3H-1
ECLab	1	1	9	3H-2
ECLab	1	1	1	3H
ECLab	9	1	12	2H
ECLab	9	1	12	3H
ECLab	9	1	7	3H
ECLab	9	1	7	1H
PGE	127	21	43	1H-1
PGE	127	21	43	1H-2
ECLab	1	1	6	1H
PGE	127	12	32	1H
ECLab	17	1	5	1H
ECLab	1	1	1	4H
LAB	506	D-0	10	1H-1
LAB	506	D-0	10	1H-2
ECLab	1	1	6	5H
ECLab	17	1	3	3H
ECLab	1	1	9	4H-1
ECLab	1	1	9	4H-2
ECLab	1	1	6	2H
ECLab	17	1	3	4H
LAB	506	D-0	7	1H-1
LAB	506	D-0	7	1H-2
ECLab	1	1	8	3H
ECLab	1	1	8	1H
LAB	506	D-0	9	1H-1
LAB	506	D-0	9	1H-2
ECLab	1	1	2	3H
ECLab	1	1	9	1H-1
ECLab	1	1	9	1H-2
ECLab	17	1	4	4H
ECLab	1	1	6	4H
ECLab	1	1	10	4H
ECLab	1	1	8	2H
ECLab	9	1	13	3H
ECLab	1	1	2	1H
ECLab	1	1	11	2H-1
ECLab	1	1	11	2H-2

Where Flaw V is blank, no flaw was reported; these represent "misses".

NEW REEL	New Row	New Column	Indication	Maximum Depth	Resolution R1		Resolution R2		Analyst A1	Analyst B1	Analyst A2	Analyst B2
					Flaw V	Call	Flaw V	Call	Flaw V	Flaw V	Flaw V	Flaw V

+Point Flaws with Destructive Exam Data and NDE Performance Test +Point Results

A-3

Table A-3

False Call Rates for Detection of PWSCC in Dented TSP Intersections
Bobbin Probes: ETSS #96012
PlusPoint Probe: ETSS #96703

Probe	# NDDs	False Calls	False Call Rate	g
Bobbin (Dents < 5V)				
Team 1 Phase 1b				
Team 2 Phase 1b				
Bobbin (All Dents)				
Team 1 Phase 1b				
Team 2 Phase 1b				
+Point (All dents)				
Team 1				
Team 2				

Table A-4

Optical	Old Reel	Old Row	Old Col	Old Loc
STCLab	212	0	7	4H
STCLab	202	0	6	2H
STCLab	202	0	4	1H
STCLab	202	0	4	2H
STCLab	202	0	1	1H
STCLab	215	0	13	3H
STCLab	212	0	5	5H
STCLab	206	0	8	3H
STCLab	215	0	13	2H
STCLab	212	0	1	3H
STCLab	212	0	3	4H
STCLab	202	0	6	4H
STCLab	212	0	3	3H
STCLab	206	0	10	5H
STCLab	206	0	8	2H
STCLab	206	0	8	4H
STCLab	206	0	10	3H
STCLab	206	0	11	3H
3	213	17	25	2H
STCLab	212	0	6	5H
STCLab	212	0	5	4H
STCLab	206	0	11	2H
STCLab	206	0	8	5H
STCLab	202	0	1	5H
STCLab	212	0	4	1H
STCLab	215	0	12	2H
STCLab	212	0	6	2H
STCLab	206	0	9	3H
STCLab	202	0	2	4H
STCLab	202	0	3	1H
STCLab	202	0	3	4H
STCLab	206	0	10	2H
STCLab	212	0	5	2H
STCLab	212	0	1	4H
STCLab	206	0	10	4H
STCLab	202	0	7	4H
STCLab	202	0	5	3H
STCLab	212	0	2	4H
STCLab	212	0	6	1H
STCLab	206	0	10	1H
STCLab	212	0	6	4H
STCLab	202	0	1	2H
STCLab	215	0	12	3H
STCLab	202	0	3	3H
STCLab	202	0	3	2H
STCLab	212	0	4	4H
STCLab	212	0	7	2H
STCLab	202	0	5	2H
STCLab	212	0	5	3H

			BOBBIN FALSE CALL RATES (Dents < 5 VOLTS)							
New REEL	New Row	New Col	Dent V	R1 Call	Team 1 PRI-1	SEC-1	R2 Call	Team 2 PRI-2	SEC-2	g

Table A-4

Optical	Old Reel	Old Row	Old Col	Old Loc	New REEL	New Row	New Col	Dent V	R1 Call	Team 1 PRI-1	SEC-1	R2 Call	Team 2 PRI-2	SEC-2	g
STCLab	212	0	1	2H											
STCLab	212	0	3	1H											
STCLab	202	0	6	3H											
3	213	19	24	2H											
STCLab	212	0	3	2H											
STCLab	206	0	9	4H											
STCLab	202	0	2	3H											
STCLab	202	0	7	5H											
STCLab	215	0	13	5H											
STCLab	206	0	9	1H											
STCLab	212	0	2	2H											
STCLab	202	0	6	5H											
STCLab	215	0	12	5H											
2	212	20	23	2H											
STCLab	212	0	1	5H											
STCLab	202	0	7	2H											
STCLab	202	0	2	1H											
STCLab	215	0	12	4H											
STCLab	215	0	12	1H											
STCLab	202	0	5	5H											
STCLab	212	0	7	5H											
STCLab	212	0	1	1H											
STCLab	212	0	6	3H											
STCLab	206	0	11	4H											
STCLab	202	0	6	1H											
STCLab	202	0	5	4H											
STCLab	206	0	8	1H											
STCLab	202	0	2	2H											
STCLab	202	0	2	5H											
STCLab	206	0	9	5H											
STCLab	215	0	13	1H											
STCLab	212	0	5	1H											
STCLab	206	0	11	1H											
STCLab	202	0	1	4H											
3	213	23	25	1H											
3	214	13	28	1H											
STCLab	212	0	2	5H											
STCLab	212	0	4	5H											
STCLab	202	0	4	4H											
STCLab	202	0	4	5H											
STCLab	215	0	13	4H											
STCLab	206	0	9	2H											
STCLab	202	0	5	1H											
STCLab	212	0	2	3H											
STCLab	212	0	4	2H											
STCLab	206	0	11	5H											
TVA	30	14	7	4H											
TVA	30	18	8	4H											
TVA	30	6	14	4H											
TVA	32	9	14	2H											

ABCWCAP_AppendixA_Part2.xls:Table A-4

Table A-4

Optical	Old Reel	Old Row	Old Col	Old Loc
TVA	32	5	15	3H
2	212	8	20	2H
2	212	20	20	2H
2	212	23	20	2H
2	212	21	21	1H
PGE-4/97	28	27	21	5H
2	212	28	21	1H
2	212	20	22	2H
PGE-4/97	28	36	22	7H
2	212	7	23	2H
PGE-4/97	28	38	23	7H
PGE-4/97	27	10	24	1H
PGE-4/97	27	17	24	1H
PGE-4/97	27	22	24	2H
PGE-4/97	28	27	24	2H
3	213	23	25	3H
3	213	27	25	2H
3	213	28	25	2H
3	213	35	26	2H
3	213	11	27	2H
3	213	16	27	1H
3	213	24	27	1H
3	214	7	28	2H
3	214	19	29	2H
3	214	26	30	1H

FALSE CALL RATE=# False calls/ # NDD Grading Units =

New REEL	New Row	New Col	Dent V	R1 Call	Team 1 PRI-1	SEC-1	R2 Call	Team 2 PRI-2	SEC-2	g

Table A-5

+Point False Call Rates for NDD Intersections (All dents)

Optical	Reel	Row	Column	Location	NEW REEL	New Row	New Column	Resolution R1 Flaw V	Resolution R1 Call	Analyst A1 Flaw V	Analyst B1 Flaw V	Resolution R2 Flaw V	Resolution R2 Call	Analyst A2 Flaw V	Analyst B2 Flaw V
STCLab	201	0	2												
STCLab	201	0	4												
STCLab	207	0	9												
STCLab	213	0	12												
2 -1R8	28	1	4												
STCLab	201	0	5												
STCLab	213	0	13												
STCLab	211	0	5												
STCLab	211	0	4												
STCLab	211	0	7												
STCLab	207	0	8												
STCLab	211	0	2												
2 -1R8	28	14	4												
STCLab	201	0	3												
17	93	16	59												
STCLab	211	0	5												
STCLab	211	0	1												
STCLab	211	0	3												
STCLab	207	0	9												
STCLab	201	0	1												
STCLab	213	0	12												
STCLab	207	0	8												
2 -1R8	28	12	3												
STCLab	211	0	3												
STCLab	201	0	3												
STCLab	201	0	1												
STCLab	211	0	6												
STCLab	211	0	6												
STCLab	207	0	11												
STCLab	201	0	5												
17	97	10	67												
2 -1R8	29	22	47												
STCLab	201	0	1												
STCLab	213	0	12												
STCLab	213	0	12												
2 -1R8	29	22	47												
17	93	9	64												
STCLab	211	0	7												
STCLab	211	0	4												
STCLab	213	0	12												
STCLab	201	0	2												
15	80	9	85												
STCLab	211	0	3												
STCLab	201	0	2												
STCLab	201	0	4												
2 -1R8	28	15	3												
15	80	6	78												
PGE	127	10	22												
STCLab	211	0	3												
STCLab	211	0	3												
STCLab	207	0	9												
STCLab	201	0	7												
STCLab	211	0	2												
2 -1R8	26	8	2												
STCLab	201	0	7												
STCLab	201	0	5												
STCLab	201	0	1												
STCLab	207	0	8												
STCLab	201	0	2												

LAB SAMPLES / Bold=Training REEL

Table A-5
+Point False Call Rates for NDD Intersections (All dents)

Optical	Reel	Row	Column
STCLab	201	0	6
STCLab	207	0	11
STCLab	211	0	5
STCLab	201	0	3
STCLab	201	0	2
STCLab	211	0	2
16	90	9	73
STCLab	207	0	8
STCLab	207	0	10
STCLab	201	0	4
STCLab	201	0	7
STCLab	211	0	4
STCLab	201	0	7
15	80	8	85
17	93	16	59
STCLab	211	0	5
STCLab	211	0	1
STCLab	207	0	10
STCLab	207	0	9
STCLab	211	0	5
STCLab	211	0	1
STCLab	213	0	13
STCLab	201	0	7
STCLab	213	0	13
STCLab	201	0	1
STCLab	207	0	11
STCLab	211	0	4
STCLab	211	0	2
STCLab	211	0	2
STCLab	201	0	6
STCLab	211	0	1
STCLab	201	0	4
STCLab	207	0	10
STCLab	213	0	13
STCLab	211	0	1
17	93	5	61
2 -1R8	26	6	2
STCLab	211	0	6
STCLab	201	0	5
STCLab	201	0	3
STCLab	211	0	6
STCLab	211	0	7
STCLab	211	0	7
STCLab	213	0	13
STCLab	207	0	8
STCLab	201	0	5
STCLab	207	0	11
STCLab	201	0	6
STCLab	211	0	6
STCLab	211	0	7
STCLab	201	0	6
STCLab	201	0	6
STCLab	207	0	10
STCLab	207	0	11
STCLab	201	0	3
STCLab	207	0	9
STCLab	211	0	4
STCLab	201	0	4
STCLab	207	0	10

LAB SAMPLES — Bold=Training REEL

Location	NEW REEL	New Row	New Column	Resolution R1 Flaw V	Resolution R1 Call	Analyst A1 Flaw V	Analyst B1 Flaw V	Resolution R2 Flaw V	Resolution R2 Call	Analyst A2 Flaw V	Analyst B2 Flaw V

A-9

Table A-5

+Point False Call Rates for NDD Intersections (All dents)

LAB SAMPLES		Bold=Training REEL		Location	NEW REEL	New Row	New Column	Resolution R1 Flaw V	Call	Analyst A1 Flaw V	Analyst B1 Flaw V	Resolution R2 Flaw V	Call	Analyst A2 Flaw V	Analyst B2 Flaw V	g
Optical	Reel	Row	Column													
2-1R8	28	4	1													
2-1R8	28	5	1													
2-1R8	26	6	2													
2-1R8	26	7	2													
2-1R8	26	9	2													
2-1R8	26	4	3													
2-1R8	26	12	3													
2-1R8	28	14	3													
2-1R8	28	10	4													
2-1R8	29	23	47													
2-1R8	29	24	47													
17	98	7	48													
17	98	20	54													
17	98	27	64													
17	97	8	67													
17	97	9	68													
17	97	18	68													
16	90	7	72													
15	80	5	84													
15	80	8	84													
15	80	12	86													
15	80	6	88													
15	80	18	88													
15	80	12	92													
15	80	7	93													
		FALSE CALL RATE=# False calls/ # NDD Grading Units =														

APPENDIX B

This Appendix has been removed from WCAP-15129 Revision 2

.

Appendix C

Data Exclusion Criteria for Axial PWSCC at Dented TSP Intersections

Data Exclusion Criteria for Axial PWSCC at Dented TSP Intersections

1.0   OBJECTIVE

This section addresses criteria for excluding data from databases used to qualify/quantify NDE analyses and/or to develop burst and leak rate correlations. Data exclusion criteria were developed by EPRI for application to the ARC for ODSCC at TSP intersections under NRC Generic Letter 95-05. The exclusion criteria defined herein are similar to the EPRI ODSCC criteria but are specific to axial PWSCC at dented TSP intersections. The use of crack depth profiles from destructive examinations is a specific application that requires an extension of the EPRI exclusion criteria.

The objective of the data exclusion criteria is to eliminate from databases, test or measurement data that that are unacceptable or inadequate due to errors in obtaining the data or the data are inappropriate for the application. The general categories identified for data exclusion are:

1.   Invalid or Inadequate Test
2.   Morphology Related Criteria
3.   Test Measurement Error
4.   Destructive Exam Crack Depth Profile Related Criteria

Categories 1 to 3 are the same broad groups used for the EPRI exclusion criteria (EPRI Report NP-7480-L, Volume 1, Rev. 2) for ODSCC and the criteria are the same or adapted to PWSCC. Category 4 is added specifically for programs utilizing detailed destructive exam information such as crack depth profiles for NDE qualification or ARC applications. The exclusion criteria are developed in Section 2. Section 3 applies the criteria to identify indications excluded from the database.

2.0   DATA EXCLUSION CRITERIA

NRC guidelines for acceptance of data used for ARC applications are based on accepting all data that do not satisfy criteria for exclusion from the database. The NRC's general criteria for exclusion of data from a database are:

- Data is associated with an invalid test.
- Data is associated with atypical degradation based on morphology criteria which are defined rigorously and applied to all data, and which can be unambiguously applied by an independent observer.
- Exclusion of data results in conservatism associated with application of the affected correlation.

This section defines the specific data exclusion criteria for application to axial PWSCC at dented TSP intersections.

Criterion 1: Invalid or Inadequate Test

1a: Unacceptable NDE Data Collection: This condition applies to specimens for which NDE data was not obtained with acceptable data acquisition techniques or probes, specimens that have been damaged for reasons other than the corrosion process and specimens exhibiting extraneous eddy

current signal effects (e.g. proximity to a test article weld or tube mark). This criterion results in the data point being excluded from NDE qualification programs and any ARC correlations based on NDE data.

1b: Inadequate or Inappropriate Burst Test: This condition applies to specimens that did not attain a true burst condition (e.g., caused by leakage in the burst test), a test fixture malfunction with inability to retest and specimens tested for other purposes (with a constraint such as a TSP when free span test is required). Specimens satisfying this criterion are excluded from use in an ARC burst correlation or burst test database for which it is assumed that TSPs displace in a SLB event. Specimens tested with a TSP and achieving an acceptable burst condition for the length of PWSCC outside the TSP may be used in burst correlations based on no SLB TSP displacement.

1c: Inadequate Leak Test: This condition applies to unacceptable leak tests such as insufficient test loop flow capacity to reach the specimen's leak rate for SLB conditions and a test fixture malfunction with inability to retest. Specimens satisfying this criterion are excluded from use in ARC leak rate correlations or leak test database.

1d: Tube Damage from Tube Pull Forces: This condition applies to crack distortion or damage such as excessive ligament tearing as indicated by increased post-pull NDE flaw measurements such as voltage or length and post-pull leak rates much higher than indicated by plant data. For application of this criterion, it must be demonstrated that the damage from the tube pulling operations such as ligament tearing are greater than expected at SLB conditions. Specimens satisfying this criterion are excluded from use in ARC leak rate correlations or leak test database and possibly from use in burst correlations.

1e: Unavailable Test Information: This condition applies to specimens for which complete testing such as leak, burst and fractography have not been performed. For example, a leak test may not have been performed and the fractography is not performed or not conclusive relative to including the specimen in a probability of leak database. This criterion is most applicable to excluding data from the probability of leak correlation when the test information is inadequate to draw a conclusion on whether the specimen would leak at SLB conditions.

Criterion 2: Morphology Related Criteria

2a: Crack Morphology Atypical of Axial PWSCC at Dented TSP: This condition applies to crack morphologies, particularly laboratory specimens, that have crack morphologies that are not characteristic of axial PWSCC at dented TSP intersections as found by pulled tube examinations. The required, pulled tube morphology is that of very narrow bands (such as having < 25° circumferential extent) of axial PWSCC that may be within or extending outside the TSP. Specimens with broad bands of cracks or multiple initiation sites extending more than about 25° as a single band are excluded by this criterion. This criterion excludes the data point from all NDE qualification efforts and any ARC databases or correlations.

Criterion 3: Probable Test Error in Leakage Measurement

No criteria except that under Criterion 1 are applied to exclude data from the database for the leak rate correlation.

Criterion 4: Destructive Exam Data Crack Depth Profile Related Criteria

4a: Incomplete Crack Length/Depth Profile: This condition applies when the length versus depth profile provided from the destructive examination is less than the length of significant cracking. Verification of cracking beyond the length profiled, such as photographs, must be obtained to support exclusion per this criterion. When indications are opened by bending rather than by a burst test, the length to be opened requires some judgment and the full extent of significant cracking may not be depth profiled as part of the tube exam. This criterion excludes the data point from all NDE sizing qualification efforts including NDE uncertainty estimates and from burst correlations with an NDE parameter. The indication may be used for NDE detection such as POD or a leak rate correlation with maximum depth if the available data is adequate to define the maximum depth.

4b: Incomplete Depth Profile: This condition applies when the crack is opened by bending or other techniques (e.g., radial grinding) than burst and it can be demonstrated that either the complete depth profile or the structurally or leakage limiting crack may not have been obtained. To apply this criterion, it must be demonstrated by destructive examination data, such as metallography, that the complete depth profile has not been defined or that the microcracks or macrocracks parallel to the crack opened by bending have depths or lengths exceeding the opened crack. An example of this criterion application could be depth profiles obtained from radial grinds, but the initial grind may have been too deep to define shallow depths. In this example, the crack length and maximum depth are defined but the average crack depth is not obtained. This criterion does not apply to a crack opened by a valid burst test which opens the structurally limiting crack. This criterion excludes the data point from NDE depth sizing qualification efforts for the data not obtained and from burst correlations with destructive exam data or a NDE parameter. The indication may be used for NDE detection such as POD or a leak rate correlation with maximum depth if the available data is adequate to define the maximum depth. If the total crack length is obtained, the indication may be used for NDE length sizing qualification.

4c: Selective Length Adjustments to Destructive Exam Crack Depth Profiles: This condition applies when the crack depth profile from destructive examination includes shallow cracking at the ends of the crack and the depths at the tails are much less than the more dominant or maximum crack depths. Under this criterion, only the shallow tails are excluded from the crack length and average depth of the crack used for qualification of NDE sizing techniques or potential burst pressure correlations. To apply this criterion, the depths of the tails excluded from the crack length must be less than 40% maximum depth, and the average depth over the length cutoff must be less than 15%. This selective length adjustment of the depth profiles is necessary to ensure that the shallow tails of cracks, which have no tube integrity implications, do not significantly impact NDE sizing uncertainty estimates.

3.0   APPLICATION TO CURRENT DATABASE

The available pulled tube and laboratory specimen indications were evaluated against the PWSCC Data Exclusion Criteria defined in Section 2. Specimens affected by application of the criteria are identified in Table C-1. Pending determination of the parameters to be correlated with burst pressure for ARC applications, a burst test data point may have potential applications in a correlation with destructive exam depth (BvD in Table C-1) and/or an NDE parameter (BvNDE). Indications P8 to P10, which were burst with a TSP and part of the crack length extending outside the TSP, are acceptable for NDE qualification, but are limited for burst correlations only under the assumption that TSPs do not displace in a SLB event. A number of specimens were pressure tested to open the cracks for destructive exam fractography of the pressurized crack opening and were not intended to be qualified burst tests. The second crack for these specimens, as identified in Table C-1, was opened after prior pressurization to burst the larger crack. Criterion 1b applies for exclusion of these data from the burst pressure correlation. In some cases, the pressurization tests resulted in burst of the indication away from the flaw such as in welded extensions to the test specimen. Since the resulting burst pressures cannot be associated with the flaw, the tests are not considered acceptable and are also excluded from the burst correlation database per Criterion 1b. Two specimens, 9-5H and 10-3H, had reported burst pressures in excess of 11 ksi (near that of undegraded tubing), and the destructive exam reported flaws exceeding 57% averaged depth over lengths greater than 0.63 inch. It would be physically impossible for flaws of this size to have burst pressures >11 ksi. Therefore, these two specimens are considered to have an unacceptable burst test. Acceptable applications for the specimen after applying the exclusion criteria are identified in the 4th column of Table C-1.

Application of Criterion 4c leads to exclusion of shallow points at the tail of a crack from the destructive exam profile and average depth used for NDE comparisons and potentially in burst evaluations. Figures C-1 to C-19 show the points excluded from the destructive exam profile for the specimens indicated in Table C-1.

Table C-1
Evaluation of Axial PWSCC Data Against Data Exclusion Criteria
Database Status – 2/00

Specimen	Basis for Excluding Indications	Exclusion Category	Remaining Data App.[1]
Plant W-1 R21C64	Field data obtained with pancake coil. NDE qualification based on + Point coil	1a	M, BvD
P8, crack 1 P9, crack 1 P10, crack 1	Indication burst with presence of TSP. Application to burst correlations limited to assumption that TSP does not displace in a SLB event.	1b	NDE, burst only for length outside TSP
Crack 2 for 9-3H, 9-4H, 9-5H, 10-3H, 11-3H	Specimen was initially burst to open crack 1. Crack 2 was cut from tube and weld into another tube section in order to pressurize the crack to open the crack for NDE fractography	1b	NDE
2-3H, 3-3H, 4-4H, 5-1H, 12-2H	Specimens burst away from flaw, typically at a weld joint or attachment to tube. Specimen lower bound burst pressure is not appropriate for use in a burst correlation.	1b	NDE
9-5H, 10-3H	Reported burst pressures were >11 ksi for indications >0.63" and 57% average depth. It is physically impossible for these large indications to correspond to the reported burst pressures, and the indications are excluded from the burst correlation.	1b	NDE
P13, cracks 1 to 3	Crack morphology of wide bands of microcracks is atypical of pulled tube PWSCC morphology	2a	None
5-1H	Complete depth profile not defined. Depth profile from radial grinding obtained at too large of depth steps to define profile. Length obtained and max. depth reasonably estimated.	4b	NDE-POD, Max. Depth, Length
9-1H, crack 2	Total crack length of significant depth was not opened by bending in destructive exam and data not valid for NDE sizing qualification. Indication can be use for NDE detection or POD as maximum depth defined.	4a	NDE-POD, Max. Depth
9-4H, crack 2	Complete depth profile not defined. Depth profile from radial grinding obtained at too large of depth steps to define profile. Length obtained and max. depth reasonably estimated.	4b	NDE-POD, Max. Depth, Length
1-3H	Shallow tails (0.05", 0.05") of crack with depths ≤ 14% excluded from crack length as avg. depth < 15% & max. depth < 40%.	4c	NDE, BvD, BvNDE
2-1H	Shallow tails (0.03", 0.11") of crack with depths ≤ 10% excluded from crack length as avg. depth < 15% & max. depth < 40%.	4c	NDE, BvD, BvNDE
2-3H	Long shallow tails (0.089", 0.212") of crack with max. depth dominantly < 9% and average depths ≤ 6% excluded from crack length as avg. depth < 15% & max. depth < 40%.	4c	NDE, BvD, BvNDE
2-4H	Shallow tails (0.11", 0.09") of crack with depths ≤ 13% excluded from crack length as avg. depth < 15% & max. depth < 40%.	4c	NDE, BvD, BvNDE
2-5H	Shallow tail (0.08") of crack with depths < 13% excluded from crack length as avg. depth < 15% & max. depth < 40%. Extensive length of crack <20% depth retained in profile.	4c	NDE, BvD, BvNDE
6-2H	Shallow tail (0.04") of crack with depths < 14% excluded from crack length as avg. depth < 15% & max. depth < 40%.	4c	NDE, BvD, BvNDE
7-1H	Shallow tail (0.19") of crack with depths ranging from 1% to 24% with an average depth < 8% excluded as avg. depth < 15% & max. depth < 40%.	4c	NDE, BvD, BvNDE
7-3H	Shallow tails (0.07", 0.35") of crack with depths ≤ 13% excluded from crack length as avg. depth < 15% & max. depth < 40%.	4c	NDE, BvD, BvNDE

| Specimen	Basis for Excluding Indications	Exclusion Category	Remaining Data App.[1]
8-2H	Shallow tails (0.05", 0.04") of crack with depths < 15% excluded from crack length as avg. depth < 15% & max. depth < 40%.	4c	NDE, BvD, BvNDE
9-2H, crack 2	Shallow tail (0.05") of crack with depths < 6% excluded from crack length as avg. depth < 15% & max. depth < 40%.	4c	NDE, BvD, BvNDE
9-3H, crack 1	Shallow tail (0.03") of crack with depths < 15% excluded from crack length as avg. depth < 15% & max. depth < 40%.	4c	NDE, BvD, BvNDE
9-3H, crack 2	Shallow tail (0.11") of crack with depths ranging from 1% to 26% with an average depth <8% excluded as avg. depth < 15% & max. depth < 40%.	4c	NDE, BvD, BvNDE
9-5H, crack 1	Shallow tails (0.05", 0.02") of crack with depths < 19% excluded from crack length as avg. depth < 15% & max. depth < 40%.	4c	NDE, BvD, BvNDE
11-3H, crack 1	Shallow tail (0.04") of crack with depths ≤ 10% excluded from crack length as avg. depth < 15% & max. depth < 40%.	4c	NDE, BvD, BvNDE
11-3H, crack 2	Long shallow tails (0.17", 0.26") of multiple microcracks (3 and 2 microcracks, respectively) with average depths ≤ 12% and 10% excluded from crack length avg. depth < 15% & max. depth < 40%.	4c	NDE, BvD, BvNDE
11-4H, crack 1	Shallow tail (0.04") of crack with depths < 23% excluded from crack length as avg. depth < 15% & max. depth < 40%.	4c	NDE, BvD, BvNDE
12-4H	Shallow tails (0.08", 0.09") of crack with depths < 5% excluded from crack length as avg. depth < 15% & max. depth < 40%.	4c	NDE, BvD, BvNDE
P9, crack 2	Shallow tail (0.09") of 3 microcracks with maximum depths 24%, 33% and 17% excluded from crack length as avg. depth < 15% & max. depth < 40%. The 33% max. depth microcrack is farther in the tail than the 17% microcrack.	4c	NDE, BvD, BvNDE
P10, crack 2	Shallow tail (0.06") of crack with depths < 28% excluded from crack length as avg. depth < 15% & max. depth < 40%.	4c	NDE, BvD, BvNDE
Notes:				
1. NDE = used in NDE qualification, BvD = used in burst pressure correlations with destructive exam depth, BvNDE = used in burst pressure correlations with NDE data, L = used in leak rate database, M = used to characterize pulled tube PWSCC morphology.				

Figure C-1
Sample 1, TSP 3H - Crack 1
Mid-Range +Point, 300 kHz
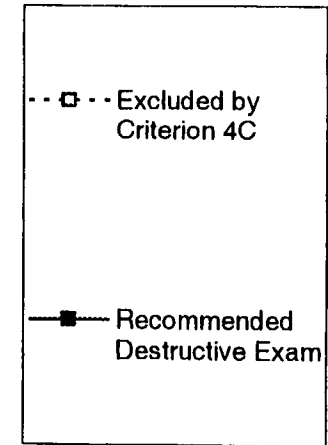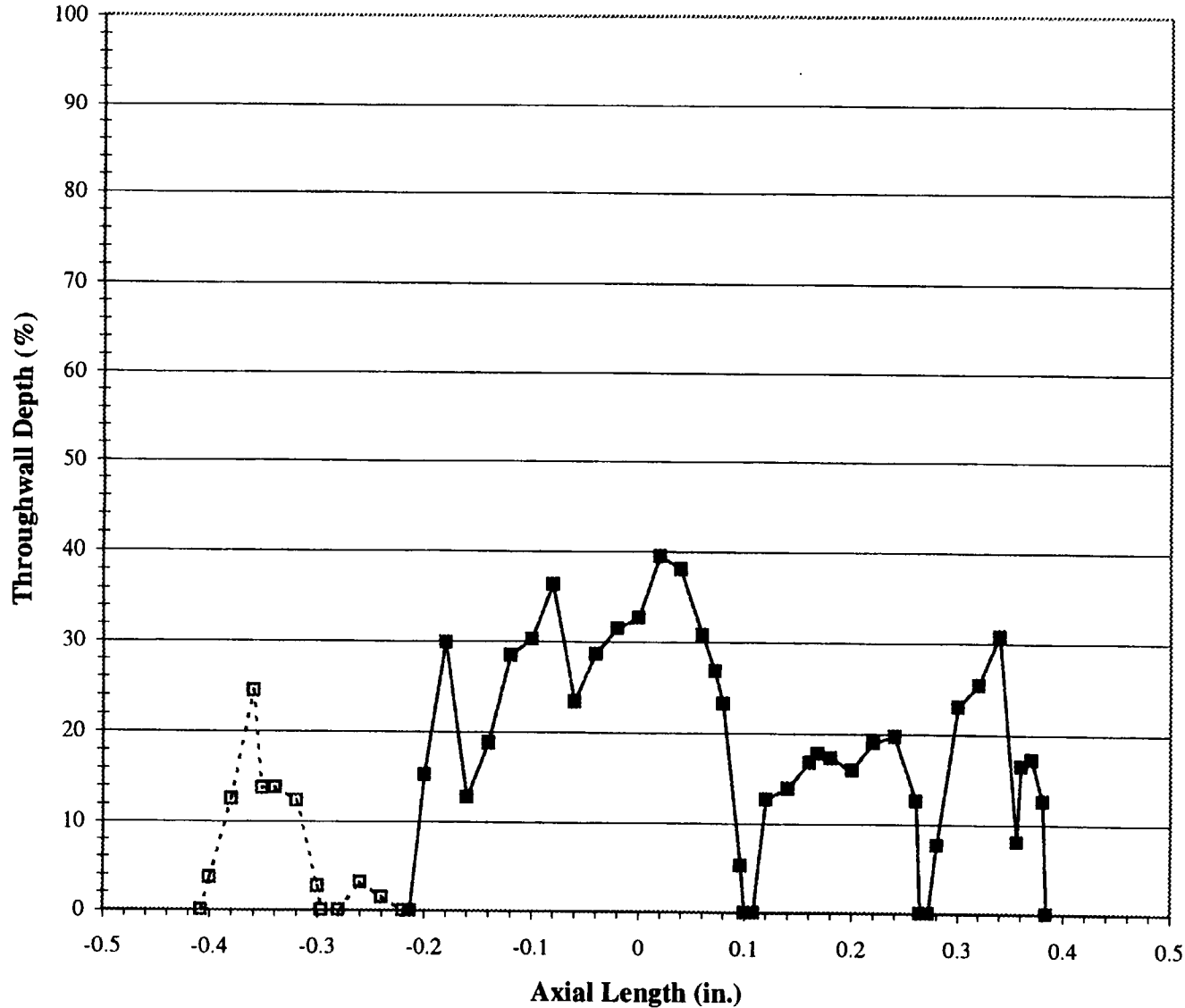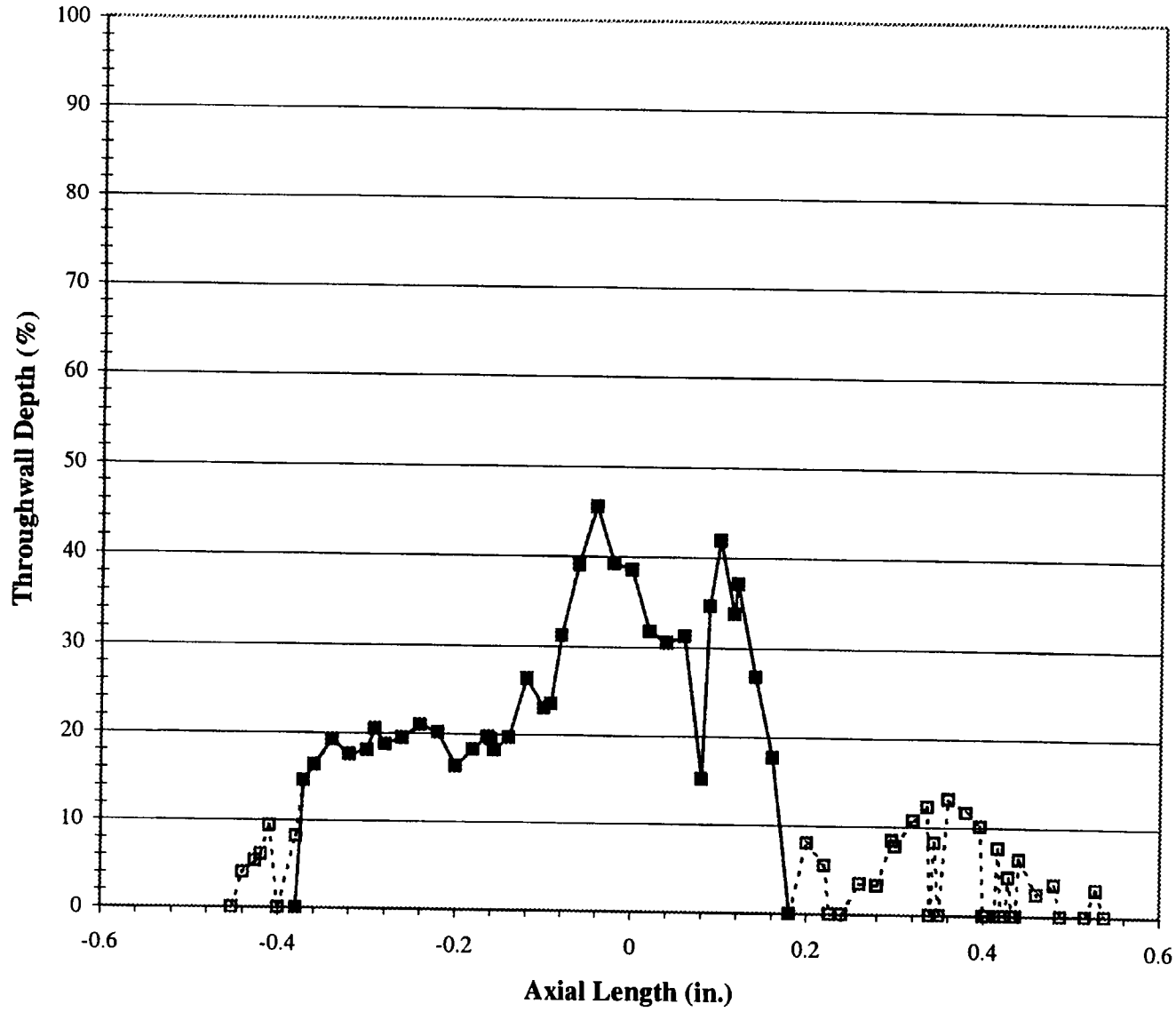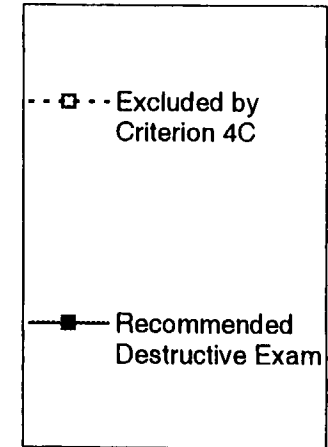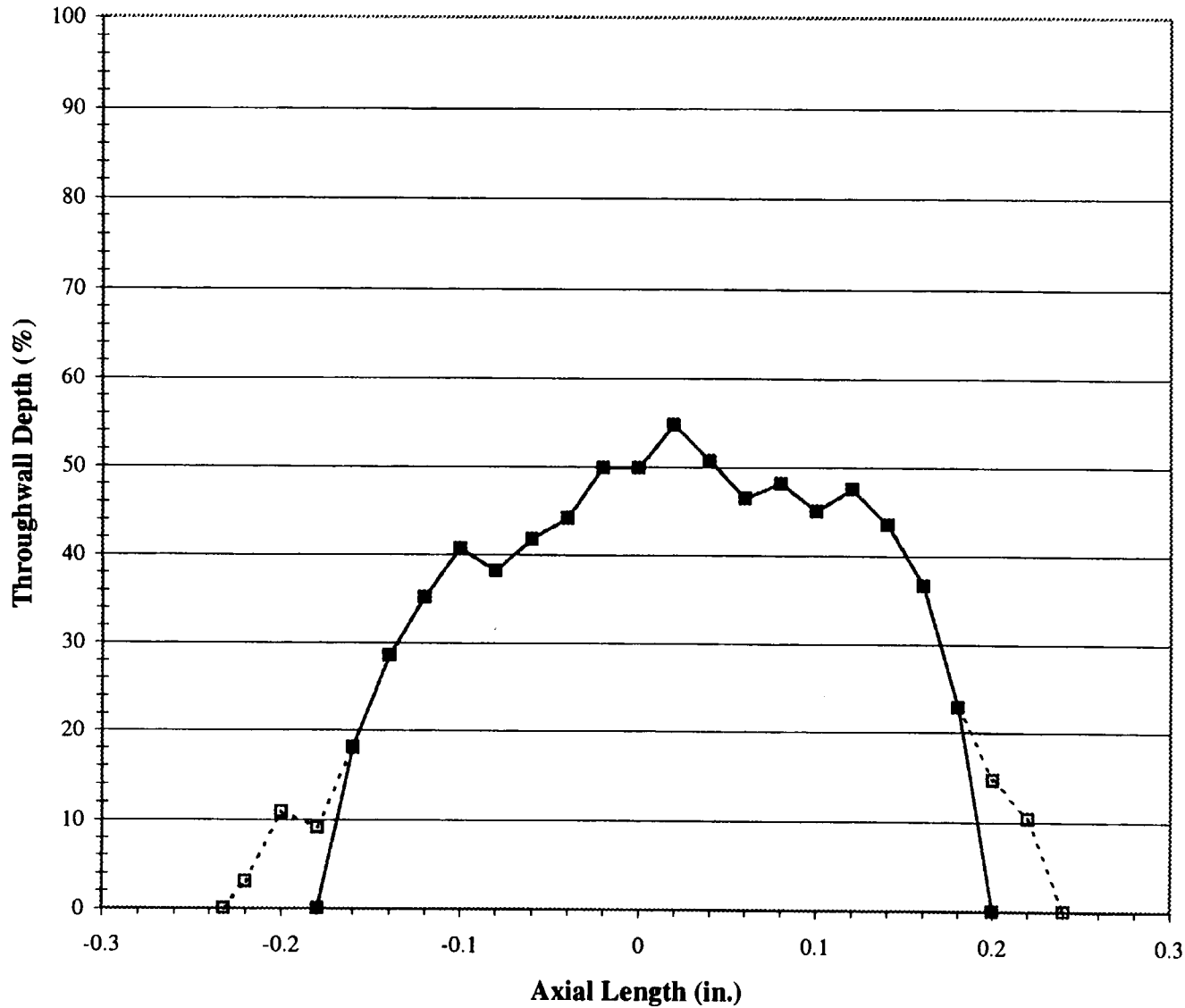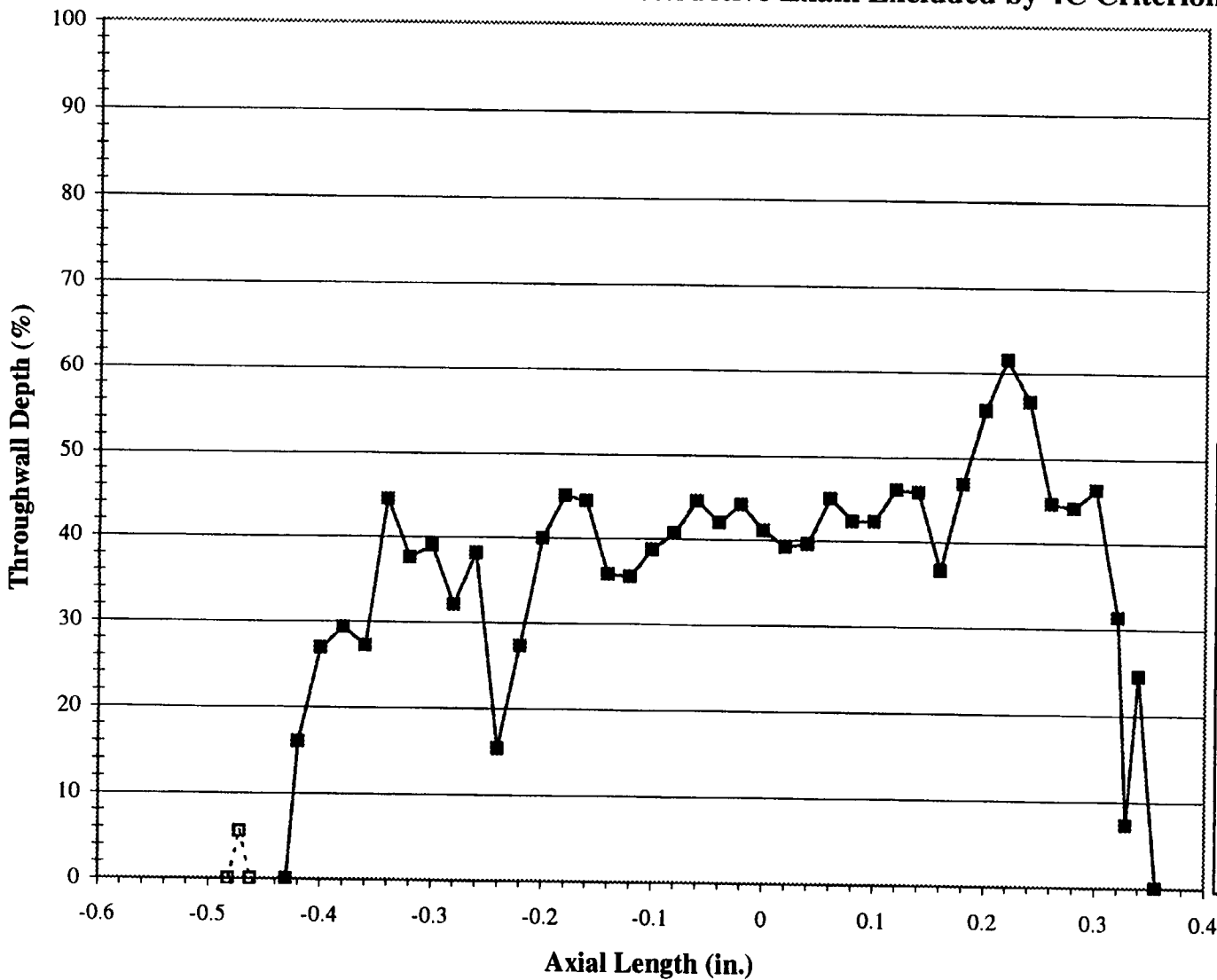**Recommended Destructive Exam and Destructive Exam Excluded by 4C Criterion**

Legend:
- - - ◻ - - Excluded by Criterion 4C
- ■ Recommended Destructive Exam

	Reported DE	Rec. DE
Max. Depth (%)	00.0	00.0
Max. Depth w/o RA(%)	55.7	55.7
Length (in.)	0.762	0.66
Avg. Depth (%)	34.43	39.18
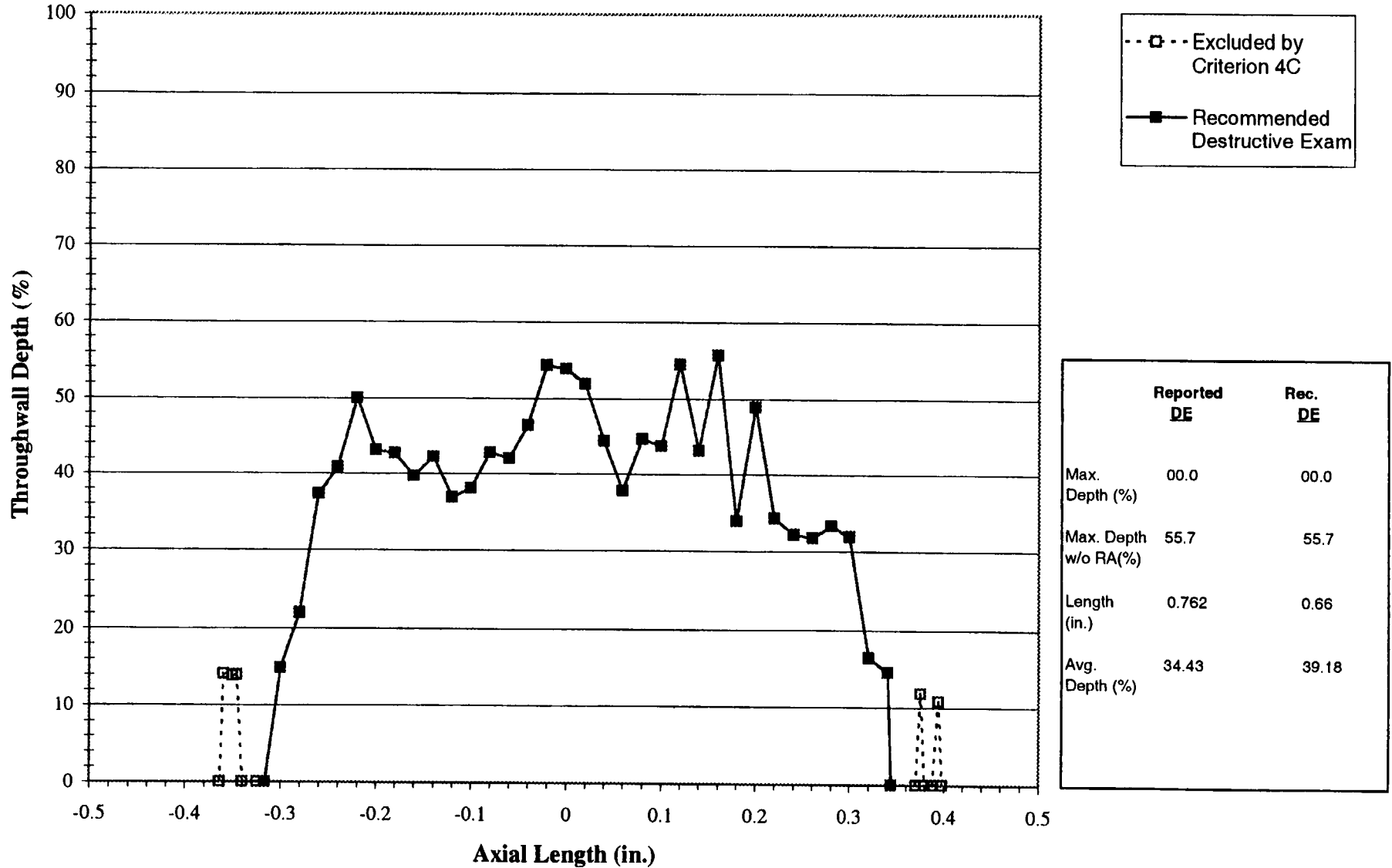
Figure C-2
Sample 2, TSP 1H - Crack 1
Mid-Range +Point, 300 kHz
Recommended Destructive Exam and Destructive Exam Excluded by 4C Criterion

Legend:
- - □ - - Excluded by Criterion 4C
—■— Recommended Destructive Exam

	Reported DE	Rec. DE
Max. Depth (%)	00.0	00.0
Max. Depth w/o RA(%)	48.0	48.0
Length (in.)	1.014	0.876
Avg. Depth (%)	20.17	22.71

Axial Length (in.)

Throughwall Depth (%)
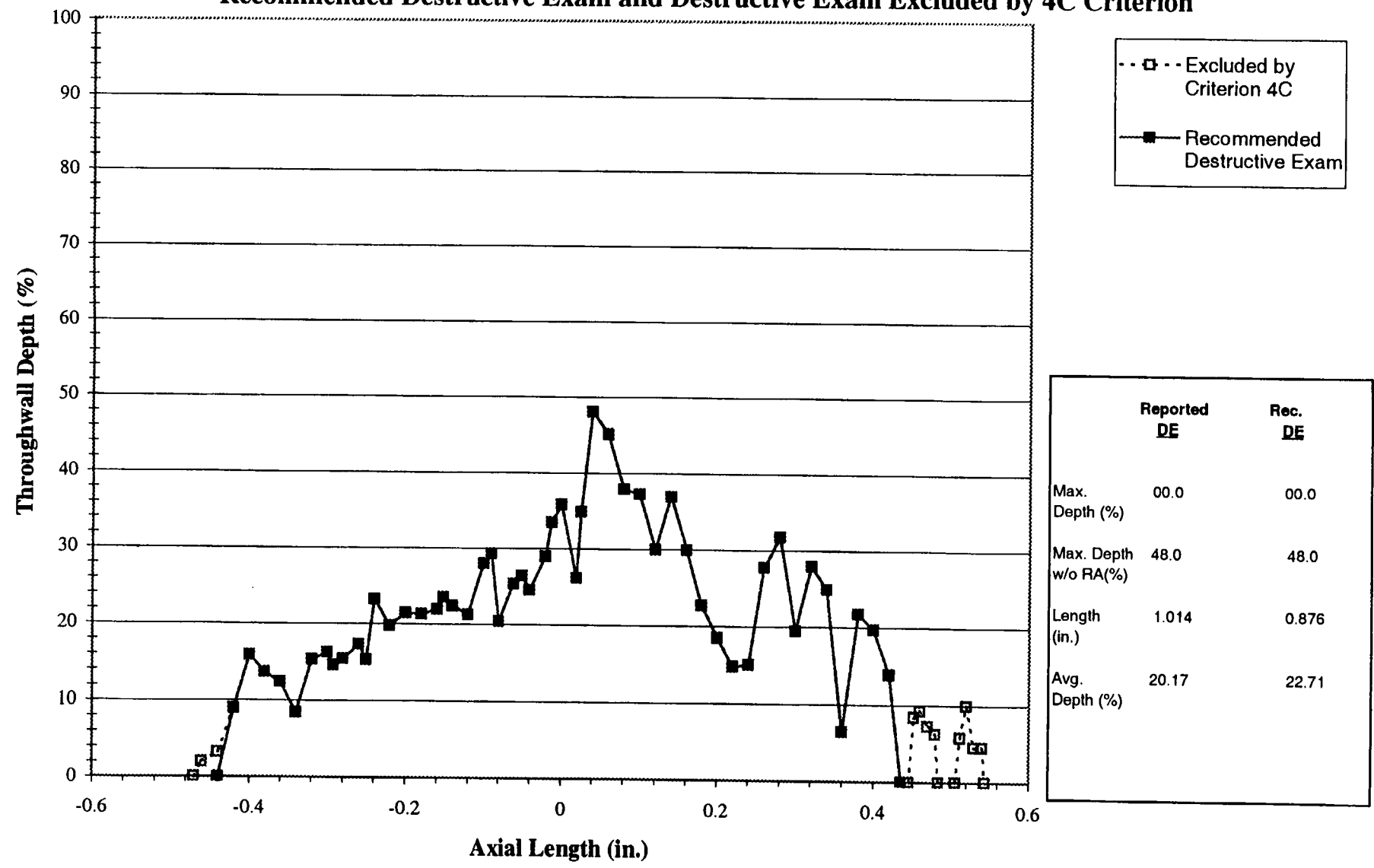
Figure C-3
Sample 2, TSP 3H - Crack 1
Mid-Range +Point, 300 kHz
Recommended Destructive Exam and Destructive Exam Excluded by 4C Criterion
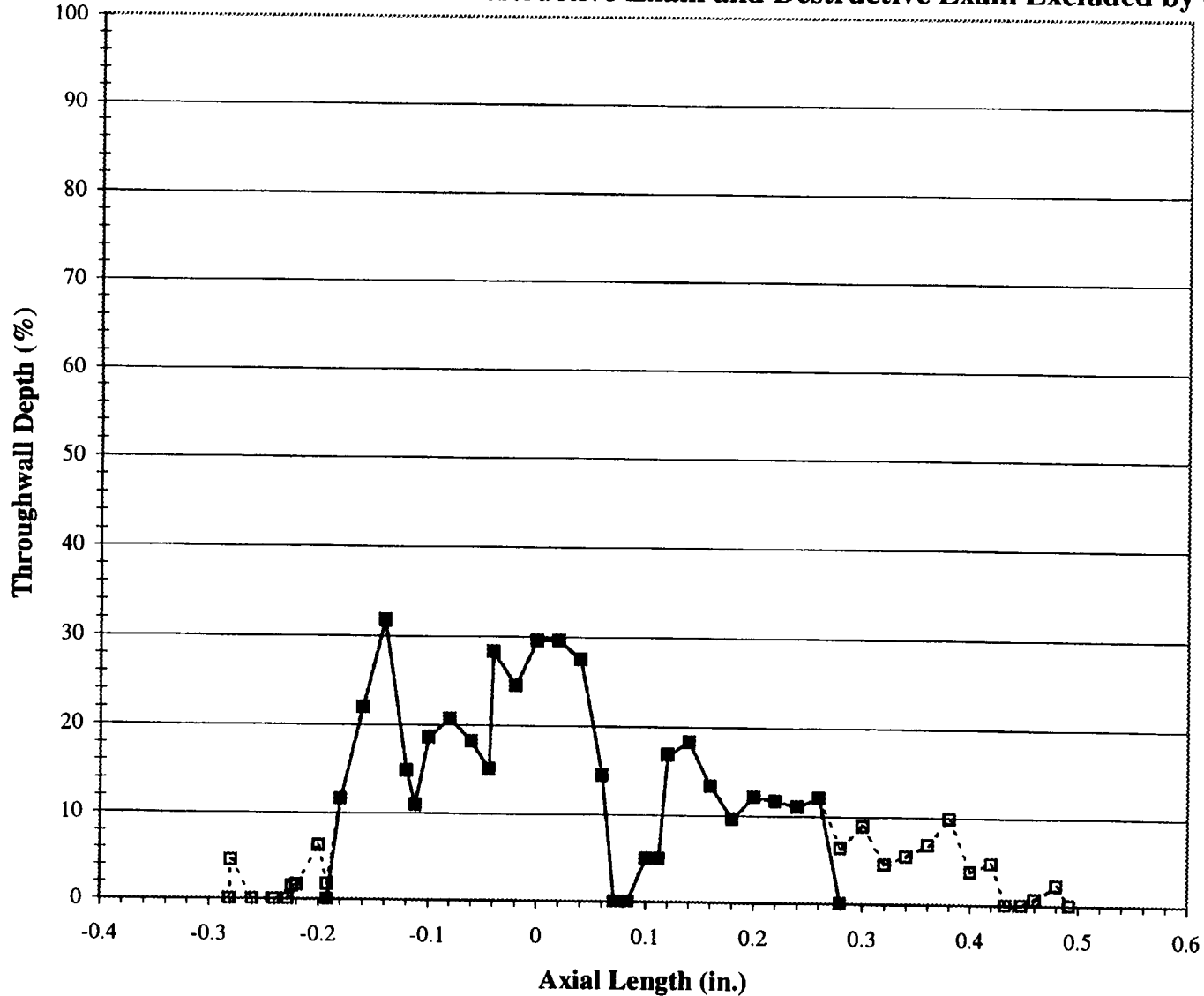
	Reported DE	Rec. DE
Max. Depth (%)	00.0	00.0
Max. Depth w/o RA(%)	31.71	31.71
Length (in.)	.773	.472
Avg. Depth (%)	11.52	16.28

Legend:
- Excluded by Criterion 4C
- Recommended Destructive Exam

Figure C-4
Sample 2, TSP 4H - Crack 1
Mid-Range +Point, 300 kHz
Recommended Destructive Exam and Destructive Exam Excluded by 4C Criterion

Legend:
- - ▫ - - Excluded by Criterion 4C
- ──■── Recommended Destructive Exam
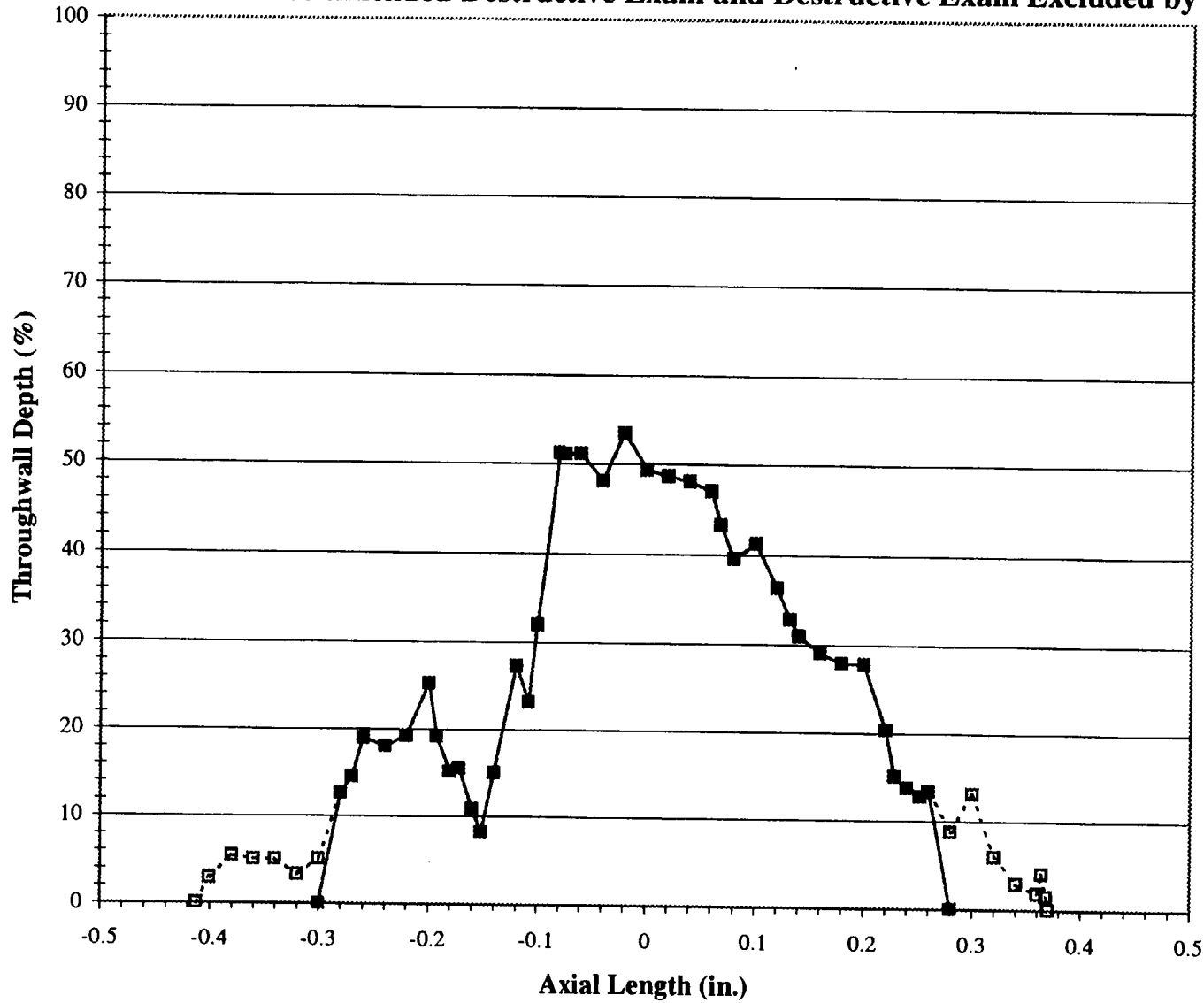
	Reported DE	Rec. DE
Max. Depth (%)	00.0	00.0
Max. Depth w/o RA(%)	53.45	53.45
Length (in.)	.782	.580
Avg. Depth (%)	23.59	29.77

Figure C-5
Sample 2, TSP 5H
Depth vs. Axial Length
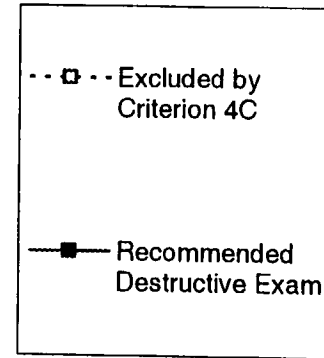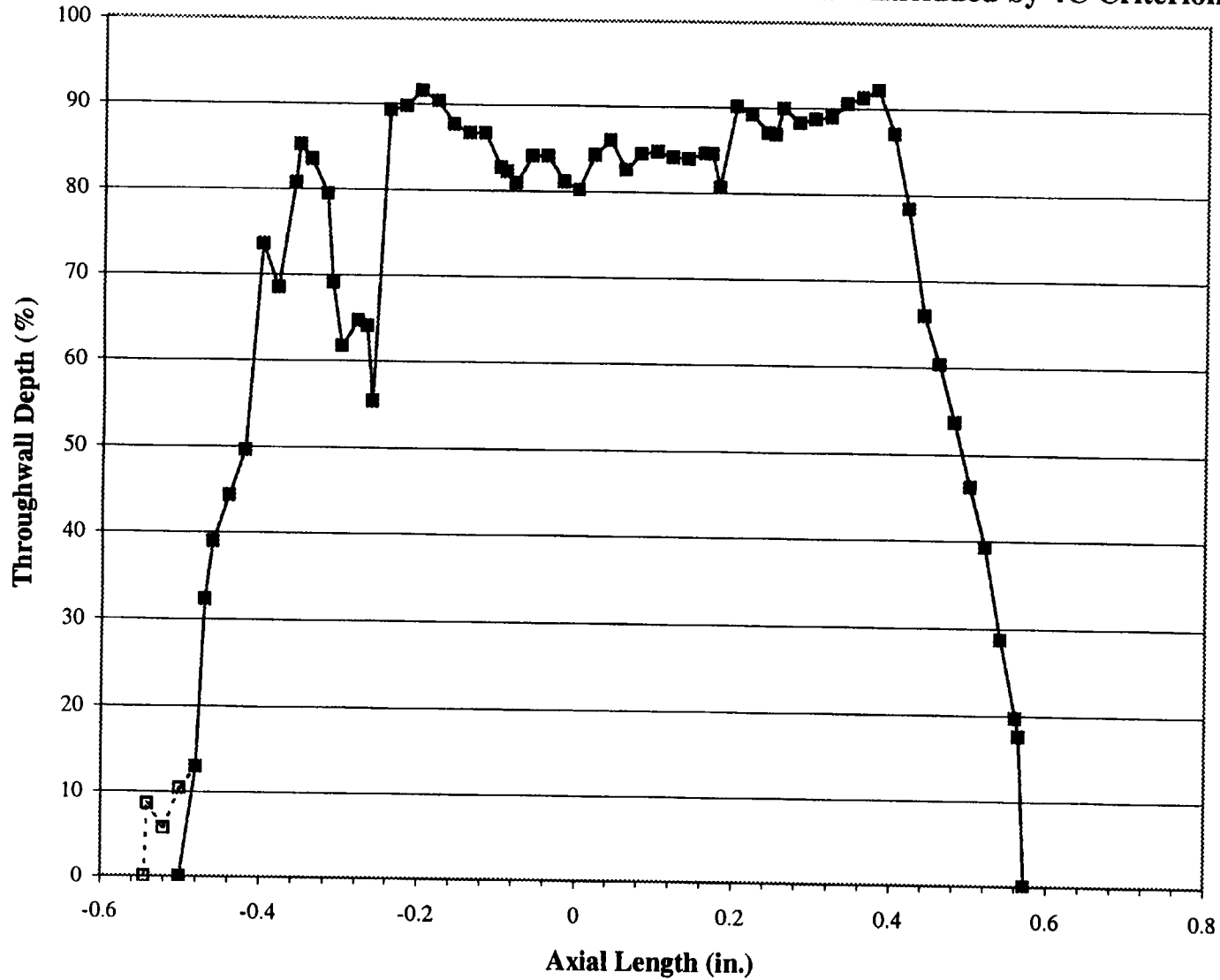## Recommended Destructive Exam and Destructive Exam Excluded by 4C Criterion

Legend:
- - - □ - - Excluded by Criterion 4C
——■—— Recommended Destructive Exam

	Reported DE	Rec. DE
Max. Depth (%)	41.0	41.0
Length (in.)	0.94	0.86
Avg. Depth (%)	17.70	18.63

Axis labels:
- Y-axis: Throughwall Depth (%)
- X-axis: Axial Length (in.)
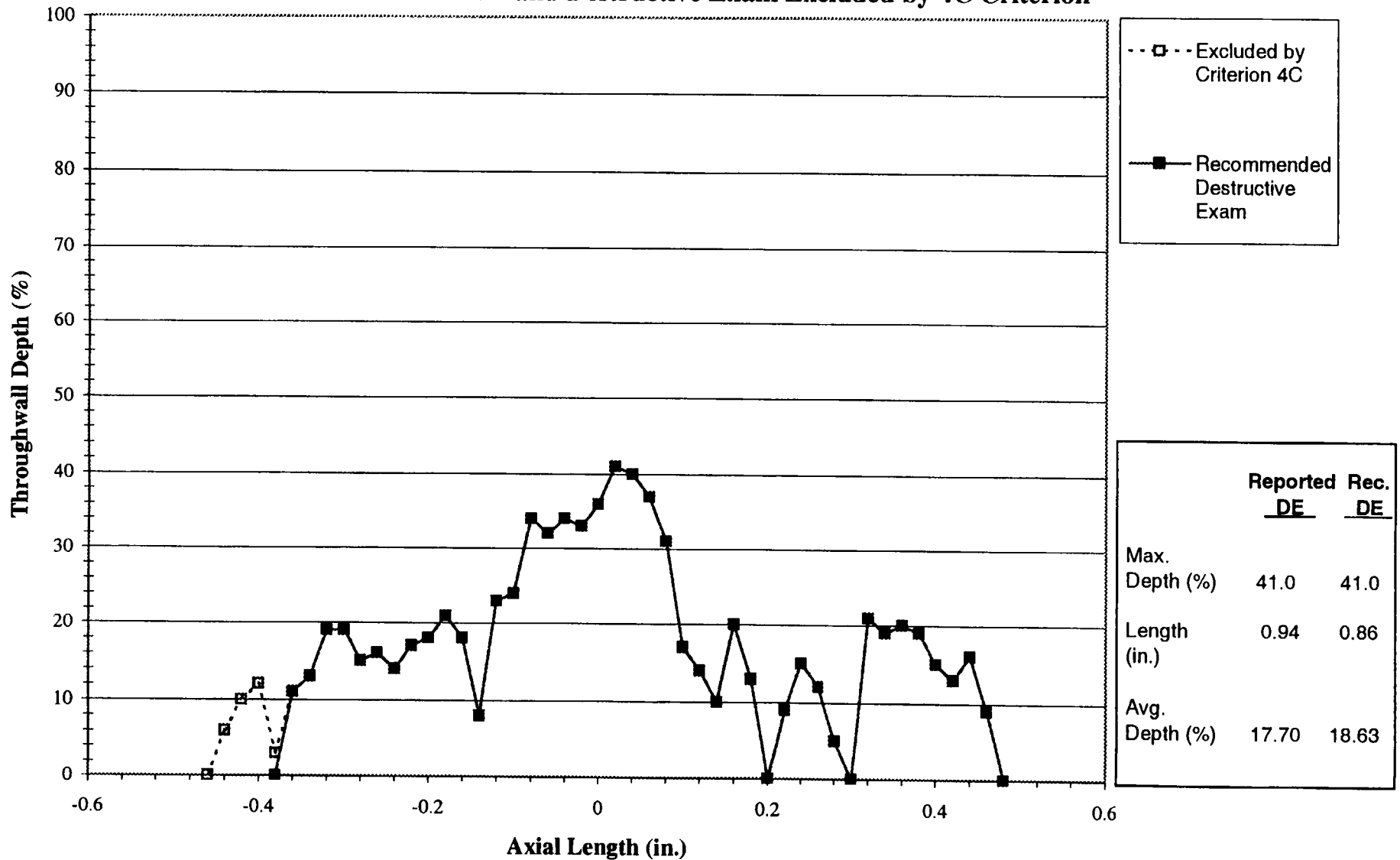
Figure C-6
Sample 6, TSP 2H - Crack 1
Mid-Range +Point, 300 kHz
Recommended Destructive Exam and Destructive Exam Excluded by 4C Criterion

Legend:
- - - □ - - Excluded by Criterion 4C
- ■ Recommended Destructive Exam
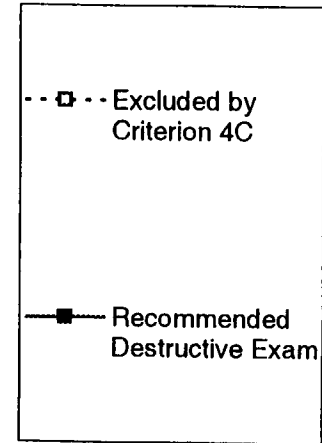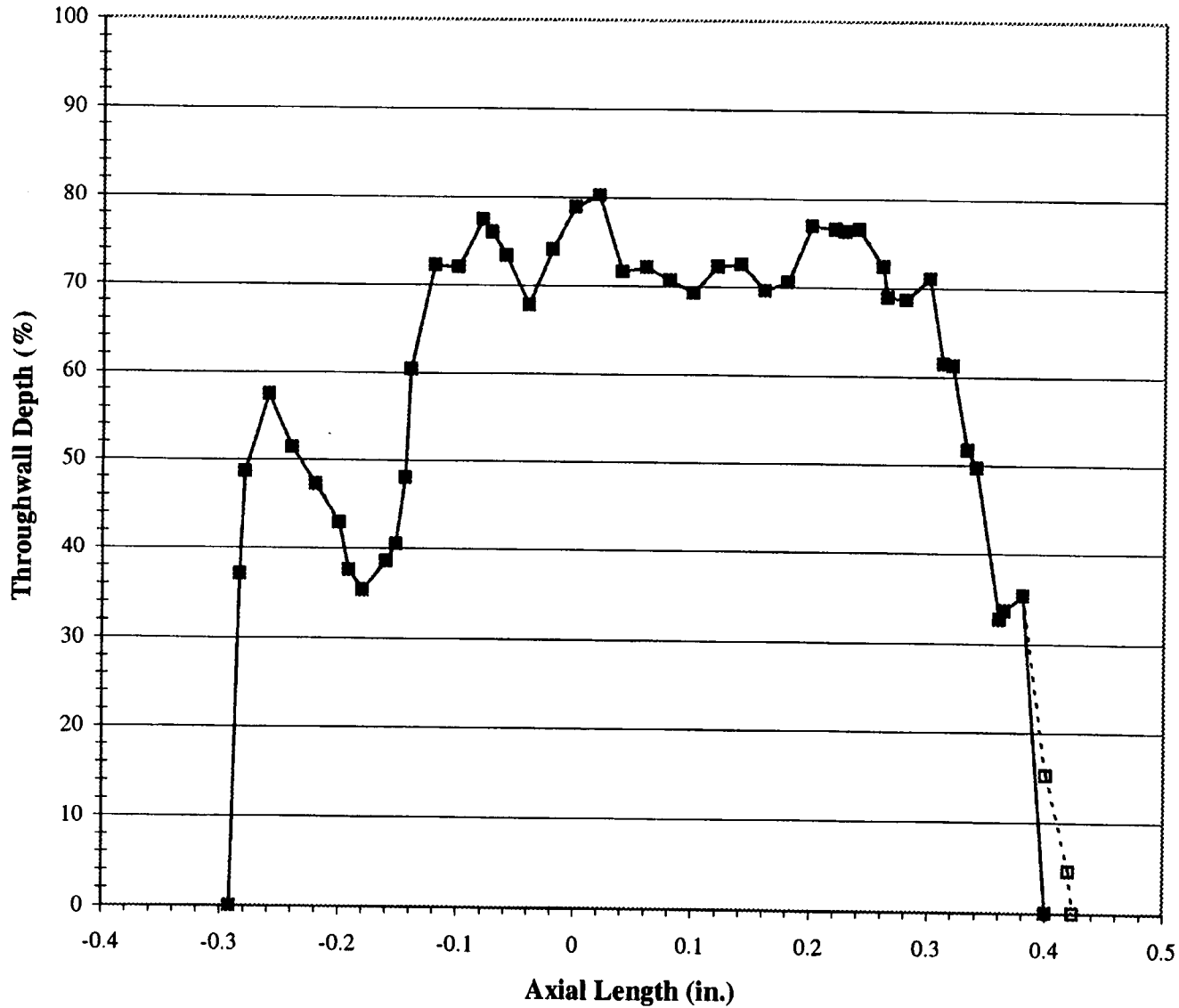
	Reported DE	Rec. DE
Max. Depth (%)	00.0	00.0
Max. Depth w/o RA(%)	80.2	80.2
Length (in.)	0.716	0.692
Avg. Depth (%)	60.52	62.10

Figure C-7
Sample 7, TSP 1H - Crack 1
Mid-Range +Point, 300 kHz
Recommended Destructive Exam and Destructive Exam Excluded by 4C Criterion

	Reported DE	Rec. DE
Max. Depth (%)	00.0	00.0
Max. Depth w/o RA(%)	39.5	39.5
Length (in.)	0.792	0.598
Avg. Depth (%)	17.99	21.53

Legend: · · ▢ · · Excluded by Criterion 4C; ■ Recommended Destructive Exam

Figure C-8
Sample 7, TSP 3H - Crack 1
Mid-Range +Point, 300 kHz
Recommended Destructive Exam and Destructive Exam Excluded by 4C Criterion

	Reported DE	Rec. DE
Max. Depth (%)	00.0	00.0
Max. Depth w/o RA(%)	45.5	45.5
Length (in.)	0.990	0.560
Avg. Depth (%)	16.29	25.18

Legend: Excluded by Criterion 4C; Recommended Destructive Exam

Figure C-9
Sample 8, TSP 2H - Crack 1
Mid-Range +Point, 300 kHz
Recommended Destructive Exam and Destructive Exam Excluded by 4C Criterion

Legend:
- Excluded by Criterion 4C
- Recommended Destructive Exam

	Reported DE	Rec. DE
Max. Depth (%)	00.0	00.0
Max. Depth w/o RA (%)	54.7	54.7
Length (in.)	0.472	0.380
Avg. Depth (%)	33.45	39.04

Figure C-10
Sample 9, TSP 2H - Crack 2
Depth vs. Axial Length
Recommended Destructive Exam and Destructive Exam Excluded by 4C Criterion

	Reported DE	Rec. DE
Max. Depth (%)	61.53	61.53
Length (in.)	0.838	0.786
Avg. Depth (%)	36.26	38.59

Legend: · · □ · · Excluded by Criterion 4C; ━■━ Recommended Destructive Exam

Y-axis: Throughwall Depth (%)
X-axis: Axial Length (in.)

Figure C-11
Sample 9, TSP 3H - Crack 1
Depth vs. Axial Length
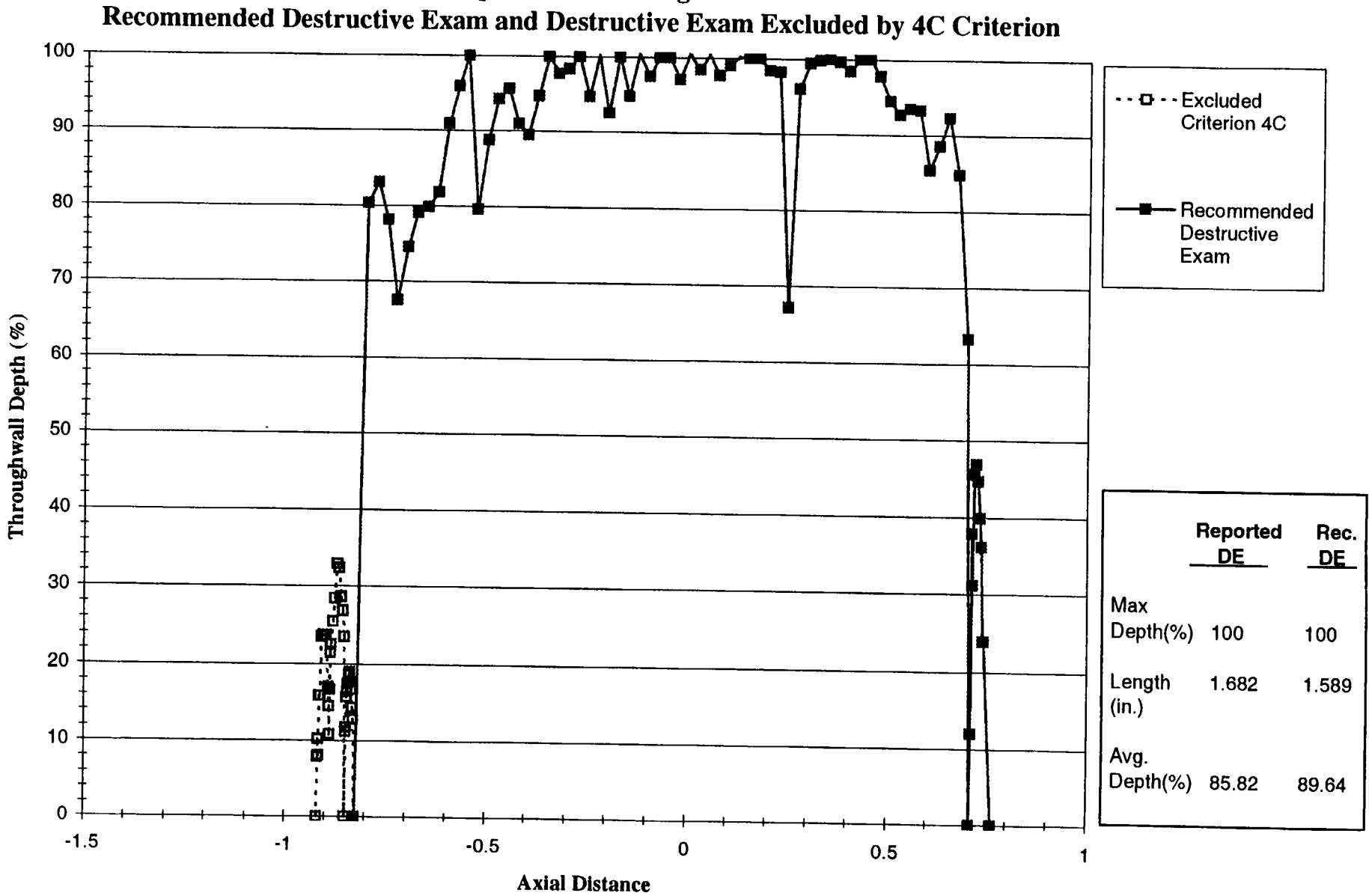**Recommended Destructive Exam and Destructive Exam Excluded by 4C Criterion**

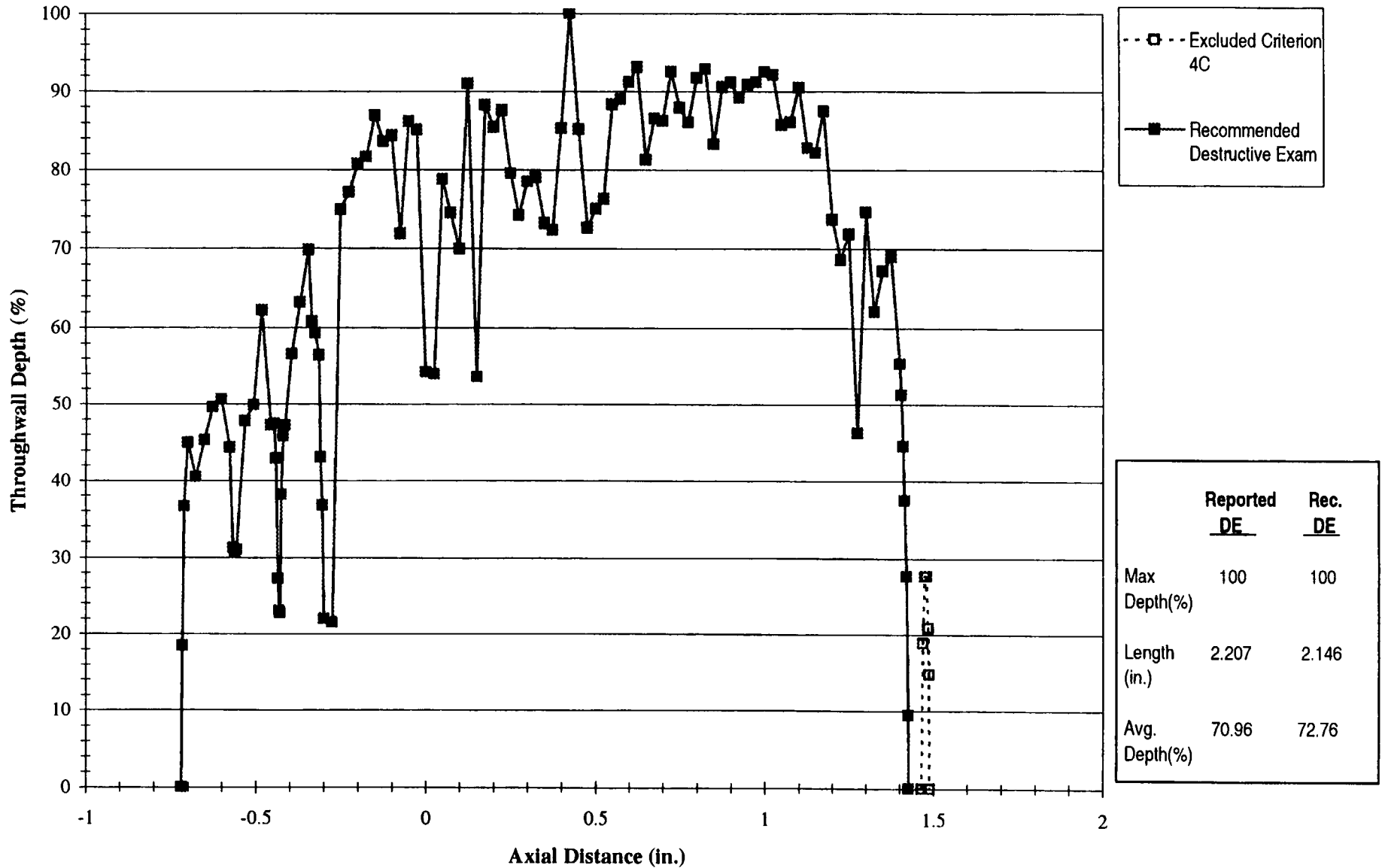|	Reported DE	Rec. DE
Max. Depth (%)	89.45	89.01
Length (in.)	0.894	0.850
Avg. Depth (%)	61.60	64.49
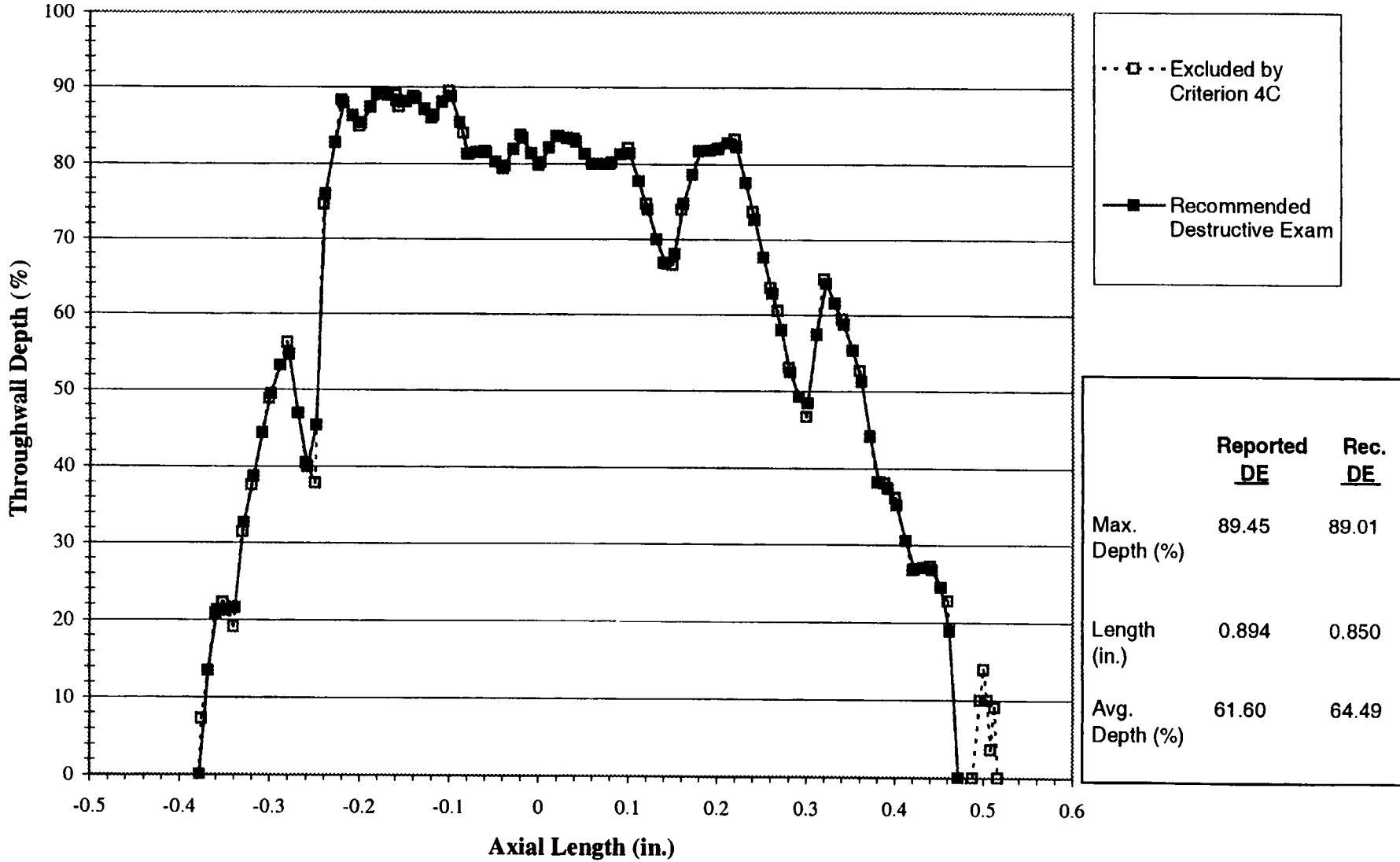
Figure C-12
Sample 9, TSP 3H - Crack 2
Depth vs. Axial Length
Recommended Destructive Exam and Destructive Exam Excluded by 4C Criterion
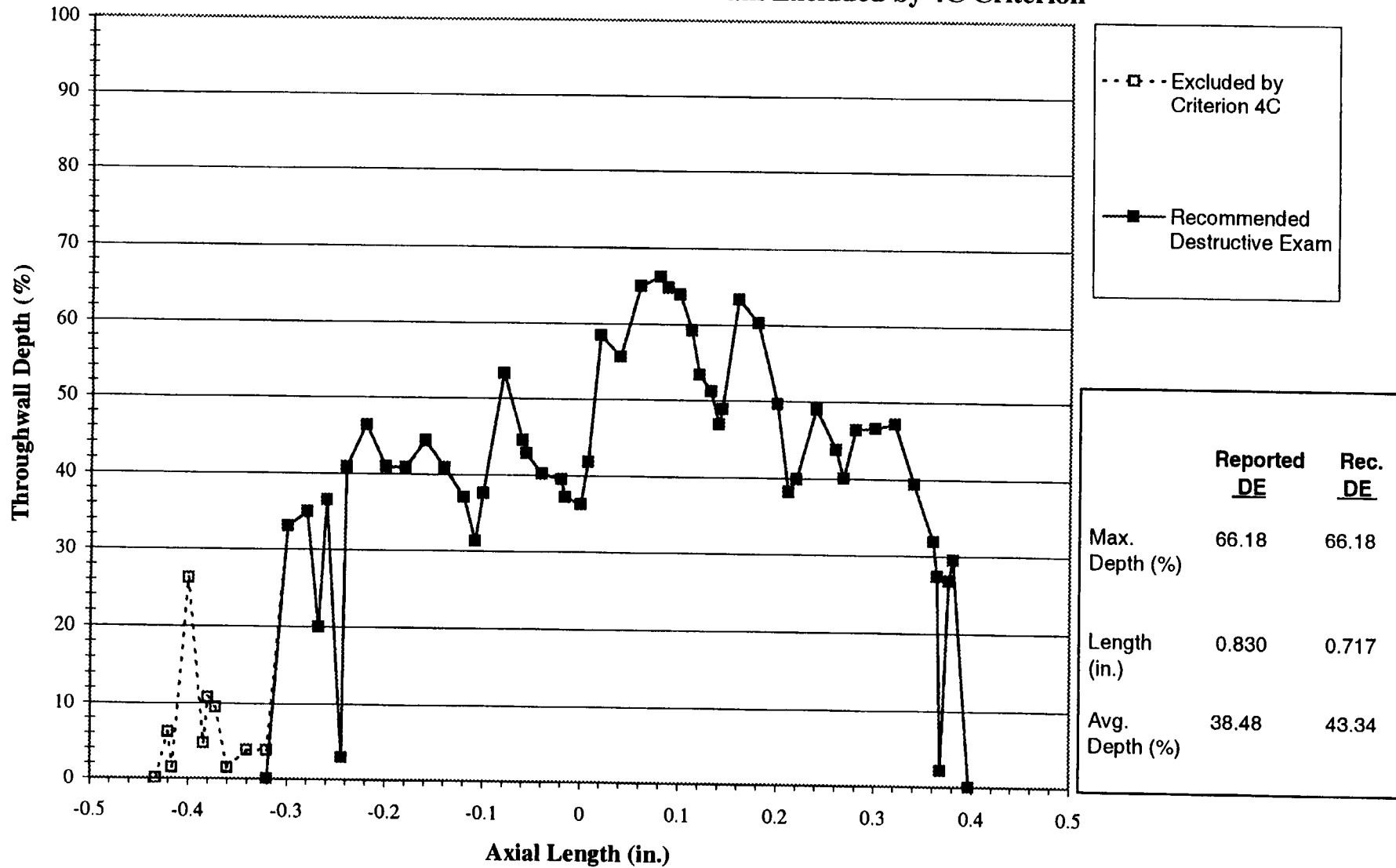
	Reported DE	Rec. DE
Max. Depth (%)	66.18	66.18
Length (in.)	0.830	0.717
Avg. Depth (%)	38.48	43.34

Legend:
- ⊡ Excluded by Criterion 4C
- ■ Recommended Destructive Exam

Throughwall Depth (%) vs. Axial Length (in.)

Figure C-13
Sample 9, TSP 5H - Crack 1
Depth vs. Axial Length
## Recommended Destructive Exam and Destructive Exam Excluded by 4C Criterion
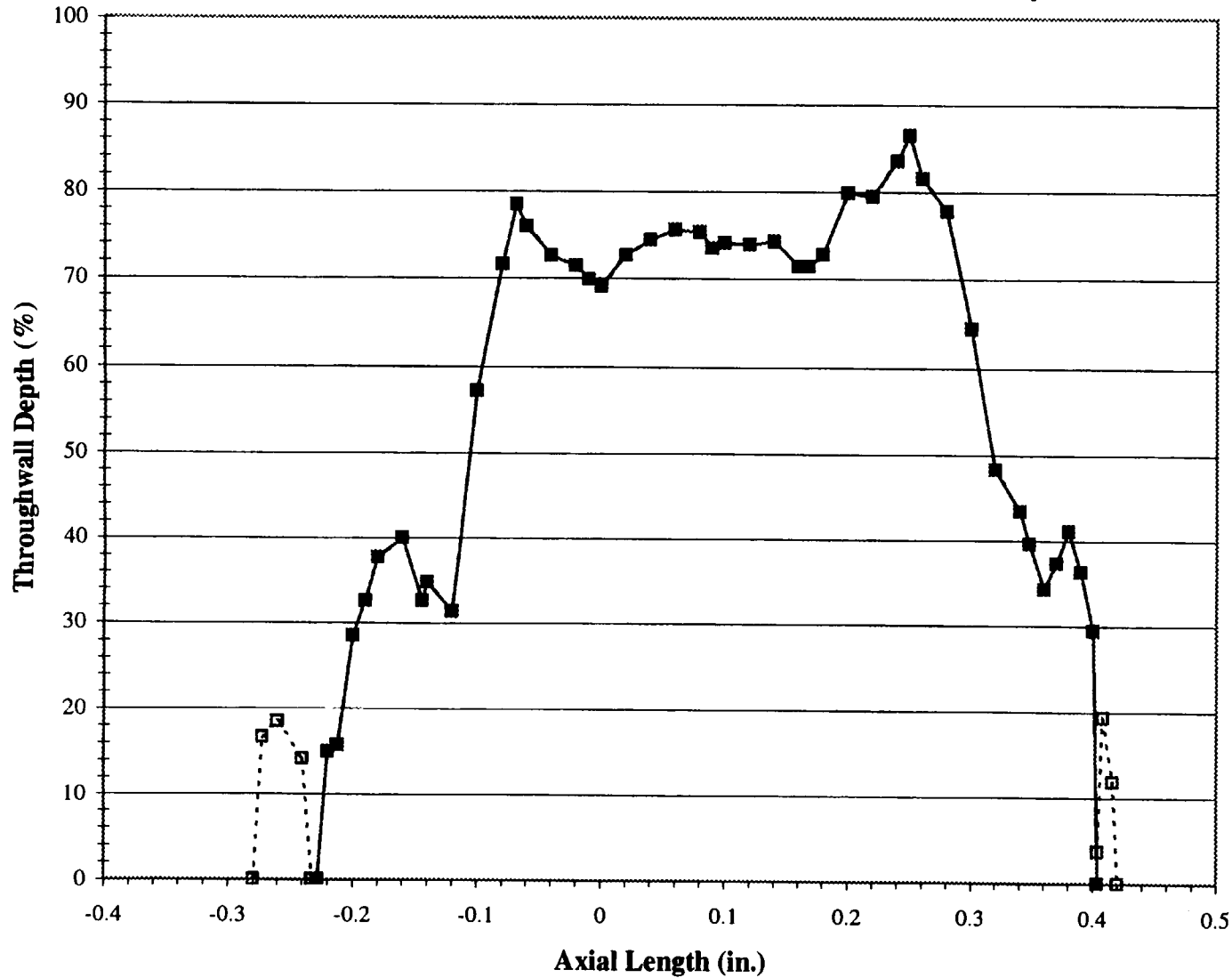
	Reported DE	Rec. DE
Max. Depth (%)	86.47	86.47
Length (in.)	0.700	0.632
Avg. Depth (%)	55.97	60.62

Legend:
- - ▫ - - Excluded by Criterion 4C
━■━ Recommended Destructive Exam

Figure C-14
Sample 11, TSP 3H - Crack 1
Depth vs. Axial Length
Recommended Destructive Exam and Destructive Exam Excluded by 4C Criterion

	Reported DE	Rec. DE
Max. Depth (%)	92.15	92.15
Length (in.)	1.116	1.072
Avg. Depth (%)	71.39	73.93

Legend:
- ··❑·· Excluded by Criterion 4C
- ■ Recommended Destructive Exam

Figure C-15
Sample 11, TSP 3H - Crack 2
Depth vs. Axial Length
Recommended Destructive Exam and Destructive Exam Excluded by 4C Criterion

	Reported DE	Rec. DE
Max. Depth (%)	55.35	55.35
Length (in.)	0.990	0.563
Avg. Depth (%)	29.61	38.56
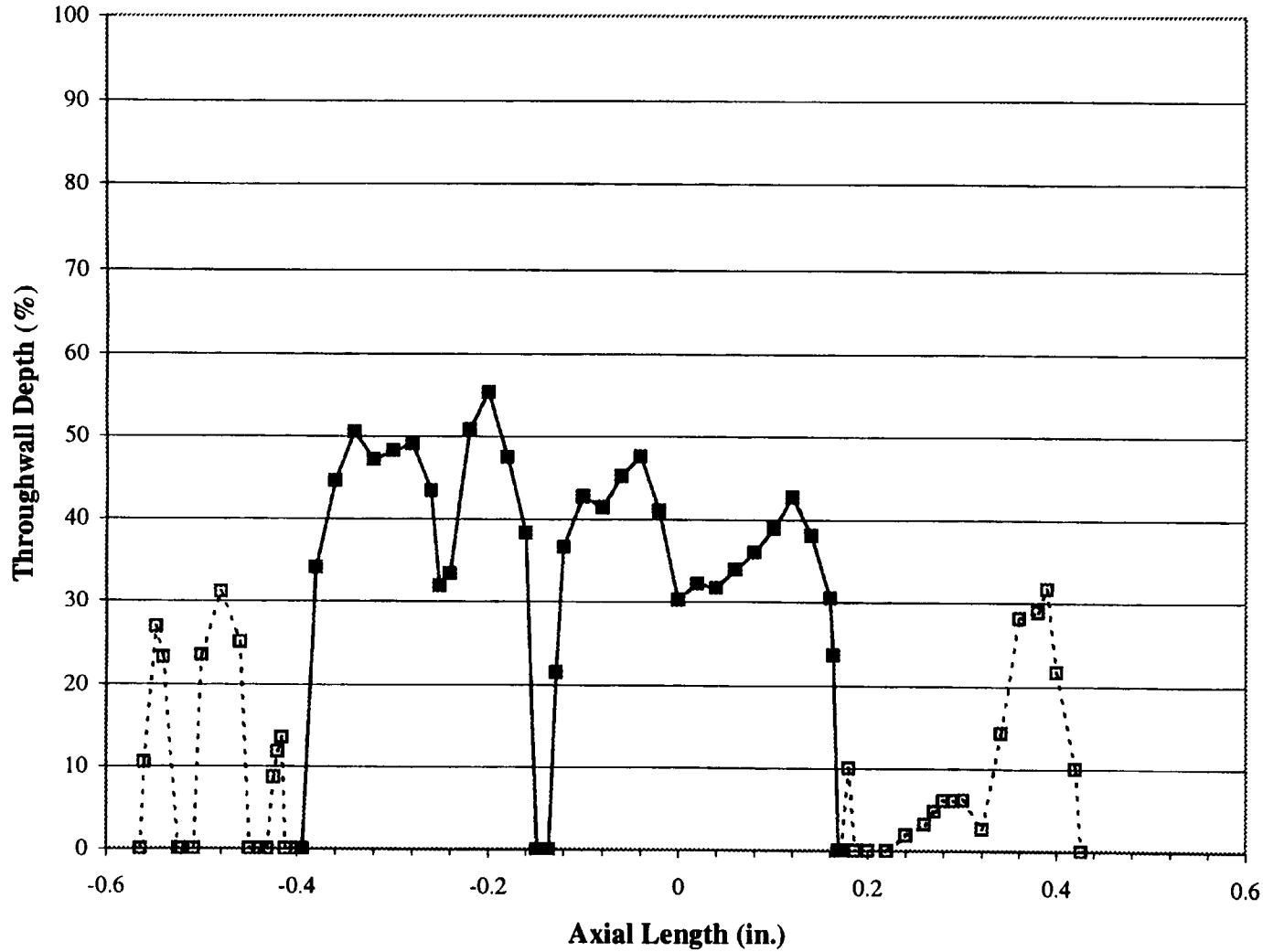
Legend:
- - ◻ - - Excluded by Criteion 4C
——■—— Recommended Destructive Exam

Figure C-16
Sample 11, TSP 4H - Crack 1
Depth vs. Axial Length
Recommended Destructive Exam and Destructive Exam Excluded by 4C Criterion
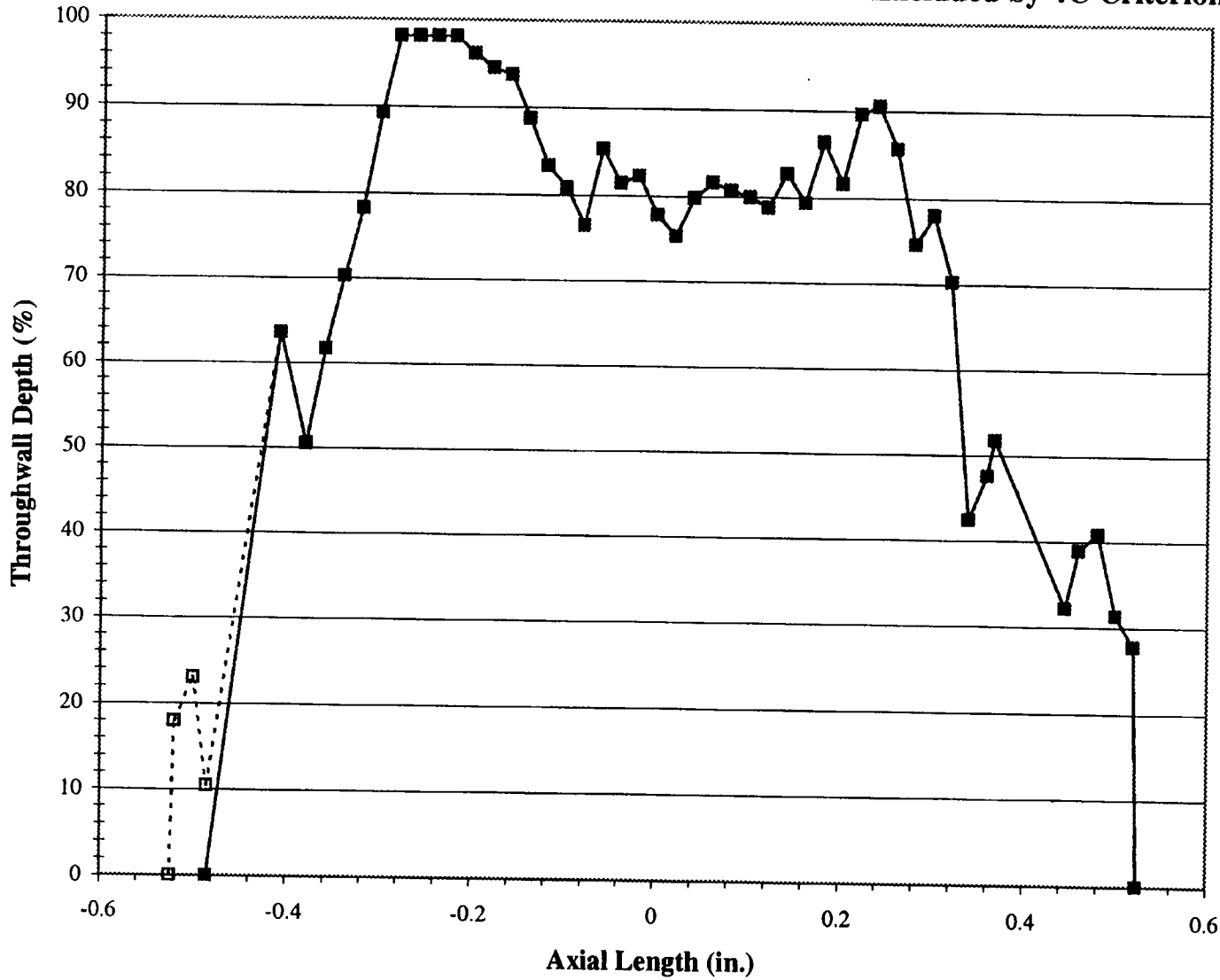
	Reported DE	Rec. DE
Max. Depth (%)	98.11	98.11
Length (in.)	1.048	1.009
Avg. Depth (%)	68.58	70.14

Figure C-17
Sample 12, TSP 4H
Depth vs. Axial Length
Recommended Destructive Exam and Destructive Exam Excluded by 4C Criterion

	Reported DE	Rec. DE
Max. Depth (%)	33.0	33.0
Length (in.)	0.53	0.36
Avg. Depth (%)	15.32	20.33

Legend: Excluded by Criterion 4C; Recommended Destructive Exam
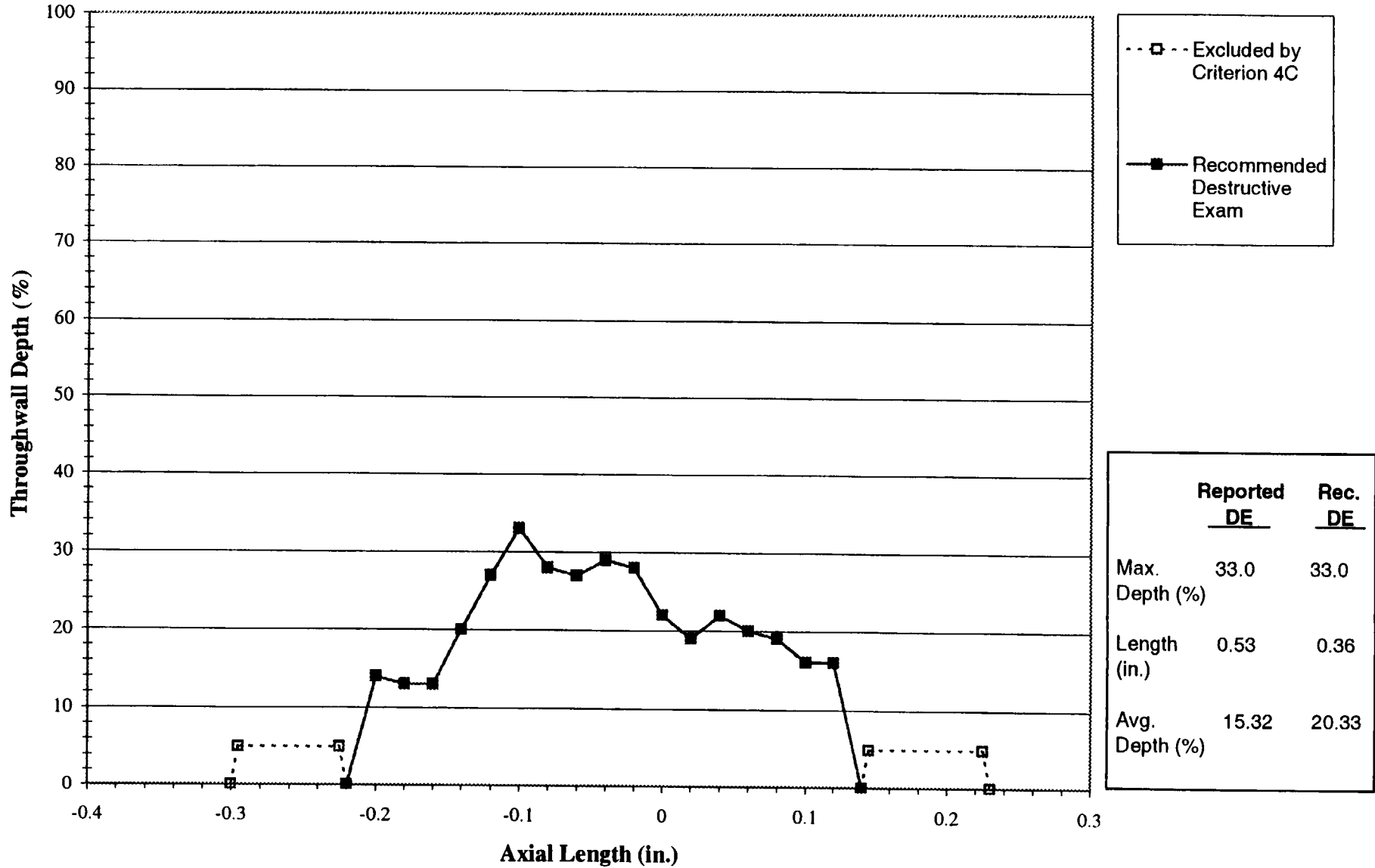
Figure C-18
Sample P9 - Crack 2
Depth vs. Axial Length
Recommended Destructive Exam and Destructive Exam Excluded by 4C Criterion

	Reported DE	Rec. DE
Max Depth(%)	100	100
Length (in.)	1.682	1.589
Avg. Depth(%)	85.82	89.64

Figure C-19
Sample P10 - Crack 2
Depth vs. Axial Length
Recommended Destructive Exam and Destructive Exam Excluded by 4C Criterion

	Reported DE	Rec. DE
Max Depth(%)	100	100
Length (in.)	2.207	2.146
Avg. Depth(%)	70.96	72.76

Legend:
- Excluded Criterion 4C
- Recommended Destructive Exam

Axis labels: Throughwall Depth (%) vs. Axial Distance (in.)

APPENDIX D

Plots of NDE Performance Test Analyses
for +Point Coil Depth Profiles with Destructive Exam Data

Figure D-1
Specimen R 1 - C 85 - 01H - Crack 1 - Year 1998
Comparison of Unadjusted, Adjusted, Burst and Voltage with Exam
NDE Depth vs. Axial Length

PWSCC ARC Release 1.1
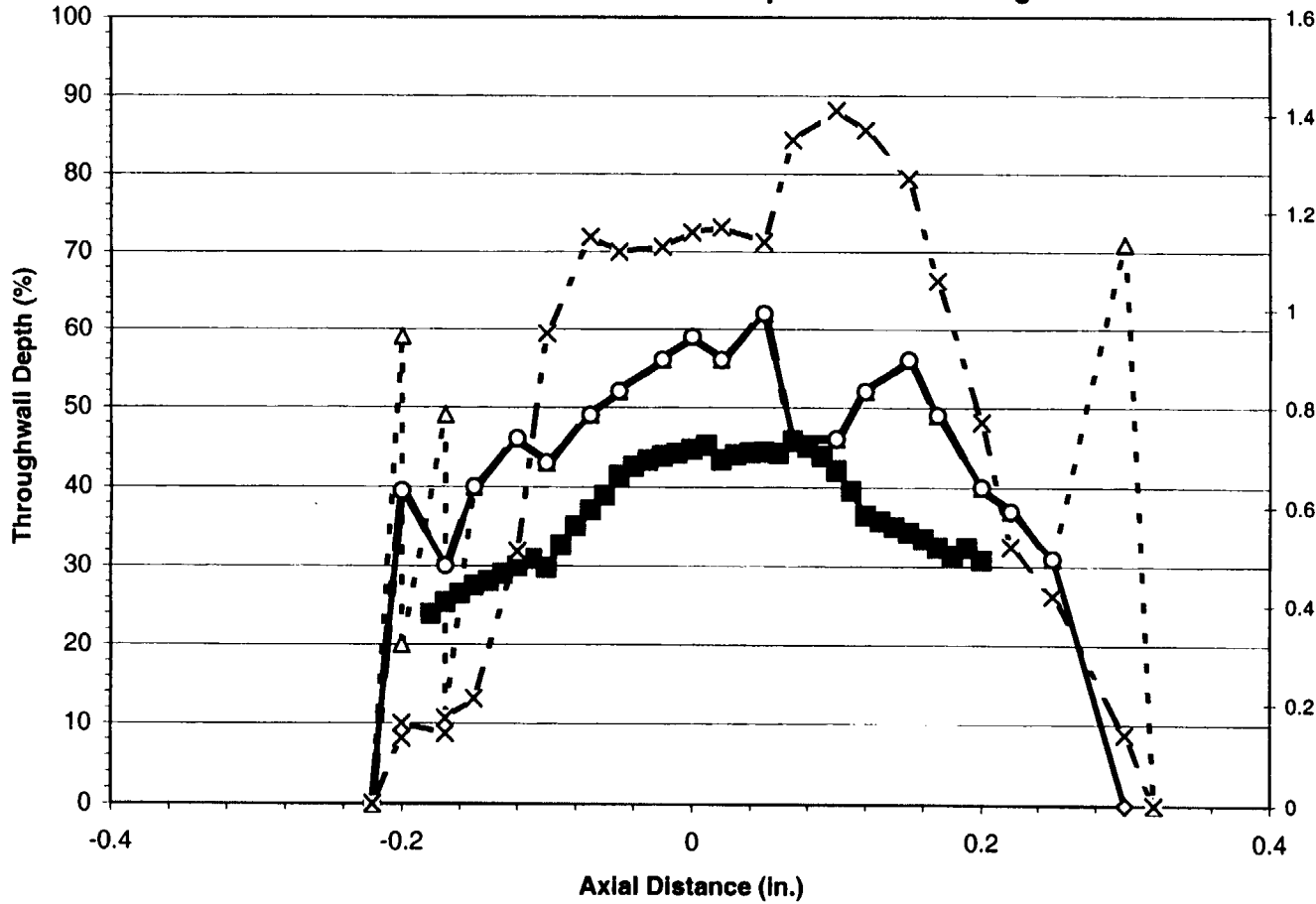
Unadjusted		
	T9093	Exam
Length	0.54	0.38
Max. Volts	1.41	
Max. Depth (%)	71.0	45.8
Avg. Depth (%)	46.1	37.1

Adjusted		
	T9093	Exam
Length	0.52	0.38
Max. Volts	1.41	
Max. Depth (%)	62.0	45.8
Avg. Depth (%)	43.1	37.1

Burst		
	T9093	Exam
Length	0.47	0.38
Max. Volts	1.41	
Max. Depth (%)	62.0	45.8
Avg. Depth (%)	46.0	37.1

Legend:
- Analyst T9093 - Unadjusted
- Analyst T9093 - Adjusted
- Analyst T9093 - Burst
- Exam
- Exam - Burst
- Analyst T9093 - Voltage

Figure D-2
Specimen R 1 - C 91 - 01H - Crack 1 - Year 1998
Comparison of Unadjusted, Adjusted, Burst and Voltage with Exam
NDE Depth vs. Axial Length

PWSCC ARC Release 1.1
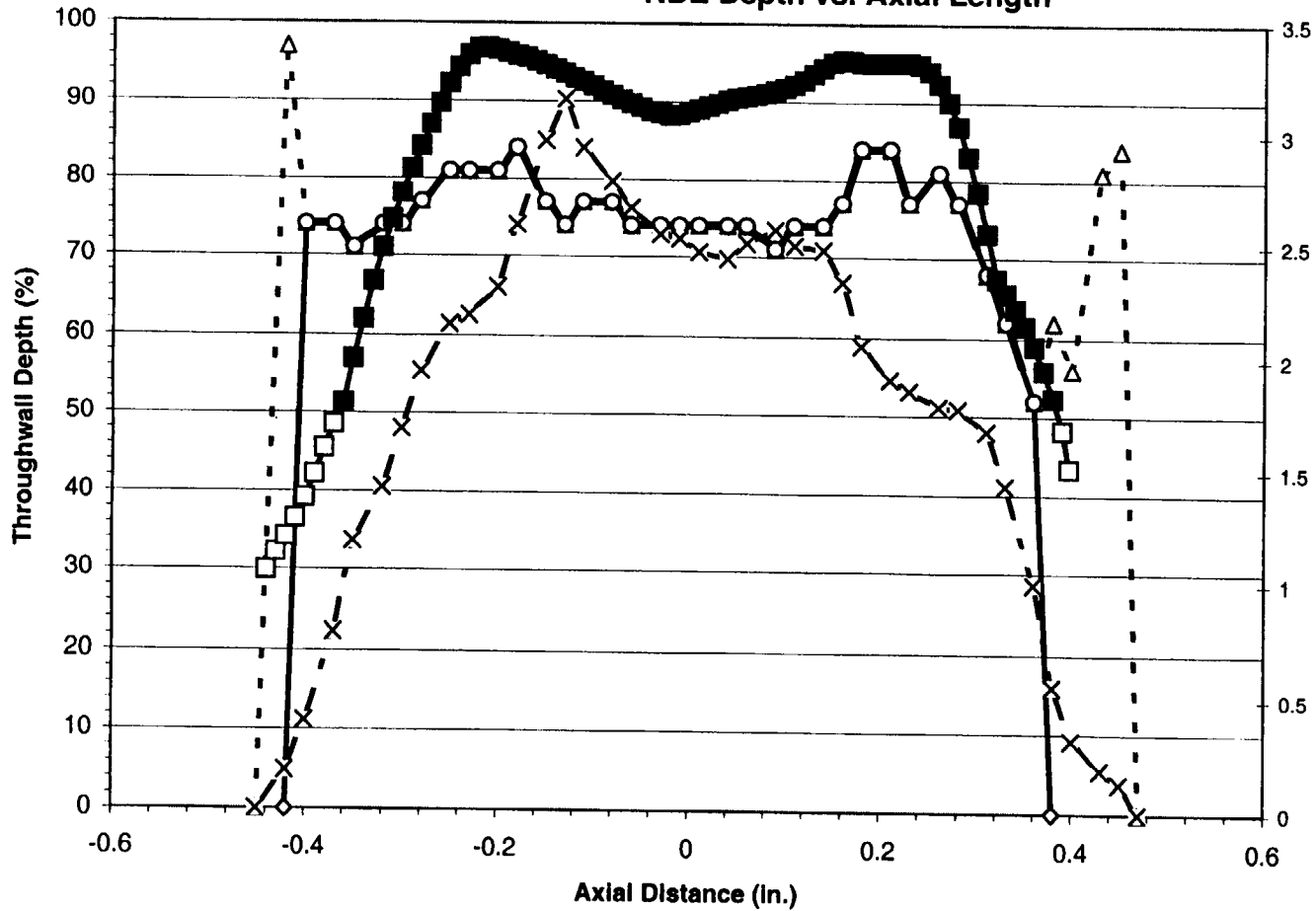
Unadjusted		
	T9093	Exam
Length	0.92	0.84
Max. Volts	3.16	
Max. Depth (%)	97.0	96.8
Avg. Depth (%)	73.2	81.4

Adjusted		
	T9093	Exam
Length	0.80	0.84
Max. Volts	3.16	
Max. Depth (%)	84.0	96.8
Avg. Depth (%)	73.2	81.4

Burst		
	T9093	Exam
Length	0.76	0.74
Max. Volts	3.16	
Max. Depth (%)	84.0	96.8
Avg. Depth (%)	75.4	86.6

Legend:
- △ - Analyst T9093 - Unadjusted —◇— Analyst T9093 - Adjusted ═O Analyst T9093 - Burst
—□— Exam ■ Exam - Burst —X— Analyst T9093 - Voltage

Figure D-3
Specimen R 1 - C 91 - 01H - Crack 2 - Year 1998
Comparison of Unadjusted, Adjusted, Burst and Voltage with Exam
NDE Depth vs. Axial Length

PWSCC ARC Release 1.1
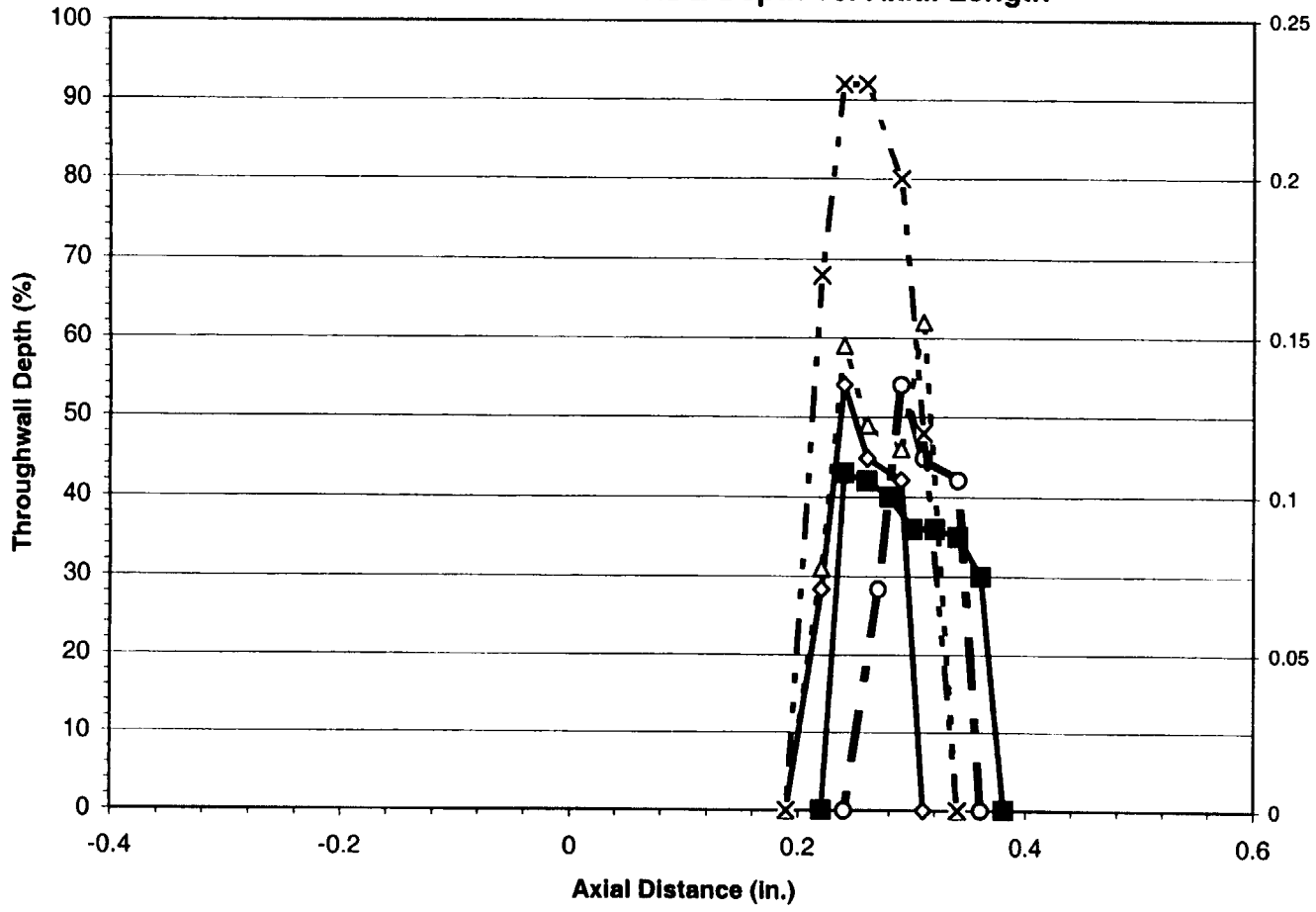
Unadjusted		
	T9093	Exam
Length	0.15	0.16
Max. Volts	0.23	
Max. Depth (%)	62.0	43.0
Avg. Depth (%)	39.2	32.8

Adjusted		
	T9093	Exam
Length	0.12	0.16
Max. Volts	0.23	
Max. Depth (%)	54.0	43.0
Avg. Depth (%)	33.0	32.8

Burst		
	T9093	Exam
Length	0.12	0.16
Max. Volts	0.23	
Max. Depth (%)	54.0	43.0
Avg. Depth (%)	33.0	32.8

- ⌀ - Analyst T9093 - Unadjusted ◇ Analyst T9093 - Adjusted ○ ·Analyst T9093 - Burst
□ Exam ■· ·Exam - Burst ✕· ·Analyst T9093 - Voltage

Figure D-4
Specimen R 2 - C 66 - 01H - Crack 1 - Year 1998
Comparison of Unadjusted, Adjusted, Burst and Voltage with Exam
NDE Depth vs. Axial Length

PWSCC ARC Release 1.1
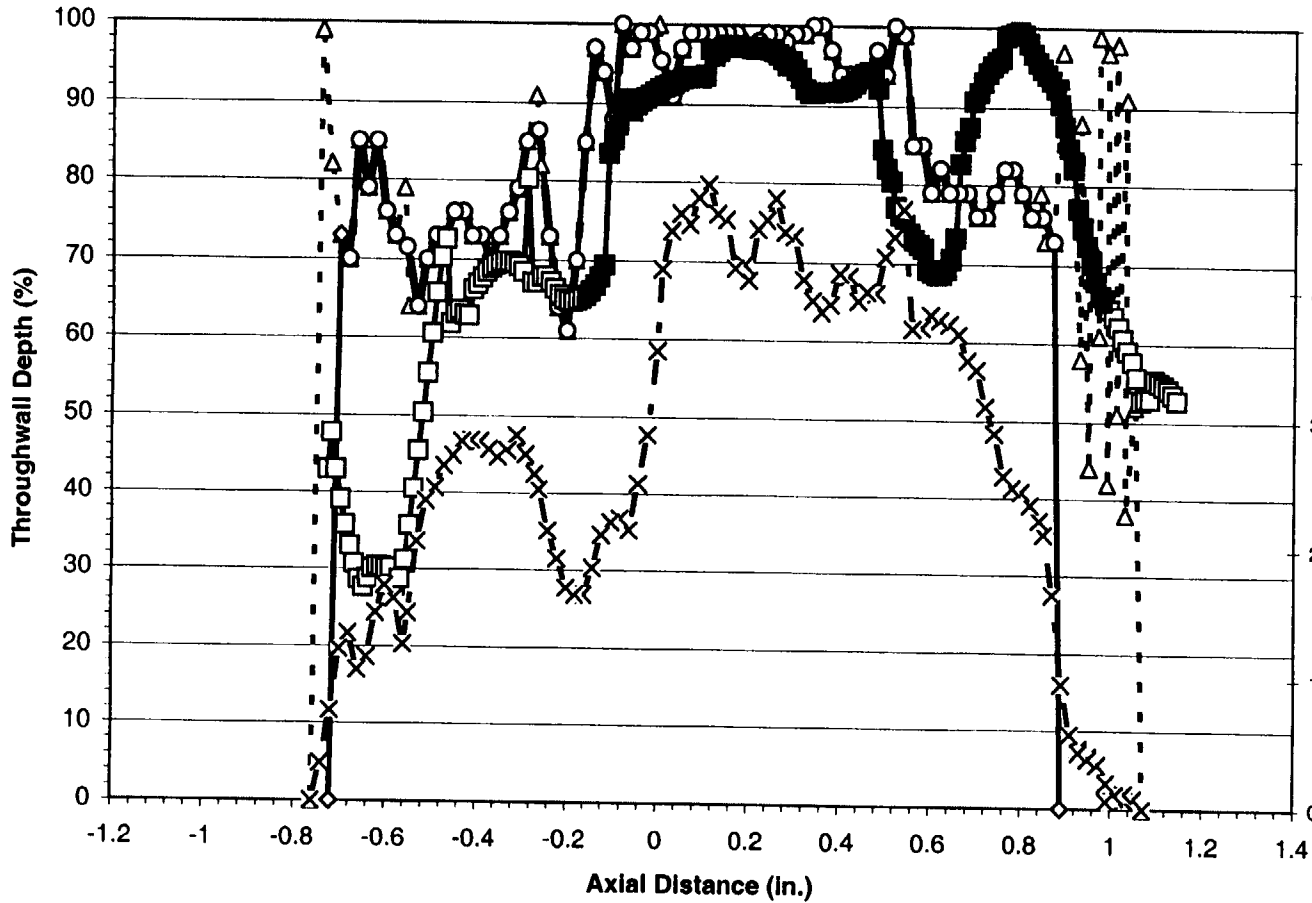
Unadjusted		
	T9093	Exam
Length	1.83	1.87
Max. Volts	4.78	
Max. Depth (%)	100.0	99.5
Avg. Depth (%)	83.4	75.3

Adjusted		
	T9093	Exam
Length	1.61	1.87
Max. Volts	4.78	
Max. Depth (%)	100.0	99.5
Avg. Depth (%)	84.4	75.3

Burst		
	T9093	Exam
Length	1.55	1.14
Max. Volts	4.78	
Max. Depth (%)	100.0	99.5
Avg. Depth (%)	85.8	88.0

Legend:
- ◁ - Analyst T9093 - Unadjusted
- ◇ - Analyst T9093 - Adjusted
- O Analyst T9093 - Burst
- □ Exam
- ■ Exam - Burst
- X Analyst T9093 - Voltage

Figure D-5
Specimen R 2 - C 66 - 01H - Crack 2 - Year 1998
Comparison of Unadjusted, Adjusted, Burst and Voltage with Exam
NDE Depth vs. Axial Length

PWSCC ARC Release 1.1
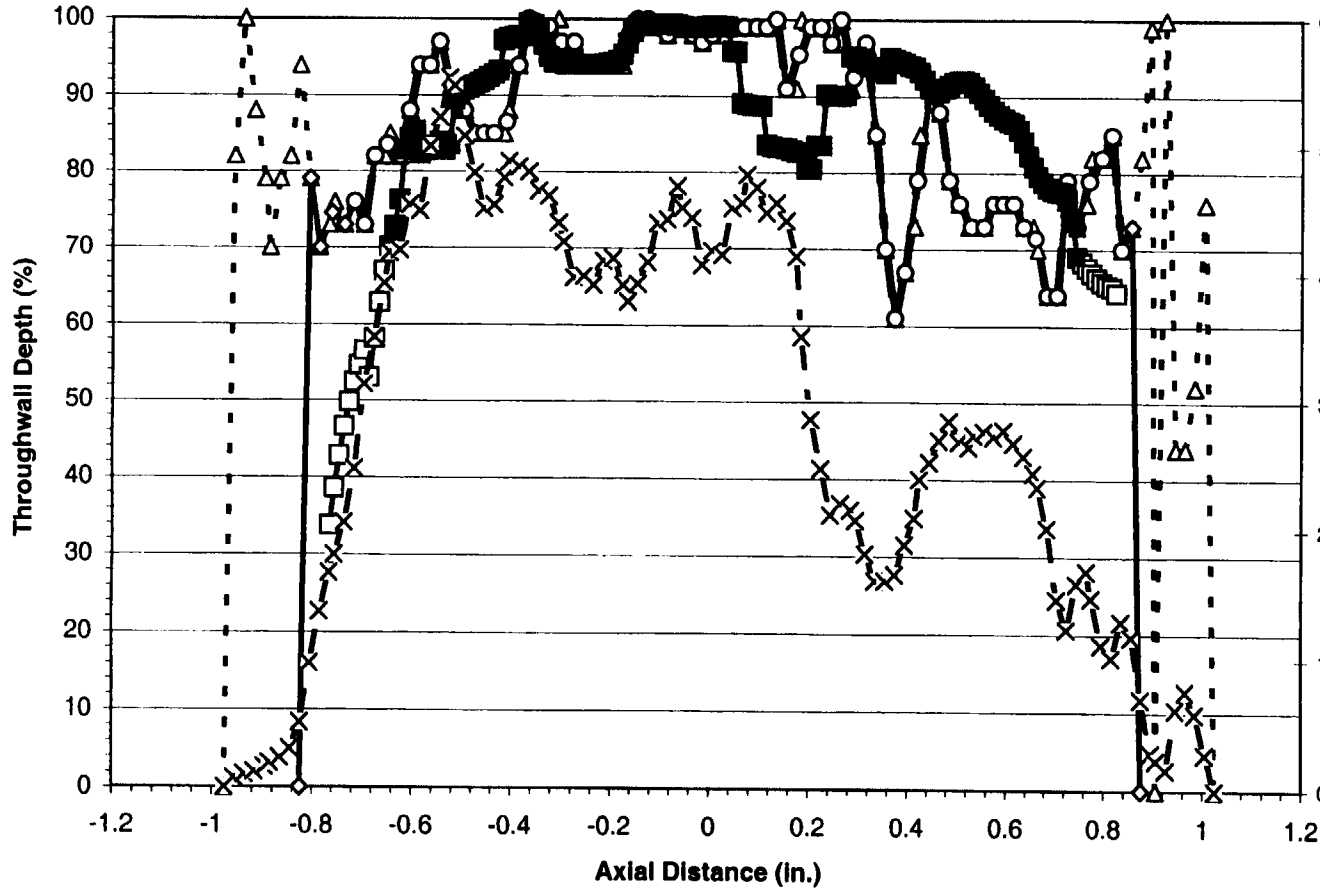
Unadjusted

	T9093	Exam
Length	2.00	1.59
Max. Volts	5.54	
Max. Depth (%)	100.0	99.4
Avg. Depth (%)	84.0	86.6

Adjusted

	T9093	Exam
Length	1.70	1.59
Max. Volts	5.51	
Max. Depth (%)	100.0	99.4
Avg. Depth (%)	85.8	86.6

Burst

	T9093	Exam
Length	1.55	1.39
Max. Volts	5.51	
Max. Depth (%)	100.0	99.4
Avg. Depth (%)	87.9	90.6

Legend: Analyst T9093 - Unadjusted; Analyst T9093 - Adjusted; Analyst T9093 - Burst; Exam; Exam - Burst; Analyst T9093 - Voltage

Figure D-6
Specimen R 5 - C 18 - 01H - Crack 1 - Year 1998
Comparison of Unadjusted, Adjusted, Burst and Voltage with Exam
NDE Depth vs. Axial Length

PWSCC ARC Release 1.1
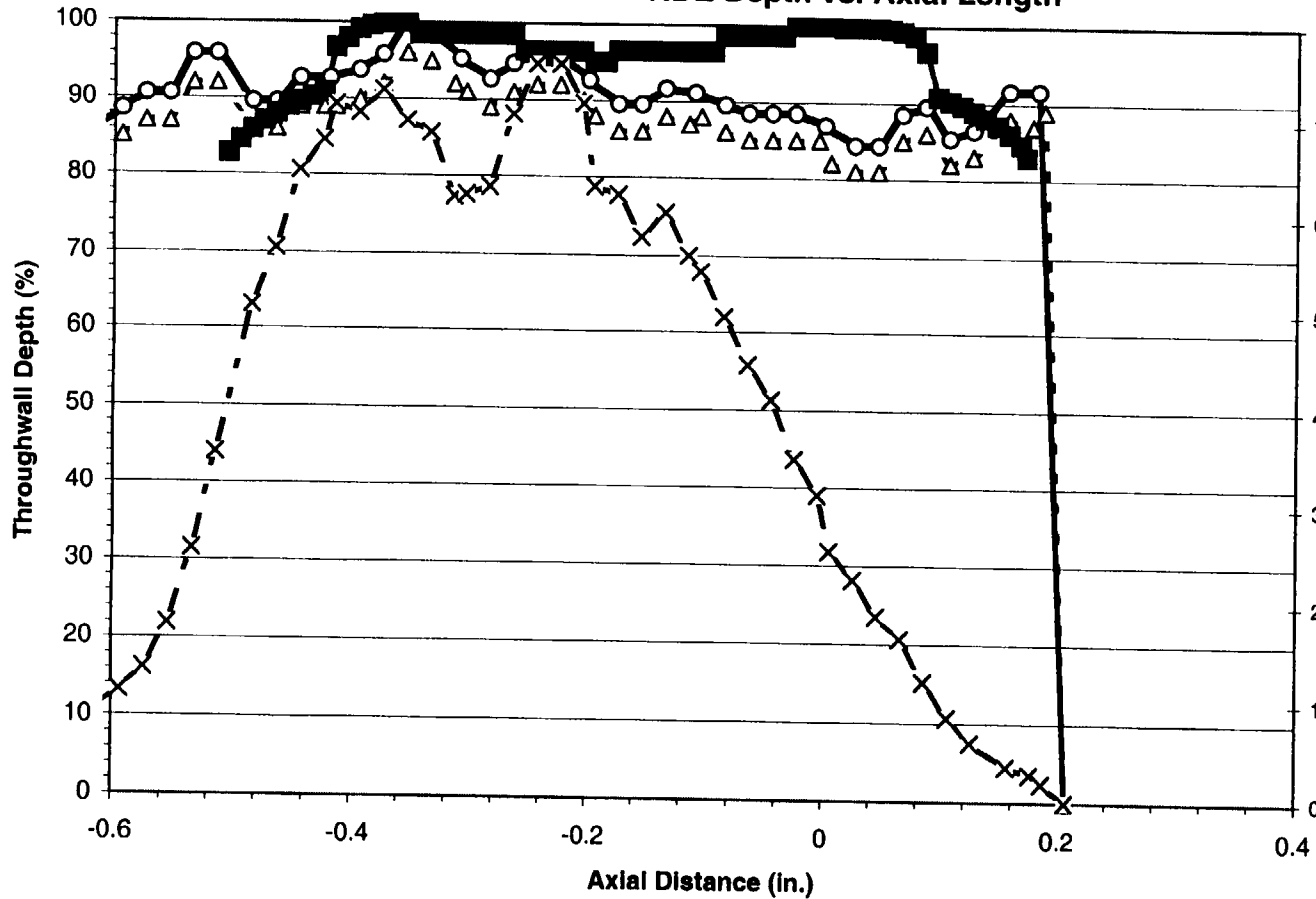
Unadjusted		
	T9093	Exam
Length	0.93	0.68
Max. Volts	7.58	
Max. Depth (%)	96.0	100.0
Avg. Depth (%)	83.1	95.6

Adjusted		
	T9093	Exam
Length	0.93	0.68
Max. Volts	7.58	
Max. Depth (%)	100.0	100.0
Avg. Depth (%)	86.3	95.6

Burst		
	T9093	Exam
Length	0.86	0.68
Max. Volts	7.58	
Max. Depth (%)	100.0	100.0
Avg. Depth (%)	89.7	95.6

Legend:
- ▲ - Analyst T9093 - Unadjusted ◇ Analyst T9093 - Adjusted ○ Analyst T9093 - Burst
- □ Exam ■ Exam - Burst ✕ Analyst T9093 - Voltage

Figure D-7
Specimen SG R 5 - C 18 - 01H - Crack 2 - Year 1998
Comparison of Unadjusted, Adjusted, Burst and Voltage with Exam
NDE Depth vs. Axial Length

PWSCC ARC Release 1.1
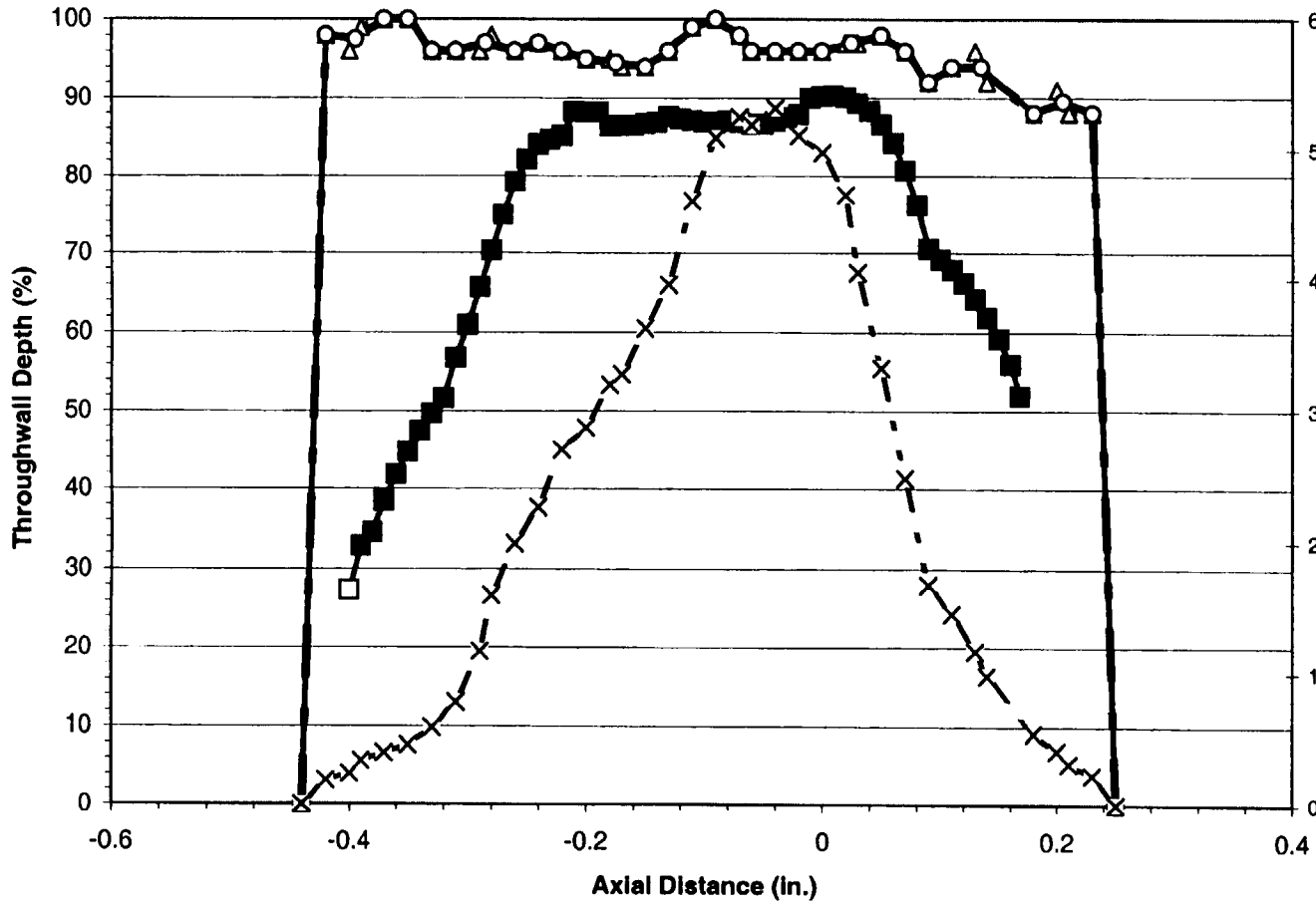
Unadjusted		
	T9093	Exam
Length	0.69	0.57
Max. Volts	5.32	
Max. Depth (%)	100.0	90.3
Avg. Depth (%)	92.7	74.6

Adjusted		
	T9093	Exam
Length	0.69	0.57
Max. Volts	5.32	
Max. Depth (%)	100.0	90.3
Avg. Depth (%)	92.7	74.6

Burst		
	T9093	Exam
Length	0.69	0.56
Max. Volts	5.32	
Max. Depth (%)	100.0	90.3
Avg. Depth (%)	92.7	75.4

Legend:
- △ - Analyst T9093 - Unadjusted
- ◇ - Analyst T9093 - Adjusted
- O - Analyst T9093 - Burst
- □ - Exam
- ■ - Exam - Burst
- X - Analyst T9093 - Voltage

Figure D-8
Specimen SG R 6 - C 24 - 01H - Crack 1 - Year 1998
Comparison of Unadjusted, Adjusted, Burst and Voltage with Exam
NDE Depth vs. Axial Length

PWSCC ARC Release 1.1
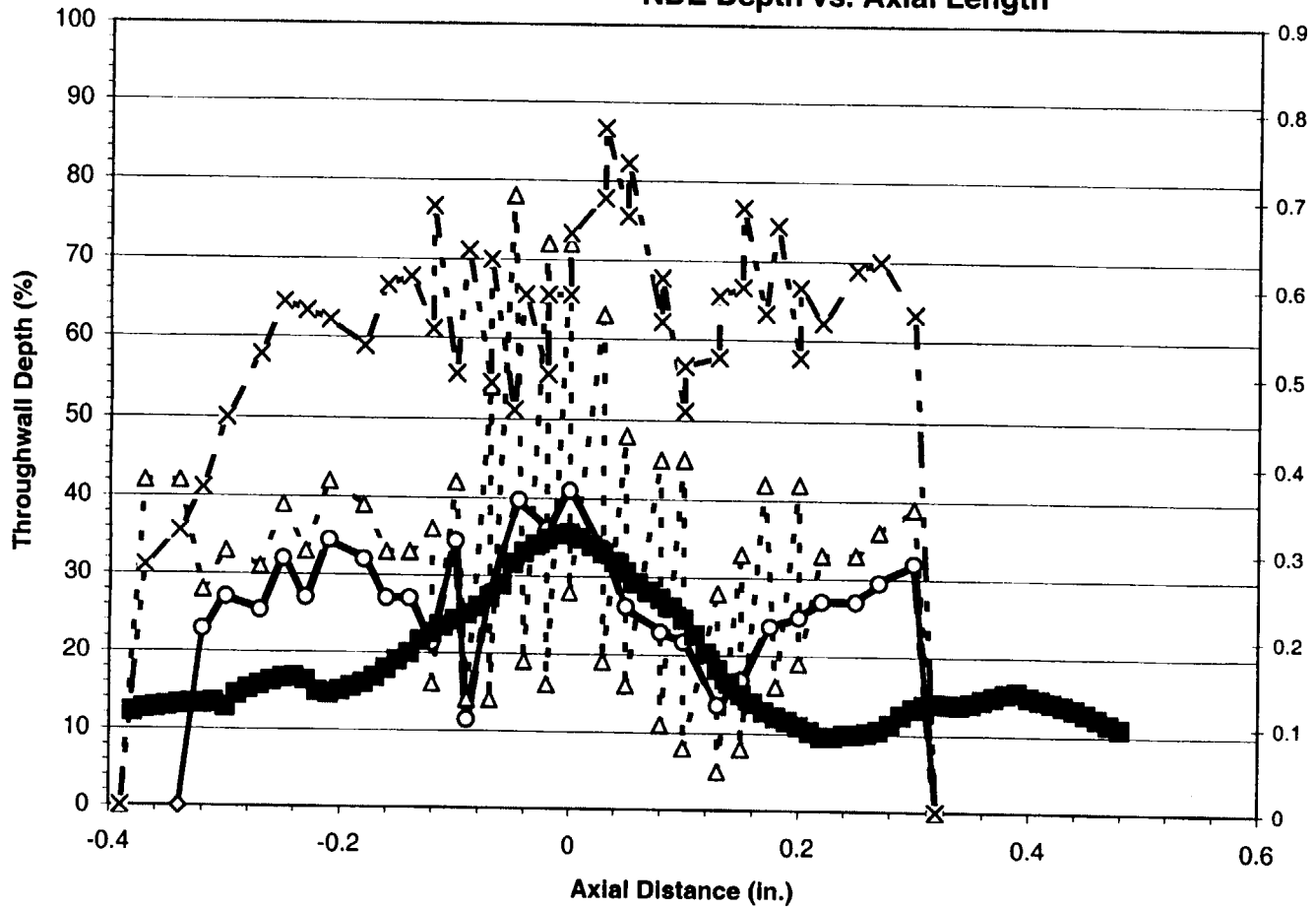
Unadjusted		
	T9093	Exam
Length	0.71	0.86
Max. Volts	0.78	
Max. Depth (%)	78.0	35.5
Avg. Depth (%)	33.4	18.3

Adjusted		
	T9093	Exam
Length	0.66	0.86
Max. Volts	0.74	
Max. Depth (%)	41.0	35.5
Avg. Depth (%)	26.7	18.3

Burst		
	T9093	Exam
Length	0.64	0.86
Max. Volts	0.74	
Max. Depth (%)	41.0	35.5
Avg. Depth (%)	27.2	18.3

Legend:
- ◬ - Analyst T9093 - Unadjusted —◇— Analyst T9093 - Adjusted —O— Analyst T9093 - Burst
—□— Exam —■- Exam - Burst —X- Analyst T9093 - Voltage

Figure D-9
Specimen R 6 - C 31 - 01H - Crack 1 - Year 1998
Comparison of Unadjusted, Adjusted, Burst and Voltage with Exam
NDE Depth vs. Axial Length

PWSCC ARC Release 1.1
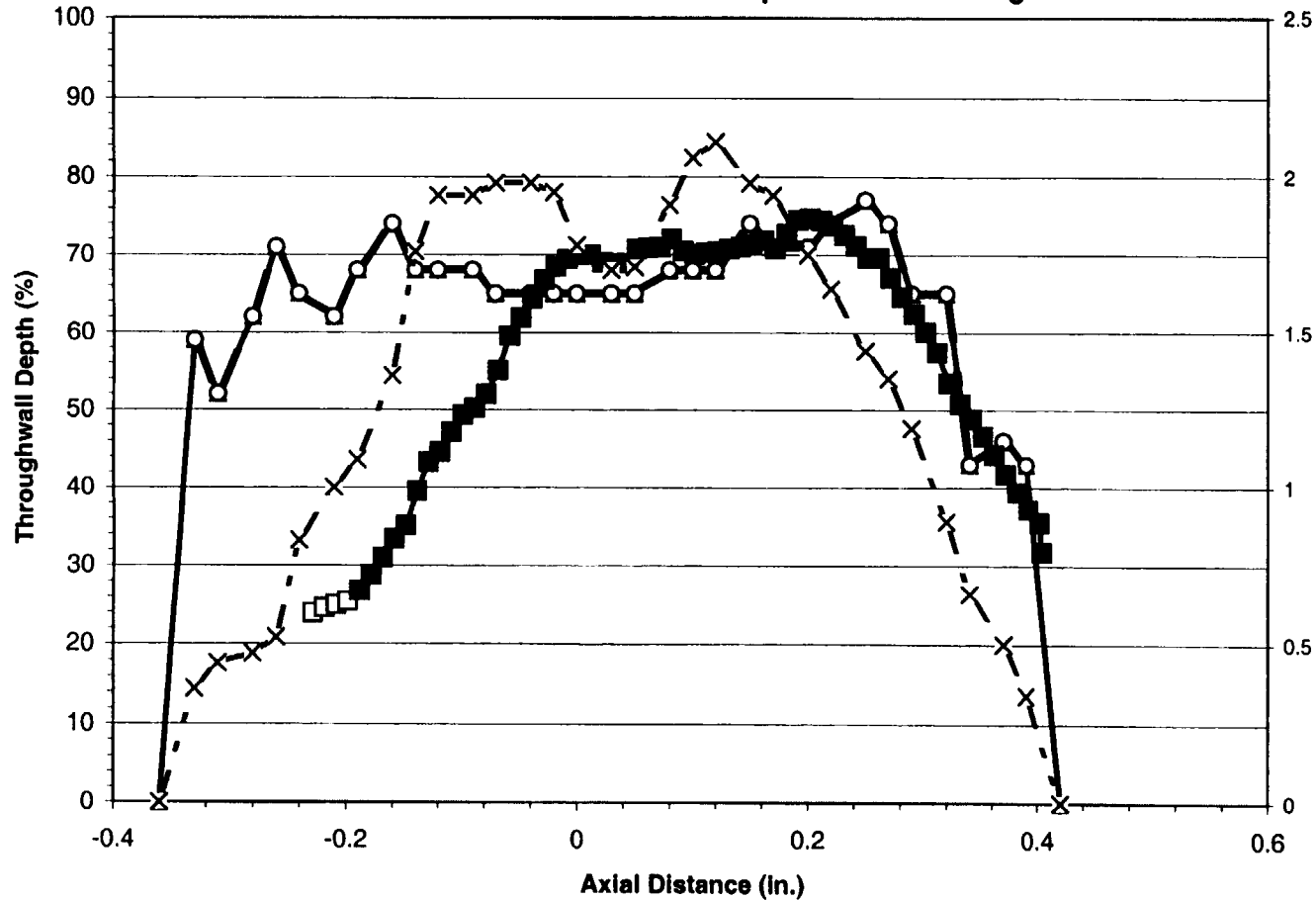
Unadjusted		
	T9093	Exam
Length	0.78	0.63
Max. Volts	2.11	
Max. Depth (%)	77.0	74.6
Avg. Depth (%)	62.3	57.5

Adjusted		
	T9093	Exam
Length	0.78	0.63
Max. Volts	2.11	
Max. Depth (%)	77.0	74.6
Avg. Depth (%)	62.3	57.5

Burst		
	T9093	Exam
Length	0.72	0.59
Max. Volts	2.11	
Max. Depth (%)	77.0	74.6
Avg. Depth (%)	65.4	59.7

Legend:
- ◬ - Analyst T9093 - Unadjusted
- ◇ Analyst T9093 - Adjusted
- ○ Analyst T9093 - Burst
- □ Exam
- ■ Exam - Burst
- ✕ Analyst T9093 - Voltage

Figure D-10
Specimen R 6 - C 31 - 01H - Crack 2 - Year 1998
Comparison of Unadjusted, Adjusted, Burst and Voltage with Exam
NDE Depth vs. Axial Length

PWSCC ARC Release 1.1
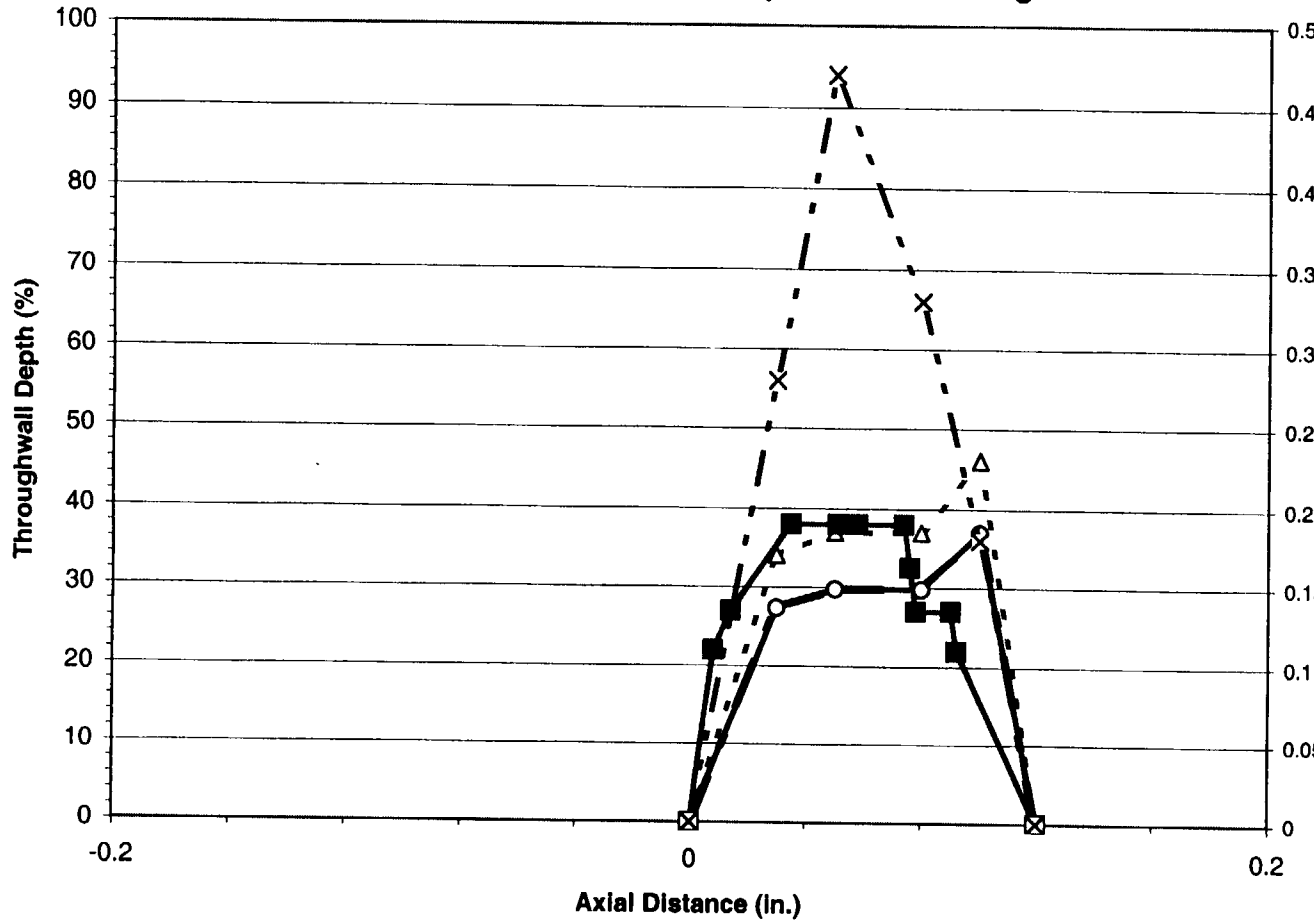
Unadjusted		
	T9093	Exam
Length	0.12	0.12
Max. Volts	0.47	
Max. Depth (%)	46.0	38.0
Avg. Depth (%)	30.2	26.8

Adjusted		
	T9093	Exam
Length	0.12	0.12
Max. Volts	0.47	
Max. Depth (%)	37.0	38.0
Avg. Depth (%)	24.3	26.8

Burst		
	T9093	Exam
Length	0.12	0.12
Max. Volts	0.47	
Max. Depth (%)	37.0	38.0
Avg. Depth (%)	24.3	26.8

- ◁ - Analyst T9093 - Unadjusted   —◇—Analyst T9093 - Adjusted   —O •Analyst T9093 - Burst
—□—Exam   —■- ·Exam - Burst   —X— ·Analyst T9093 - Voltage

Figure D-11
Specimen R 6 - C 64 - 01H - Crack 1 - Year 1998
Comparison of Unadjusted, Adjusted, Burst and Voltage with Exam
NDE Depth vs. Axial Length

PWSCC ARC Release 1.1
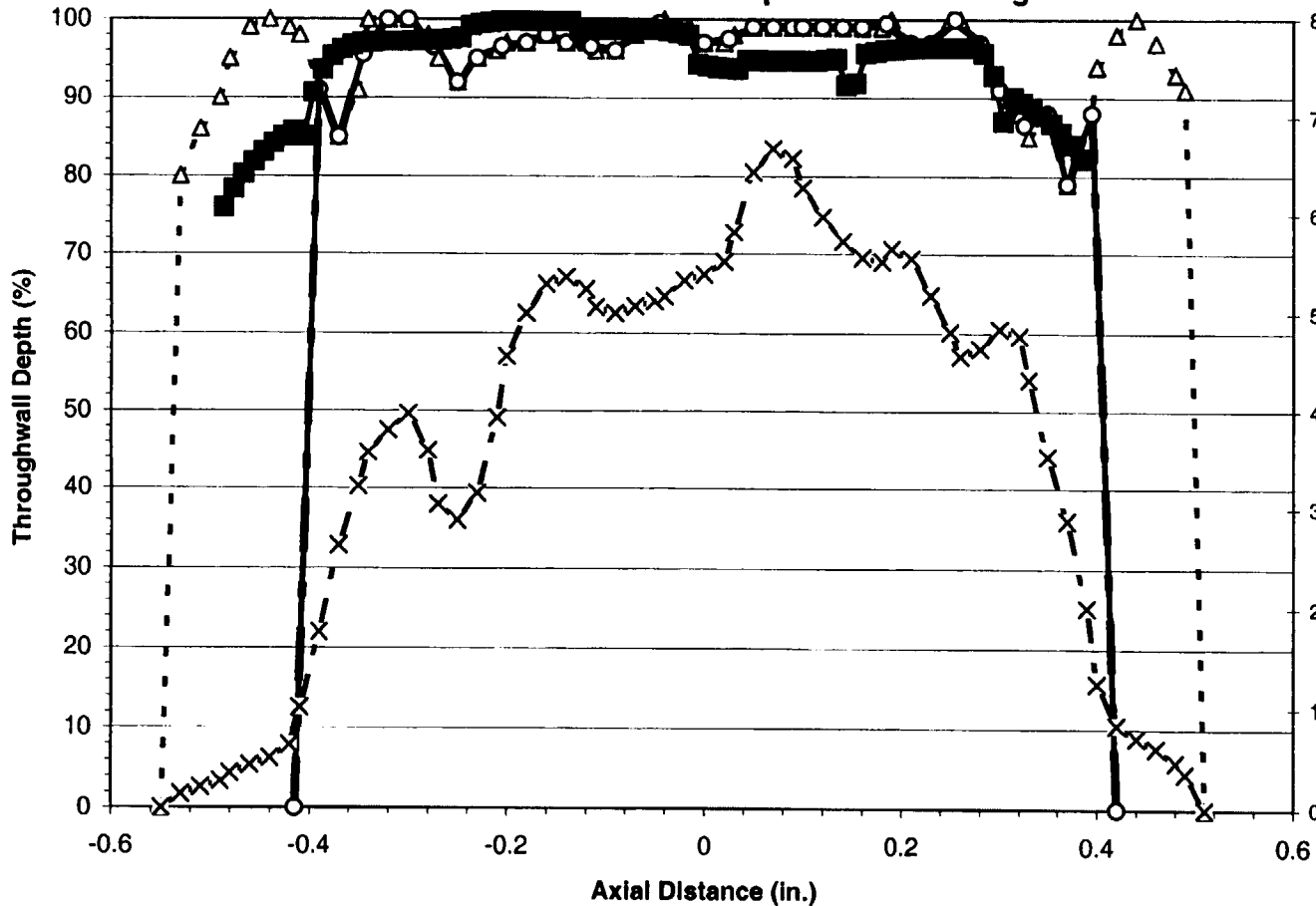
Unadjusted		
	T9093	Exam
Length	1.06	0.87
Max. Volts	6.68	
Max. Depth (%)	100.0	99.8
Avg. Depth (%)	93.5	94.3

Adjusted		
	T9093	Exam
Length	0.83	0.87
Max. Volts	6.68	
Max. Depth (%)	100.0	99.8
Avg. Depth (%)	92.7	94.3

Burst		
	T9093	Exam
Length	0.83	0.87
Max. Volts	6.68	
Max. Depth (%)	100.0	99.8
Avg. Depth (%)	92.7	94.3

Legend:
- △ - Analyst T9093 - Unadjusted
- ◇ - Analyst T9093 - Adjusted
- ○ Analyst T9093 - Burst
- □ Exam
- ■ Exam - Burst
- ✕ Analyst T9093 - Voltage

Figure D-12
Specimen R 6 - C 64 - 01H - Crack 2 - Year 1998
Comparison of Unadjusted, Adjusted, Burst and Voltage with Exam
NDE Depth vs. Axial Length

PWSCC ARC Release 1.1
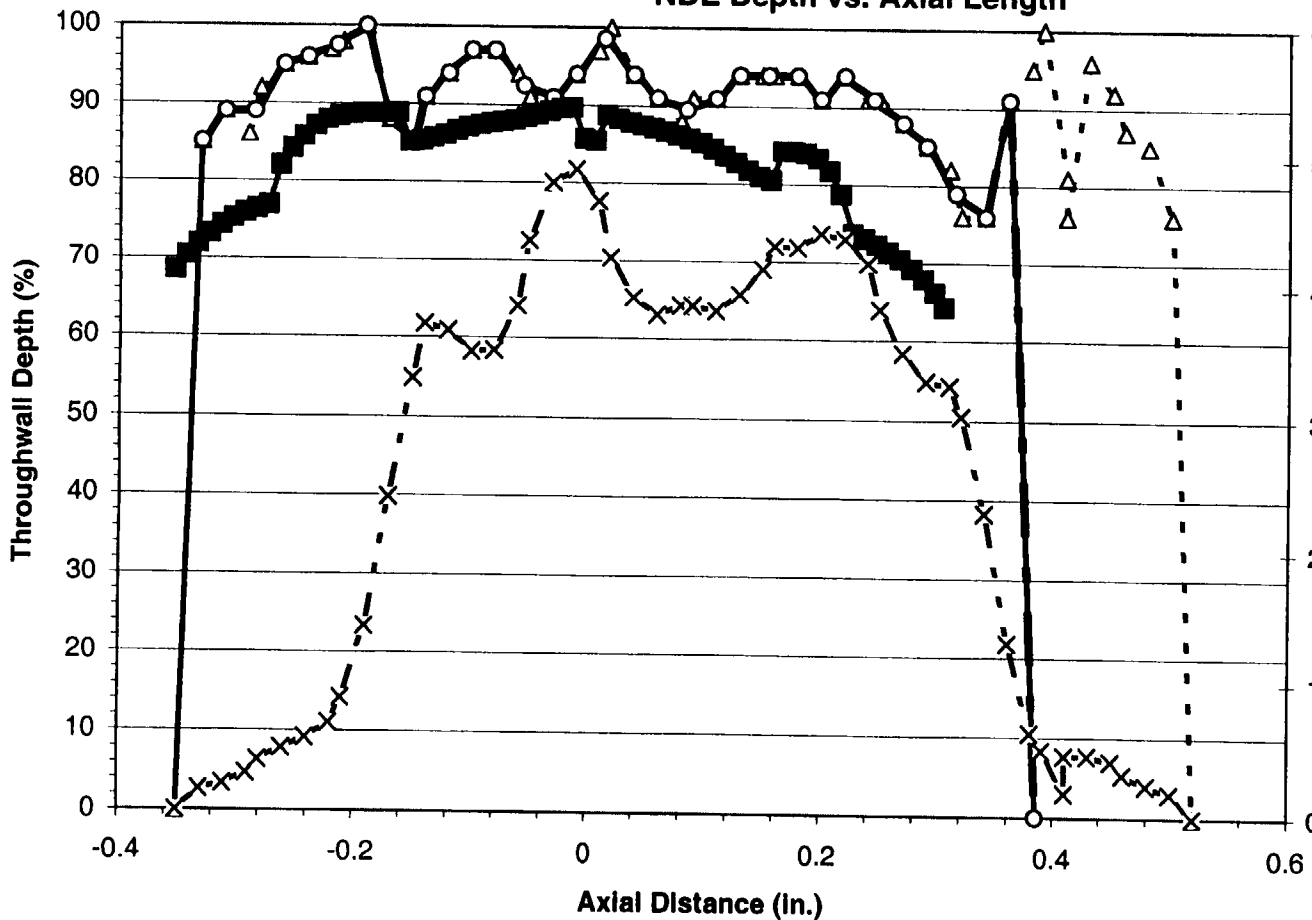
Unadjusted		
	T9093	Exam
Length	0.87	0.66
Max. Volts	4.90	
Max. Depth (%)	100.0	89.7
Avg. Depth (%)	88.7	82.5

Adjusted		
	T9093	Exam
Length	0.74	0.66
Max. Volts	4.90	
Max. Depth (%)	100.0	89.7
Avg. Depth (%)	88.6	82.5

Burst		
	T9093	Exam
Length	0.72	0.66
Max. Volts	4.90	
Max. Depth (%)	100.0	89.7
Avg. Depth (%)	89.9	82.5

- -△- Analyst T9093 - Unadjusted —◇— Analyst T9093 - Adjusted —O— Analyst T9093 - Burst
- —□— Exam —■- Exam - Burst —X- Analyst T9093 - Voltage

Figure D-13
Specimen R 9 - C 7 - 01H - Crack 1 - Year 1998
Comparison of Unadjusted, Adjusted, Burst and Voltage with Exam
NDE Depth vs. Axial Length

PWSCC ARC Release 1.1
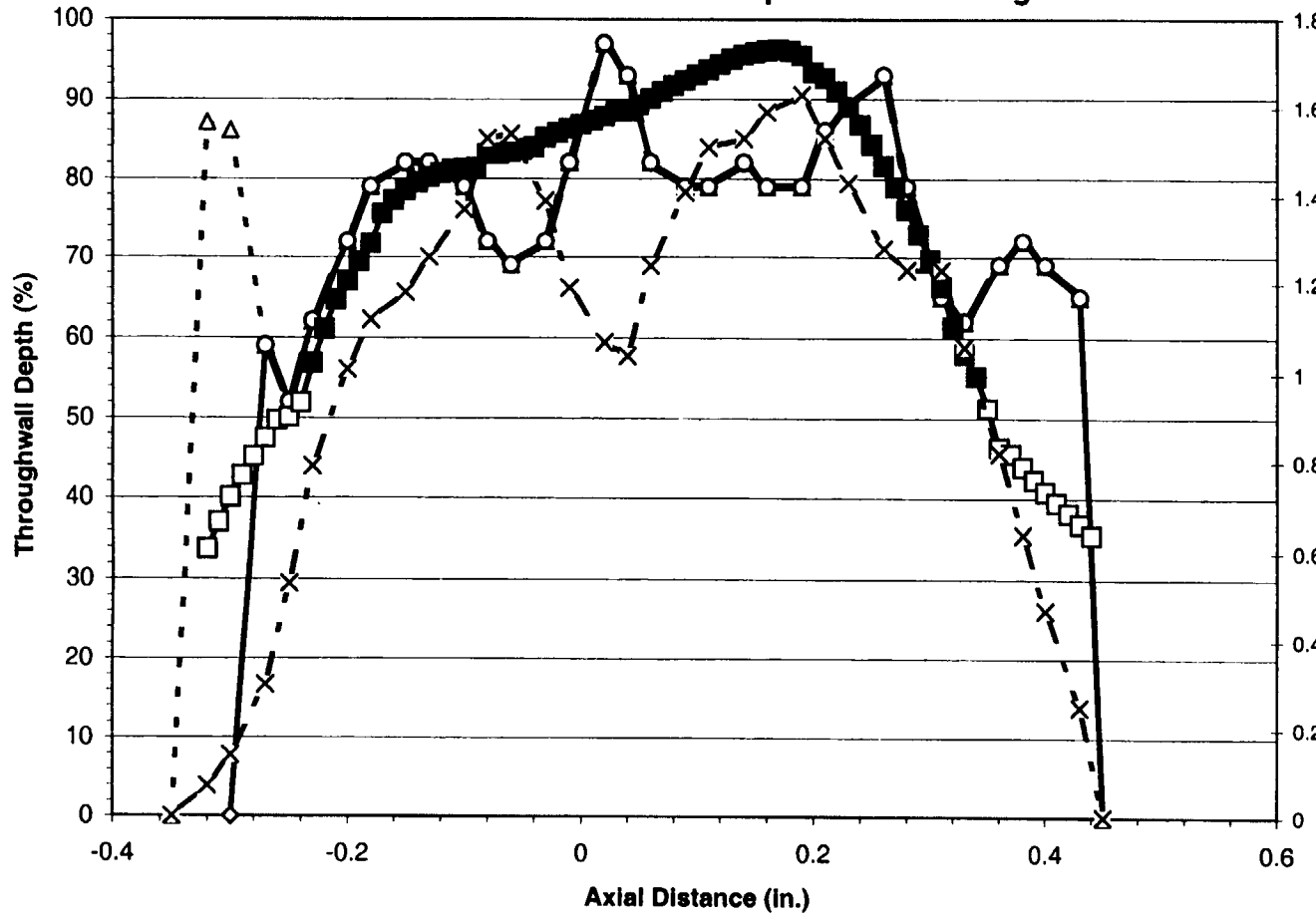
Unadjusted		
	T9093	Exam
Length	0.80	0.76
Max. Volts	1.63	
Max. Depth (%)	97.0	96.2
Avg. Depth (%)	74.3	73.2

Adjusted		
	T9093	Exam
Length	0.75	0.76
Max. Volts	1.63	
Max. Depth (%)	97.0	96.2
Avg. Depth (%)	73.5	73.2

Burst		
	T9093	Exam
Length	0.70	0.57
Max. Volts	1.63	
Max. Depth (%)	97.0	96.2
Avg. Depth (%)	76.6	82.9

Legend:
- △ - Analyst T9093 - Unadjusted
- ◇ - Analyst T9093 - Adjusted
- ○ Analyst T9093 - Burst
- □ Exam
- ■ Exam - Burst
- X - Analyst T9093 - Voltage

Figure D-14
Specimen R 9 - C 7 - 01H - Crack 2 - Year 1998
Comparison of Unadjusted, Adjusted, Burst and Voltage with Exam
NDE Depth vs. Axial Length

PWSCC ARC Release 1.1
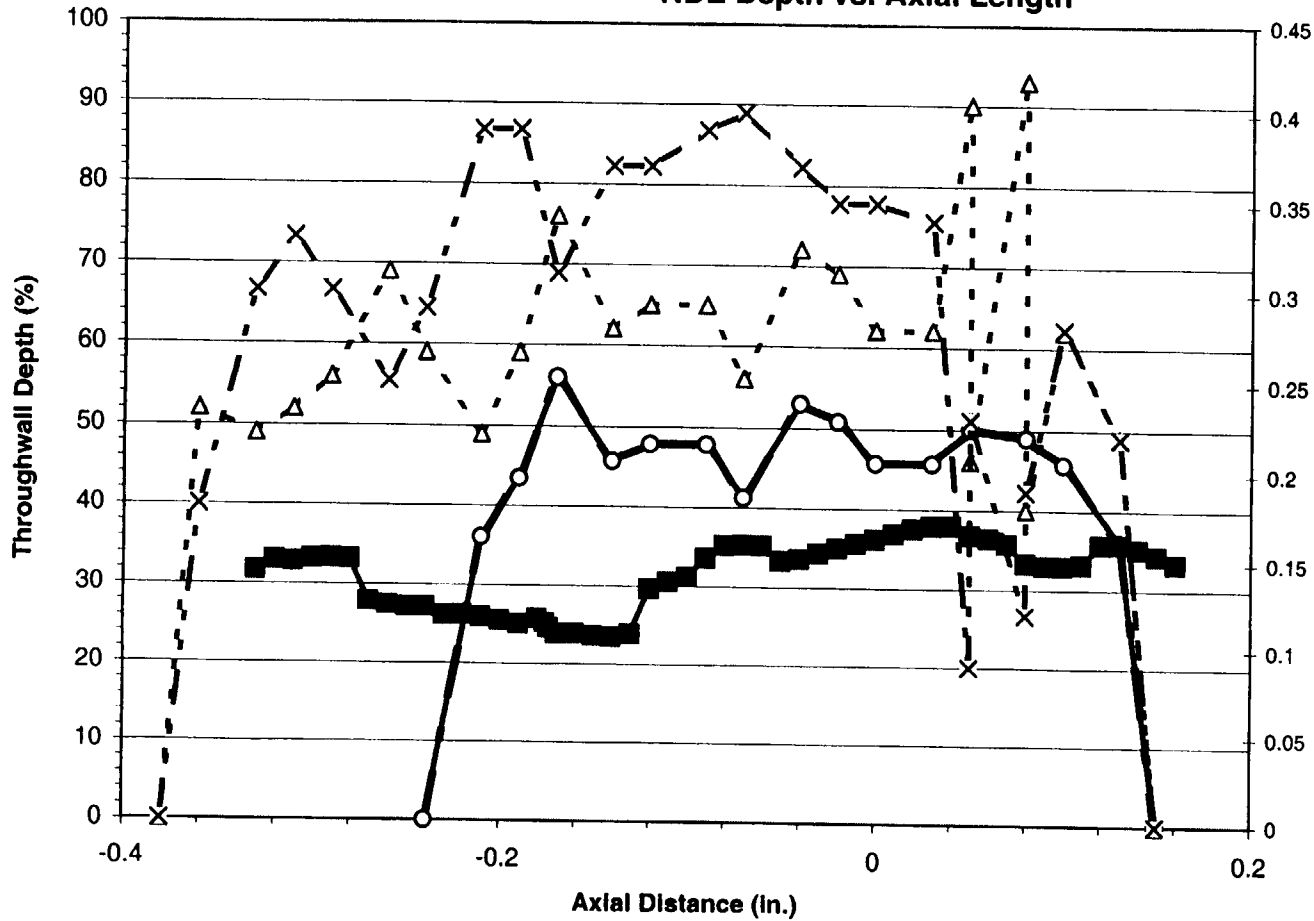
Unadjusted		
	T9093	Exam
Length	0.53	0.49
Max. Volts	0.40	
Max. Depth (%)	93.0	38.0
Avg. Depth (%)	58.7	31.7

Adjusted		
	T9093	Exam
Length	0.39	0.49
Max. Volts	0.40	
Max. Depth (%)	56.0	38.0
Avg. Depth (%)	43.3	31.7

Burst		
	T9093	Exam
Length	0.39	0.49
Max. Volts	0.40	
Max. Depth (%)	56.0	38.0
Avg. Depth (%)	43.3	31.7

- △ - Analyst T9093 - Unadjusted   ◇ Analyst T9093 - Adjusted   O Analyst T9093 - Burst
□ Exam   ■ Exam - Burst   X Analyst T9093 - Voltage

**Figure D-15
Specimen R 9 - C 19 - 01H - Crack 1 - Year 1998
Comparison of Unadjusted, Adjusted, Burst and Voltage with Exam
NDE Depth vs. Axial Length**

PWSCC ARC Release 1.1

Figure D-16
Specimen R 9 - C 19 - 01H - Crack 2 - Year 1998
Comparison of Unadjusted, Adjusted, Burst and Voltage with Exam
NDE Depth vs. Axial Length

PWSCC ARC Release 1.1
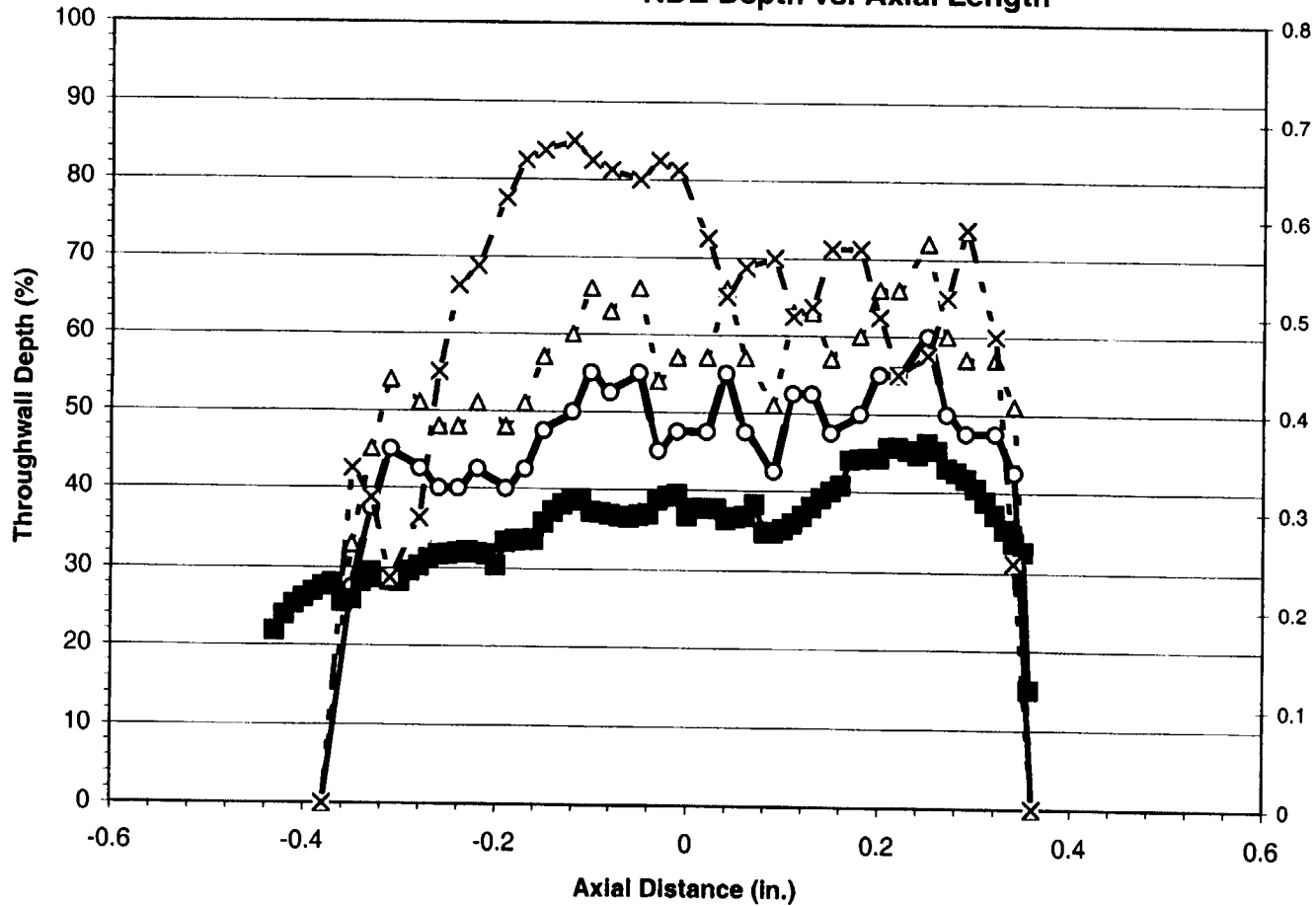
Unadjusted		
	T9093	Exam
Length	0.74	0.79
Max. Volts	0.68	
Max. Depth (%)	72.0	46.3
Avg. Depth (%)	54.7	35.6

Adjusted		
	T9093	Exam
Length	0.74	0.79
Max. Volts	0.68	
Max. Depth (%)	60.0	46.3
Avg. Depth (%)	45.6	35.6

Burst		
	T9093	Exam
Length	0.69	0.79
Max. Volts	0.68	
Max. Depth (%)	60.0	46.3
Avg. Depth (%)	47.7	35.6

Legend:
- ▵ - Analyst T9093 - Unadjusted
—◇— Analyst T9093 - Adjusted
—O— Analyst T9093 - Burst
—□— Exam
—■— Exam - Burst
—X— Analyst T9093 - Voltage

Figure D-17
Specimen R 9 - C 37 - 01H - Crack 1 - Year 1998
Comparison of Unadjusted, Adjusted, Burst and Voltage with Exam
NDE Depth vs. Axial Length

PWSCC ARC Release 1.1
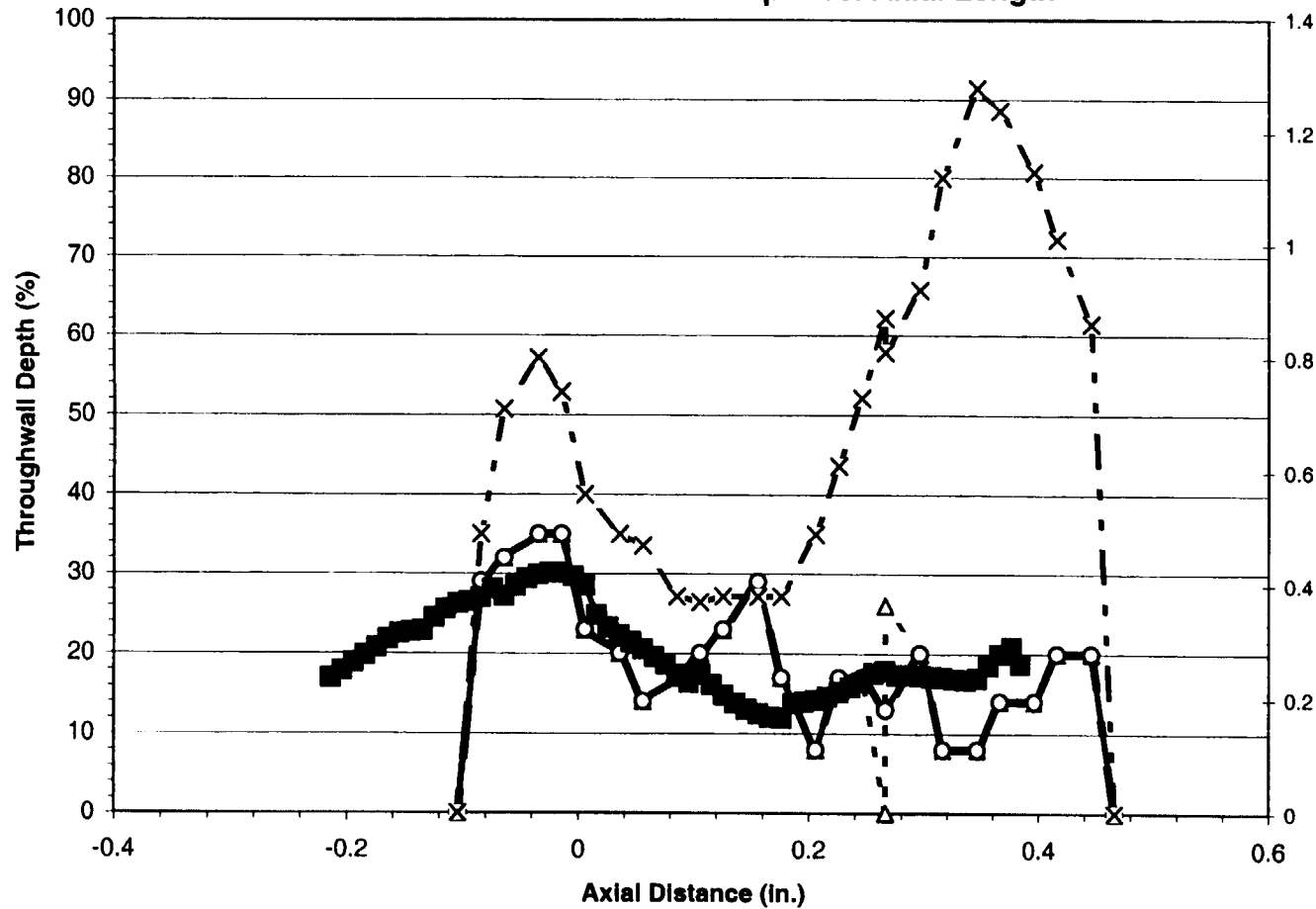
Unadjusted		
	T9093	Exam
Length	0.57	0.60
Max. Volts	1.28	
Max. Depth (%)	35.0	30.1
Avg. Depth (%)	18.9	20.1

Adjusted		
	T9093	Exam
Length	0.57	0.60
Max. Volts	1.28	
Max. Depth (%)	35.0	30.1
Avg. Depth (%)	18.8	20.1

Burst		
	T9093	Exam
Length	0.57	0.60
Max. Volts	1.28	
Max. Depth (%)	35.0	30.1
Avg. Depth (%)	18.8	20.1

Legend:
- -△- Analyst T9093 - Unadjusted
- —◇— Analyst T9093 - Adjusted
- —O— Analyst T9093 - Burst
- —□— Exam
- —■— Exam - Burst
- —X— Analyst T9093 - Voltage

Figure D-18
Specimen R 9 - C 64 - 01H - Crack 1 - Year 1998
Comparison of Unadjusted, Adjusted, Burst and Voltage with Exam
NDE Depth vs. Axial Length

PWSCC ARC Release 1.1
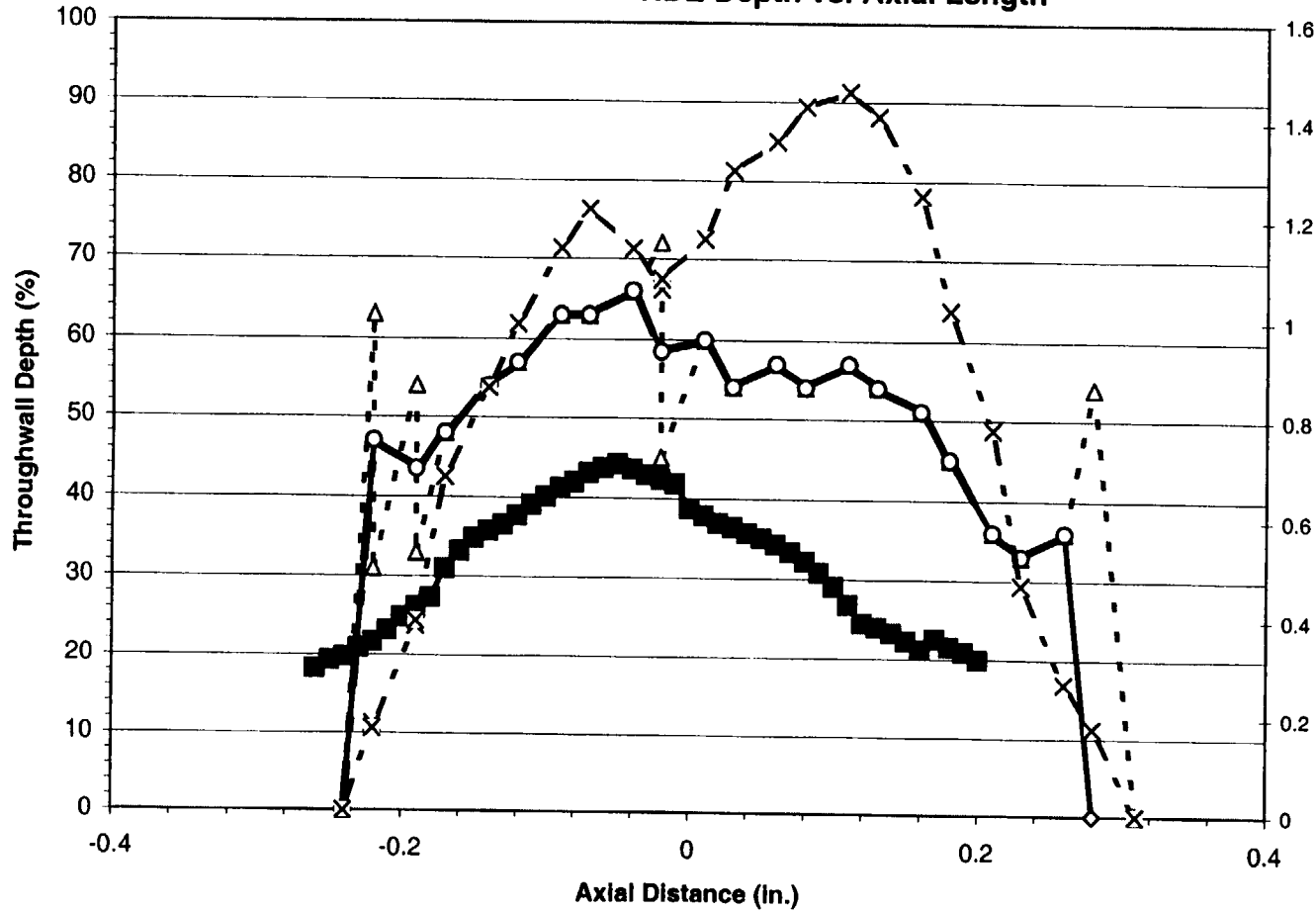
Unadjusted		
	T9093	Exam
Length	0.55	0.46
Max. Volts	1.46	
Max. Depth (%)	72.0	44.2
Avg. Depth (%)	49.7	31.8

Adjusted		
	T9093	Exam
Length	0.52	0.46
Max. Volts	1.46	
Max. Depth (%)	66.0	44.2
Avg. Depth (%)	49.9	31.8

Burst		
	T9093	Exam
Length	0.50	0.46
Max. Volts	1.46	
Max. Depth (%)	66.0	44.2
Avg. Depth (%)	51.1	31.8

Legend:
- Analyst T9093 - Unadjusted
- Analyst T9093 - Adjusted
- Analyst T9093 - Burst
- Exam
- Exam - Burst
- Analyst T9093 - Voltage

Figure D-19
Specimen R 13 - C 7 - 01H - Crack 1 - Year 1998
Comparison of Unadjusted, Adjusted, Burst and Voltage with Exam
NDE Depth vs. Axial Length

PWSCC ARC Release 1.1
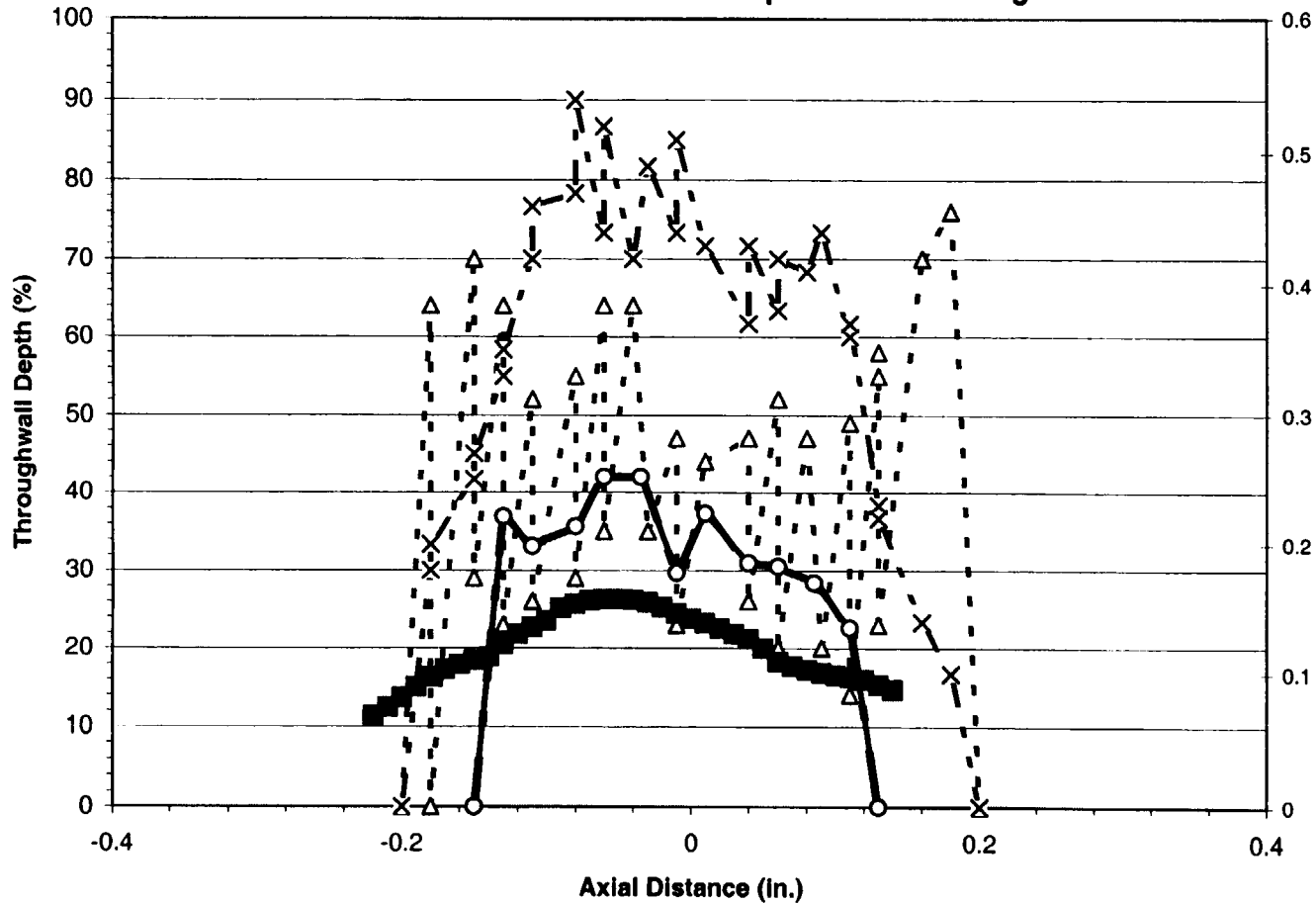
Unadjusted		
	T9093	Exam
Length	0.40	0.36
Max. Volts	0.54	
Max. Depth (%)	76.0	26.3
Avg. Depth (%)	40.5	20.2

Adjusted		
	T9093	Exam
Length	0.28	0.36
Max. Volts	0.51	
Max. Depth (%)	42.0	26.3
Avg. Depth (%)	31.2	20.2

Burst		
	T9093	Exam
Length	0.28	0.36
Max. Volts	0.51	
Max. Depth (%)	42.0	26.3
Avg. Depth (%)	31.2	20.2

Legend:
- ◁ - Analyst T9093 - Unadjusted
- ◇ Analyst T9093 - Adjusted
- ○ Analyst T9093 - Burst
- □ Exam
- ■ Exam - Burst
- X Analyst T9093 - Voltage

Figure D-20
Specimen R 13 - C 16 - 01H - Crack 1 - Year 1998
Comparison of Unadjusted, Adjusted, Burst and Voltage with Exam
NDE Depth vs. Axial Length

PWSCC ARC Release 1.1
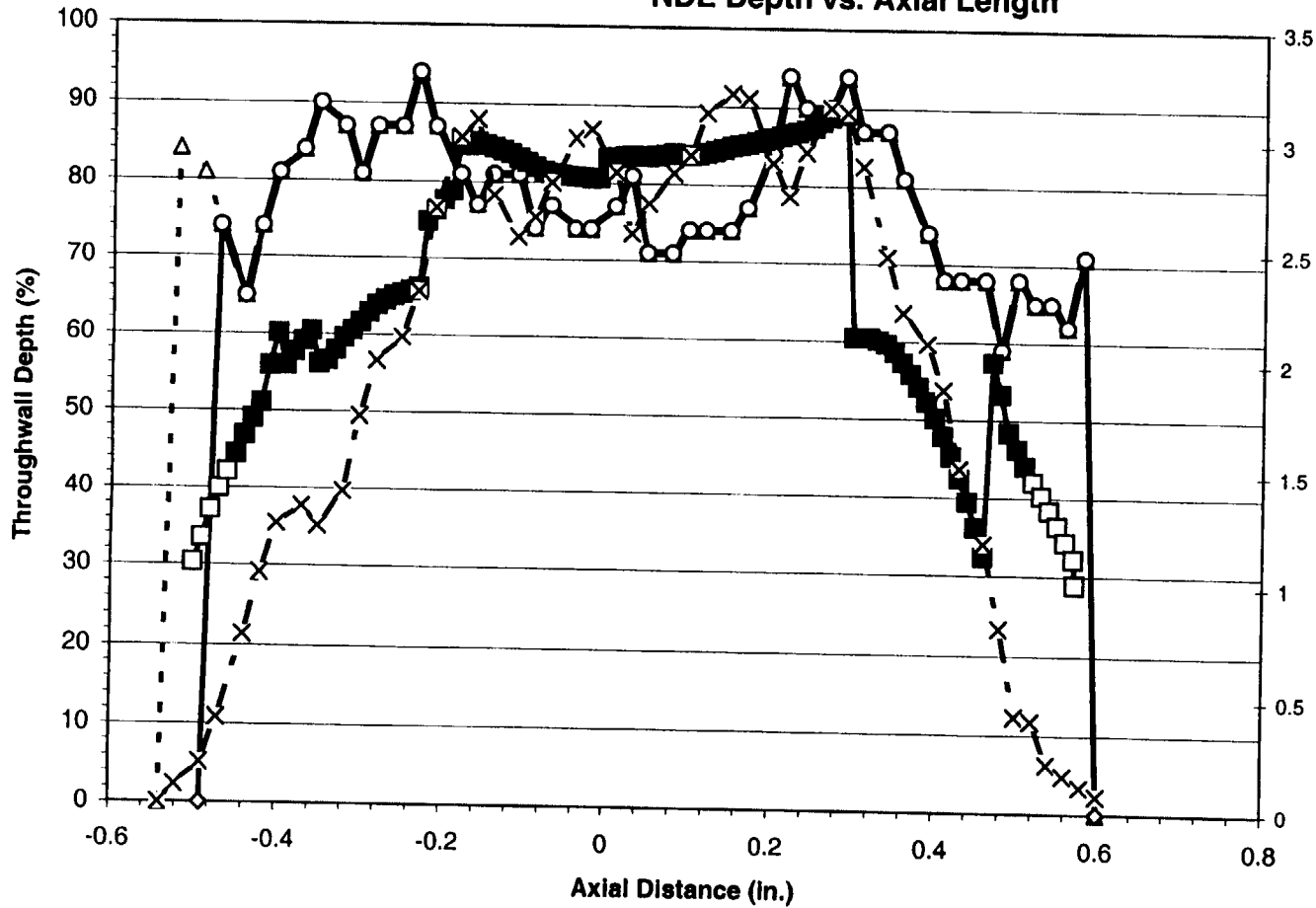
Unadjusted		
	T9093	Exam
Length	1.14	1.07
Max. Volts	3.21	
Max. Depth (%)	94.0	89.3
Avg. Depth (%)	76.9	67.2

Adjusted		
	T9093	Exam
Length	1.09	1.07
Max. Volts	3.21	
Max. Depth (%)	94.0	89.3
Avg. Depth (%)	76.7	67.2

Burst		
	T9093	Exam
Length	1.05	0.96
Max. Volts	3.21	
Max. Depth (%)	94.0	89.3
Avg. Depth (%)	78.2	70.6

Legend:
- ▵ - Analyst T9093 - Unadjusted ◇ Analyst T9093 - Adjusted ◯ Analyst T9093 - Burst
- □ Exam ■ Exam - Burst X Analyst T9093 - Voltage

Figure D-21
Specimen R 13 - C 16 - 01H - Crack 2 - Year 1998
Comparison of Unadjusted, Adjusted, Burst and Voltage with Exam
NDE Depth vs. Axial Length

PWSCC ARC Release 1.1
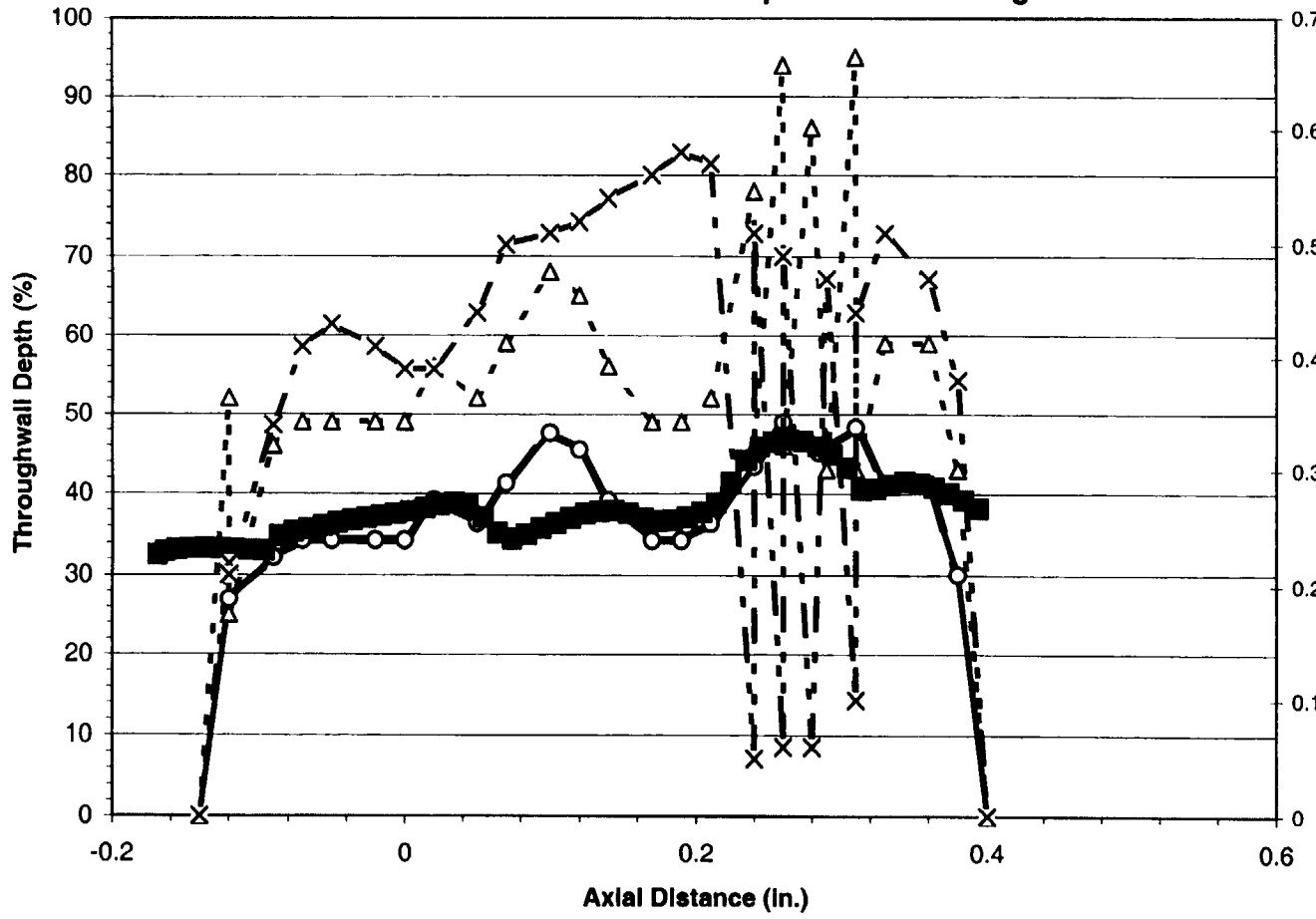
Unadjusted		
	T9093	Exam
Length	0.54	0.56
Max. Volts	0.58	
Max. Depth (%)	95.0	46.7
Avg. Depth (%)	53.1	38.2

Adjusted		
	T9093	Exam
Length	0.54	0.56
Max. Volts	0.58	
Max. Depth (%)	49.0	46.7
Avg. Depth (%)	37.2	38.2

Burst		
	T9093	Exam
Length	0.50	0.56
Max. Volts	0.58	
Max. Depth (%)	49.0	46.7
Avg. Depth (%)	39.0	38.2

- ◁ - Analyst T9093 - Unadjusted   ◇ Analyst T9093 - Adjusted   ○ Analyst T9093 - Burst
□ Exam   ■ Exam - Burst   X Analyst T9093 - Voltage

Figure D-22
Specimen R 13 - C 34 - 01H - Crack 1 - Year 1998
Comparison of Unadjusted, Adjusted, Burst and Voltage with Exam
NDE Depth vs. Axial Length

PWSCC ARC Release 1.1
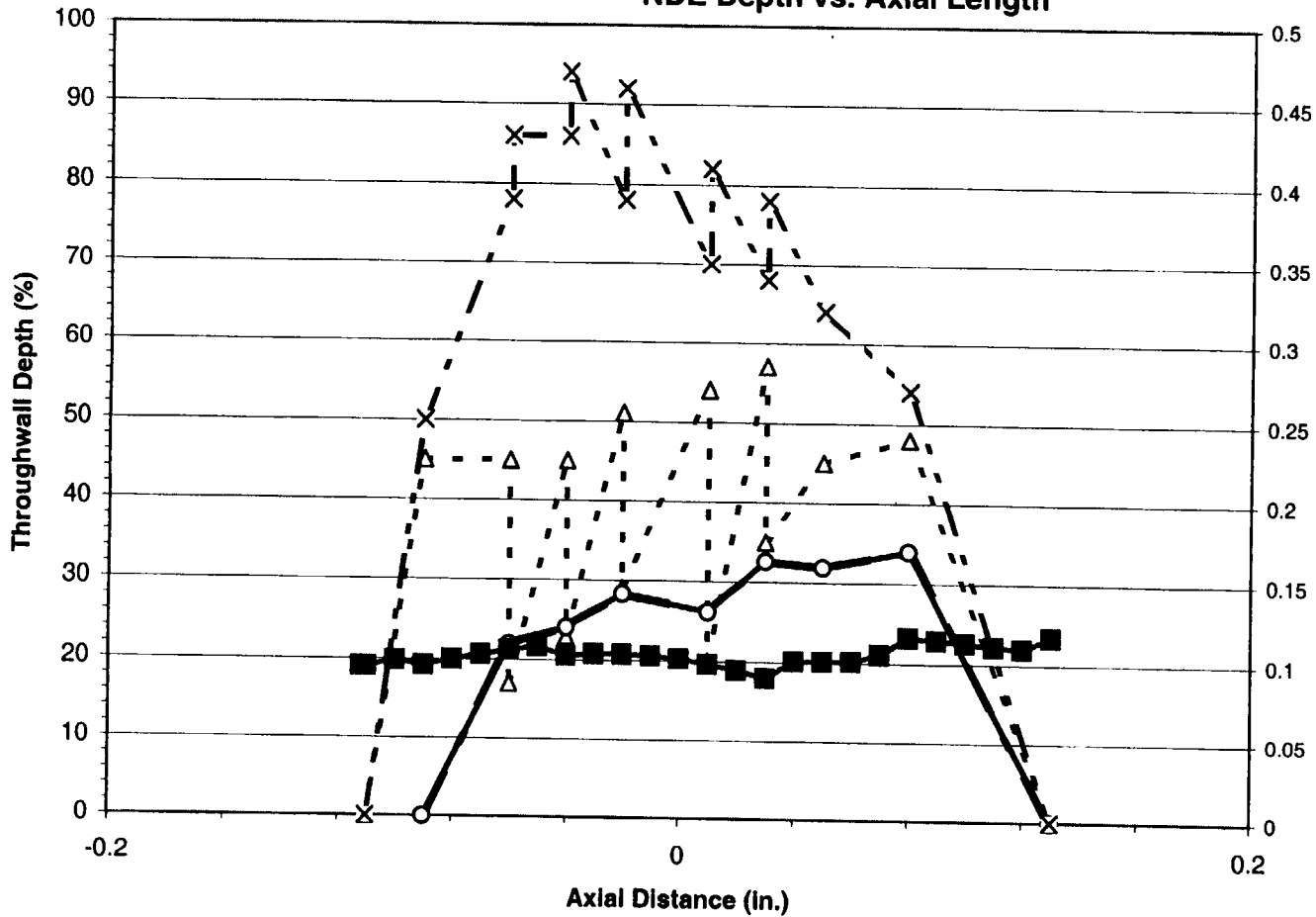
Unadjusted		
	T9093	Exam
Length	0.24	0.24
Max. Volts	0.47	
Max. Depth (%)	57.0	23.4
Avg. Depth (%)	34.9	20.7

Adjusted		
	T9093	Exam
Length	0.22	0.24
Max. Volts	0.45	
Max. Depth (%)	34.0	23.4
Avg. Depth (%)	23.6	20.7

Burst		
	T9093	Exam
Length	0.22	0.24
Max. Volts	0.45	
Max. Depth (%)	34.0	23.4
Avg. Depth (%)	23.6	20.7

- △ - Analyst T9093 - Unadjusted —◇— Analyst T9093 - Adjusted —O •Analyst T9093 - Burst
—□— Exam   —■- ·Exam - Burst   —X- ·Analyst T9093 - Voltage

Figure D-23
Specimen R 13 - C 59 - 01H - Crack 1 - Year 1998
Comparison of Unadjusted, Adjusted, Burst and Voltage with Exam
NDE Depth vs. Axial Length

PWSCC ARC Release 1.1
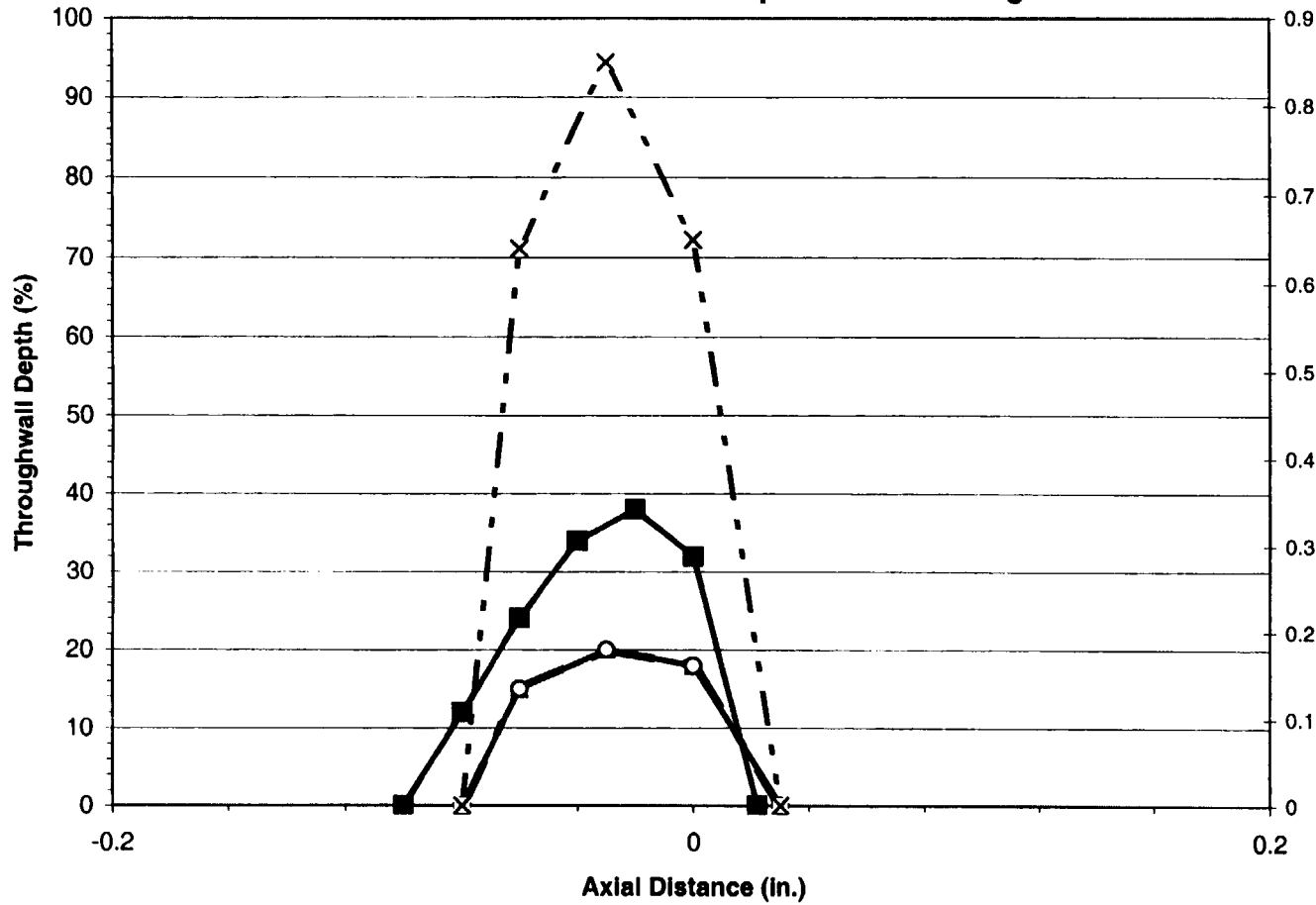
Unadjusted		
	T9093	Exam
Length	0.11	0.12
Max. Volts	0.85	
Max. Depth (%)	20.0	38.0
Avg. Depth (%)	13.8	23.2

Adjusted		
	T9093	Exam
Length	0.11	0.12
Max. Volts	0.85	
Max. Depth (%)	20.0	38.0
Avg. Depth (%)	13.8	23.2

Burst		
	T9093	Exam
Length	0.11	0.12
Max. Volts	0.85	
Max. Depth (%)	20.0	38.0
Avg. Depth (%)	13.8	23.2

Legend:
- ◬ - Analyst T9093 - Unadjusted —◇— Analyst T9093 - Adjusted —O— Analyst T9093 - Burst
- —□— Exam —■— Exam - Burst —X— Analyst T9093 - Voltage

Figure D-24
Specimen R 13 - C 85 - 01H - Crack 1 - Year 1998
Comparison of Unadjusted, Adjusted, Burst and Voltage with Exam
NDE Depth vs. Axial Length

PWSCC ARC Release 1.1
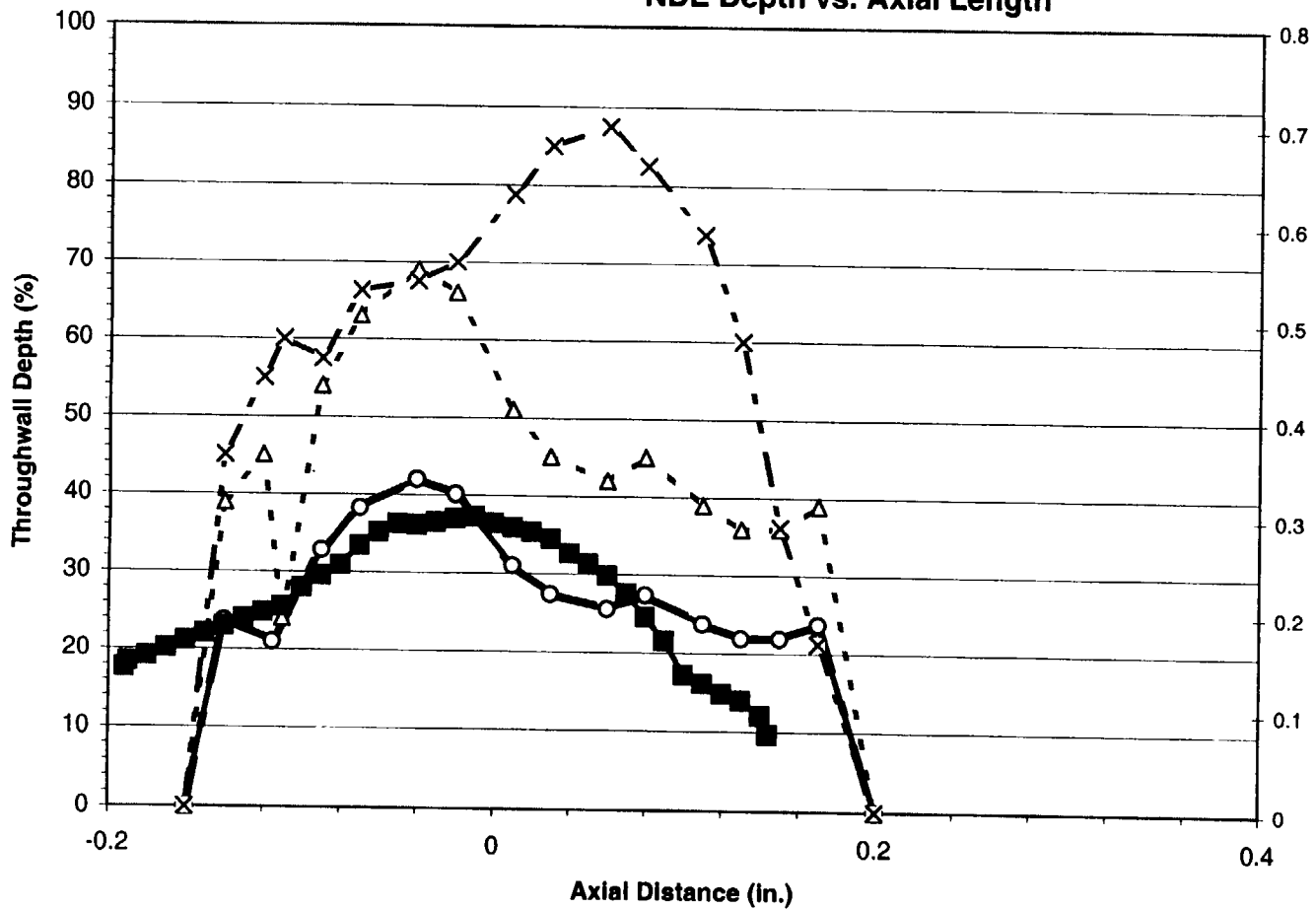
Unadjusted		
	T9093	Exam
Length	0.36	0.34
Max. Volts	0.70	
Max. Depth (%)	69.0	37.3
Avg. Depth (%)	43.9	27.3

Adjusted		
	T9093	Exam
Length	0.36	0.34
Max. Volts	0.70	
Max. Depth (%)	42.0	37.3
Avg. Depth (%)	26.8	27.3

Burst		
	T9093	Exam
Length	0.36	0.34
Max. Volts	0.70	
Max. Depth (%)	42.0	37.3
Avg. Depth (%)	26.8	27.3

Legend:
- △ - Analyst T9093 - Unadjusted —◇— Analyst T9093 - Adjusted —○ Analyst T9093 - Burst
—□— Exam —■- Exam - Burst —X- Analyst T9093 - Voltage

Figure D-25
Specimen R 17 - C 43 - 01H - Crack 1 - Year 1998
Comparison of Unadjusted, Adjusted, Burst and Voltage with Exam
NDE Depth vs. Axial Length

PWSCC ARC Release 1.1
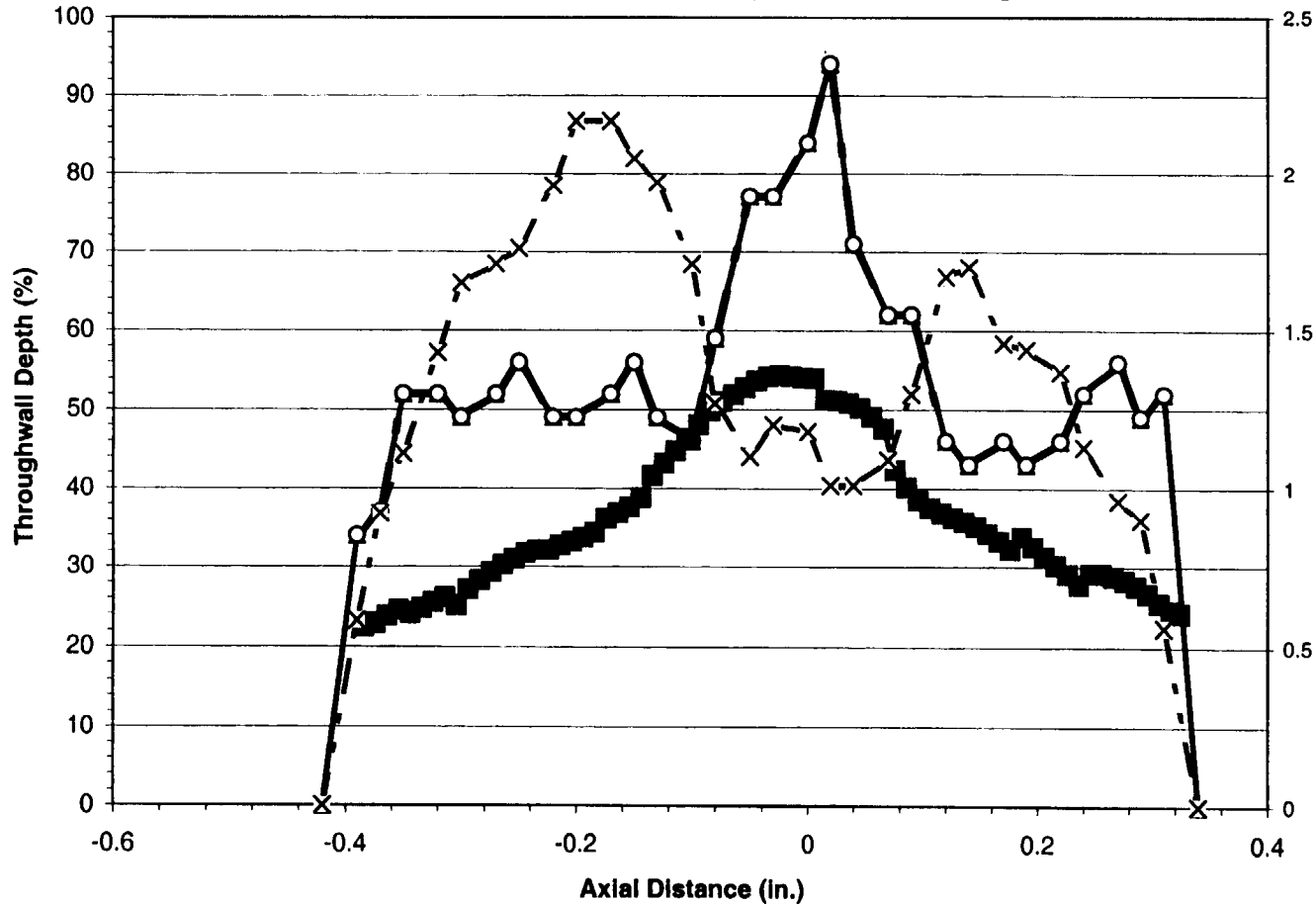
Unadjusted		
	T9093	Exam
Length	0.76	0.71
Max. Volts	2.17	
Max. Depth (%)	94.0	54.3
Avg. Depth (%)	52.8	36.7

Adjusted		
	T9093	Exam
Length	0.76	0.71
Max. Volts	2.17	
Max. Depth (%)	94.0	54.3
Avg. Depth (%)	52.8	36.7

Burst		
	T9093	Exam
Length	0.70	0.71
Max. Volts	2.17	
Max. Depth (%)	94.0	54.3
Avg. Depth (%)	55.5	36.7

Legend:
- ◁ - Analyst T9093 - Unadjusted —◇— Analyst T9093 - Adjusted —O— Analyst T9093 - Burst
—□— Exam —■- Exam - Burst —X- Analyst T9093 - Voltage

Figure D-26
Specimen R 17 - C 58 - 01H - Crack 1 - Year 1998
Comparison of Unadjusted, Adjusted, Burst and Voltage with Exam
NDE Depth vs. Axial Length

PWSCC ARC Release 1.1
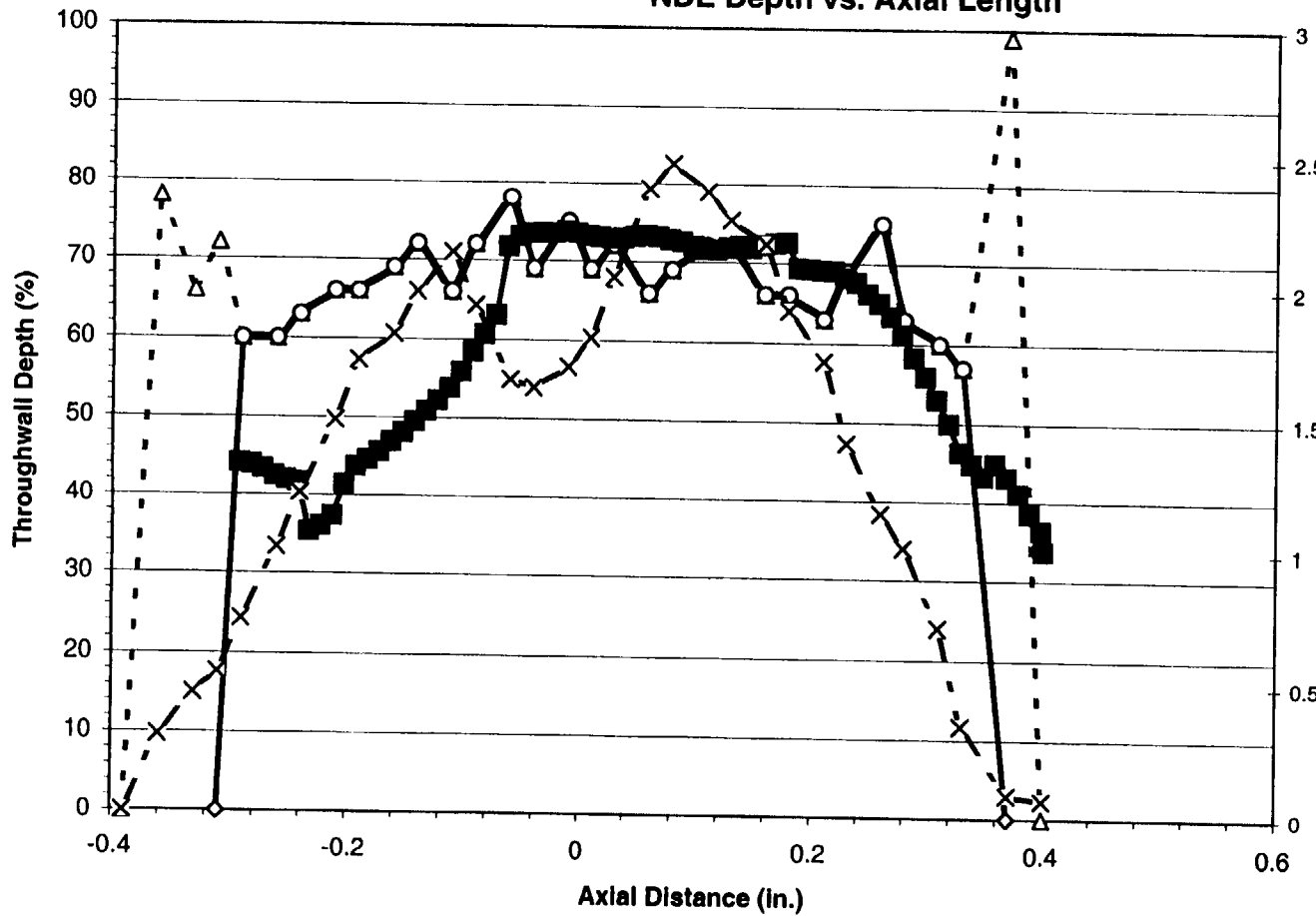
Unadjusted		
	T9093	Exam
Length	0.79	0.69
Max. Volts	2.48	
Max. Depth (%)	99.0	73.7
Avg. Depth (%)	66.7	59.1

Adjusted		
	T9093	Exam
Length	0.68	0.69
Max. Volts	2.48	
Max. Depth (%)	78.0	73.7
Avg. Depth (%)	64.4	59.1

Burst		
	T9093	Exam
Length	0.62	0.69
Max. Volts	2.48	
Max. Depth (%)	78.0	73.7
Avg. Depth (%)	67.9	59.1

Legend: Analyst T9093 - Unadjusted · Analyst T9093 - Adjusted · Analyst T9093 - Burst · Exam · Exam - Burst · Analyst T9093 - Voltage

Figure D-27
Specimen R 19 - C 38 - 01H - Crack 1 - Year 1998
Comparison of Unadjusted, Adjusted, Burst and Voltage with Exam
NDE Depth vs. Axial Length

PWSCC ARC Release 1.1
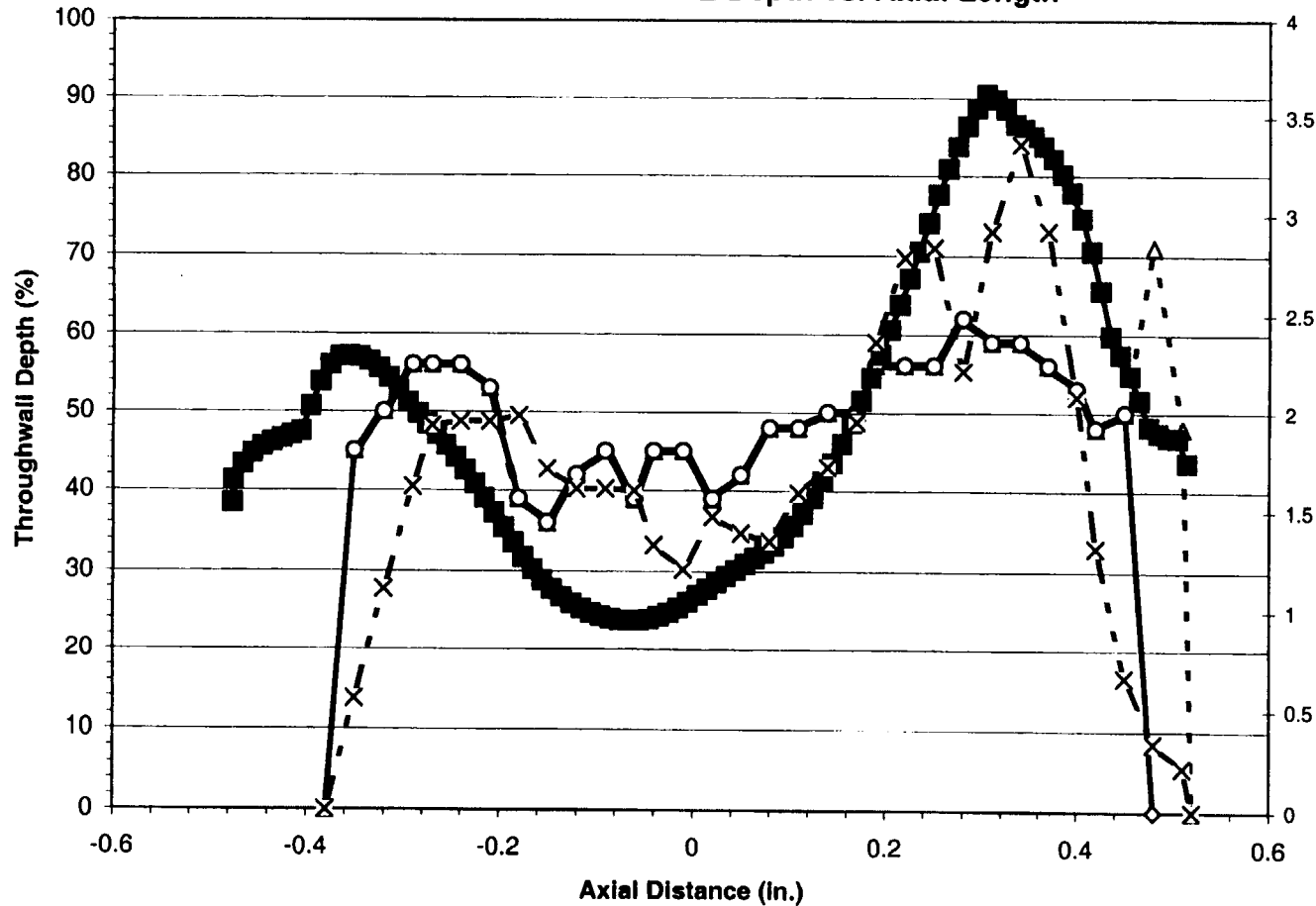
Unadjusted		
	T9093	Exam
Length	0.90	0.99
Max. Volts	3.36	
Max. Depth (%)	71.0	90.5
Avg. Depth (%)	49.2	49.3

Adjusted		
	T9093	Exam
Length	0.86	0.99
Max. Volts	3.36	
Max. Depth (%)	62.0	90.5
Avg. Depth (%)	47.9	49.3

Burst		
	T9093	Exam
Length	0.80	0.99
Max. Volts	3.36	
Max. Depth (%)	62.0	90.5
Avg. Depth (%)	49.7	49.3

Legend:
- △ - Analyst T9093 - Unadjusted —◇— Analyst T9093 - Adjusted —O— Analyst T9093 - Burst
—□— Exam —■— Exam - Burst —X— Analyst T9093 - Voltage

Figure D-28
Specimen R 19 - C 38 - 01H - Crack 2 - Year 1998
Comparison of Unadjusted, Adjusted, Burst and Voltage with Exam
NDE Depth vs. Axial Length

PWSCC ARC Release 1.1
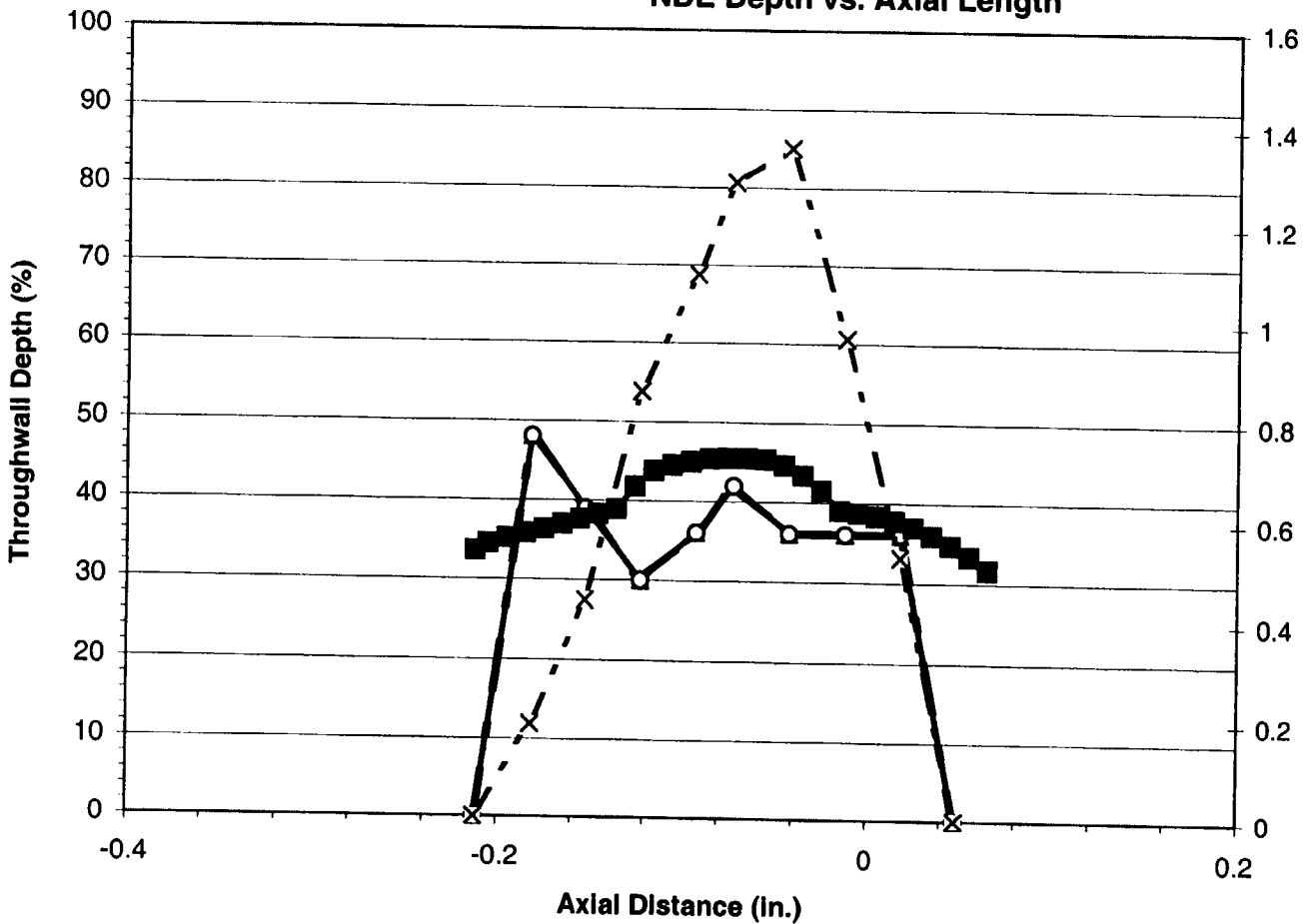
Unadjusted		
	T9093	Exam
Length	0.26	0.28
Max. Volts	1.36	
Max. Depth (%)	48.0	45.5
Avg. Depth (%)	33.5	39.6

Adjusted		
	T9093	Exam
Length	0.26	0.28
Max. Volts	1.36	
Max. Depth (%)	48.0	45.5
Avg. Depth (%)	33.5	39.6

Burst		
	T9093	Exam
Length	0.26	0.28
Max. Volts	1.36	
Max. Depth (%)	48.0	45.5
Avg. Depth (%)	33.5	39.6

Legend:
- ◬ - Analyst T9093 - Unadjusted ◇ Analyst T9093 - Adjusted ○ Analyst T9093 - Burst
- □ Exam ■ Exam - Burst X Analyst T9093 - Voltage

Figure D-29
Specimen R 21 - C 13 - 01H - Crack 1 - Year 1998
Comparison of Unadjusted, Adjusted, Burst and Voltage with Exam
NDE Depth vs. Axial Length

PWSCC ARC Release 1.1
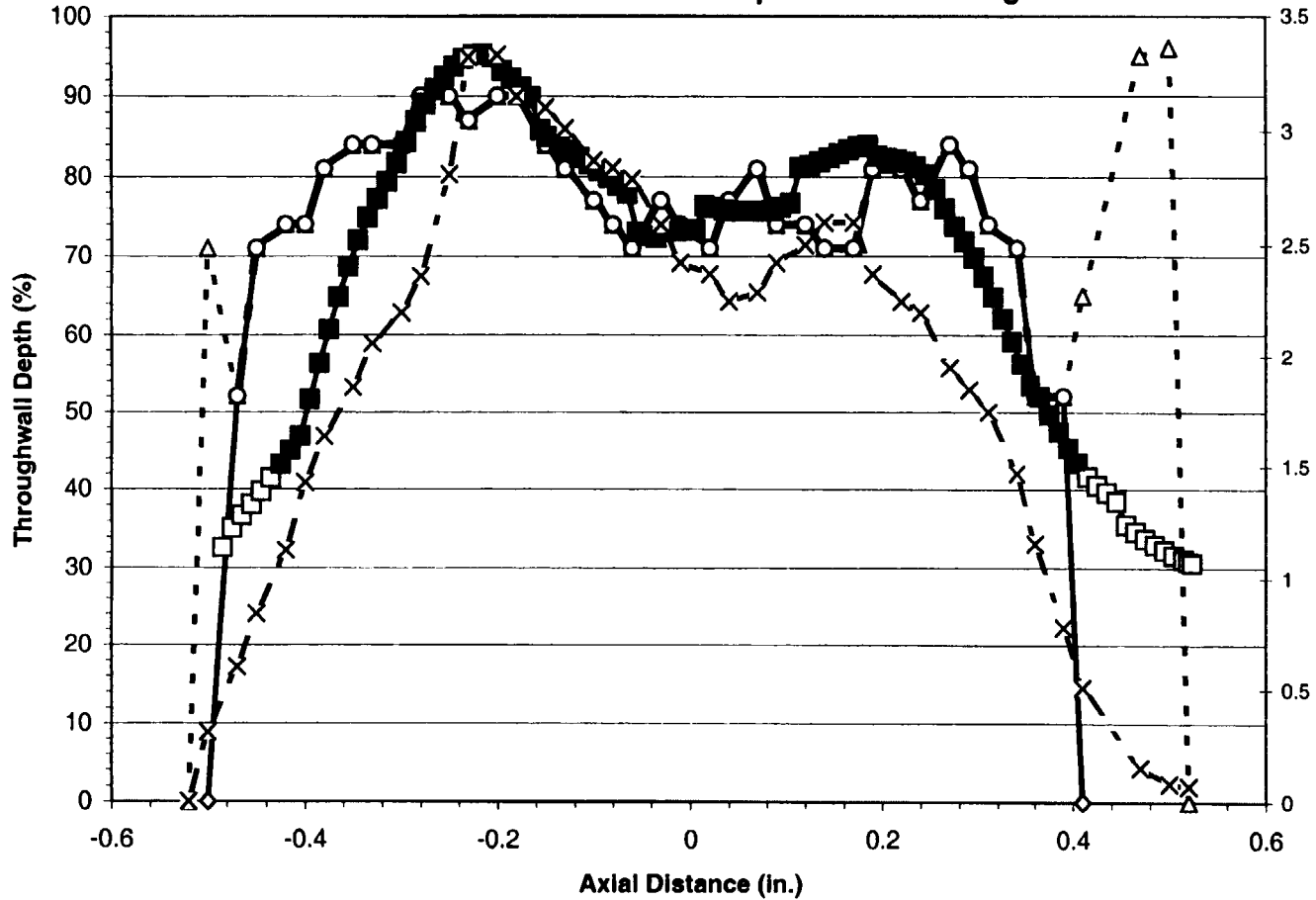
Unadjusted		
	T9093	Exam
Length	1.04	1.01
Max. Volts	3.33	
Max. Depth (%)	96.0	95.3
Avg. Depth (%)	75.9	68.7

Adjusted		
	T9093	Exam
Length	0.91	1.01
Max. Volts	3.33	
Max. Depth (%)	90.0	95.3
Avg. Depth (%)	74.6	68.7

Burst		
	T9093	Exam
Length	0.86	0.83
Max. Volts	3.33	
Max. Depth (%)	90.0	95.3
Avg. Depth (%)	77.4	75.6

Legend:
- △ - Analyst T9093 - Unadjusted
- ◇ - Analyst T9093 - Adjusted
- ○ Analyst T9093 - Burst
- □ Exam
- ■ Exam - Burst
- X - Analyst T9093 - Voltage

Figure D-30
Specimen R 21 - C 13 - 01H - Crack 2 - Year 1998
Comparison of Unadjusted, Adjusted, Burst and Voltage with Exam
NDE Depth vs. Axial Length

PWSCC ARC Release 1.1
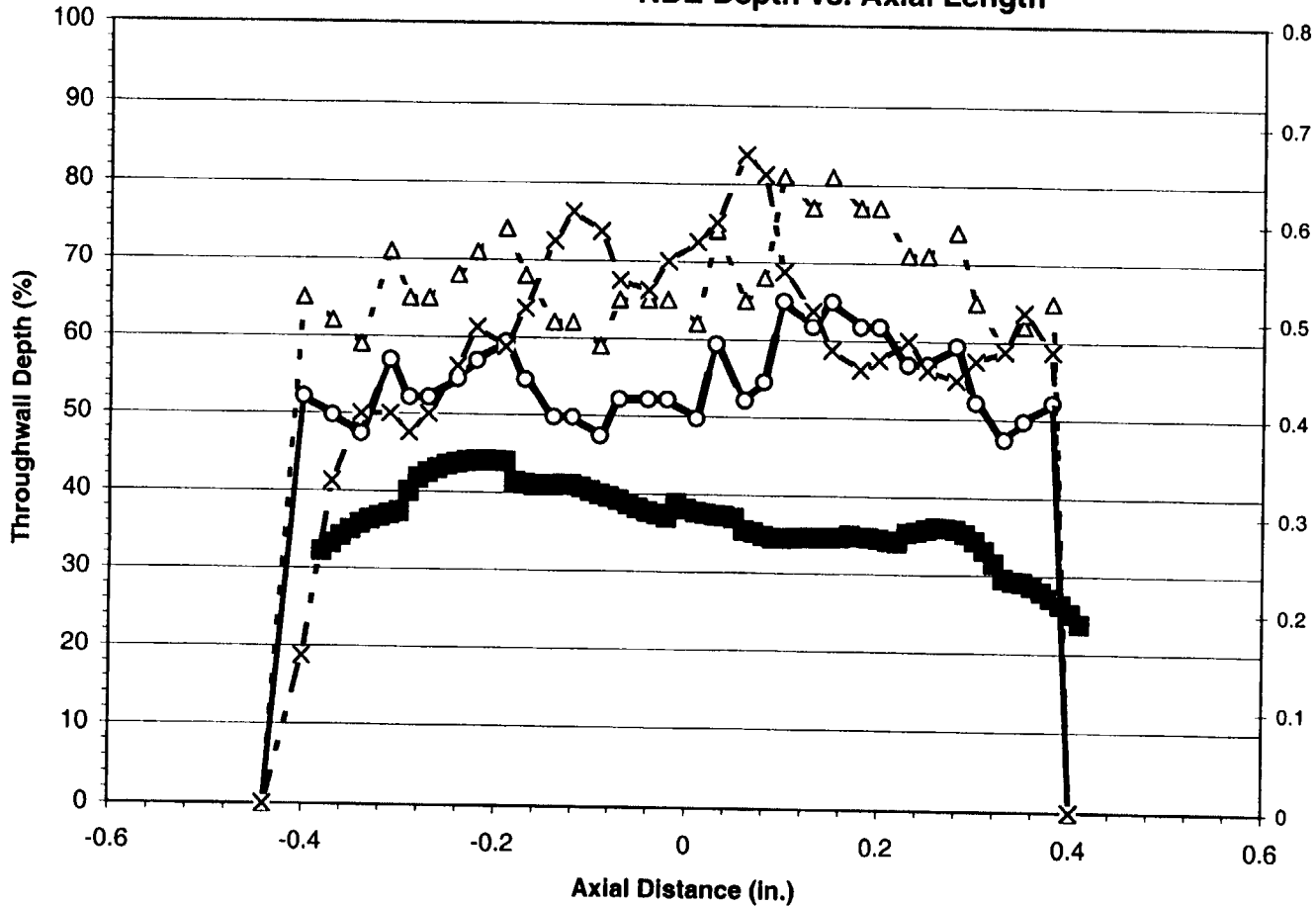
Unadjusted		
	T9093	Exam
Length	0.84	0.79
Max. Volts	0.67	
Max. Depth (%)	81.0	44.0
Avg. Depth (%)	65.4	36.6

Adjusted		
	T9093	Exam
Length	0.84	0.79
Max. Volts	0.67	
Max. Depth (%)	65.0	44.0
Avg. Depth (%)	52.5	36.6

Burst		
	T9093	Exam
Length	0.78	0.79
Max. Volts	0.67	
Max. Depth (%)	65.0	44.0
Avg. Depth (%)	54.5	36.6

Legend:
- Analyst T9093 - Unadjusted
- Analyst T9093 - Adjusted
- Analyst T9093 - Burst
- Exam
- Exam - Burst
- Analyst T9093 - Voltage

Figure D-31
Specimen R 21 - C 28 - 01H - Crack 1 - Year 1998
Comparison of Unadjusted, Adjusted, Burst and Voltage with Exam
NDE Depth vs. Axial Length

PWSCC ARC Release 1.1
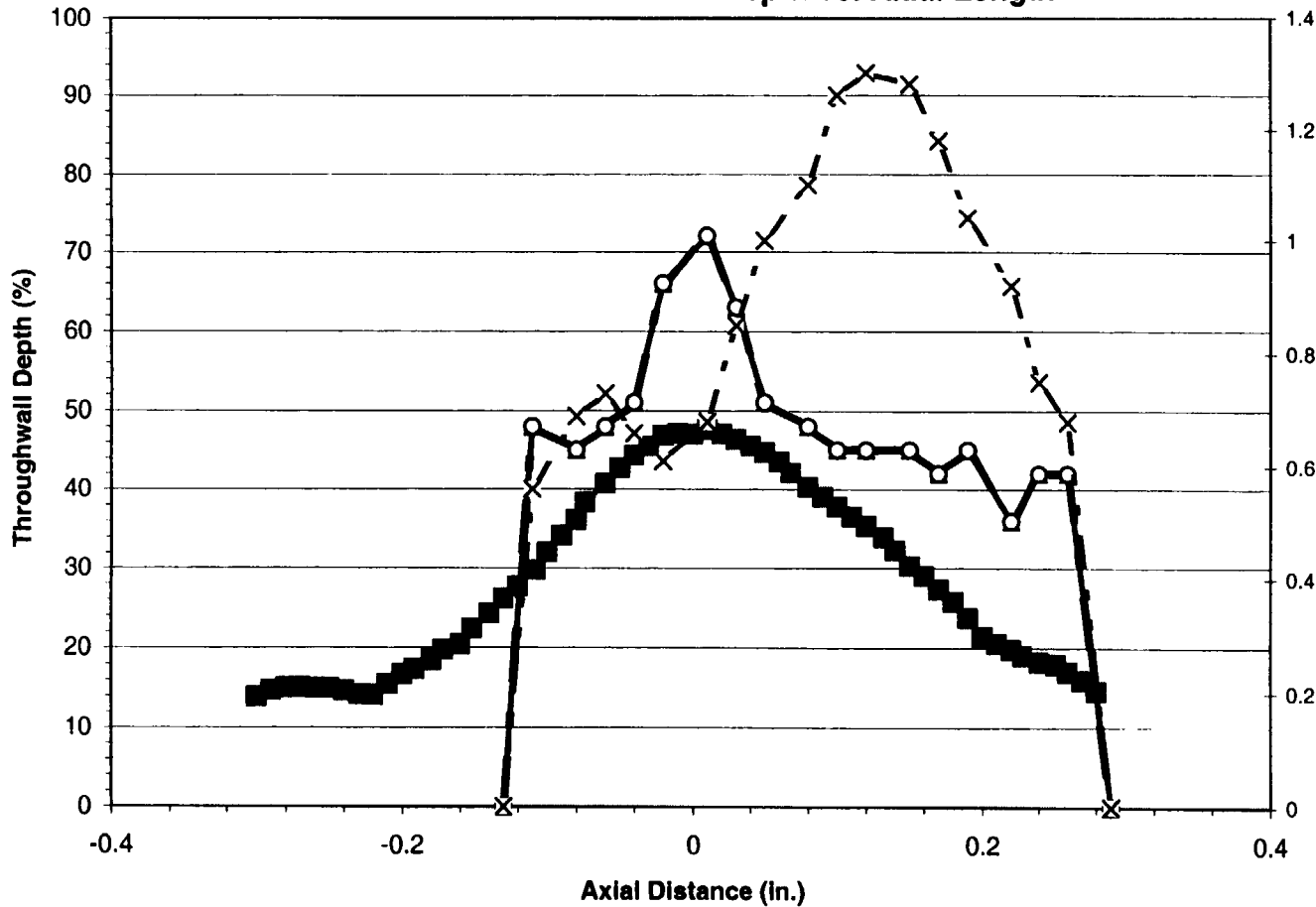
Unadjusted		
	T9093	Exam
Length	0.42	0.58
Max. Volts	1.30	
Max. Depth (%)	72.0	47.6
Avg. Depth (%)	46.2	29.0

Adjusted		
	T9093	Exam
Length	0.42	0.58
Max. Volts	1.30	
Max. Depth (%)	72.0	47.6
Avg. Depth (%)	46.2	29.0

Burst		
	T9093	Exam
Length	0.42	0.58
Max. Volts	1.30	
Max. Depth (%)	72.0	47.6
Avg. Depth (%)	46.2	29.0

- ⌂ - Analyst T9093 - Unadjusted —◇— Analyst T9093 - Adjusted ━━O •Analyst T9093 - Burst
—□—Exam ━■- ·Exam - Burst —X- ·Analyst T9093 - Voltage

Figure D-32
Specimen R 21 - C 31 - 01H - Crack 1 - Year 1998
Comparison of Unadjusted, Adjusted, Burst and Voltage with Exam
NDE Depth vs. Axial Length

PWSCC ARC Release 1.1
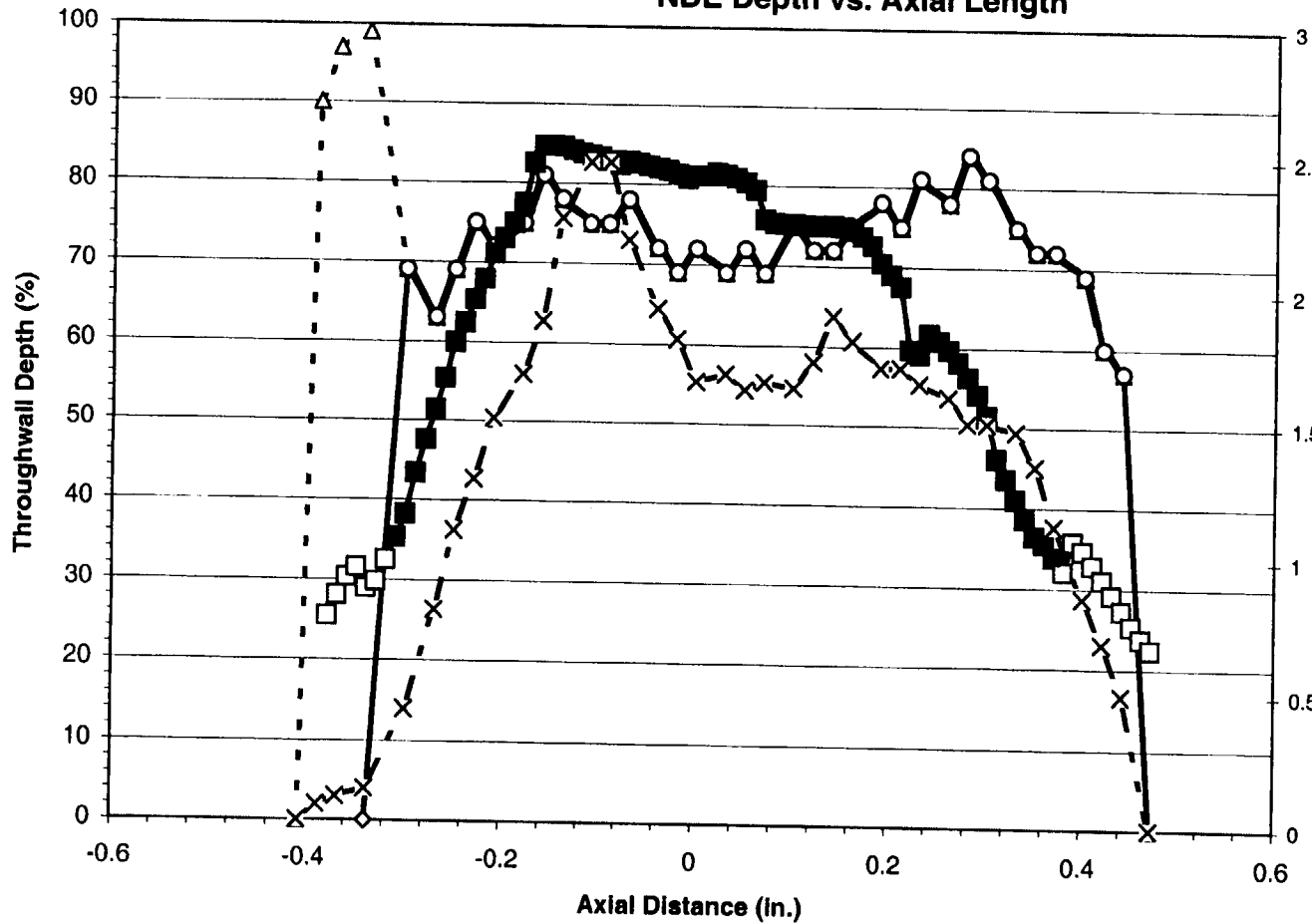
Unadjusted		
	T9093	Exam
Length	0.88	0.85
Max. Volts	2.48	
Max. Depth (%)	99.0	84.6
Avg. Depth (%)	73.0	60.9

Adjusted		
	T9093	Exam
Length	0.81	0.85
Max. Volts	2.48	
Max. Depth (%)	84.0	84.6
Avg. Depth (%)	69.8	60.9

Burst		
	T9093	Exam
Length	0.74	0.68
Max. Volts	2.48	
Max. Depth (%)	84.0	84.6
Avg. Depth (%)	73.4	68.6

Legend:
- △ - Analyst T9093 - Unadjusted
- ◇ - Analyst T9093 - Adjusted
- O Analyst T9093 - Burst
- □ Exam
- ■ Exam - Burst
- X - Analyst T9093 - Voltage

6/30/003:18 PM

Figure D-33
Specimen R 21 - C 31 - 01H - Crack 2 - Year 1998
Comparison of Unadjusted, Adjusted, Burst and Voltage with Exam
NDE Depth vs. Axial Length

PWSCC ARC Release 1.1
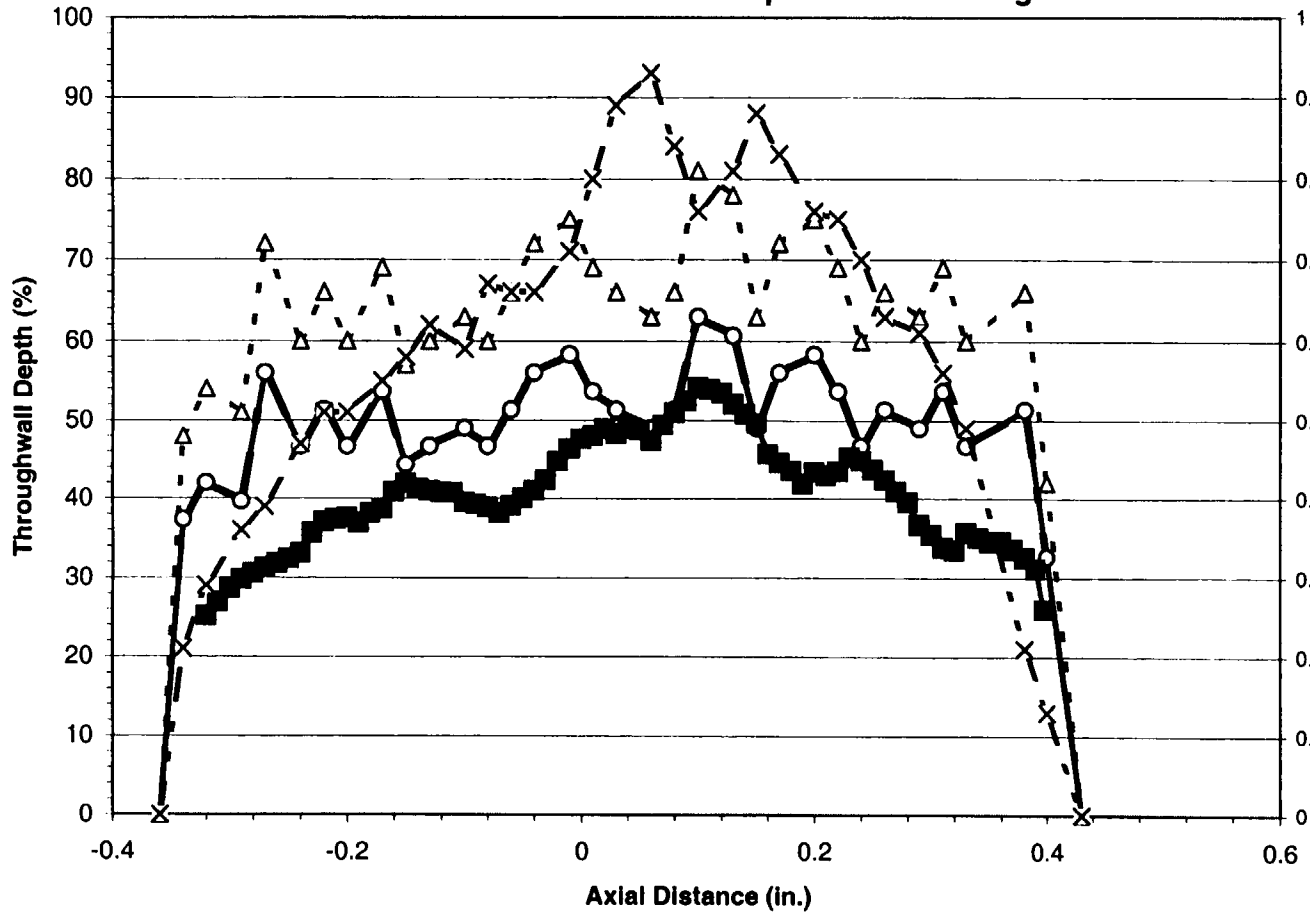
Unadjusted		
	T9093	Exam
Length	0.79	0.72
Max. Volts	0.93	
Max. Depth (%)	81.0	54.1
Avg. Depth (%)	62.4	40.7

Adjusted		
	T9093	Exam
Length	0.79	0.72
Max. Volts	0.93	
Max. Depth (%)	63.0	54.1
Avg. Depth (%)	48.6	40.7

Burst		
	T9093	Exam
Length	0.74	0.72
Max. Volts	0.93	
Max. Depth (%)	63.0	54.1
Avg. Depth (%)	50.7	40.7

Legend: - △ - Analyst T9093 - Unadjusted —◇— Analyst T9093 - Adjusted —○ •Analyst T9093 - Burst —□—Exam —■- ·Exam - Burst —X- ·Analyst T9093 - Voltage

Figure D-34
Specimen R 21 - C 73 - 01H - Crack 1 - Year 1998
Comparison of Unadjusted, Adjusted, Burst and Voltage with Exam
NDE Depth vs. Axial Length

PWSCC ARC Release 1.1
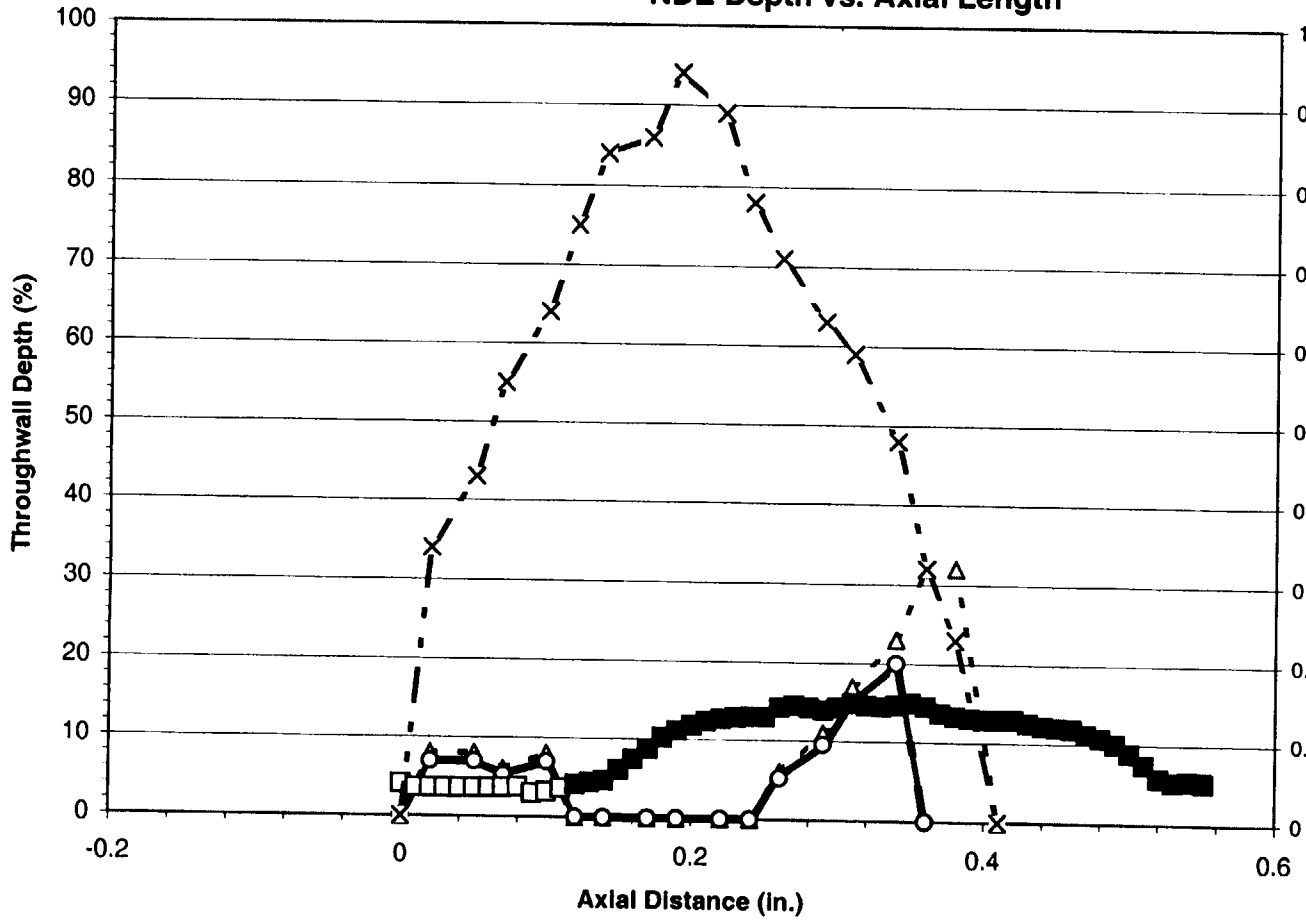
Unadjusted		
	T9093	Exam
Length	0.41	0.55
Max. Volts	0.94	
Max. Depth (%)	32.0	15.0
Avg. Depth (%)	8.8	9.6

Adjusted		
	T9093	Exam
Length	0.36	0.55
Max. Volts	0.94	
Max. Depth (%)	20.0	15.0
Avg. Depth (%)	5.3	9.6

Burst		
	T9093	Exam
Length	0.36	0.43
Max. Volts	0.94	
Max. Depth (%)	20.0	15.0
Avg. Depth (%)	5.3	11.2

- △ - Analyst T9093 - Unadjusted ◇ Analyst T9093 - Adjusted ◯ •Analyst T9093 - Burst
□ Exam ■ ·Exam - Burst ✕ ·Analyst T9093 - Voltage

Figure D-35
Specimen R 21 - C 79 - 01H - Crack 1 - Year 1998
Comparison of Unadjusted, Adjusted, Burst and Voltage with Exam
NDE Depth vs. Axial Length

PWSCC ARC Release 1.1
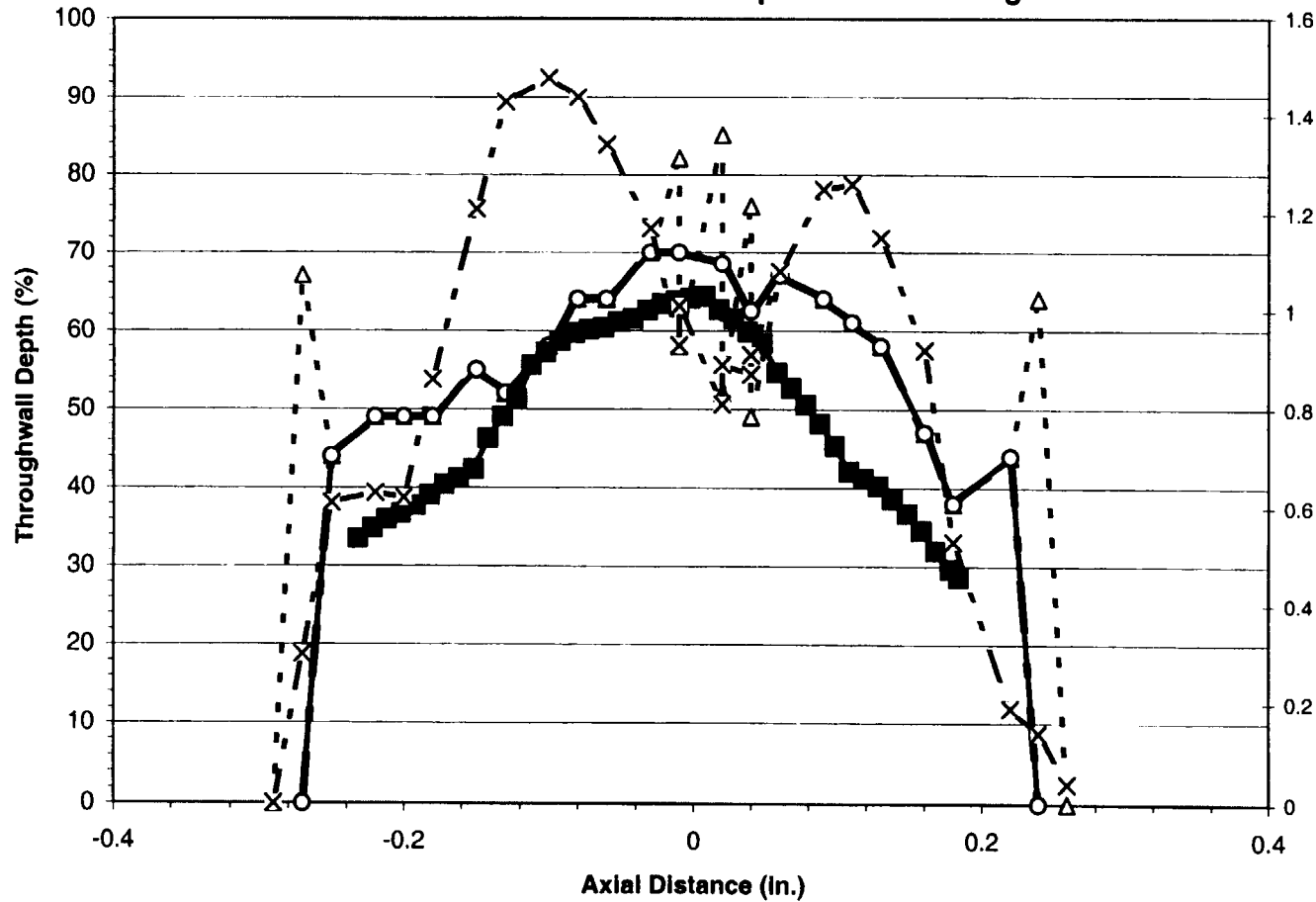
Unadjusted		
	T9093	Exam
Length	0.55	0.42
Max. Volts	1.48	
Max. Depth (%)	85.0	64.3
Avg. Depth (%)	54.9	49.4

Adjusted		
	T9093	Exam
Length	0.51	0.42
Max. Volts	1.48	
Max. Depth (%)	70.0	64.3
Avg. Depth (%)	54.1	49.4

Burst		
	T9093	Exam
Length	0.51	0.42
Max. Volts	1.48	
Max. Depth (%)	70.0	64.3
Avg. Depth (%)	54.1	49.4

Legend:
- △ - Analyst T9093 - Unadjusted —◇— Analyst T9093 - Adjusted —O ▪Analyst T9093 - Burst
- —□— Exam —■- ·Exam - Burst —X- ·Analyst T9093 - Voltage

Figure D-36
Specimen R 21 - C 85 - 01H - Crack 1 - Year 1998
Comparison of Unadjusted, Adjusted, Burst and Voltage with Exam
NDE Depth vs. Axial Length

PWSCC ARC Release 1.1
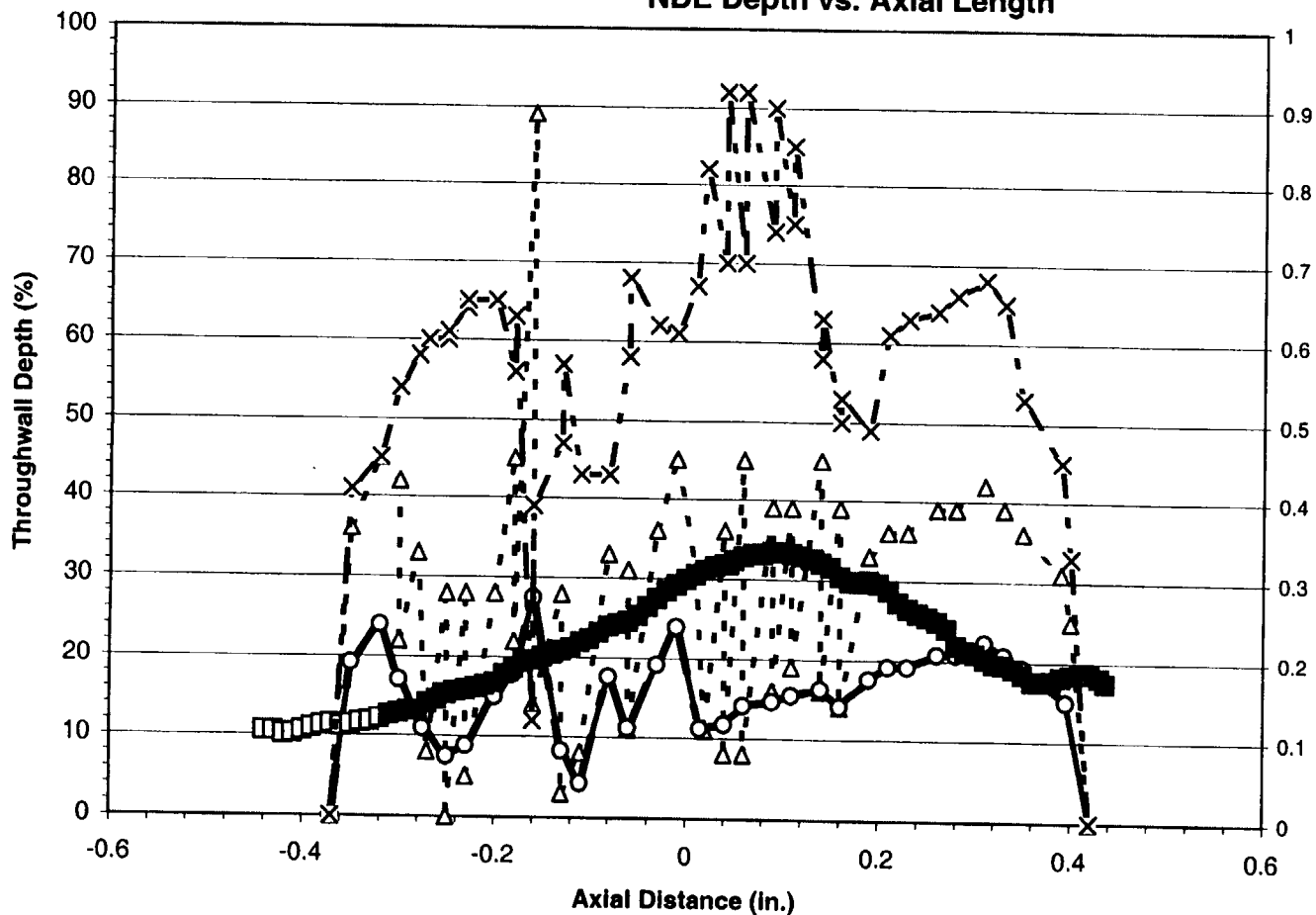
Unadjusted		
	T9093	Exam
Length	0.79	0.88
Max. Volts	0.92	
Max. Depth (%)	89.0	33.4
Avg. Depth (%)	29.0	21.8

Adjusted		
	T9093	Exam
Length	0.79	0.88
Max. Volts	0.82	
Max. Depth (%)	27.5	33.4
Avg. Depth (%)	15.8	21.8

Burst		
	T9093	Exam
Length	0.77	0.75
Max. Volts	0.82	
Max. Depth (%)	27.5	33.4
Avg. Depth (%)	16.1	23.6

Legend:
- Δ - Analyst T9093 - Unadjusted
—◇— Analyst T9093 - Adjusted
—O— Analyst T9093 - Burst
—□— Exam
—■- Exam - Burst
—X- Analyst T9093 - Voltage

Figure D-37
Specimen R 23 - C 15 - 01H - Crack 1 - Year 1998
Comparison of Unadjusted, Adjusted, Burst and Voltage with Exam
NDE Depth vs. Axial Length

PWSCC ARC Release 1.1
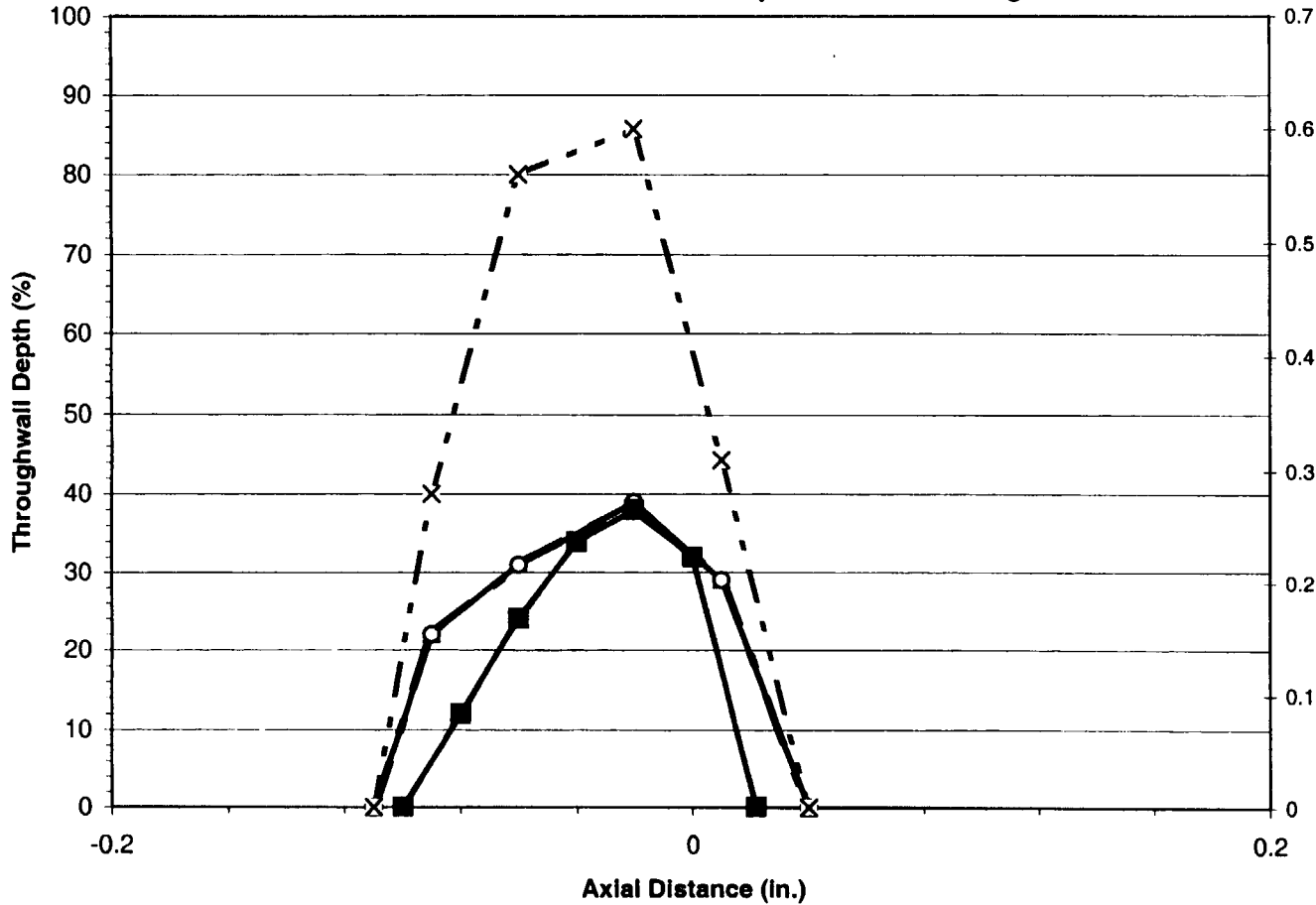
Unadjusted		
	T9093	Exam
Length	0.15	0.12
Max. Volts	0.60	
Max. Depth (%)	39.0	38.0
Avg. Depth (%)	25.8	23.2

Adjusted		
	T9093	Exam
Length	0.15	0.12
Max. Volts	0.60	
Max. Depth (%)	39.0	38.0
Avg. Depth (%)	25.8	23.2

Burst		
	T9093	Exam
Length	0.15	0.12
Max. Volts	0.60	
Max. Depth (%)	39.0	38.0
Avg. Depth (%)	25.8	23.2

- ◬ - Analyst T9093 - Unadjusted ◇ Analyst T9093 - Adjusted ○ Analyst T9093 - Burst
  □ Exam ■ Exam - Burst X Analyst T9093 - Voltage

Figure D-38
Specimen R 25 - C 40 - 01H - Crack 1 - Year 1998
Comparison of Unadjusted, Adjusted, Burst and Voltage with Exam
NDE Depth vs. Axial Length

PWSCC ARC Release 1.1
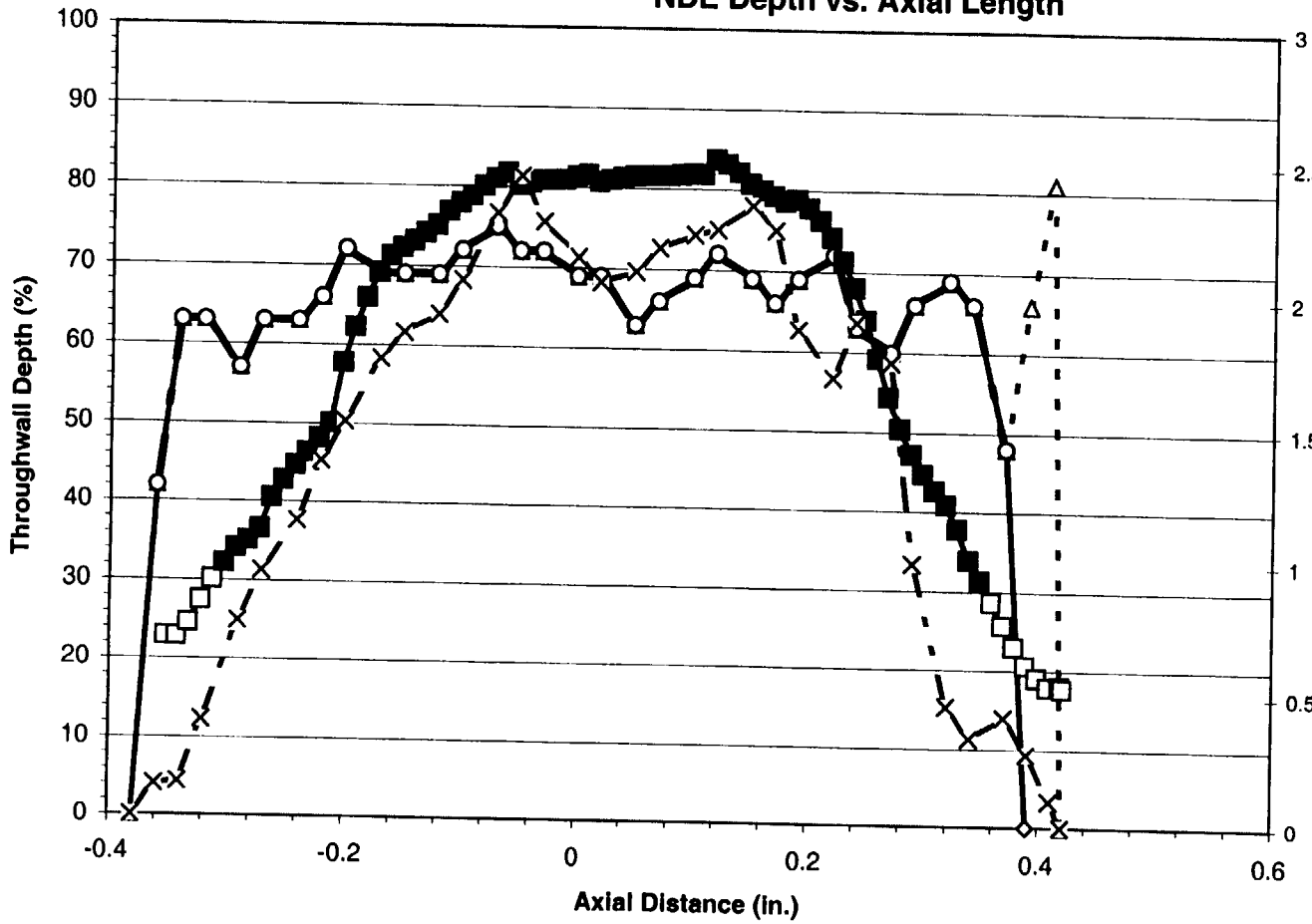
Unadjusted		
	T9093	Exam
Length	0.80	0.77
Max. Volts	2.44	
Max. Depth (%)	81.0	83.7
Avg. Depth (%)	65.1	60.5

Adjusted		
	T9093	Exam
Length	0.77	0.77
Max. Volts	2.44	
Max. Depth (%)	75.0	83.7
Avg. Depth (%)	64.3	60.5

Burst		
	T9093	Exam
Length	0.73	0.65
Max. Volts	2.44	
Max. Depth (%)	75.0	83.7
Avg. Depth (%)	66.6	67.4

- ◁ - Analyst T9093 - Unadjusted ──◇── Analyst T9093 - Adjusted ──O- ▪Analyst T9093 - Burst
──□── Exam ──■- ᐧExam - Burst ──X- ᐧAnalyst T9093 - Voltage

6/30/003:18 PM

Figure D-39
Specimen R 25 - C 52 - 01H - Crack 1 - Year 1998
Comparison of Unadjusted, Adjusted, Burst and Voltage with Exam
NDE Depth vs. Axial Length

PWSCC ARC Release 1.1
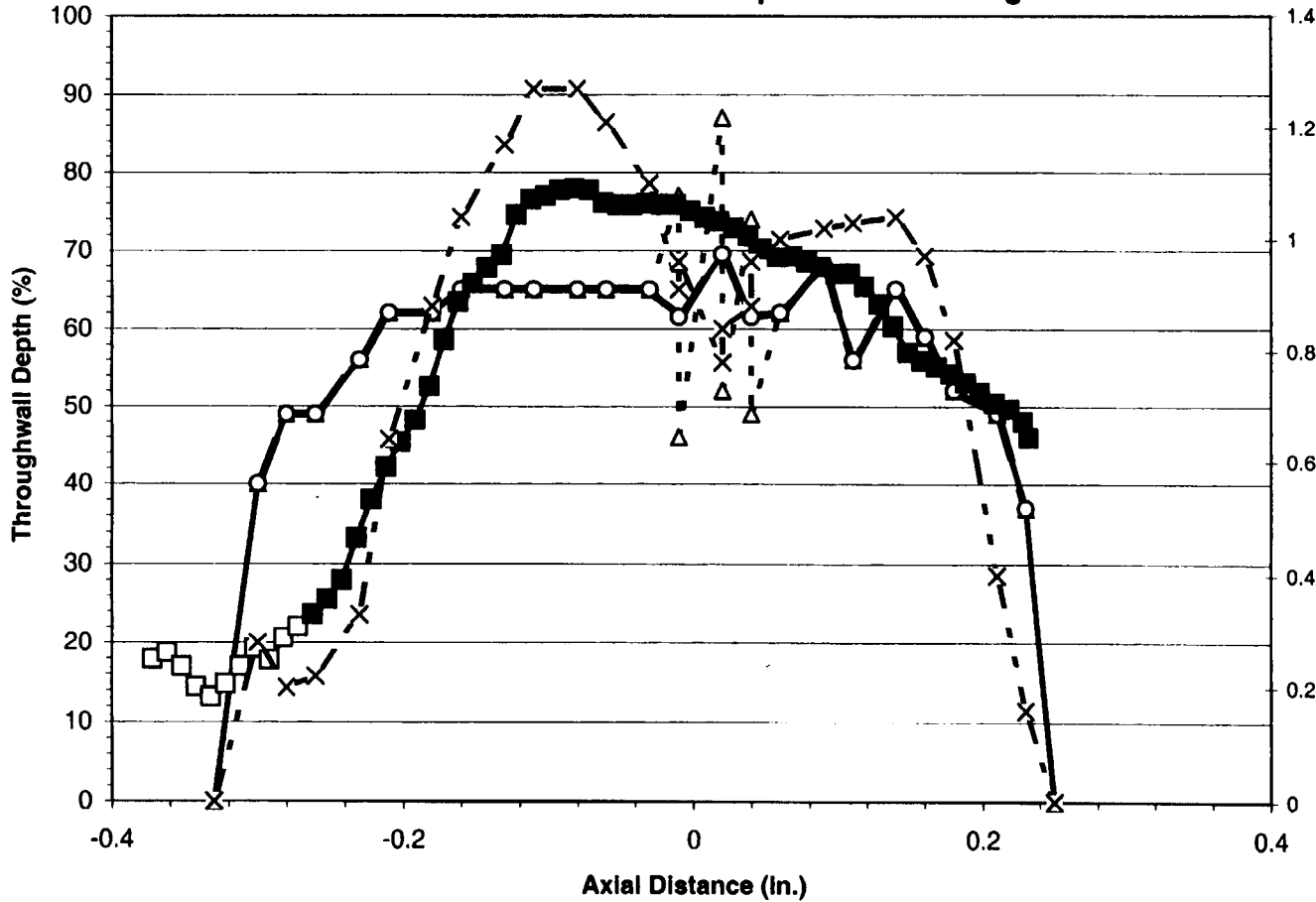
Unadjusted	T9093	Exam
Length	0.58	0.60
Max. Volts	1.27	
Max. Depth (%)	87.0	77.9
Avg. Depth (%)	56.6	54.1

Adjusted	T9093	Exam
Length	0.58	0.60
Max. Volts	1.27	
Max. Depth (%)	69.5	77.9
Avg. Depth (%)	56.3	54.1

Burst	T9093	Exam
Length	0.53	0.49
Max. Volts	1.27	
Max. Depth (%)	69.5	77.9
Avg. Depth (%)	59.8	62.2

Figure D-40
Specimen R 25 - C 79 - 01H - Crack 1 - Year 1998
Comparison of Unadjusted, Adjusted, Burst and Voltage with Exam
NDE Depth vs. Axial Length

PWSCC ARC Release 1.1
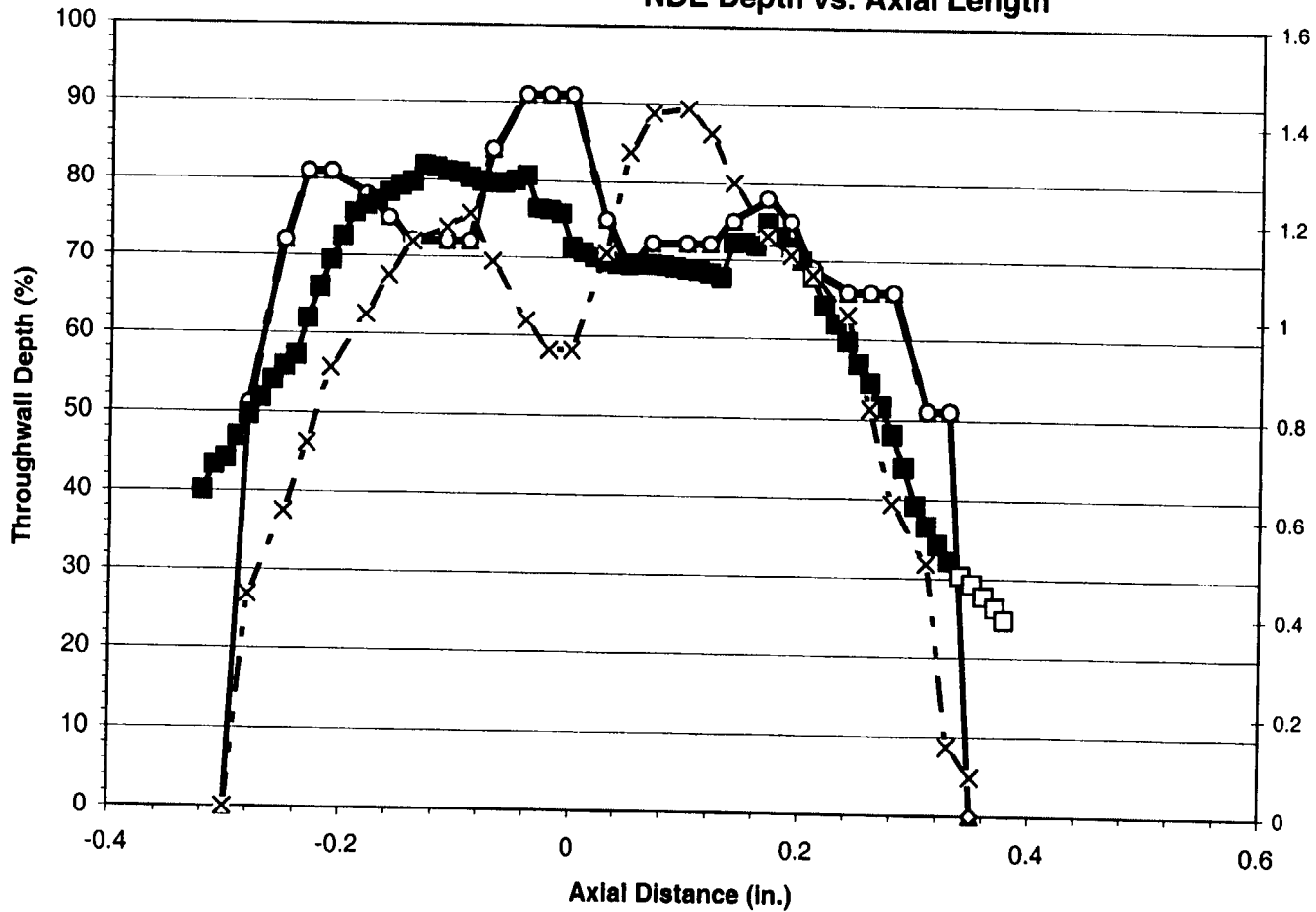
Unadjusted		
	T9093	Exam
Length	0.65	0.70
Max. Volts	1.43	
Max. Depth (%)	91.0	81.8
Avg. Depth (%)	70.7	63.6

Adjusted		
	T9093	Exam
Length	0.65	0.70
Max. Volts	1.43	
Max. Depth (%)	91.0	81.8
Avg. Depth (%)	70.7	63.6

Burst		
	T9093	Exam
Length	0.61	0.65
Max. Volts	1.43	
Max. Depth (%)	91.0	81.8
Avg. Depth (%)	73.6	66.2

Legend:
- Δ - Analyst T9093 - Unadjusted
- ◇ Analyst T9093 - Adjusted
- O Analyst T9093 - Burst
- □ Exam
- ■ Exam - Burst
- X - Analyst T9093 - Voltage

6/30/003:18 PM

Figure D-41
Specimen R 27 - C 77 - 01H - Crack 1 - Year 1998
Comparison of Unadjusted, Adjusted, Burst and Voltage with Exam
NDE Depth vs. Axial Length

PWSCC ARC Release 1.1
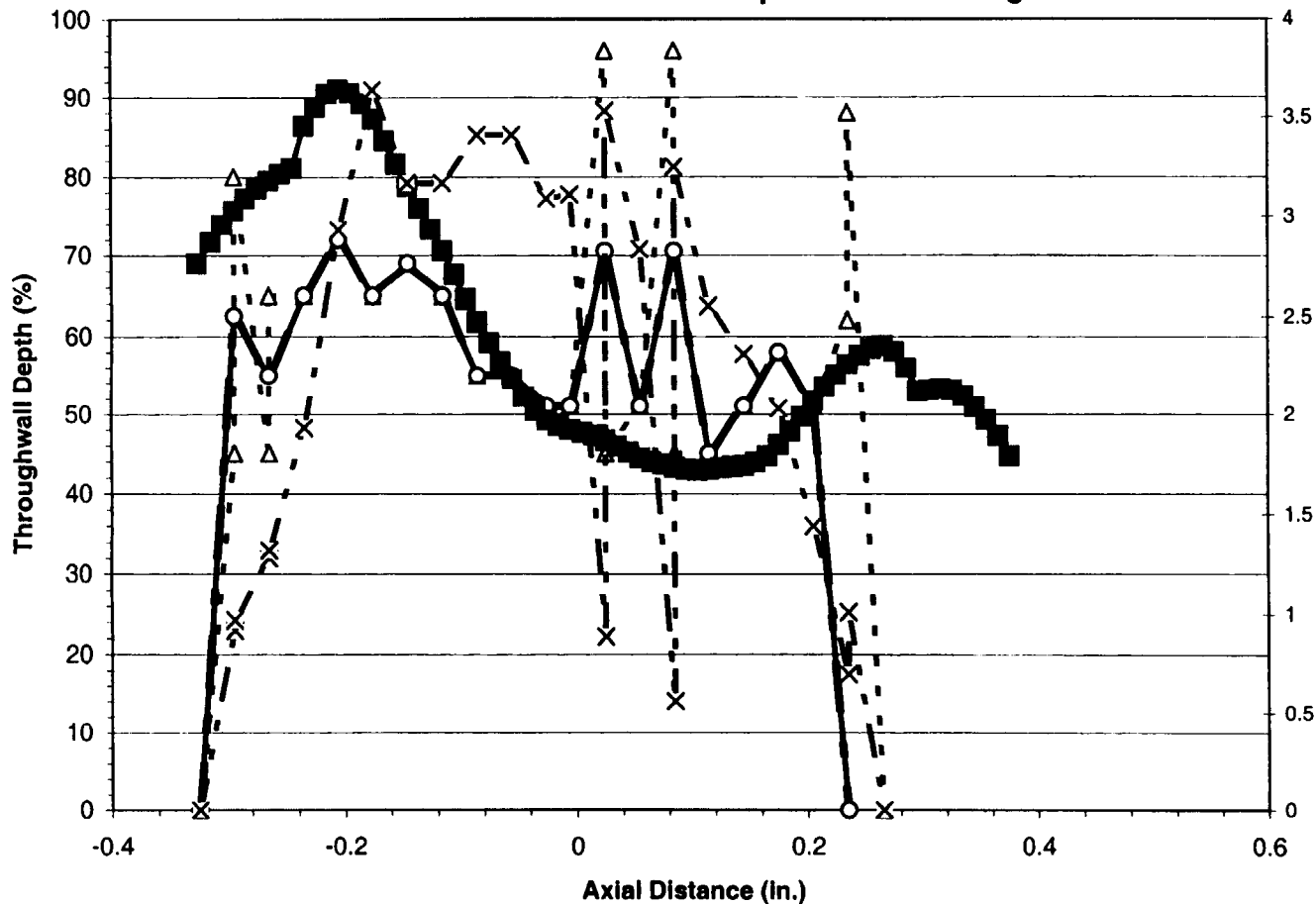
Unadjusted		
	T9093	Exam
Length	0.59	0.70
Max. Volts	3.64	
Max. Depth (%)	96.0	91.1
Avg. Depth (%)	57.0	59.9

Adjusted		
	T9093	Exam
Length	0.56	0.70
Max. Volts	3.64	
Max. Depth (%)	72.0	91.1
Avg. Depth (%)	56.0	59.9

Burst		
	T9093	Exam
Length	0.56	0.70
Max. Volts	3.64	
Max. Depth (%)	72.0	91.1
Avg. Depth (%)	56.0	59.9

Legend:
- △ - Analyst T9093 - Unadjusted
- ◇ - Analyst T9093 - Adjusted
- ○ - Analyst T9093 - Burst
- □ - Exam
- ■ - Exam - Burst
- X - Analyst T9093 - Voltage

Figure D-42
Specimen R 29 - C 34 - 01H - Crack 1 - Year 1998
Comparison of Unadjusted, Adjusted, Burst and Voltage with Exam
NDE Depth vs. Axial Length

PWSCC ARC Release 1.1
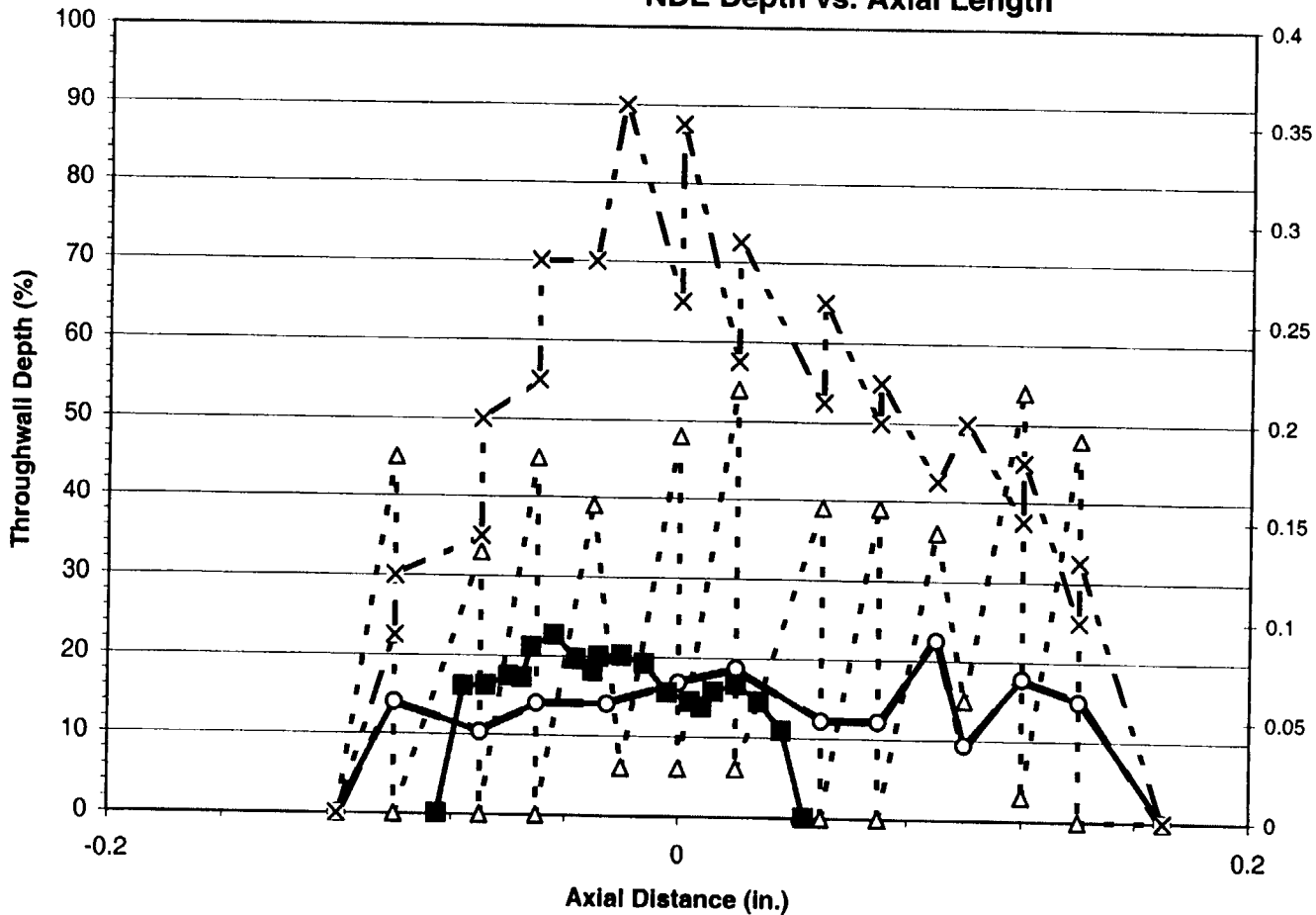
Unadjusted		
	T9093	Exam
Length	0.29	0.13
Max. Volts	0.36	
Max. Depth (%)	54.0	22.7
Avg. Depth (%)	20.9	16.1

Adjusted		
	T9093	Exam
Length	0.29	0.13
Max. Volts	0.32	
Max. Depth (%)	22.5	22.7
Avg. Depth (%)	13.4	16.1

Burst		
	T9093	Exam
Length	0.29	0.13
Max. Volts	0.32	
Max. Depth (%)	22.5	22.7
Avg. Depth (%)	13.4	16.1

- ◬ - Analyst T9093 - Unadjusted   —◇—Analyst T9093 - Adjusted   —O ▪Analyst T9093 - Burst
—□—Exam   —▪- ʹExam - Burst   —X- ʹAnalyst T9093 - Voltage

Figure D-43
Specimen R 29 - C 16 - 01H - Crack 1 - Year 1998
Comparison of Unadjusted, Adjusted, Burst and Voltage with Exam
NDE Depth vs. Axial Length

PWSCC ARC Release 1.1
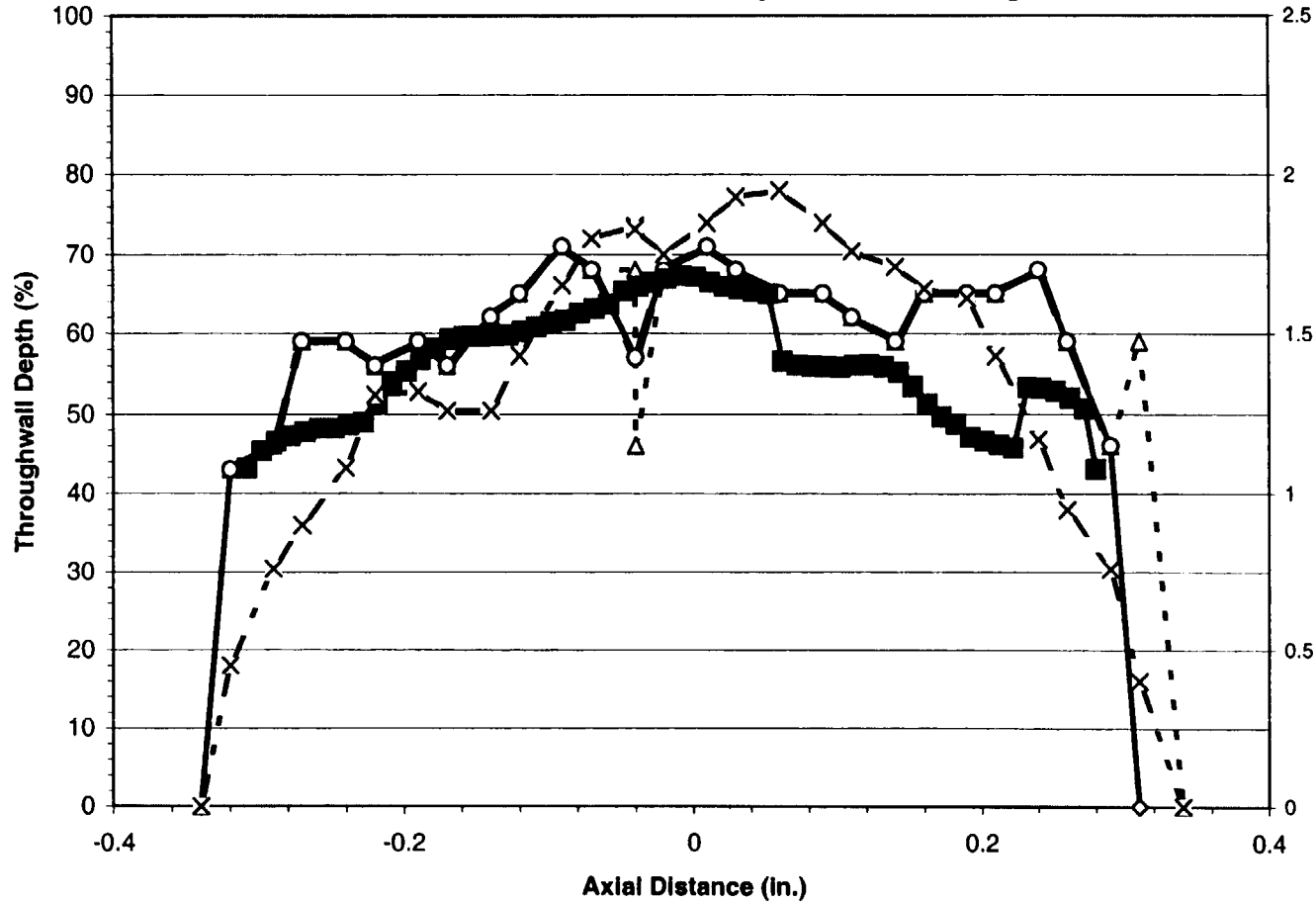
Unadjusted		
	T9093	Exam
Length	0.68	0.59
Max. Volts	1.95	
Max. Depth (%)	71.0	67.3
Avg. Depth (%)	58.7	56.1

Adjusted		
	T9093	Exam
Length	0.65	0.59
Max. Volts	1.95	
Max. Depth (%)	71.0	67.3
Avg. Depth (%)	59.2	56.1

Burst		
	T9093	Exam
Length	0.61	0.59
Max. Volts	1.95	
Max. Depth (%)	71.0	67.3
Avg. Depth (%)	61.7	56.1

Legend: Analyst T9093 - Unadjusted; Analyst T9093 - Adjusted; Analyst T9093 - Burst; Exam; Exam - Burst; Analyst T9093 - Voltage

Figure D-44
Specimen R 29 - C 41 - 01H - Crack 1 - Year 1998
Comparison of Unadjusted, Adjusted, Burst and Voltage with Exam
NDE Depth vs. Axial Length

PWSCC ARC Release 1.1
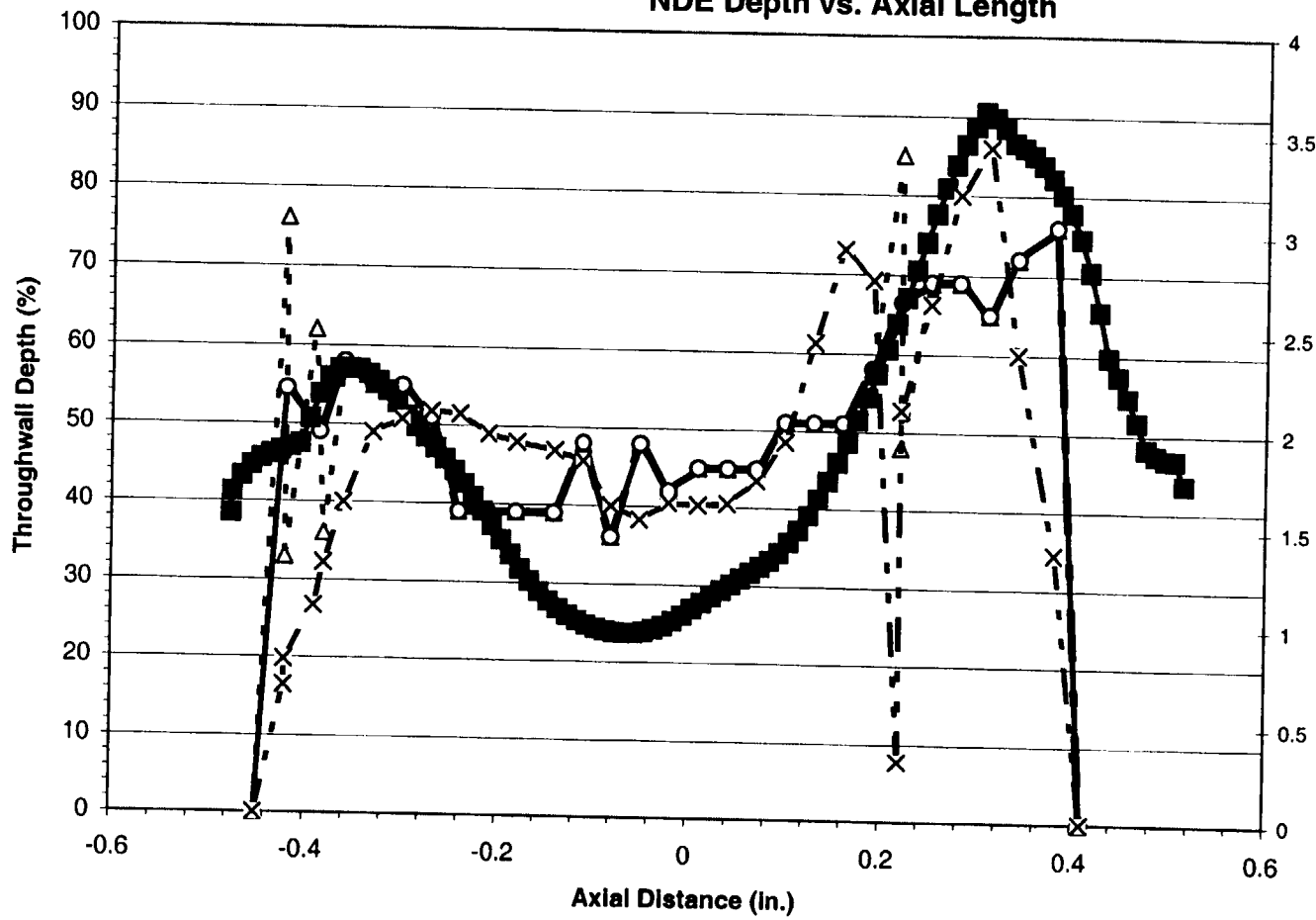
Unadjusted		
	T9093	Exam
Length	0.86	0.99
Max. Volts	3.44	
Max. Depth (%)	85.0	90.5
Avg. Depth (%)	50.7	49.3

Adjusted		
	T9093	Exam
Length	0.86	0.99
Max. Volts	3.44	
Max. Depth (%)	76.0	90.5
Avg. Depth (%)	50.7	49.3

Burst		
	T9093	Exam
Length	0.83	0.99
Max. Volts	3.44	
Max. Depth (%)	76.0	90.5
Avg. Depth (%)	51.5	49.3

Legend:
- △ - Analyst T9093 - Unadjusted —◇—Analyst T9093 - Adjusted —O— ·Analyst T9093 - Burst
- □—Exam —■- ·Exam - Burst —X- ·Analyst T9093 - Voltage

6/30/003:18 PM

Figure D-45
Specimen R 29 - C 41 - 01H - Crack 2 - Year 1998
Comparison of Unadjusted, Adjusted, Burst and Voltage with Exam
NDE Depth vs. Axial Length

PWSCC ARC Release 1.1
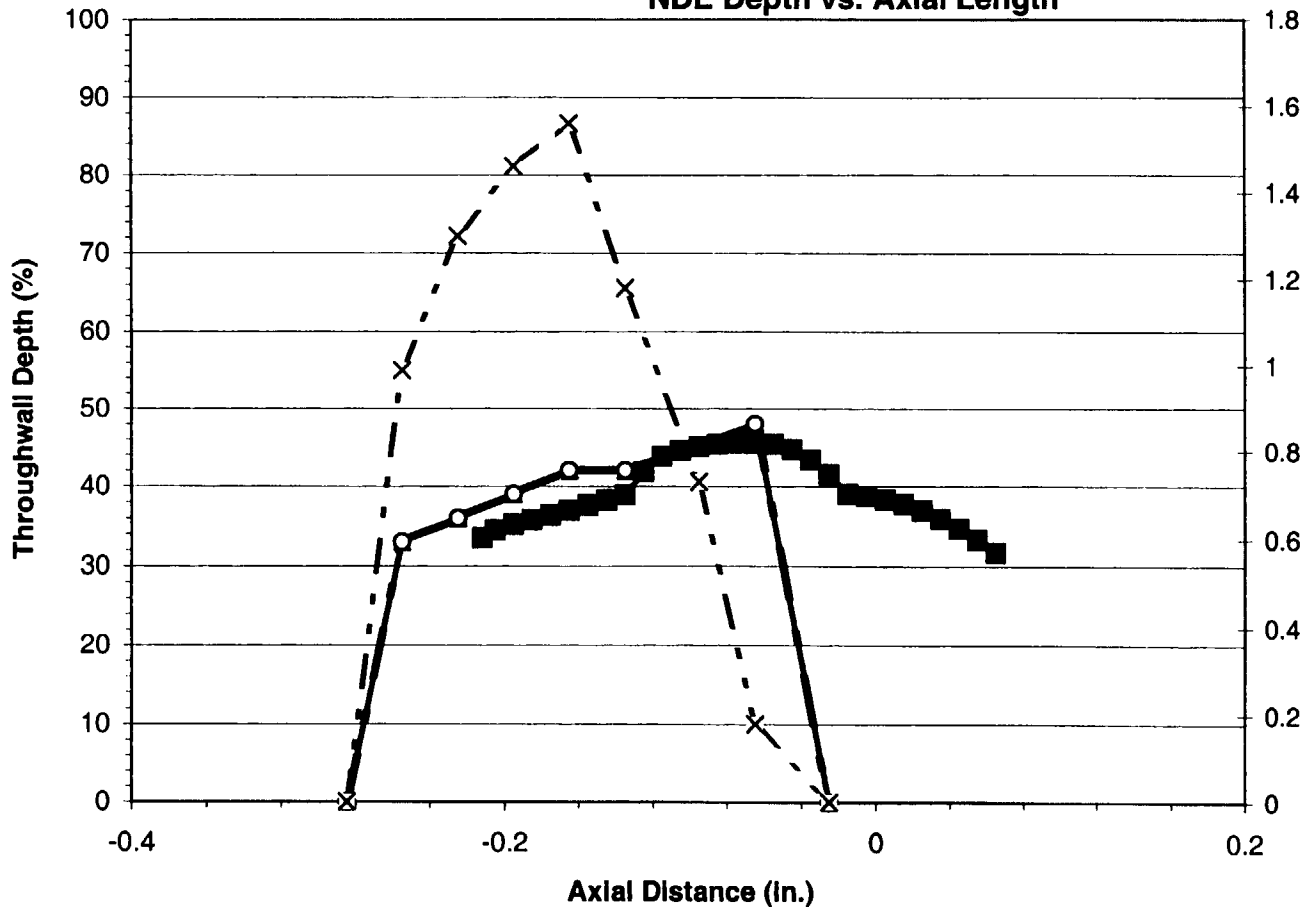
Unadjusted		
	T9093	Exam
Length	0.26	0.28
Max. Volts	1.56	
Max. Depth (%)	48.0	45.5
Avg. Depth (%)	35.5	39.6

Adjusted		
	T9093	Exam
Length	0.26	0.28
Max. Volts	1.56	
Max. Depth (%)	48.0	45.5
Avg. Depth (%)	35.5	39.6

Burst		
	T9093	Exam
Length	0.26	0.28
Max. Volts	1.56	
Max. Depth (%)	48.0	45.5
Avg. Depth (%)	35.5	39.6

- ▲ - Analyst T9093 - Unadjusted ◇ Analyst T9093 - Adjusted O Analyst T9093 - Burst
□ Exam ■ Exam - Burst X- Analyst T9093 - Voltage

Figure D-46
Specimen R 29 - C 67 - 01H - Crack 1 - Year 1998
Comparison of Unadjusted, Adjusted, Burst and Voltage with Exam
NDE Depth vs. Axial Length

PWSCC ARC Release 1.1
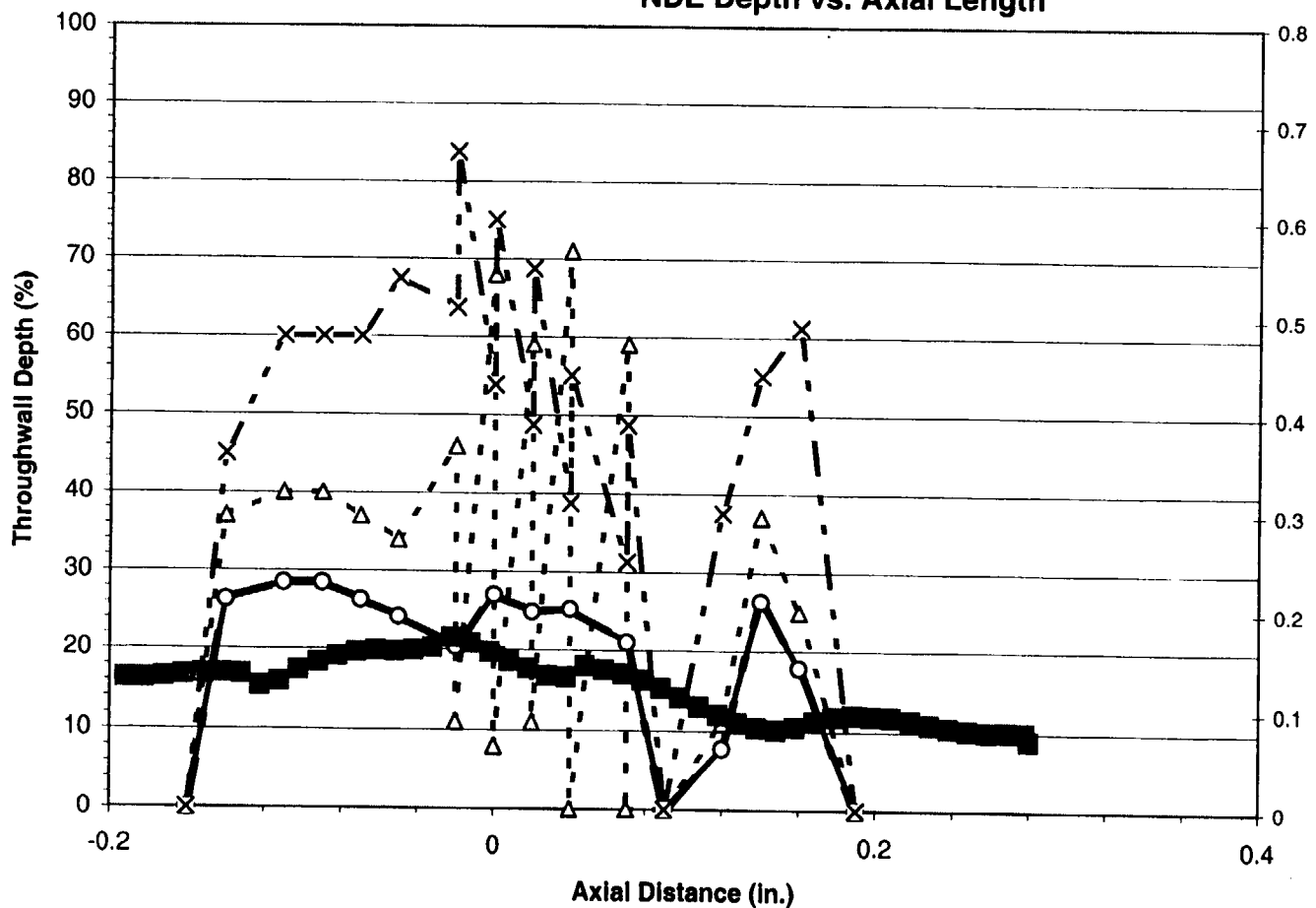
Unadjusted		
	T9093	Exam
Length	0.35	0.47
Max. Volts	0.67	
Max. Depth (%)	71.0	21.5
Avg. Depth (%)	28.0	15.2

Adjusted		
	T9093	Exam
Length	0.35	0.47
Max. Volts	0.59	
Max. Depth (%)	28.5	21.5
Avg. Depth (%)	19.9	15.2

Burst		
	T9093	Exam
Length	0.35	0.47
Max. Volts	0.59	
Max. Depth (%)	28.5	21.5
Avg. Depth (%)	19.9	15.2

- △ - Analyst T9093 - Unadjusted   ◇ Analyst T9093 - Adjusted   ○ Analyst T9093 - Burst
□ Exam   ■ Exam - Burst   X Analyst T9093 - Voltage

Figure D-47
Specimen R 30 - C 45 - 01H - Crack 1 - Year 1998
Comparison of Unadjusted, Adjusted, Burst and Voltage with Exam
NDE Depth vs. Axial Length

PWSCC ARC Release 1.1
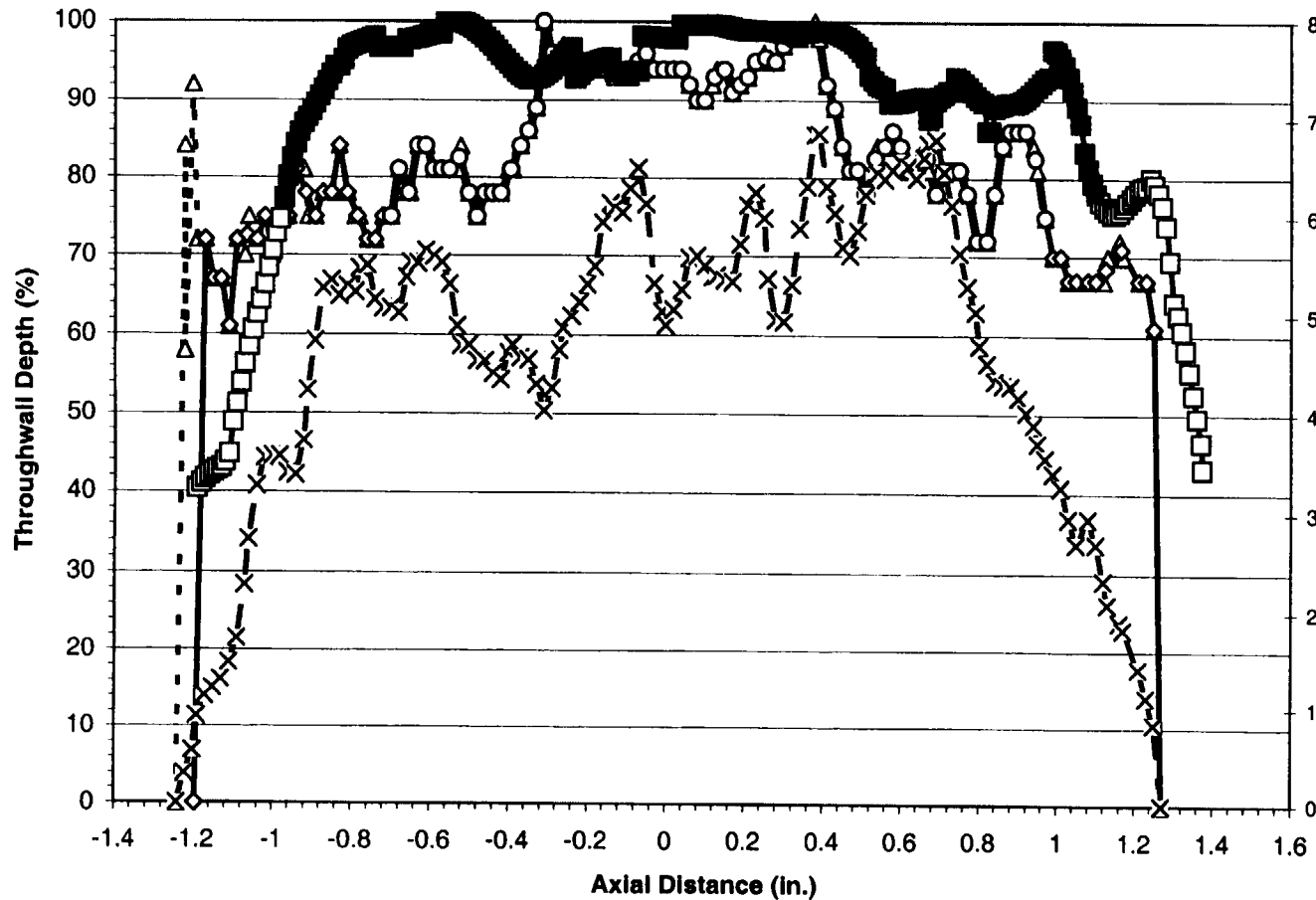
Unadjusted		
	T9093	Exam
Length	2.51	2.56
Max. Volts	6.85	
Max. Depth (%)	100.0	100.0
Avg. Depth (%)	81.5	88.7

Adjusted		
	T9093	Exam
Length	2.46	2.56
Max. Volts	6.84	
Max. Depth (%)	100.0	100.0
Avg. Depth (%)	81.5	88.7

Burst		
	T9093	Exam
Length	1.67	2.07
Max. Volts	6.84	
Max. Depth (%)	100.0	100.0
Avg. Depth (%)	87.1	94.6

Legend: Analyst T9093 - Unadjusted; Analyst T9093 - Adjusted; Analyst T9093 - Burst; Exam; Exam - Burst; Analyst T9093 - Voltage

Figure D-48
Specimen R 30 - C 45 - 01H - Crack 2 - Year 1998
Comparison of Unadjusted, Adjusted, Burst and Voltage with Exam
NDE Depth vs. Axial Length

PWSCC ARC Release 1.1
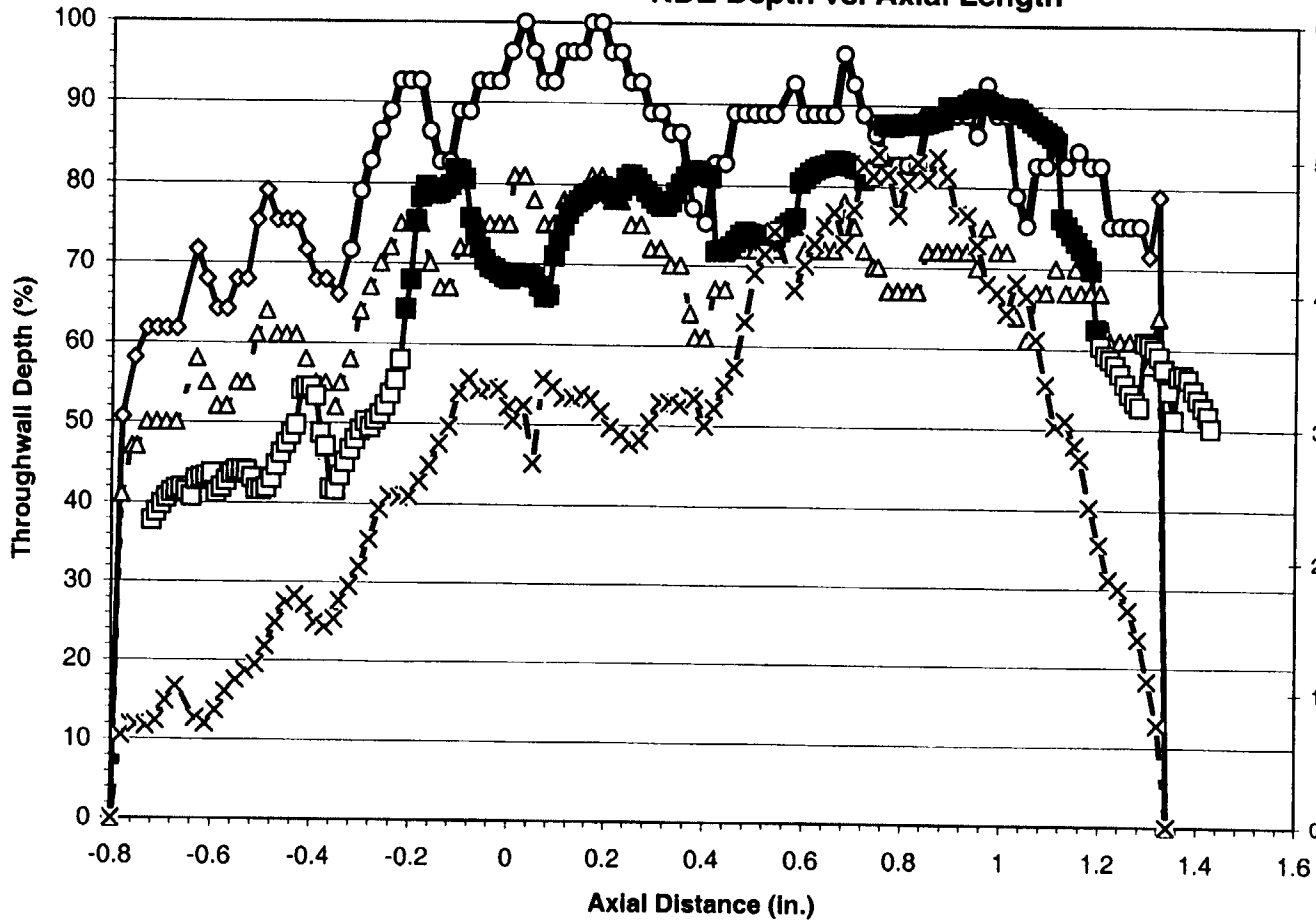
Unadjusted		
	T9093	Exam
Length	2.14	2.15
Max. Volts	5.04	
Max. Depth (%)	81.0	90.9
Avg. Depth (%)	66.5	69.0

Adjusted		
	T9093	Exam
Length	2.14	2.15
Max. Volts	5.02	
Max. Depth (%)	100.0	90.9
Avg. Depth (%)	82.2	69.0

Burst		
	T9093	Exam
Length	1.60	1.40
Max. Volts	5.02	
Max. Depth (%)	100.0	90.9
Avg. Depth (%)	87.8	79.5

- △ - Analyst T9093 - Unadjusted   —◇— Analyst T9093 - Adjusted   ●O ●Analyst T9093 - Burst
—□—Exam   ■- ·Exam - Burst   —X- ·Analyst T9093 - Voltage

Figure D-49
Specimen R 33 - C 34 - 01H - Crack 1 - Year 1998
Comparison of Unadjusted, Adjusted, Burst and Voltage with Exam
NDE Depth vs. Axial Length

PWSCC ARC Release 1.1
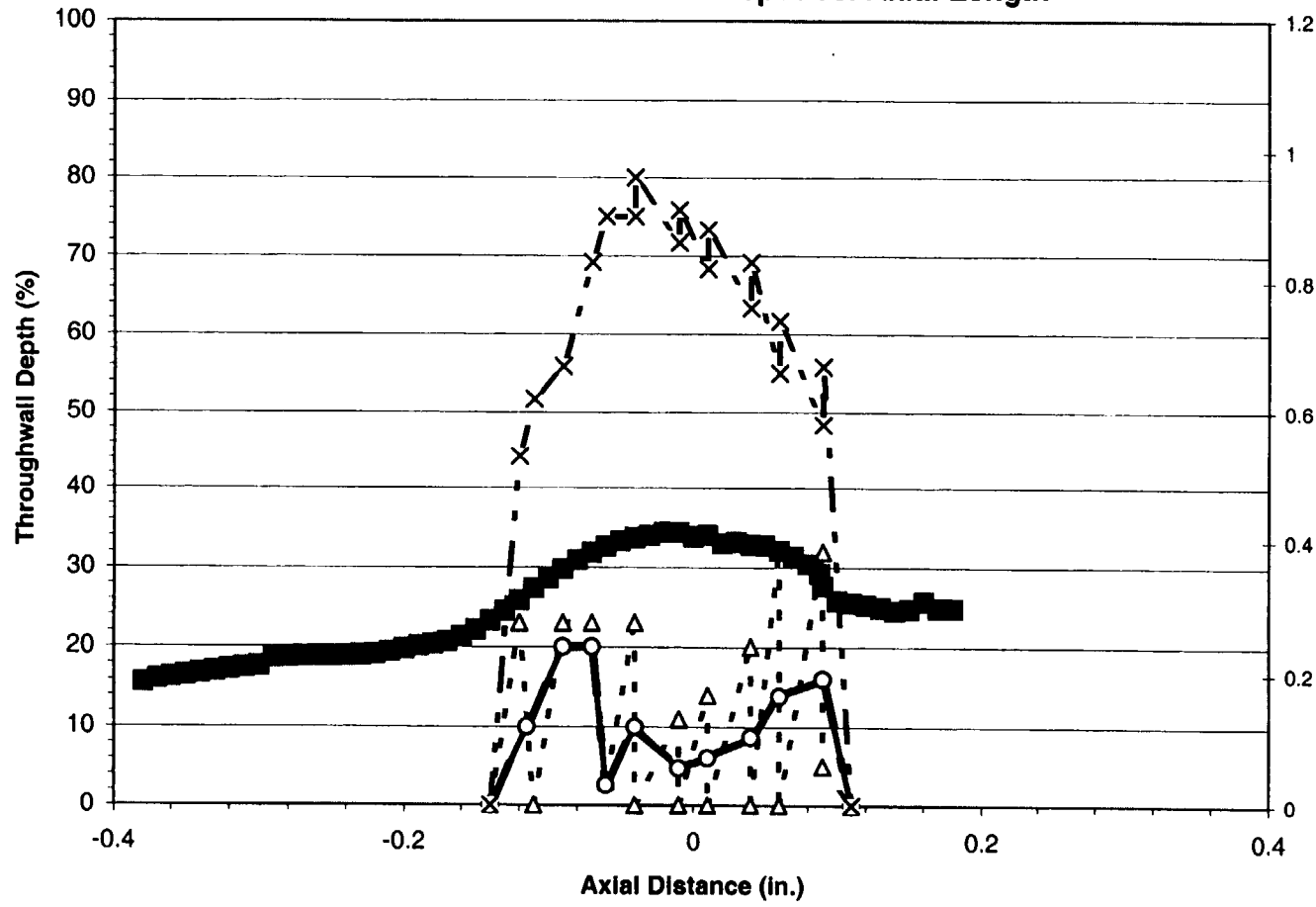
Unadjusted		
	T9093	Exam
Length	0.25	0.56
Max. Volts	0.96	
Max. Depth (%)	32.0	34.4
Avg. Depth (%)	11.6	24.9

Adjusted		
	T9093	Exam
Length	0.25	0.56
Max. Volts	0.93	
Max. Depth (%)	20.0	34.4
Avg. Depth (%)	10.1	24.9

Burst		
	T9093	Exam
Length	0.25	0.56
Max. Volts	0.93	
Max. Depth (%)	20.0	34.4
Avg. Depth (%)	10.1	24.9

Legend:
- △ - Analyst T9093 - Unadjusted   —◇— Analyst T9093 - Adjusted   —O— Analyst T9093 - Burst
—□— Exam   —■— Exam - Burst   —X— Analyst T9093 - Voltage

Figure D-50
Specimen R 33 - C 58 - 01H - Crack 1 - Year 1998
Comparison of Unadjusted, Adjusted, Burst and Voltage with Exam
NDE Depth vs. Axial Length

PWSCC ARC Release 1.1
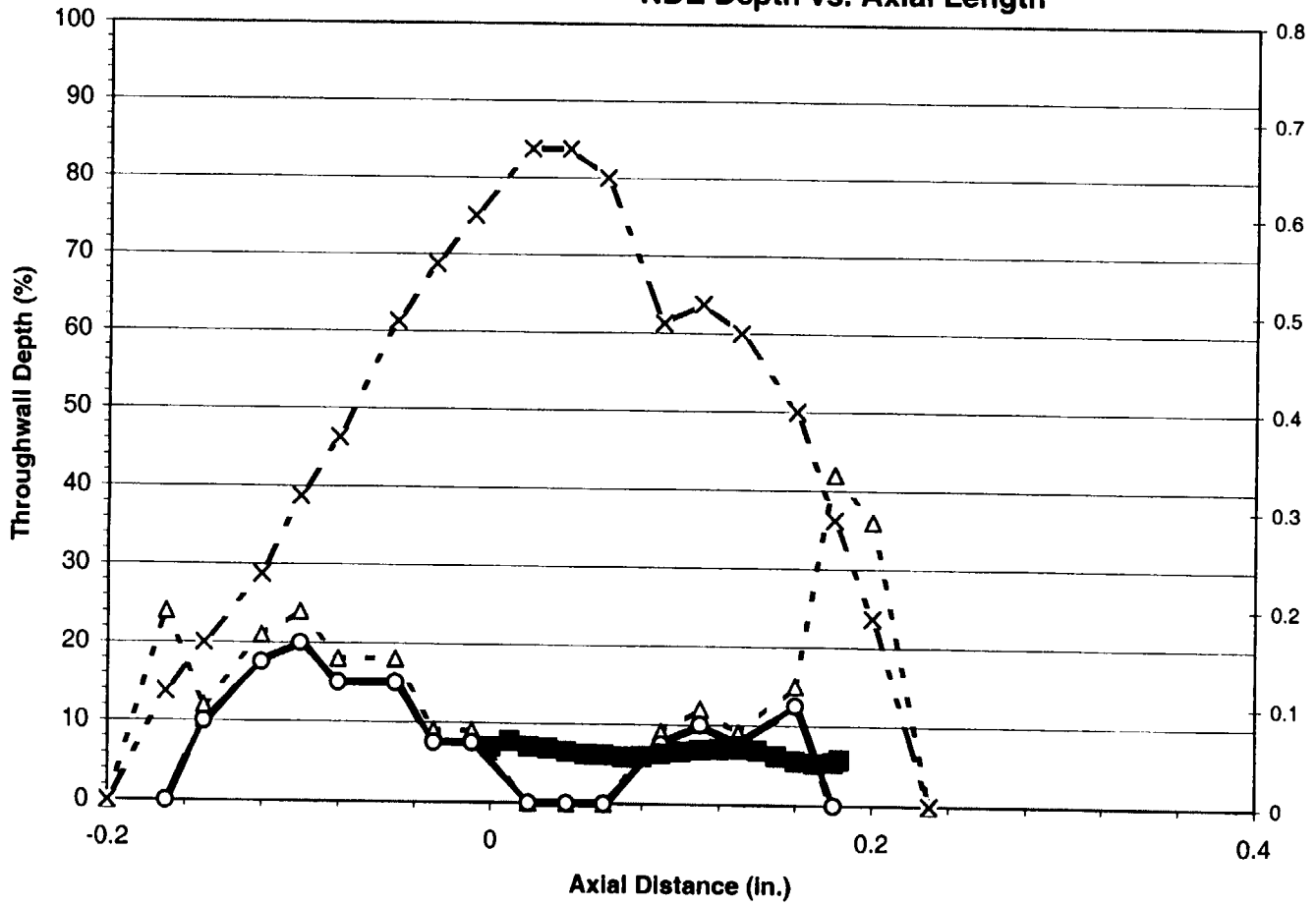
Unadjusted		
	T9093	Exam
Length	0.43	0.18
Max. Volts	0.67	
Max. Depth (%)	42.0	7.7
Avg. Depth (%)	14.0	6.4

Adjusted		
	T9093	Exam
Length	0.35	0.18
Max. Volts	0.67	
Max. Depth (%)	20.0	7.7
Avg. Depth (%)	8.7	6.4

Burst		
	T9093	Exam
Length	0.35	0.18
Max. Volts	0.67	
Max. Depth (%)	20.0	7.7
Avg. Depth (%)	8.7	6.4

- ◁ - Analyst T9093 - Unadjusted —◇—Analyst T9093 - Adjusted —O— Analyst T9093 - Burst
—□—Exam —■- Exam - Burst —X- Analyst T9093 - Voltage

Figure D-51
Specimen R 37 - C 31 - 01H - Crack 1 - Year 1998
Comparison of Unadjusted, Adjusted, Burst and Voltage with Exam
NDE Depth vs. Axial Length

PWSCC ARC Release 1.1
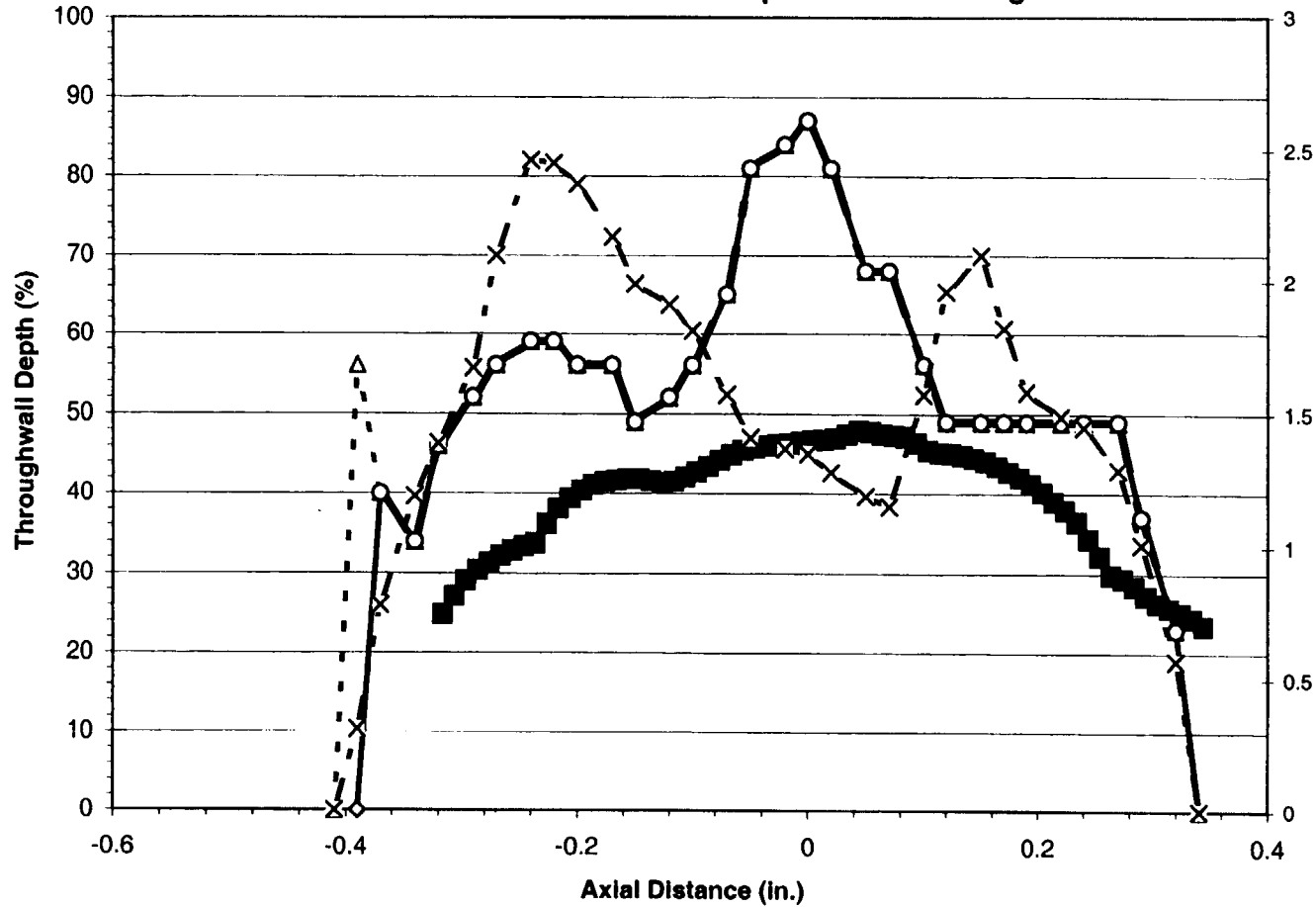
Unadjusted		
	T9093	Exam
Length	0.75	0.66
Max. Volts	2.46	
Max. Depth (%)	87.0	47.9
Avg. Depth (%)	53.8	39.4

Adjusted		
	T9093	Exam
Length	0.73	0.66
Max. Volts	2.46	
Max. Depth (%)	87.0	47.9
Avg. Depth (%)	53.7	39.4

Burst		
	T9093	Exam
Length	0.69	0.66
Max. Volts	2.46	
Max. Depth (%)	87.0	47.9
Avg. Depth (%)	55.9	39.4

Legend:
- - ◬ - Analyst T9093 - Unadjusted
- ◇ Analyst T9093 - Adjusted
- ○ Analyst T9093 - Burst
- □ Exam
- ■ - Exam - Burst
- X - Analyst T9093 - Voltage

Figure D-52
Specimen R 37 - C 52 - 01H - Crack 1 - Year 1998
Comparison of Unadjusted, Adjusted, Burst and Voltage with Exam
NDE Depth vs. Axial Length

PWSCC ARC Release 1.1
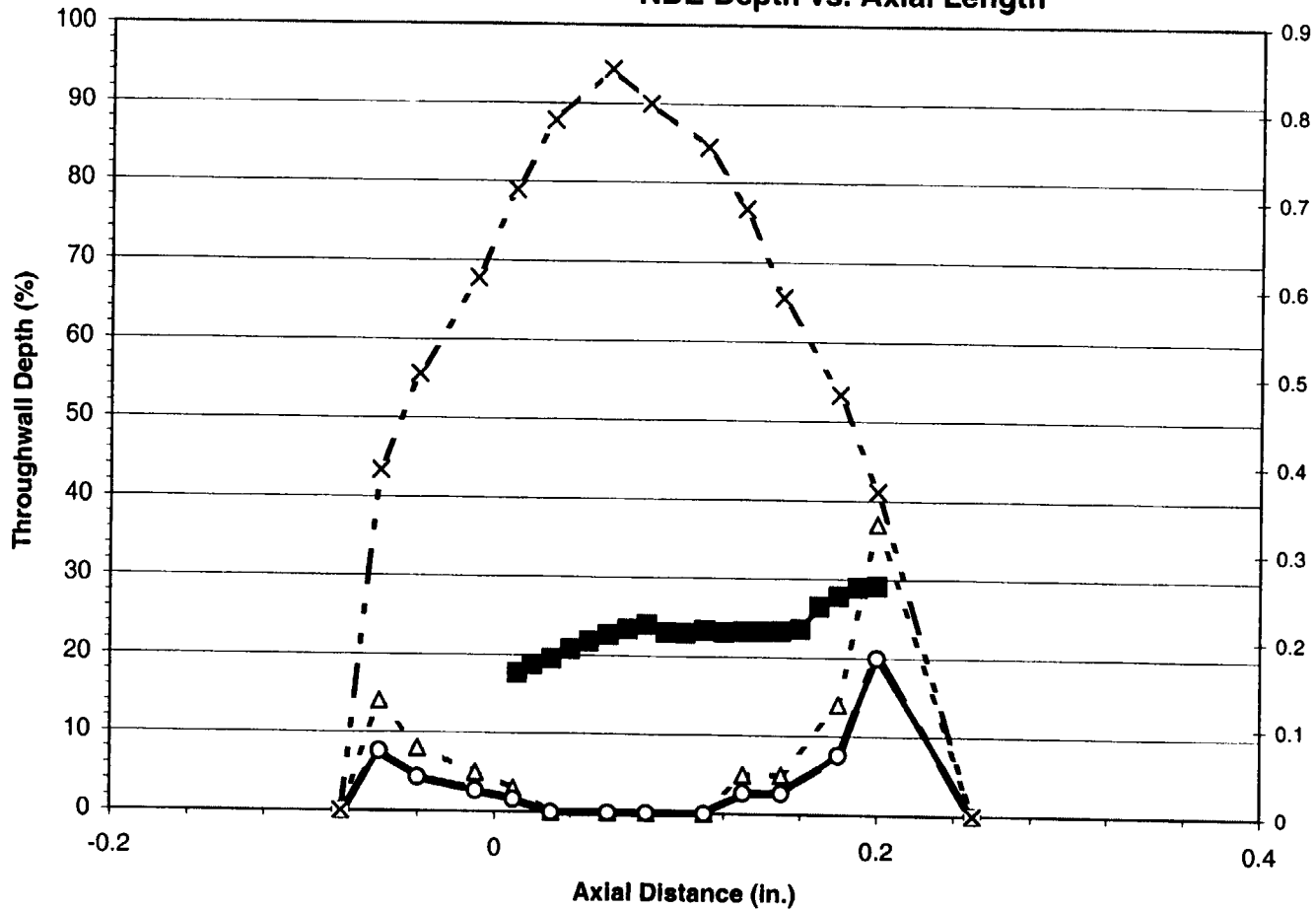
Unadjusted		
	T9093	Exam
Length	0.33	0.19
Max. Volts	0.85	
Max. Depth (%)	37.0	29.1
Avg. Depth (%)	7.7	23.4

Adjusted		
	T9093	Exam
Length	0.33	0.19
Max. Volts	0.85	
Max. Depth (%)	20.0	29.1
Avg. Depth (%)	4.2	23.4

Burst		
	T9093	Exam
Length	0.33	0.19
Max. Volts	0.85	
Max. Depth (%)	20.0	29.1
Avg. Depth (%)	4.2	23.4

- ◬ - Analyst T9093 - Unadjusted   —◇—Analyst T9093 - Adjusted   —O— Analyst T9093 - Burst
—□—Exam   —■— Exam - Burst   —X— Analyst T9093 - Voltage

6/30/00 3:19 PM

Figure D-53
Specimen R 39 - C 28 - 01H - Crack 1 - Year 1998
Comparison of Unadjusted, Adjusted, Burst and Voltage with Exam
NDE Depth vs. Axial Length

PWSCC ARC Release 1.1
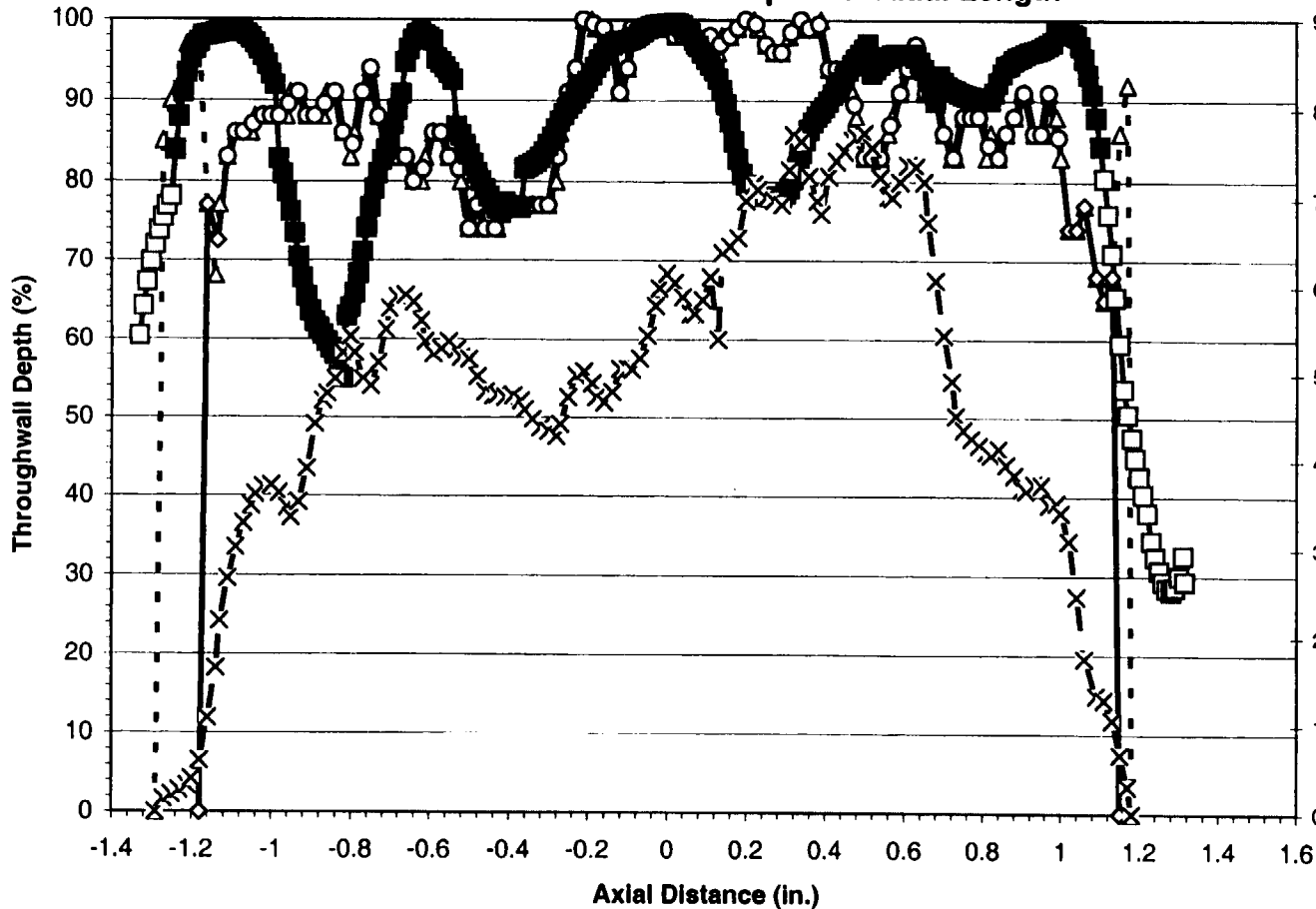
Unadjusted		
	T9093	Exam
Length	2.47	2.64
Max. Volts	7.74	
Max. Depth (%)	100.0	99.6
Avg. Depth (%)	87.6	84.8

Adjusted		
	T9093	Exam
Length	2.33	2.64
Max. Volts	7.74	
Max. Depth (%)	100.0	99.6
Avg. Depth (%)	87.2	84.8

Burst		
	T9093	Exam
Length	2.11	2.34
Max. Volts	7.74	
Max. Depth (%)	100.0	99.6
Avg. Depth (%)	89.4	88.8

Legend:
- ◁ - Analyst T9093 - Unadjusted
- ◇ Analyst T9093 - Adjusted
- ○ Analyst T9093 - Burst
- □ Exam
- ■ Exam - Burst
- ✕ Analyst T9093 - Voltage

Figure D-54
Specimen R 39 - C 28 - 01H - Crack 2 - Year 1998
Comparison of Unadjusted, Adjusted, Burst and Voltage with Exam
NDE Depth vs. Axial Length

PWSCC ARC Release 1.1
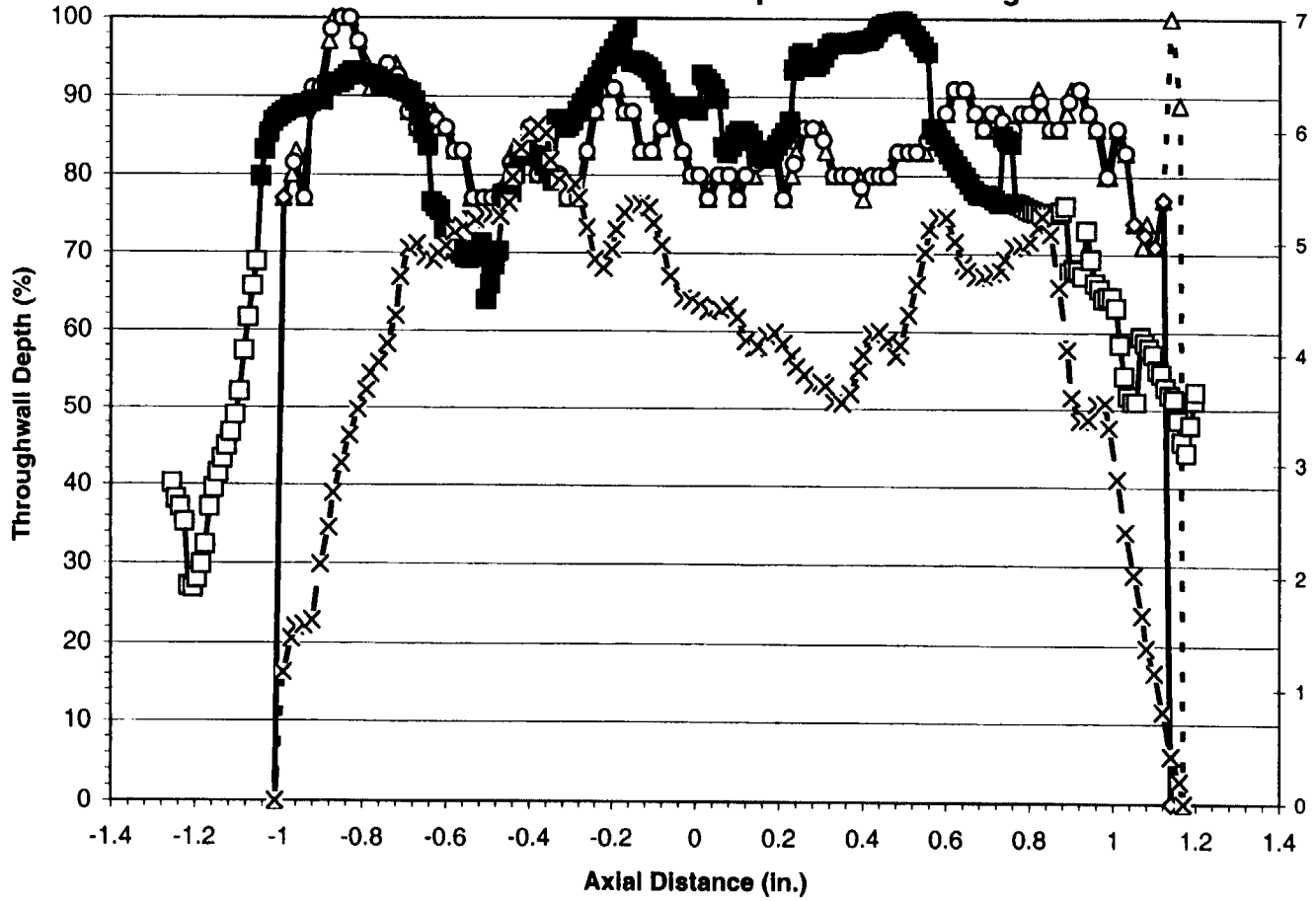
Unadjusted		
	T9093	Exam
Length	2.18	2.45
Max. Volts	6.04	
Max. Depth (%)	100.0	99.7
Avg. Depth (%)	83.9	79.4

Adjusted		
	T9093	Exam
Length	2.15	2.45
Max. Volts	6.04	
Max. Depth (%)	100.0	99.7
Avg. Depth (%)	83.5	79.4

Burst		
	T9093	Exam
Length	2.00	1.81
Max. Volts	6.04	
Max. Depth (%)	100.0	99.7
Avg. Depth (%)	84.9	87.4

- ◬ - Analyst T9093 - Unadjusted ◇ Analyst T9093 - Adjusted O Analyst T9093 - Burst
□ Exam ■ Exam - Burst X Analyst T9093 - Voltage

Figure D-55
Specimen R 41 - C 64 - 01H - Crack 1 - Year 1998
Comparison of Unadjusted, Adjusted, Burst and Voltage with Exam
NDE Depth vs. Axial Length

PWSCC ARC Release 1.1
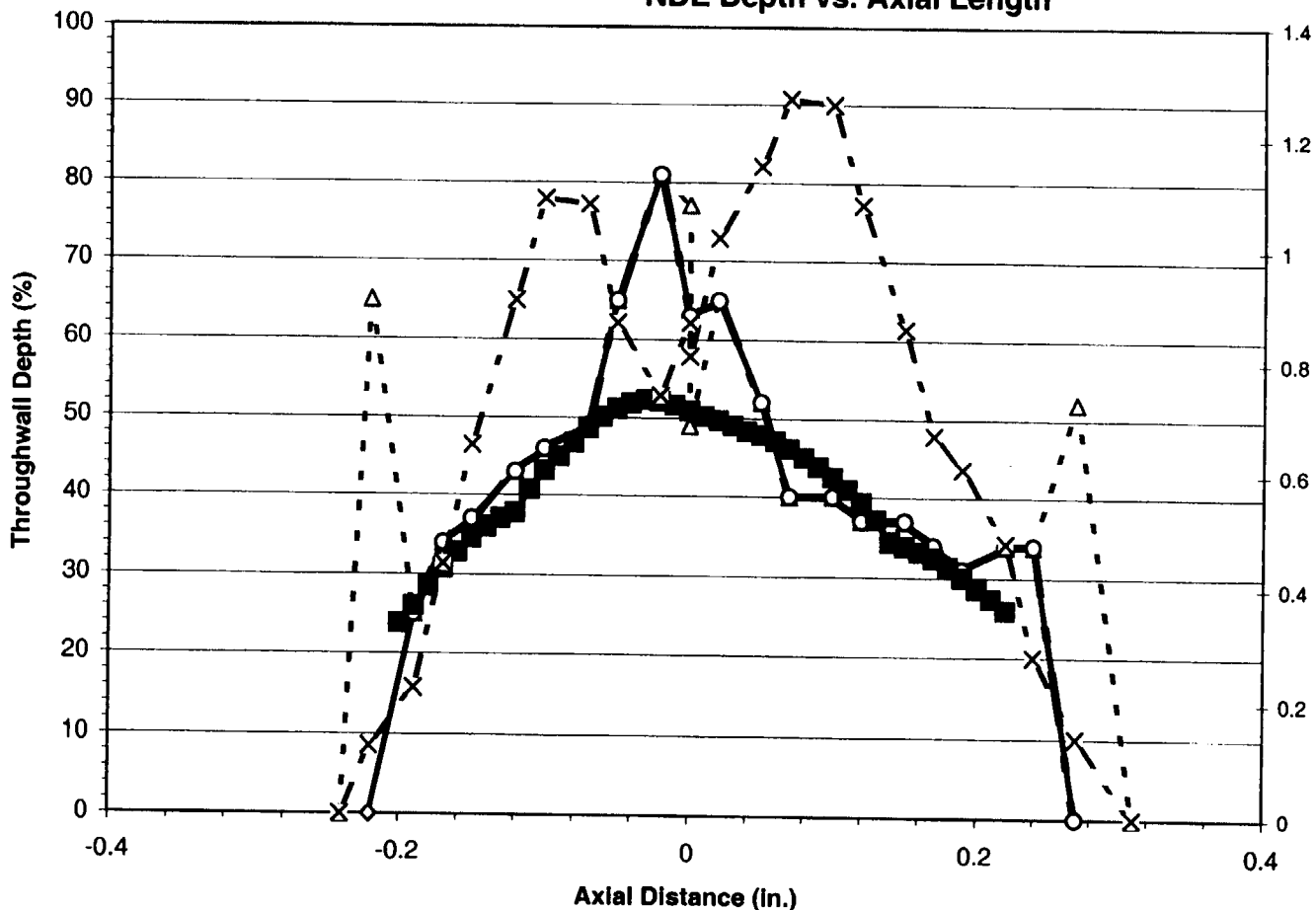
Unadjusted		
	T9093	Exam
Length	0.55	0.42
Max. Volts	1.27	
Max. Depth (%)	81.0	52.2
Avg. Depth (%)	43.6	40.7

Adjusted		
	T9093	Exam
Length	0.49	0.42
Max. Volts	1.27	
Max. Depth (%)	81.0	52.2
Avg. Depth (%)	41.9	40.7

Burst		
	T9093	Exam
Length	0.46	0.42
Max. Volts	1.27	
Max. Depth (%)	81.0	52.2
Avg. Depth (%)	43.8	40.7

Legend: - △ - Analyst T9093 - Unadjusted, Analyst T9093 - Adjusted, Analyst T9093 - Burst, Exam, Exam - Burst, Analyst T9093 - Voltage

Figure D-56
Specimen R 43 - C 40 - 01H - Crack 1 - Year 1998
Comparison of Unadjusted, Adjusted, Burst and Voltage with Exam
NDE Depth vs. Axial Length

PWSCC ARC Release 1.1
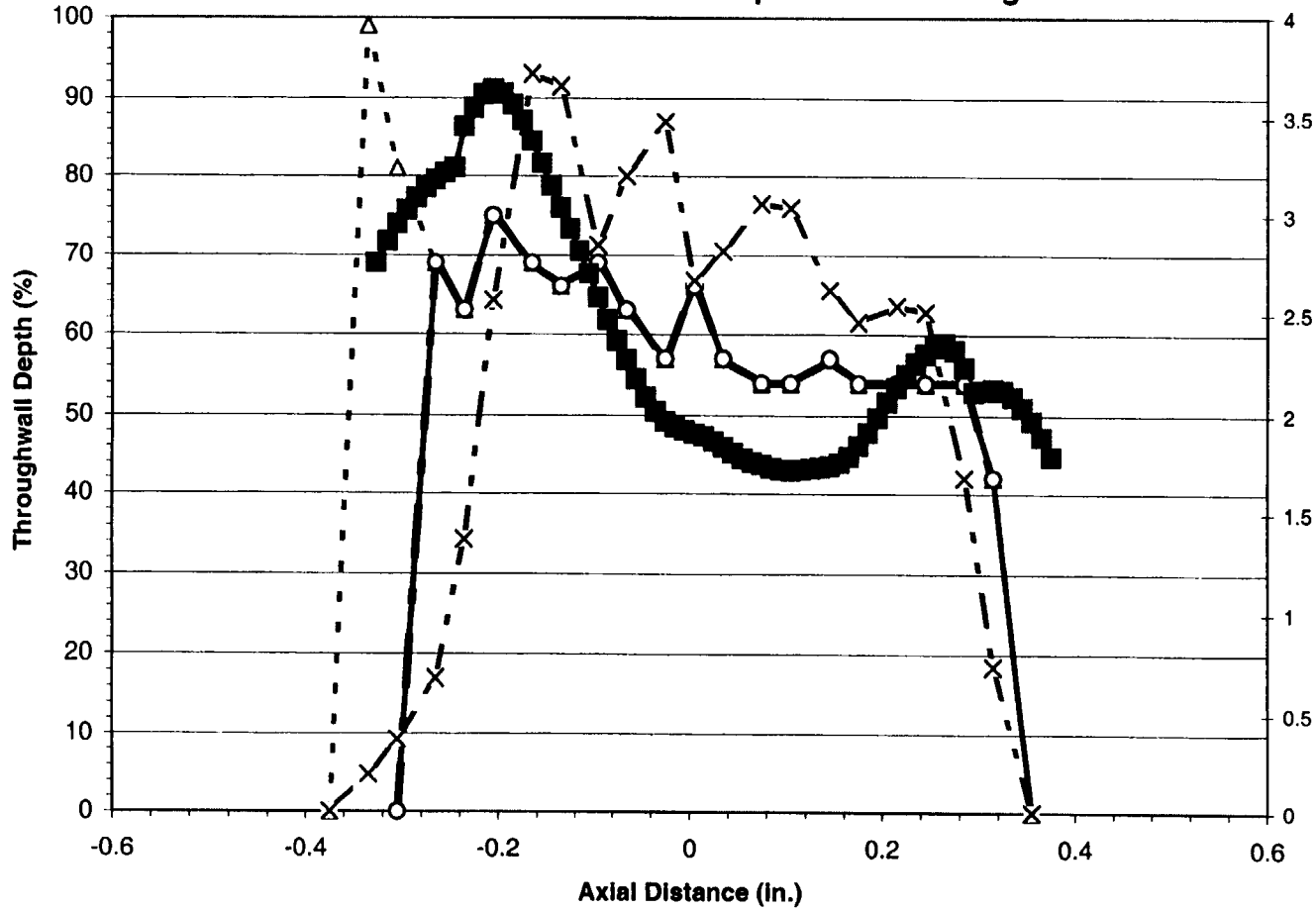
Unadjusted		
	T9093	Exam
Length	0.73	0.70
Max. Volts	3.72	
Max. Depth (%)	99.0	91.1
Avg. Depth (%)	59.4	59.9

Adjusted		
	T9093	Exam
Length	0.66	0.70
Max. Volts	3.72	
Max. Depth (%)	75.0	91.1
Avg. Depth (%)	56.1	59.9

Burst		
	T9093	Exam
Length	0.62	0.70
Max. Volts	3.72	
Max. Depth (%)	75.0	91.1
Avg. Depth (%)	58.4	59.9

Legend:
- Analyst T9093 - Unadjusted
- Analyst T9093 - Adjusted
- Analyst T9093 - Burst
- Exam
- Exam - Burst
- Analyst T9093 - Voltage